

bradscholars

Applications of Raman Spectroscopic Techniques in Forensic and Security Contexts. The detection of drugs of abuse and explosives in scenarios of forensic and security relevance using benchtop and portable Raman spectroscopic instrumentation

Item Type	Thesis
Authors	Ali, Esam M.A.
Rights	<p>http://creativecommons.org/licenses/by-nc-nd/3.0/
The University of Bradford theses are licenced under a http://creativecommons.org/licenses/by-nc-nd/3.0/>Creative Commons Licence.</p>
Download date	2026-06-10 05:37:05
Link to Item	http://hdl.handle.net/10454/5267

Chapter 1

Introduction

1.1 Aims and Objectives

The aim of the research work presented in this thesis is to develop Raman spectroscopic techniques for the detection of drugs of abuse and explosives in scenarios of forensic and security relevance.

To achieve this aim, three main objectives were addressed. The first is to investigate the applicability of Raman spectroscopic techniques for the detection and identification of drugs of abuse and explosives on some biomaterials of forensic relevance including undyed natural and synthetic fibres and dyed textile specimens, nail and skin. Residues of illicit drugs and explosives on these substrates can provide useful information. Handling, transportation or re-packaging of drugs of abuse and explosives will inevitably leave the clothing, and other possessions of persons involved in these activities contaminated with these substances. The nails and skin of the person may also be contaminated due to the handling of these substances. Therefore, the detection of controlled substances and explosives can be used as part of the evidence to establish a link between an individual and these substances. The application of confocal Raman microscopy for the *in-situ* detection and identification of particulates of several drugs of abuse and explosives on different substrates has been investigated. Pure and ‘street’ (formulations seized by the police) samples of cocaine hydrochloride, MDMA and amphetamine sulphate were used as examples in this study. Pure and commercially formulated materials of the explosives pentaerythritol tetranitrate (PETN), trinitrotoluene (TNT), and ammonium nitrate and the explosives precursors hexamethylenetetraamine (HMTA) and pentaerythritol have also been studied. Several parameters have been investigated during the course of this

study. The ability of the technique to discriminate between the analyte and the substrate matrix and the sensitivity of this approach that allows molecular information to be obtained in conjunction with microscopic evaluation of evidential materials have been addressed. The rapidity of confocal Raman spectroscopy to obtain data - an important factor for law enforcement agencies and forensic scientists, and the potential for application as a preliminary forensic screening procedure have also been investigated. Furthermore, the advantageous attributes of the technique over other chemical analytical approaches with regards to the necessity of sample preparation or pretreatment and the preservation of the integrity of the evidential material for future analysis have been studied.

The second objective is investigating the applications of benchtop and portable Raman spectroscopic techniques for the *in-situ* detection of drugs of abuse namely cocaine hydrochloride, MDMA and amphetamine sulphate in clothing impregnated with these drugs. Raman spectra were obtained from a set of undyed natural and synthetic fibres and dyed textiles impregnated with these drugs. The spectra were collected using three Raman spectrometers; one benchtop dispersive spectrometer coupled to a fibre-optic probe and two portable spectrometers. The application of these techniques to identify drugs of abuse in garments impregnated with these drugs has been investigated.

The third objective is to evaluate a portable prototype Raman spectrometer (DeltaNu Advantage 1064) equipped with 1064 nm laser for the analysis of drugs of abuse and explosives. The feasibility of the instrument for the analysis of the samples both as neat materials and whilst contained in plastic and glass containers has been investigated. The advantages, disadvantages and the analytical potential in the forensics arena of this instrument have been discussed.

1.2 Thesis Structure

This thesis is composed of 10 chapters addressing the three objectives of the research work. The second chapter describes the legislation related to drugs of abuse, the chemical structure and effects of the commonly abused drugs. It also illustrates the classification and structure of explosives. The third chapter describes the most commonly used analytical techniques for the analysis of drugs of abuse and explosives. The advantages, disadvantages and limitations of each technique have been discussed. The theory, principles and instrumentation of Raman spectroscopy has been discussed in chapter four. Chapter five discusses the application of Raman spectroscopy for the analysis of drugs of abuse and explosives. Chapters six to ten include the experimental work and results of the research work carried out in this study. Chapter six illustrates detection and identification of drugs of abuse and explosives on human nail using Raman spectroscopy. The application of confocal Raman microspectroscopy for the *in-situ* detection of drugs-of-abuse and explosives on clothing has been addressed in chapter seven. The application of fibre-optic Raman spectroscopy to the *in-situ* identification of drugs of abuse, namely cocaine hydrochloride, MDMA and amphetamine sulphate, on a variety of fibres and textiles impregnated with the drugs has been detailed in chapter eight. Chapter nine demonstrates the use of confocal Raman microspectroscopy for the detection of drugs of abuse and explosives on skin. The feasibility of a new prototype portable Raman spectrometer equipped with 1064nm excitation for the identification of drugs of abuse and explosives has been discussed in chapter ten. Chapter eleven comprises the conclusions of this research study and suggestions for future work.

Chapter 2

Drugs of Abuse and Explosives

2.1 Drugs of Abuse

2.1.1 Definition ^[1, 2]

The term ‘drug of abuse’ describes any substance that, because of some desirable effects, is used for a purpose other than therapeutic action. Another definition of the term is any substance for which the possession or supply is restricted by law because of its potential harmful effect on the user. Such drugs are known as controlled or scheduled substances and comprise both licit materials (i.e. those manufactured under licence), the illicit products of clandestine factories and some natural products. In 2000, it was estimated by the World Health Organization (WHO) that there were about 185 million global illicit drugs abusers, 2 billion users of alcohol and 1.3 billion smokers (Figure 2.1). As a proportion of disease burden, illicit drugs have the greatest impact in developed countries –Western and North Europe, North America and Australia. They have the least impact in Central and Southern Africa. ^[3]

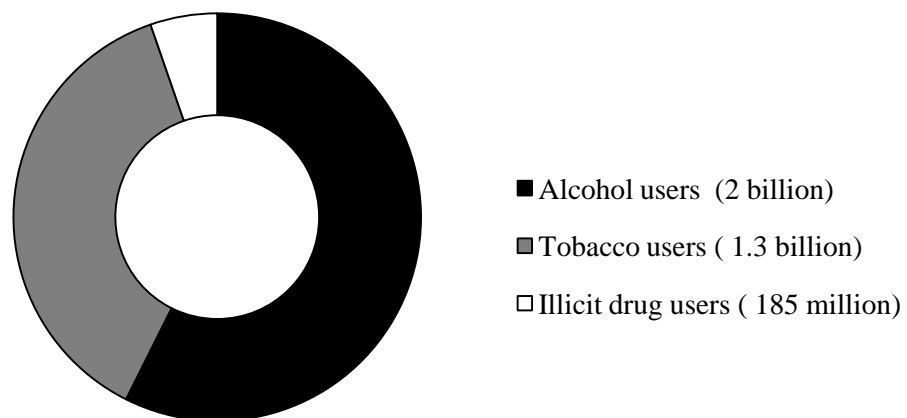


Figure 2.1 World extent of psychoactive substance use (Adapted from Ref. 3)

2.1.2 Drug legislation in the UK ^[4,5]

In the United Kingdom, drugs of abuse are regulated under the Misuse of Drugs Act (1971) and the Misuse of Drugs Regulations

2.1.2.1 The Misuse of Drugs Act (1971)

The misuse of drugs act (1971) prohibits certain activities with respect to controlled drugs (e.g. possession, possession with intent to supply, production) without a licence.

The drugs are listed in Schedule 2 of the act and are divided into three classes: class A, B and C. These classes represent, in descending order, the propensity of the substances to cause social harm. Associated with each class are the maximum penalties for offences involving controlled drugs, decreasing in severity in the order A to C. For Class A drugs, the maximum penalty for some offences is life imprisonment, for Class B and C is 14 years. The list below shows examples of each class:

- Class A drugs: cocaine (including crack), N-methyl-3,4 methylenedioxyamphetamine (MDMA, ecstasy), LSD (lysergic acid diethylamide), mescaline, opium, morphine and some derivatives, phencyclidine, psilocin. Injectable forms of drugs in Class B.
- Class B drugs: Amphetamine, methamphetamine, cannabis, barbiturates, codeine, dihydrocodeine, methcathinone , and methylphenidate.
- Class C drugs: Benzodiazepines, gamma hydroxybutyrate (GHB), ketamine.

The list of drugs in Schedule 2 may be varied by a Statutory Instrument known as a Modification Order. There have been 14 such Orders since 1971, most of which have served to incorporate changes agreed by member states of the United Nations.

2.1.2.2 The Misuse of Drugs Regulations (Updated 2001) ^[5]

These regulations define those people who are authorised to produce, possess and supply controlled drugs. The drugs are divided into five schedules with decreasing levels of control over import, export, possession, production, supply and record keeping.

Schedule 1: These drugs cannot be prescribed, have little therapeutic value and licences are issued only for research purposes. Only those persons specified in the Act or licensed by the Home Office may possess or supply these drugs. Schedule 1 drugs include cannabis, cannabidiol, cathinone, coca leaf, ecstasy and related drugs, designer opioids derived from fentanyl, LSD, psilocin, and raw opium.

Schedule 2: Possession of these drugs by a member of the public is only lawful when acting under the directions of a doctor. For persons that supply them, the drugs are subject to very strict requirements for storage and documentation. Schedule 2 drugs include amphetamine, cocaine, opioids, gamma-butyrolactone (GBL), phencyclidine and methylphenidate.

Schedule 3: Drugs included in this Schedule are subject to the same regulations as schedule 2 except that the documentation of supply is less rigorous. Drugs included are barbiturates, buprenorphine, diethylpropion, temazepam, flunitrazepam, and cathine.

Schedule 4: Drugs included in this schedule are divided into two parts: Part I which comprises mostly benzodiazepines and GHB and Part II which contains growth hormones, anabolic steroids, human chorionic gonadotrophins and clenbuterol.

Schedule 5: These are preparations containing very low concentrations of substances belonging to schedules 2 and 3 *e.g.* codeine and ethylmorphine. Suppliers and producers must keep transaction records of their dealings.

2.1.3 Drug Dependence ^[2, 6]

The abuse of drugs can result in psychological dependence, which is an inappropriate compulsion to take the substance regularly. Some drugs can result in physical dependence and the drug is taken to make the user feel good, or more usually to avoid withdrawal. Withdrawal reaction comprises a collection of signs and symptoms so it is known as withdrawal syndrome. It occurs if the chronic use of a drug is stopped abruptly, if an antagonist is given or if the dose is reduced suddenly. Tolerance occurs when repeated administration of a drug eventually produces a reduced effect, such that larger doses are required to achieve the same response. This may lead a user to take amounts that would be fatal. The method of administration of a drug plays an important part in the speed of onset and intensity of the desired effects. There are three basic methods by which drugs of abuse are taken: by injection, orally and via the airways.

- **Injection:** Many drugs are commonly taken by intravenous injection, including heroin, cocaine hydrochloride, amphetamine and temazepam. This route affords rapid access to the circulation and then to the brain, allowing fast onset of intense psychoactive effect. Intravenous injection may lead to several complications such as abscesses, collapsed veins and intrarterial injection may cause gangrene. This route also carries the risk of contracting infections such as HIV and hepatitis.
- **Oral administration:** Many drugs can be taken orally such as ecstasy, LSD and alcohol. Also, many of the plants and abused medicines are taken by mouth. Compared to administration by injection or via airways, the psychotropic effects can take a longer time to develop.

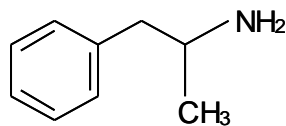
- Administration via airways: volatile substances can be taken by inhalation. Other compounds need to be heated before inhalation such as heroin, crack cocaine, cannabis resin and methamphetamine. Tobacco, heroin and cannabis can be smoked. In addition, dry powders such as amphetamine and cocaine hydrochloride can be inhaled into the nose (snorting).

At street level no drugs are pure and even prescription medicines contain excipients. A variety of cheap, inert or pharmacologically active adulterants are used to dilute or bulk out 'cut' illicit drugs including glucose, aspirin, paracetamol, caffeine, lidocaine, mannitol and lactose. In addition to the effects of the drug of abuse, the adulterant may cause harmful side effects. Contamination of street preparations of drugs of abuse with poisons such as arsenic oxides, strychnine, quinine and hyoscyne has been described. [7-10]

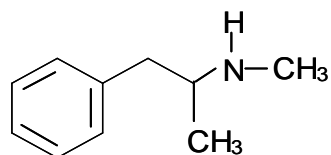
2.1.4 Drugs of abuse

2.1.4.1 Amphetamines [2, 11-14]

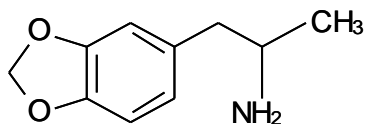
Amphetamine is a synthetic stimulant drug, commonly known as speed, whizz or uppers. There are a large number of amphetamines which are controlled substances. Figure (2.2) shows the chemical structure of amphetamine and those of some of its derivatives. Amphetamine is a racemic mixture of dextro and levorotatory amphetamine; *D*-amphetamine is the most active and is the form used therapeutically. Many of its derivatives have been abused. The drug is mixed with a wide variety of adulterants and diluents such as caffeine, glucose, baby milk and talc. The effects of these substances on the user can be extremely harmful. Amphetamine can be snorted, taken orally, smoked or injected. Amphetamine can cause breathing difficulties and the heart rate to increase, pupils to widen, appetite to lessen and a reduction in the



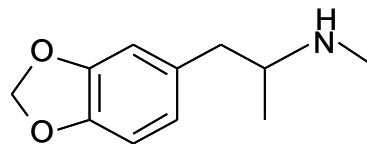
Amphetamine



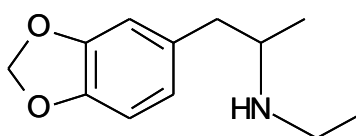
Methamphetamine



3,4-Methylenedioxyamphetamine (MDA)



3,4-Methylenedioxy-N-methylamphetamine (MDMA)



3,4-Methylenedioxy-N-ethylamphetamine (MDEA)

Figure 2.2 Structures of commonly encountered amphetamines

need for sleep. Feelings of increased confidence, talkativeness, cheerfulness and feeling more alert and energetic can result. Ecstasy is almost invariably taken orally and referred to as a ‘club drug’, because of its links with young people who regularly attend nightclubs. MDMA has become one of the main drugs of abuse in many countries in Northern Europe. Ecstasy abusers seek a state of tranquil euphoria in which there is a high degree of emotional empathy between associates, greater insight into personal problems and an expanded mental perspective. Users feel at ‘peace with the world’ and violent and aggressive feelings are suppressed. For all amphetamines, the stimulant effects gradually dissipate and as they begin to wear off, they may be succeeded by a period of restlessness, anxiety, tiredness and depression (a ‘crash’). Prolonged amphetamine use can result in psychological dependence. Tolerance may develop resulting in an increase in the amount needed to achieve the desired effect.

2.1.4.2 Cocaine [1, 2, 11, 13, 15]

Cocaine is a central nervous system (CNS) stimulant drug. It occurs naturally in the leaves of two plants indigenous to South America; *Erythroxylum coca* and *Erythroxylum novogranatense*. The leaves contain about 1% cocaine and can be chewed as a drug. Coca paste or cocaine can be produced from the leaves of the plant. Cocaine hydrochloride (known as snow, Coke or C) is a white powder which typically smells of HCl. This is the commonest form of the drug used and is often mixed with various diluents and adulterants. This salt can be re-converted to the free base form comprising hard, waxy lumps commonly known as ‘rocks’ or ‘crack’. Cocaine hydrochloride can be snorted from a line of white powder and the drug is absorbed through the mucous membrane of the nose. Alternatively, it can be injected. Cocaine free base is volatile and can be administered by smoking. Figure (2.3) shows the chemical structure of cocaine hydrochloride and crack cocaine. When cocaine hydrochloride is injected or crack cocaine is smoked, the user experiences a sudden ‘rush’ of exhilaration as the drug enters the brain very quickly. This sudden intense feeling is not a feature of nasal insufflation of the hydrochloride salt because absorption across the mucous membrane is relatively slow and feeling of euphoria

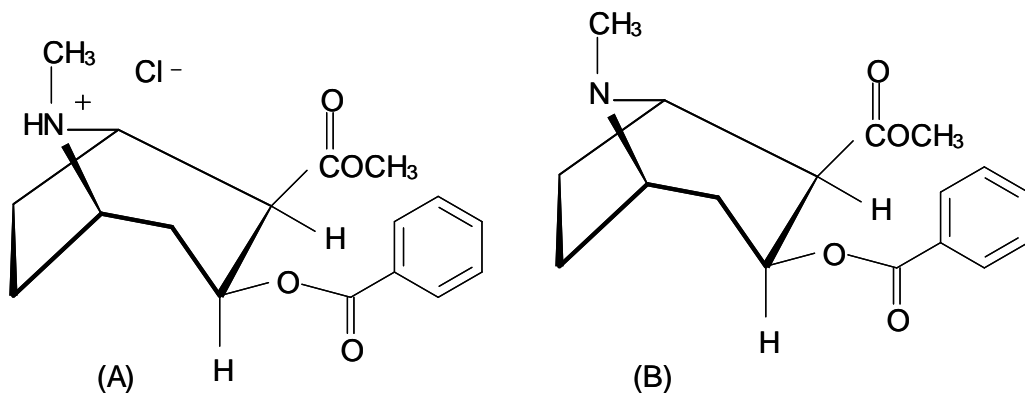


Figure 2.3 Structures of A: Cocaine hydrochloride B: Crack Cocaine

takes longer to develop. The mental effects encountered include feeling of euphoria, alertness, excitement and rapid flow of thought. Cocaine is a CNS stimulant; it helps to combat fatigue, increases capacity to do work and promotes clearer thinking and concentration. Unwanted side-effects include increased irritability, insomnia, and restlessness. With high doses, the user may exhibit confused and disorganized behaviour, irritability, fear, paranoia, hallucinations, and may become extremely antisocial and aggressive, possibly leading to stroke, heart attack or death. The use of needles for intravenous injection of cocaine is a possible mode for HIV infection.

2.1.4.3 Opioids [1, 2, 11, 14, 15, 16]

This group of drugs are extracted from the opium poppy (*papaver somniferum*), native to Asia Minor. The opium market continues to be dominated by the large levels of cultivation and production in Afghanistan. The active drugs can be found in the latex that exudes from incisions made in the unripe capsule of the flowering head. The alkaloids that occur in the poppy include morphine, noscapine, codeine, papaverine

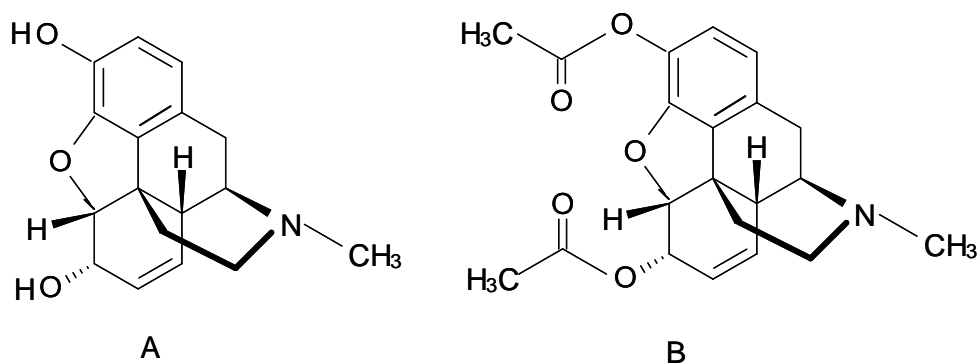


Figure 2.4 Structure of A: Morphine

B: Diacetylmorphine (Heroin)

and thebaine. Morphine (Figure 2.4 A) is responsible for most of the psychotropic activity and comprises 9-17% of the weight of the dried opium. Alkaloids derived from the opium poppy that have morphine-like action are termed opiates, whereas synthetic derivatives are termed opioids. In recent years, the term opioids has been

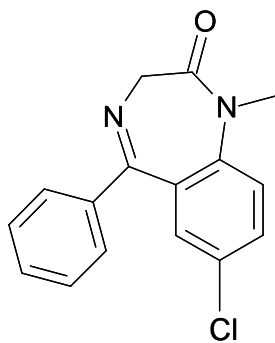
understood to encompass opiates. Prescription opioids that are abused include morphine, methadone, codeine, diamorphine (heroin), fentanyl, tramadol, and pethidine. Opium is purified to form crude morphine. Diamorphine is prepared by the acetylation of morphine. Heroin (Figure 2.4B) is the most widely used opioid because of its potency, availability, and rapid brain access after administration. It is known as ‘Junke’, ‘H’, or ‘Horse’ and usually supplied as a brown or off-white powder. In ‘street’ preparations, it is generally found mixed with other substances including paracetamol, sugar, diazepam and other opioids.

2.1.4.4 Benzodiazepines ^[1, 2, 13,17]

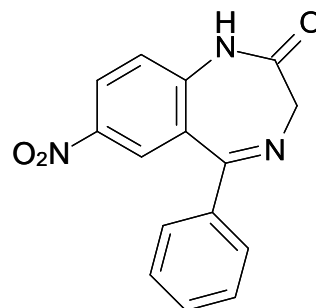
There are over 30 benzodiazepines (Figure 2.5) in common use worldwide and abuse is restricted largely to pharmaceutical preparations. The inappropriate use of benzodiazepines falls into three main categories:

- 1- Overprescribing of hypnotic and anxiolytic benzodiazepines has resulted in large numbers of people becoming dependent upon them (benzodiazepine dependents).
- 2- Recreational abuse of benzodiazepines on the street by known users of illicit substances (benzodiazepine abusers).
- 3- Involuntary administration *e.g.* use in sedating individuals prior to sexual assault.

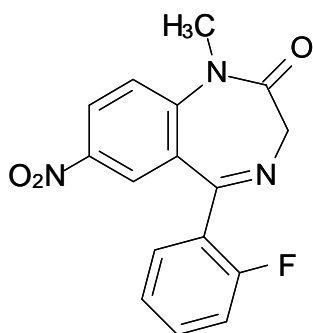
The most commonly abused benzodiazepines are diazepam, nitrazepam, flunitrazepam, flurazepam and lorazepam. They may be used in conjunction with heroin or in their own right. Benzodiazepines are obtained by purchase on the black market or from legitimate receivers of benzodiazepines prescriptions. Flunitrazepam (Rohypnol) has been used in ‘date rape’ crimes to incapacitate victims before sexual assaults.



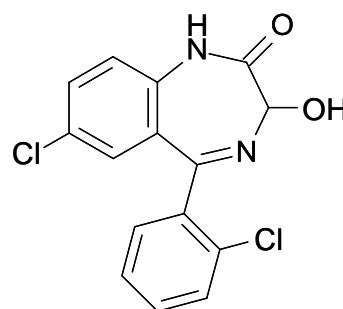
A: Diazepam



B: Nitrazepam



A: Flunitrazepam



D: Lorazepam

Figure 2.5 Chemical structures of some benzodiazepines

2.1.4.5 Cannabis ^[1, 2, 13]

Cannabis refers to a variety of preparations derived from the Indian hemp, *Cannabis sativa*. The plant is native to India, Bangladesh and Pakistan, but is now much more widely distributed, mainly because of man's intervention. It is the most commonly used, widely cultivated, and extensively trafficked illicit drug. Glandular hairs called trichomes, which secrete the resin, are abundant in the flowering heads and surrounding leaves. The major pharmacologically active constituents of the resin are called cannabinoids. There are over 60 of these but the most important psychoactive compound is delta-9-tetrahydrocannabinol (THC) [Figure 2.6]. The main types of cannabis sold at the street level are:

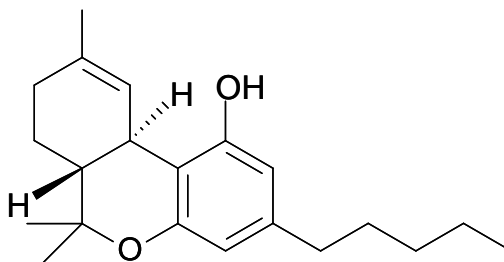


Figure 2.6 delta-9-tetrahydrocannabinol (THC)

a- Marijuana: This term is more popular in USA and refers to the grey-green dried and crushed heads and small leaves of the cannabis plant. It contains up to 5% THC.

b- Hashish: refers to the cannabis resin alone, after removal from the plant. The term is derived from the Arabic 'hashish al keif' which means dried herb of pleasure. It is typically brown in colour with a toffee-like texture when pure but the colour may vary according to geographical source and purity. Hashish can contain up to 20% THC.

c- Hash oil: refers to a concentrated resin extract and is the most potent form of cannabis. It is a greenish-black viscous liquid and can comprise 60% or more THC.

Cannabis products are administered in a number of different ways. The most common one is mixing with tobacco and smoking. Marijuana herb can be rolled into cigarettes or mixed with tobacco. Hashish or hash oil is mixed with tobacco prior to rolling the cigarette. It can also be smoked in a special pipe.

2.1.4.6 Gamma-hydroxybutyric acid ^[1, 2, 18]

Gamma-hydroxybutyric acid (Figure 2.7) was originally developed as an anaesthetic and hypnotic drug in the early 1960s. It acts as a CNS depressant and is chemically related to the brain neurotransmitter gamma-aminobutyric acid (GABA). The related

compounds gamma butyrolactone (GBL) and 1, 4-butanediol are converted to GHB after ingestion. These compounds are marketed as dietary supplements and solvents. Thus, an individual who ingest these chemicals will experience pharmacological effects similar to those of GHB. GHB is usually supplied as odourless white powder,

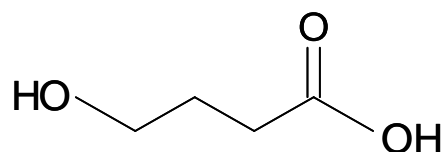


Figure 2.7 Gamma-hydroxybutyric acid (GHB)

capsule, tablets or ready dissolved in water. Street names of GHB include ‘GBH’, ‘liquid X’ and ‘liquid ecstasy’. GHB is abused due to its sedative, relaxant and euphoric properties. It has been used to commit drug facilitated sexual crimes (DFSA).

2.1.5 Cutting agents ^[10, 13, 14]

In addition to identifying and quantifying the drug of abuse, the forensic analyst often must identify the cutting agents added to many drug exhibits. A similar term, excipients, is used to refer to inactive ingredients in commercial preparations *e.g.* lactose and mannitol. Cutting agents are chosen on the basis of their physical or chemical similarity to the controlled drugs. They are used to stretch the supply of a drug of abuse and maximize the profits. Diluents are substances that have no pharmacological properties *e.g.* baking soda, starch and sugar. Adulterants are active substances usually (but not always) have effects similar to the controlled drug. The taste of a cutting agent is a crude measure of its chemical similarity to the controlled

drug. For example, cocaine is cut with procaine or lidocaine which have similar local anaesthetic effects. Also, cocaine can be cut with caffeine; both have a stimulant effect. Contaminants are substances that accidentally find their way to the sample during the extraction, purification or transportation processes e.g. arsenic and barium.

2.2 Explosives ^[14, 19-22]

An explosive is a material, either a pure single substance or a mixture of substances, which is capable of producing an explosion by its own energy. The explosive substance is an unstable material that produces an explosion or detonation by means of a very rapid, self-propagating transformation of the material into more stable substances, always with the liberation of heat and the formation of gases. This transformation is accompanied by loud sound and shock. Explosives can be classified according to their performance and uses to three classes; primary, secondary and propellants.

a- Primary explosives:

Primary explosives are sensitive to modest stimuli such as heat, spark, or friction; application of the correct stimulus will lead to a detonation. They possess the ability to transmit the detonation to less sensitive explosives. Primary explosives have a high degree of sensitivity to detonation through shock, friction, electric spark or high temperatures and explode whether they are confined or unconfined. Primary explosives in common use include lead azide, lead styphnate, potassium dinitrobenzofurozan, mercury azide, and mercury fulminate.

b- Secondary explosives:

Secondary explosives (also known as high explosives) cannot be detonated readily by heat or shock and are generally more powerful than primary explosives. They are less

sensitive than primary explosives and can only be initiated to detonation by the shock produced by the explosion of a primary explosive. Some common military explosives are shown in Figure 2.8.

c- Propellants:

Propellants are combustible substances containing within themselves all the oxygen needed for their combustion. Propellants only burn and do not explode; burning usually proceeds rather violently and is accompanied by a flame or sparks and a crackling sound, but not by a sharp, loud bang as in the case of detonating explosives.

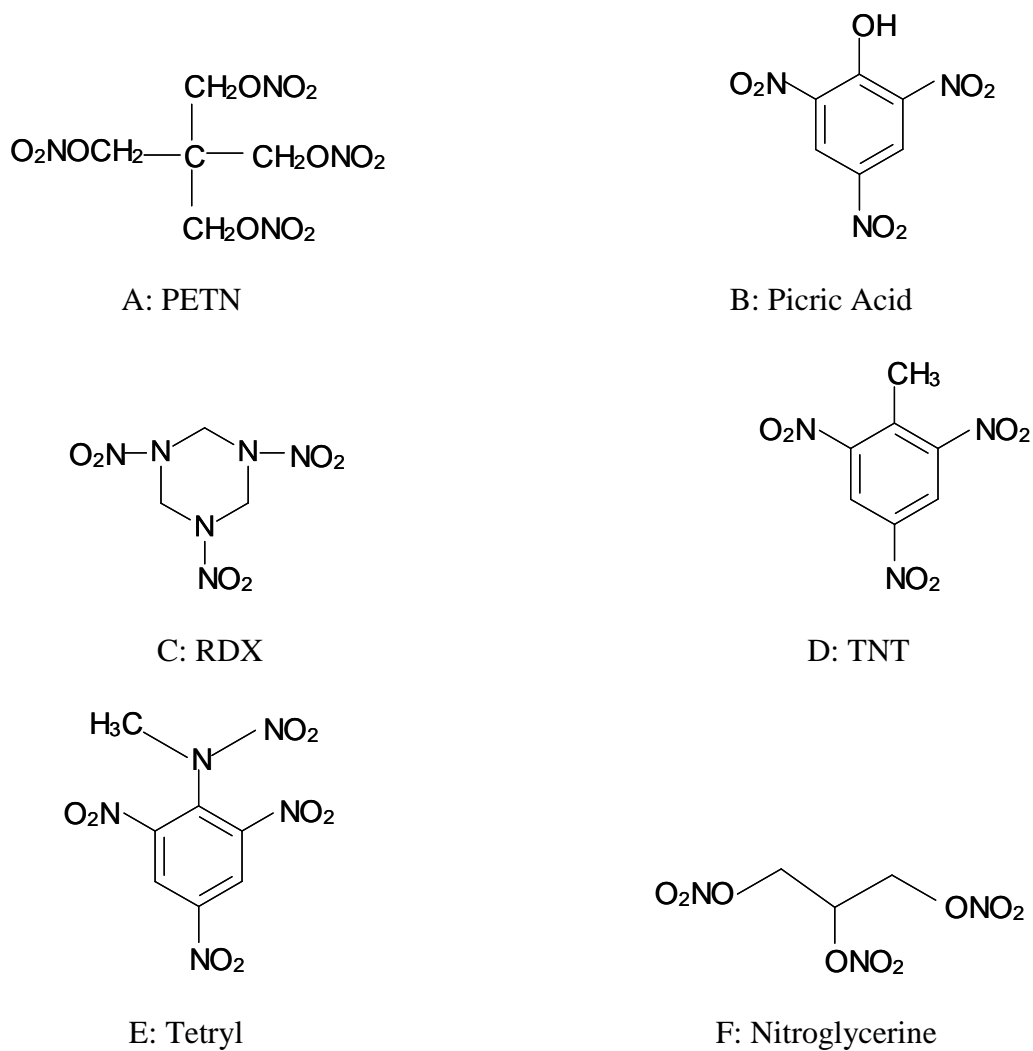


Figure 2.8 Some common secondary explosives [Adapted from reference 19].

Smokeless powders are widely used in gun propellants for small arms and shotguns. Smokeless powders containing nitrocellulose as the only energetic ingredient are referred to as “single-base” propellants, whereas those that also contain nitroglycerine are known as “double-base” propellants.

2.2.1 Plastic explosives

Most explosives are powders and do not readily hold a shape. So, plasticizers are added to make a mouldable material. Plastic explosives contain one or more of the explosives listed above, moulded in an inert, flexible binder. A wide variety of plasticizers are added, but the maximum level is usually 10–15% because most plasticizers are inert and would degrade explosive output. Examples of plastic explosives are C-4, Semtex H, and PE4. Because most of these explosives are sensitive to initiation by impact or friction, they may be desensitized by coating with wax, oil or grease.

2.2.2 Polymer Bonded Explosives

Polymer bonded explosives (PBXs) were developed to decrease the sensitivity of the newly-synthesized explosive crystals by embedding them in a rubber-like polymeric matrix. PBXs based on RDX and RDX/PETN are known as Semtex. Energetic polymers were added in explosive compositions to increase the explosive performance. This makes the explosives more vulnerable to accidental initiation by impact compared to traditional explosive compositions. The addition of plasticizers has reduced the sensitivity of PBXs whilst improving their processability and mechanical properties. Examples of PBXs are PETN in polyester and styrene copolymer and RDX in a nylon and aluminium matrix.

Chapter 3

Forensic Analysis of Drugs of Abuse and Explosives

3.1 Forensic Analysis of Drugs of Abuse

Items received by the forensic laboratory and suspected of containing drugs of abuse occur in four main forms: powders, tablets and capsules, living plants or dried vegetable matter, and liquids. The forensic chemist must ensure that the material provided is suitable for the analysis to be carried out, carry out the correct analysis, achieve quality data of certain standard, interpret the data and present them in written and /or verbal forms. Figure 3.1 shows a general scheme for the analysis of drugs of abuse. ^[13]

3.1.1 Physical Examination ^[1, 23]

The physical appearance generally gives a good idea of the drug present e.g. cannabis. It is therefore possible to go directly to the specific test rather than use a screening technique. Tablets such as prescription medications or clandestinely synthesized tablets are common forms of physical evidence. In cases where the evidence is or appears to be commercially manufactured tablets, identification can be made visually using references such as the physician's desk reference. In other cases the pills may have other markings or imprints such as crosses or imprints. Amphetamines, methamphetamine, and MDMA are often sold illicitly in tablet form, although typically the pills are cruder than those produced commercially. While the physical appearance can give a good idea about the drug present, the identity of the drug can only be established after chemical analysis.

3.1.2 Screening tests

3.1.2.1 Presumptive (colour) tests ^[1, 14, 24]

Colour tests give valuable indication of the content of the sample material. These tests

continue to be popular for several reasons. They rely on simple chemical reactions which produce visible results that can be interpreted with the naked eye. The reagents and laboratory materials required to perform the tests are inexpensive and readily available. The tests can be performed by unskilled operator without extensive training. They can also be employed in the field by the security and law enforcement agents. One of the most important and widely used colour tests is the Marquis test. A yellow to orange colour is obtained if amphetamine or methamphetamine is present in the tested sample while opiates yield an indigo colour. The main purpose of these primary colour tests is to narrow the list of substances possibly present in an unknown sample. These tests are only presumptive and suffer from several disadvantages. They cannot discriminate between drugs of the same type *i.e.* they cannot discriminate between derivatives. Additionally, they are susceptible to false positive results, and the colour produced can be influenced by the salt form of the drug or the presence of other agents in the sample.

3.1.2.2 Thin Layer Chromatography ^[1, 14]

TLC is a simple, quick, and inexpensive procedure that gives the forensic analyst a quick answer as to how many components are in a mixture. TLC is also used to support the identity of a compound in a mixture when the R_f of a compound is compared with the R_f of a known compound. A TLC plate is a sheet of glass, metal, or plastic which is coated with a thin layer of a solid adsorbent (usually silica or alumina). A small amount of the mixture to be analyzed is spotted near the bottom of this plate. The TLC plate is then placed in a shallow pool of a solvent in a developing chamber so that only the very bottom of the plate is in the liquid. This liquid, or the eluent, is the mobile phase, and it slowly rises up the TLC plate by capillary action. As the solvent moves past the applied spot, an equilibrium is established for each

component of the mixture between the molecules of that component which are adsorbed on the solid and the molecules which are in solution. In principle, the components will vary in solubility and in the strength of their adsorption to the adsorbent and some components will be carried farther up the plate than others. When the solvent has reached the top of the plate, the plate is removed from the developing chamber, dried, and the separated components of the mixture are visualized. If the compounds are coloured, visualization is straightforward. Non-coloured compounds are visualized using ultraviolet radiation or by spraying the plate with a detection reagents. Colour tests reagents can be used for visualising the compounds which increases the selectivity of the detection. The major drawback of TLC is its low sensitivity and low specificity, thus negative results of TLC are not always negative by other methods.

3.1.3 Confirmatory tests

3.1.3.1 Chromatography ^[25]

Chromatography involves a sample being dissolved in a mobile phase (which may be a gas or a liquid) which is then forced through an immobile, immiscible stationary phase. The phases are selected such that components of the sample have differing solubilities in each phase. A component which is quite soluble in the stationary phase will take longer to travel through it than a component which is not soluble in the stationary phase but soluble in the mobile phase. As a result of these differences in mobilities, sample constituents will become separated from each other as they travel through the stationary phase. Chromatographic techniques use columns packed with a stationary phase, through which the mobile phase is forced. The sample is transported through the column by continuous addition of the mobile phase ; a process called

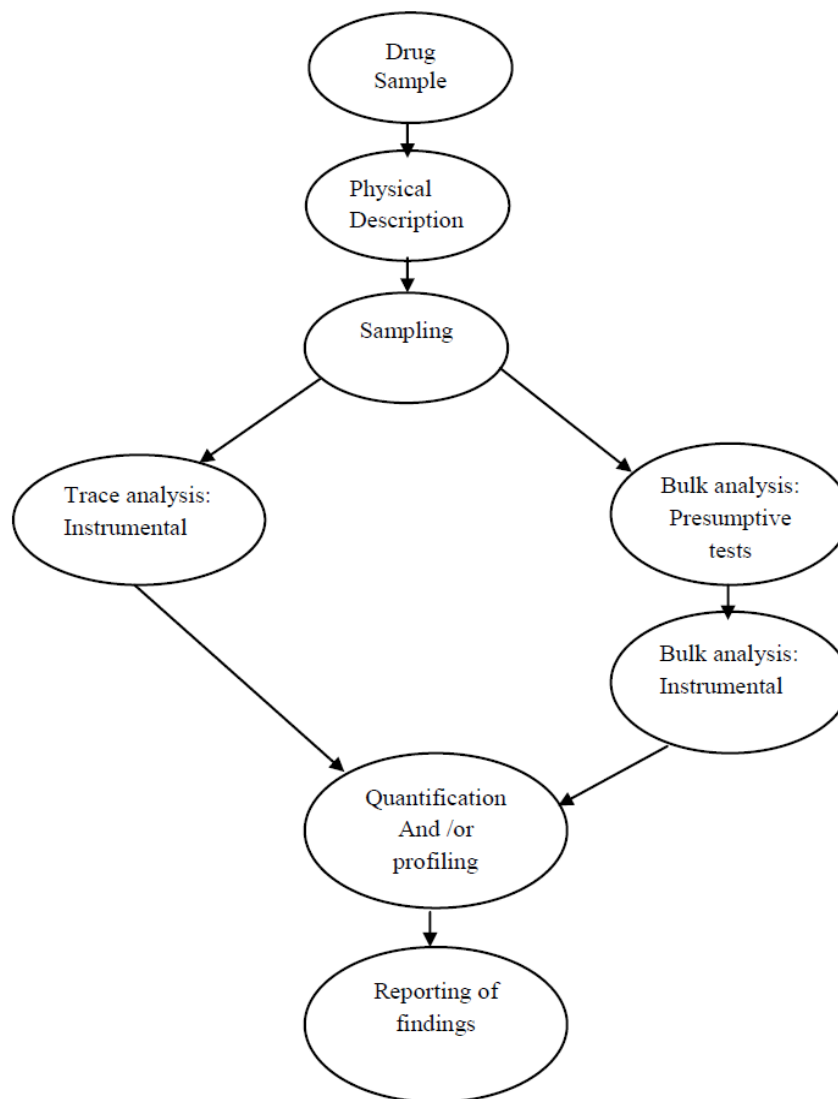


Figure 3.1 General scheme for drug analysis [Adapted from reference 13]

elution. The time elapsed between sample injection and an analyte peak reaching a detector at the end of the column is termed the retention time (t_R). In many chemical analyses, the compound of interest is found as a part of a complex mixture and the role of the chromatographic technique is to separate the components of that mixture to allow their identification or quantitative determination. The main disadvantages of chromatography are difficulties in establishing specific separation methods (mobile and stationary phases) may lead to a lack of specificity. Identification depends on the comparison of the retention time of an unknown with those of reference materials

determined under similar experimental conditions. There are, however, so many compounds that even if the retention times of an unknown sample and a reference material are identical, the analyst cannot say with absolute certainty that the two compounds are the same. Despite a range of chromatographic conditions are available to the analyst, it is not always possible to effect the complete separation of all of the components of a mixture which may prevent the precise and accurate identification of the analyte of interest.

3.1.3.1.1 Gas Chromatography-Mass Spectrometry ^[26]

GC separates the components of a mixture in time, and the mass spectrometer provides information that helps in the structural identification of each component. The basic principle of GC/ MS involves the volatilization of the sample in a heated inlet port, separation of the sample components in a specially prepared column, and detection of each component by a detector. A carrier gas, such as helium or hydrogen, is used to transfer the sample from the inlet port, through the column, and into the detector. Separation of the sample components is determined by the distribution of each component between the carrier gas (mobile phase) and the column (stationary phase). Samples to be analysed by GC-MS must be volatile, thermally stable and low polarity. Involatile, thermally labile and polar substances must be derivatised prior to GC-MS analysis. Identification and chemical profiling of MDMA in ecstasy tablets was undertaken using GC-MS. Based on the chemical profiles, and regardless of their different physical characteristics, tablets obtained in different seizures could be determined as to whether or not they could have come from a common source. The impurities detected in the MDMA tablets also served as excellent chemical markers from which plausible synthetic route of the MDMA tablets were inferred. ^[27, 28] Also, a gas chromatographic procedure with mass spectrometric detection (GC-MS) was

established to detect amphetamines, MDMA, MDEA and MDA, cocaine and pharmacologically active impurities in ecstasy tablets.^[29] In addition, several drugs of abuse were detected in contaminated USA paper currency and Euro banknotes using GC-MS analysis.^[30, 31]

The GC column can be connected to a Fourier-transform infrared spectrometer (GC-FTIR). The separated molecules elute to the flow cell of the IR detector. In the flow cell the molecules are bathed with infrared radiation. The absorption spectrum is a fingerprint of the molecule.^[32, 33] GC-FTIR has been successfully applied to the detection of amphetamines.^[34]

3.1.3.1.2 High Performance Liquid Chromatography^[35]

HPLC is based on selective partitioning of the molecules of interest between two different phases. Here, the mobile phase is a solvent or solvent mixture that flows under high pressure over beads coated with the solid stationary phase. While travelling through the column, molecules in the sample partition selectively between the mobile and the stationary phases. Those molecules that interact with the stationary phase will lag behind those that partition preferentially with the mobile phase. As a result, the sample introduced at the front of the column will emerge in separate bands (called peaks), with the bands emerging first being the components that interacted least with the stationary phase and as a result moved quicker through the column. The components that emerge last will be the ones that interacted most with the stationary phase and thus moved the slowest through the column. A detector is placed at the end of the column to identify the components of the sample that elute. HPLC is especially useful for compounds that are thermally labile. HPLC has some advantages over GC because of the variety and combinations of mobile phases that can be selected. Many different types of detectors are available for HPLC such as the refractive index

detector (RI), UV/VIS detectors, fluorescence detectors and mass spectrometer detector (HPLC-MS). MDMA concentration was analyzed in ecstasy tablets using HPLC.^[36] Although the tablet weights were uniform, MDMA concentration showed a remarkable variability, indicating poor manufacturing control thus imposing additional health risks to the users. Also, four methylenedioxyated amphetamines were quantified in tablets from illicit drug seizures.^[37] Quantitative determination of cocaine hydrochloride^[38] and comparison of illegal cocaine samples using HPLC were reported.^[39] In addition, the technique was successfully applied for the identification of heroin^[40], cannabinoids^[41], and benzodiazepines.^[42]

3.1.3.1.3 Liquid Chromatography-Mass spectrometry (LC-MS)^[43]

Liquid chromatography-mass spectrometry is an analytical technique that combines the physical separation capabilities of liquid chromatography (or HPLC) with the mass analysis capabilities of mass spectrometry. The primary advantage HPLC/MS has over GC/MS is that it is capable of analysing a much wider range of components. Compounds that are thermally labile, exhibit high polarity or have a high molecular mass may all be analysed using HPLC/MS, even proteins may be routinely analysed. Components eluting from the chromatographic column are introduced to the mass spectrometer via a specialised interface. The two most commonly used interfaces for HPLC/MS are the electrospray ionisation and the atmospheric pressure chemical ionisation interfaces. LC-MS was applied for the detection of drugs of abuse, namely amphetamine, cocaine and heroin, in seized drug samples,^[44] in air^[45], in pharmaceutical products^[46] and on Euro banknotes.^[47]

3.1.3.1.4 HPLC-FTIR^[48]

This technique comprises the interfacing between HPLC and FT-IR spectrometer. The interface can be achieved in two ways:

a - Flow-cell LC–FT-IR: Coupling of LC and FT-IR is achieved by letting the column effluent pass directly through a flow cell with IR-transparent windows.

b - Solvent-elimination: LC–FT-IR: An interface is used which effects the evaporation of the eluent and deposition of the analytes on a substrate suitable for IR detection.

3.1.3.2 Mass Spectrometry ^[26, 29, 49]

Mass spectral analyses involve the formation of gaseous ions from an analyte (M) and subsequent measurement of the mass-to-charge ratio (m/z) of these ions. The commonly used ionization methods include Electron Ionization (EI), Chemical Ionization (CI), Secondary Ion Mass Spectrometry (SIMS), Thermospray (TSP), and Electrospray Ionization (ESI). Depending on the ionization method used, the sample is converted to molecular ions and their fragments. The mass spectrometer separates the ions generated upon ionization according to their mass-to-charge ratio to give a graph of ion abundance vs. m/z . Mixtures are often pre-separated by gas or liquid chromatography, so that a mass spectrum can be obtained for each individual component to thereby facilitate sample characterization. The exact m/z value of the molecular ion reveals the ion's elemental composition and, thus, allows for the compositional analysis of the sample. If the molecular ions are unstable and decompose completely, the resulting fragmentation patterns can be used as a fingerprint for the identification of the sample. Fragment ions also provide important information about the primary structure of the sample molecules. Tandem mass spectrometry (MS/MS) is very useful in structural determinations and can be visualized as multiple mass spectrometers placed in tandem. This technique performs gas-phase purification of a specified m/z value using the first mass spectrometer. This is achieved by allowing only the ion of interest to be transmitted while simultaneously

discriminating against (rejecting) all other ions. The transmitted ion is then fragmented to yield product or fragment ions from the precursor species. These ions can then be rationalized to a structure. Mass spectrometric methods have experienced a steadily increasing use due to their high sensitivity (<10⁻¹⁵ mol suffice for analysis), selectivity (minor components can be analyzed within a mixture), specificity (exact mass and fragmentation patterns serve as particularly specific compositional characteristics), and speed (data acquisition possible within seconds). Several studies have appeared in the literature addressing the application of mass spectrometry to the detection and the identification of drugs of abuse. It has been applied for the screening of solid dosage forms of drugs of abuse ^[50], and the detection of drugs and their metabolites in dusted latent fingerprints.^[51] Also, ion trap mass spectrometry was applied for the examination of complex mixtures containing drugs of abuse ^[52] and street market confiscated drugs were analysed using electrospray ionization mass spectrometry. ^[53] Moreover, desorption electrospray ionization (DESI)-mass spectrometry was applied to the analysis of mixtures of explosives and drugs from a variety of fabrics, including cotton, silk, denim, polyester, rayon, spandex, leather and their blends. ^[54]

3.1.3.3 X-ray powder diffraction ^[55]

X-ray diffraction is a common technique for the study of crystal structures and atomic spacing. The three-dimensional structure of crystalline materials is defined by regular, repeating planes of atoms that form a crystal lattice. X-ray diffraction is based on constructive interference of monochromatic X-rays and a crystalline sample. These X-rays are generated by a cathode ray tube, filtered to produce monochromatic radiation, collimated to concentrate, and directed toward the sample. The interaction of the

incident rays with the sample to be analyzed produces constructive interference (and a diffracted ray) when conditions satisfy Bragg's Law ($n\lambda=2d \sin \theta$). This Law relates the wavelength of electromagnetic radiation to the diffraction angle and the lattice spacing in a crystalline sample. By scanning the sample through a range of 2θ angles, all possible diffraction directions of the lattice should be attained due to the random orientation of the powdered material. Measuring the diffraction pattern therefore allows deducing the distribution of atoms in a material. Typically, this is achieved by the comparison of d -spacings with standard reference patterns. The main advantages of X-ray diffraction methods in forensic science are the unique character of the diffraction patterns of crystalline substances, the ability of the technique to distinguish between elements and their oxides, and to identify chemical compounds, polymorphic forms, and mixed crystals by a non-destructive examination.

XRD is usually employed to identify the chemical form of the drug (salt, base or acid), to identify any diluents or adulterants present in the sample, and to compare one seizure with another. X-ray diffraction has been applied for the detection of heroin^[56] and illicit drugs in parcels.^[57] It also was applied to analyze various trace elements in small amounts of drugs of abuse.^[58, 59] Several elements such as iodine, phosphorus, calcium, sulfur, and potassium were found as contaminants in the seized samples.

3.1.3.4 Spectroscopy^[14]

Confirmation of the identity of the drug often requires the use of at least one spectroscopic technique. The spectra obtained are 'fingerprints' unique to each chemical compound and provide confirmatory information for unequivocal identification of most drugs of abuse. Usually the acquired spectra of the unknown are compared visually with reference spectra by an experienced analyst or tentatively

identified by a computerized library search. The combination of the separation capability of chromatography with the identification capabilities of the spectroscopic techniques is clearly therefore advantageous, particularly as many compounds with similar or identical retention characteristics have quite different spectra and can therefore be differentiated. This extra specificity allows quantitation to be carried out which, with chromatography alone, would not be possible. A variety of spectroscopic techniques can be found in many forensic laboratories including NMR spectroscopy, IR spectroscopy, and Raman spectroscopy.

3.1.3.4.1 NMR Spectroscopy ^[60]

NMR is based on the absorption of energy in the radiofrequency region of electromagnetic spectrum by the nuclei of atoms. NMR spectra arise from a property that some nuclei have, usually called spin. Spinning of charged nuclei generates a magnetic field. When a sample is subjected to an external magnetic field, the nuclei align themselves with or against the applied magnetic field. Protons that align with the applied field are in the lower-energy α -spin state and protons that align against the field are in the higher-energy β -spin state. When the sample is subjected to radiofrequency radiation (rf radiation) whose energy corresponds to the difference in energy between the α - and β -spin states, the α - and β -spin states are made to interconvert i.e. flipping the spin. This flipping of the proton from one magnetic alignment to the other by the radio waves is known as the resonance condition. When the nuclei relax to their original states, they emit electromagnetic signals with frequencies that depend on the difference in energy between the α - and β -spin states. Since NMR experiment started with excess of nuclei in the α -spin states, there is a net absorption of energy which is displayed as a plot of frequency versus amount of absorbed energy. Nuclei in different parts of the molecule experience different local

magnetic fields according to the molecular structure, and so they absorb the rf radiation at different frequencies. This difference is called the chemical shift. NMR has been applied to distinguish between drugs that have effects similar to narcotics and stimulants.^[61] NMR in conjunction with MS and IR has been used for the identification and detection of contaminants in synthesized amphetamines ^[62] and for the characterization of derivatives of MDMA. ^[63] It also has been applied for the detection of aminorex material in confiscated drug samples. ^[64]

3.1.3.4.2 UV/Visible Spectroscopy ^[65]

Ultraviolet-visible spectroscopy (UV=200-400nm, VIS = 400-780 nm) corresponds to electronic excitations between the energy levels that correspond to the molecular orbitals of the systems. In particular, electronic transitions involving p orbitals and lone pairs (n = non-bonding) are important and so UV-VIS spectroscopy is of most use for identifying conjugated systems which tend to have stronger absorptions. The lowest energy transition is that between the highest occupied molecular orbital (HOMO) and the lowest unoccupied molecular orbital (LUMO) in the ground state. The absorption of the electromagnetic radiation excites an electron to the LUMO and creates an excited state (Figure 3.2). The more highly conjugated the system, the smaller the HOMO-LUMO gap, and therefore the lower the frequency and longer the wavelength. The part of the molecule which is responsible for the absorption is called

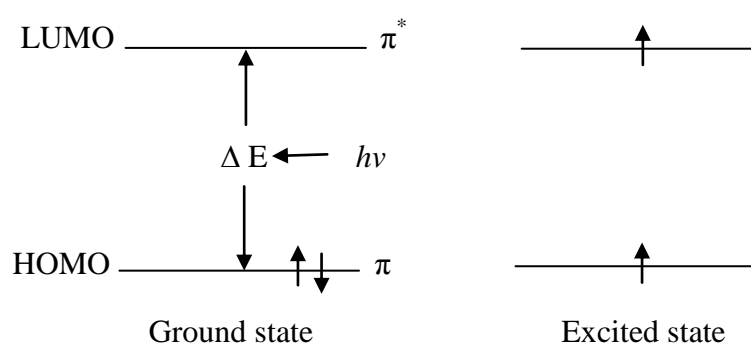


Figure 3.2 Excitation of electrons between molecular orbitals [adapted from reference 65]

the chromophore, of which the most common are C=C (π to π^*) and C=O (n to π^*) system. The UV/VIS spectrum represents the absorption of light as a plot of wavelength (λ), in nanometer, of the absorbed radiation versus the intensity of the absorption. Identification of amphetamine and related illicit drugs by 2nd derivative ultraviolet spectrometry has been reported. [66] Also, amphetamines have been detected using high-performance liquid-chromatography with ultraviolet detection [67] and capillary zone electrophoresis with ultraviolet detection has been used for the enantiomeric separation of methamphetamine and related analogs in methamphetamine seizures. [68]

3.1.3.4.3 Infrared Spectroscopy [69, 70]

Infrared spectroscopy is considered one of the most important analytical techniques available to scientists. One of the great advantages of IR-spectroscopy is that virtually any sample in almost any state may be studied. Liquids, solutions, pastes, powders, films, fibres, gases and surfaces can all be examined with a sensible choice of a sampling technique. Infrared spectroscopy is a technique that probes the vibrations of the atoms of a molecule. The infrared region of the electromagnetic spectrum extends from 14,000 to 10 cm^{-1} and the region of most interest for chemical analysis is the mid-infrared region (4,000 cm^{-1} to 400 cm^{-1}) which corresponds to changes in vibrational energies within molecules. Not all possible vibrations within a molecule will result in an absorption peak in the infrared region. To be infrared active the vibration must result in a change of dipole moment during the vibration. This is the selection rule for infrared spectroscopy. This means that for homonuclear diatomic molecules such as hydrogen (H_2), nitrogen (N_2) and oxygen (O_2) no infrared absorption is observed, as these molecules have zero dipole moment and stretching of the bonds will not produce one. For heteronuclear diatomic molecules such as carbon

monoxide (CO) and hydrogen chloride (HCl), which possess a permanent dipole moment, infrared activity occurs because stretching of this bond leads to a change in dipole moment. An infrared spectrum is obtained by passing infrared radiation through a sample and determining what fraction of the incident radiation is absorbed at a particular energy. The energy at which any peak in an absorption spectrum appears corresponds to the frequency of a vibration of a part of the molecule. Tape-lifted model particles of drugs of abuse were analysed using Fourier transform infrared spectroscopy^[71] and several drugs of abuse were analysed by GC/IR/MS.^[72]

3.1.3.4.4 Terahertz Spectroscopy

Terahertz radiation has been demonstrated to be an effective probe for inter and intramolecular vibrational modes of crystalline materials yielding unique molecularly specific spectra. Broadband terahertz time-domain spectroscopy has been applied for the analysis of several drugs of abuse concealed in envelopes.^[73] Principal component analysis was employed to cluster terahertz spectra of a wide range of samples of drugs of abuse containing cocaine hydrochloride, ecstasy and heroin.^[74]

3.2 Forensic Analysis of Explosives

The detection of explosives has become a subject of major interest in recent years. Incidents involving the explosion of airplanes, terrorist attacks on buildings, and suicide bombers attacking crowds of people or busses, have been making headlines with far more regularity than anyone but the terrorists would like. Detection of explosives is of significant importance in several applications such as finding hidden explosives in airport luggage, screening of personnel for explosives and environmental monitoring of explosives-contaminated sites.^[75]

Detection of explosives is based on a wide variety of technologies that focus on either

bulk explosives or traces of explosives. Bulk explosives can be detected directly by detecting the chemical composition of the explosive material or indirectly by imaging characteristic shapes of the explosive charge, detonators, and wires. Trace detection relies on vapours emitted from the explosive or on explosive particles that are deposited on nearby surfaces. Explosive detection is not an easy task, and combinations of the various techniques offer increased sensitivity and selectivity. ^[21]

3.2.1 Bulk Detection Methods

Bulk detection methods are suitable for the detection of explosives with low vapour pressure and inspection of sealed containers. The general technique is to direct a form of radiation at the object under investigation, detect the resulting radiation emanating from the object and determine whether that received signal carries the signature of an explosive. The most common example of these techniques is the basic X-ray inspection system seen at most airport security check points.

3.2.1.1 X-ray techniques

X-rays have been used for many years to search for explosives and other contraband in luggage and cargo containers. Since X-ray radiation is ionizing, there are health concerns when people are exposed to it. There are several X-ray techniques which include:

a- Transmission X-ray imaging: These systems require a detector on the opposite side of the target i.e. a bag from the transmitter. Transmission systems give good resolution images and detect shapes of objects shadowed as a result of their high X-ray absorption. ^[20,76-78]

b- Dual energy systems

The basic principle of DXA data acquisition is based on the differences between

an object attenuation at high and low x-ray levels. As the x-ray beam passes through the object, detectors measure the level of x-ray radiation that is absorbed by it. An algorithm is used which interprets each pixel, and creates an image for the item under investigation. This procedure yields precise, high quality images at very low doses of radiation. ^[79, 80]

c- Computed tomography (CT): ^[81, 82]

Computed tomography, widely used in the medical field, has been adapted to explosives detection. X-ray transmission information is collected at multiple angles around the item being inspected within a particular plane (usually perpendicular to the plane of the conveyor belt and the direction of the belt motion). This information is then used for producing 2-D and 3-D cross-sectional images of an object from flat X-ray images. The image represents the X-ray attenuation of the objects in the collection plane. Characteristics of the internal structure of an analyzed object such as dimensions and shape are readily available from CT images.

3.2.1.2 Neutron and gamma ray techniques ^[19,21]

These techniques are based on the excitation of elements by neutrons which in turn produce secondary gamma rays that are characteristic of the object elemental composition. Neutrons are uncharged particles, so when they irradiate materials they interact by way of nuclear interactions with the neutrons and protons in the nucleus of the atoms of the target material. Neutrons have a greater penetration range and because of this ability to penetrate deep into dense materials, neutron interrogation has been proposed for explosive detection in small items, such as passenger bags, as well as for large cargo containers. When neutrons interact with materials, they are sensitive to the structure of the nucleus. Thus, neutrons probe not only to the elemental content

of the target material, but also the isotopic mixture.

a- Thermal neutron activation (TNA): Thermal neutrons can be captured by ^{14}N nuclei and result in γ -rays of a specific energy. The distribution and level of γ -rays at this energy can in principle be used to detect nitrogen-rich explosives. [83]

b - Pulsed fast neutron analysis (PFNA): Fast neutrons are used to bombard the target. The induced gamma rays are measured to detect the explosives. The system is based on 3-D images of elemental ratios of O, N, and C. [84]

c - γ -Ray nuclear resonance absorption (NRA): An accelerator generates γ -rays to penetrate the screened item. The γ -rays are preferentially absorbed by nitrogen nuclei. A significant decrease in the number of detected γ -rays indicates the possible presence of explosives. [85]

The major disadvantage of these techniques is the health hazards issues which may limit their use for the detection of explosives.

3.2.1.3 Nuclear quadrupole resonance (NQR) [86, 87]

A low intensity radio frequency pulse (0.5-6 MHz) is applied to the screened object. ^{14}N nuclei orient themselves to the electromagnetic field. When the electromagnetic field is removed, the nuclei relax emitting a unique radio signal. NQR provides a chemical specificity as the signal is related to the particular molecular configuration of the nuclei possessing the quadrupole moment. The NQR detection is restricted to crystalline solids; amorphous materials, and liquids are not detected.

3.2.1.4 Terahertz spectroscopy [88-90]

Terahertz spectroscopy is a spectroscopic technique that uses the terahertz frequency radiation (100-10 GHz i.e. between infrared and microwave frequency) of the electromagnetic spectrum for the investigation and structure elucidation of materials. Terahertz radiation can penetrate clothing, bags and packaging material and because

its radiation is safe, it can be used for screening people. Since each explosive has a unique terahertz absorption spectrum, it can be used to differentiate between various explosives.

3.2.2 Trace Detection Methods

Trace analysis of explosives is of major importance in forensic and environmental applications. In forensics, the applications include analysis of post-explosion residues and identification of traces of explosives on suspects' hands, clothing and other related items. In the environmental field, the applications include analysis of explosives and their degradation products in soil and water. These analyses are important because of the toxicity of most explosives and the fact that many areas in the vicinity of explosives and munitions manufacturing plants are contaminated.^[91]

Trace detection methods measure traces of characteristic volatile compounds that evaporate from the explosives or particulate matter present on the outside of the explosive container or other surfaces. Vapour samples are collected from the target area or object by drawing ambient air into the detector. Trace detection is a particularly challenging task as saturated vapour pressures for many of the common explosives are very low. Particulate samples are collected by wiping surfaces with a paper filter trap or with hand-held vacuum, followed by desorption into the detector.^[75, 92] In addition, chemical preconcentrators have been developed to increase the sensitivity of the detection. Most preconcentrators are mainly based on drawing in a large volume of air, which includes the explosives, from the air stream onto a chemical filter, followed by vaporising these explosives into the detector.

3.2.2.1 Ion Mobility Spectrometry (IMS) ^[93, 94]

A sample, gaseous or in solution, is introduced into an ionization region such as

atmospheric pressure chemical ionization (APCI), photo-ionization, and electrospray ionization. Analyte ions are accelerated by an electric field down a drift region against a flow of drift gas. This results in separation of the analyte ions according to ion mobility, which depends on mass, charge, size, and shape. The drift time depends on the ionic mass; heavier ions move at a slower speed and therefore have a longer drift time. Under the influence of this electric field, ions move toward the detector, nominally a Faraday plate, and create a signal (i.e. current flow) at the detector. The ion mobility spectrum consists of a plot of ion current as a function of drift time. Ion mobility spectrometers have advantages in terms of simplicity, small size, and short response time. Because of these criteria, ion mobility spectrometry has become the most widely used technology for the detection of trace levels of explosives on handbags and carry on-luggage in airports. Post-blast residues from nitroglycerin, C-4, DETA Sheet, SEMTEX, and ammonium nitrate explosives have also been detected on items of forensic and evidentiary value. ^[95]

3.2.2.2 Mass Spectrometric techniques

Mass spectrometry has become a routine technique for forensic analysis of explosives and one of the technologies used for vapour and trace detection of hidden explosives. Mass spectrometry is recognized for its superior performance with regard to sensitivity and specificity. Mass spectrometry is more informative than Ion Mobility Spectrometry in terms of identifying organic compounds in trace amounts. ^[96] Several ionization methods including electrospray ionization (ESI) ^[97] and atmospheric pressure chemical ionization (APCI) ^[98] have been used, depending on the type of explosives. The thermal lability of many explosives, with the requirements of high sensitivity, makes LC/MS a method of choice for the analysis of explosives. ^[99] Also, a study comparing detection limits for GC/MS analysis of organic explosives has been

reported. ^[100] Moreover, Tandem mass spectrometry has been used in mass spectrometric explosives detection in order to increase selectivity.^[101] Tandem mass spectrometry (MS/MS) allows inducing fragmentation and mass analyzing the fragment ions. This is accomplished by generating fragments from a selected ion and then mass analyzing the fragment ions. ^[75, 102]

3.2.2.3 Canines ^[103]

Canines have highly sensitive olfactory system and dogs have been trained to sniff explosives. Dogs are mobile and can clear a large space such as an auditorium or inspect a building floor by floor to ensure the absence of explosives. However, this method suffers from several disadvantages such as the high cost, the decrease of performance over time, behavioural variations and the need for an assigned handler for best performance.

3.2.2.4 Electronic noses (Microsensors) ^[104]

Electronic noses are handheld and mobile devices, called electronic or artificial noses, which mimic bomb-sniffing dogs without having their drawbacks. An electronic nose is usually composed of a chemical sensing system and a pattern-recognition system. Each vapour presented to the sensing system produces a signature or “fingerprint”. Presenting many different chemicals to the sensor yields a database of fingerprints, which the pattern-recognition system uses to recognize and automatically identify each chemical. Fluorescent polymer sensors are used as chemical detectors. These materials fluoresce intensely in the presence of ultraviolet light when no nitroaromatic explosive compounds are present, but are prevented from fluorescing when those compounds are introduced. Upon encountering a nitroaromatic molecule, the tailored fluorescing polymer binds with it. If the air sample contains explosive vapour, the photomultiplier detector will sense a decrease in light intensity triggering an alarm.

Chapter 4

Principles, Theory and Instrumentation of Raman Spectroscopy

4.1 Vibrational spectroscopy ^[105]

Infrared and Raman spectroscopy are complementary techniques that are used for structural elucidation of materials. They provide information on the chemical structures and physical characteristics of materials; they are used for the identification of substances by ‘fingerprinting’. Also, they are used for quantitative or semi-quantitative analysis. These spectroscopic techniques are based on the vibrations of the atoms of a molecule. An infrared spectrum is commonly obtained by passing infrared radiation through a sample and determining what fraction of the incident radiation is absorbed at a particular energy. The energy at which any peak in an absorption spectrum appears corresponds to the frequency of a vibration of a part of a sample molecule. Raman spectroscopy is based on the Raman Effect, which is the inelastic scattering of photons by the sample molecules. One of the great advantages of vibrational spectroscopy is that virtually any sample in any physical state may be studied. Liquids, solutions, powders, films, fibres, gases and surfaces can all be examined with a choice of a suitable sampling technique.

4.1.1 Molecular vibrations ^[106]

IR and Raman spectra results from transitions between quantized vibrational energy states. Molecular vibrations can range from the simple motion of the two atoms of a diatomic molecule to the more complex motion of every atom in a large polyatomic molecule. A mode of vibration in a molecule is a periodic contortion in which the centre of mass of the molecule or its orientation does not change as a result of the vibration and all of the atoms pass through their linear equilibrium position coincidentally. The position of a molecule in three dimensional space can be described

by using an x , y and z co-ordinate for each atom. This means that a molecule comprised of n atoms has $3n$ Cartesian co-ordinates required to describe its shape, position and orientation. The motion can be described by a change Δx , Δy and Δz in these Cartesian axes. There are $3n$ fundamental distinct molecular motions which are called degrees of freedom. Molecular motions consist of translations, rotations and vibrations. Three of the degrees of freedom are translations of the whole molecule along the x , y or z axis. A non-linear molecule also has three pure rotations about these axes while a linear molecule has only two. The translational and rotational degrees of freedom, which do not change the relative positions of the atoms in the molecule, are often called non-genuine modes. Thus, a non-linear molecule possesses $3n-6$ fundamental modes of vibration, whilst a linear molecule has $3n-5$. Of these, the number of stretching modes is equal to the number of bonds in the molecule ($n-1$ for an acyclic molecule) and the remainder of the vibrations are bending modes. During these normal modes of vibrations all the atoms move in phase and with the same frequency. Various atoms in a molecule may be regarded as balls of different masses and the covalent bonds between them as weightless tiny springs holding such balls together. There are two types of fundamental molecular vibrations (Figure 4.1):

1- Stretching vibrations: in stretching vibrations, the distance between two atoms increase or decrease, but the atoms remain in the same bond axis. Stretching vibrations are of two types:

a- Symmetrical stretching: in this mode of vibration, the movement of atoms with respect to the common (or central) atom is in the same direction along the same bond axis.

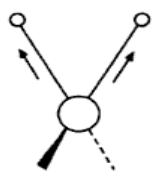
b- Asymmetrical stretching: in this vibrational mode, one atom approaches the common atom while the other departs away from it.

2- Bending Vibrations (Deformations): In such vibrations, the positions of the atoms change with respect to their original bond axes. Bending vibrations are of four types:

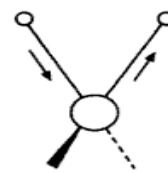
a - Scissoring: In this mode of vibration, the movement of atoms is in the opposite direction with change in their bond axes as well as in the bond angle they form with the central atom.

b - Rocking: in this vibration, the movement of atoms takes place in the same direction with change in their bond axes. Scissoring and rocking are in-plane bendings.

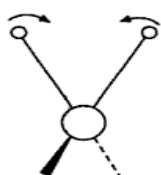
c - Wagging: in this vibration, two atoms simultaneously move above and below the plane with respect to the common atom.



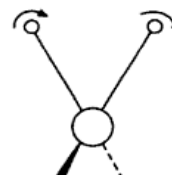
Symmetrical stretching



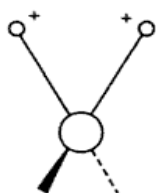
Asymmetrical stretching



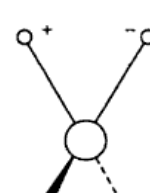
Scissoring



Rocking



Wagging



Twisting

Figure 4.1 Stretching and Bending vibrations (+ and – signs indicate movement perpendicular to the plane of the paper).

d - Twisting: in this vibration, one of the atom moves up and the other moves down the plane with respect to the common atom.

4.2 Theory of the Raman Effect ^[107,108]

The first experimental observation of the inelastic scattering of light was made by Raman and Krishnan in 1928. When a compound is irradiated with monochromatic radiation, the radiation is transmitted, absorbed or scattered by the molecule. Of the scattered radiation, a majority of the photons are scattered at the same frequency as the incident radiation frequency. This form of scattering has been termed elastic or Rayleigh scattering. Additionally, a very small proportion of the photons (about $1/10^6$) are scattered at frequencies arrayed above and below the frequency of the Rayleigh line. The differences between the incident frequency of radiation and shifted frequencies correspond to the frequency of the molecular vibrations present in the molecules of the sample. These wavelength-shifted frequencies are termed inelastic scattering, and a collection of these wavelength-shifted frequencies comprises the Raman spectrum.

4.2.1 The classical theory of the Raman Effect ^[109]

When the oscillating electric field of the incoming radiation interacts with the atoms of the molecule (Figure 4.2), the electron cloud of the molecule is distorted and induces an electric dipole moment. This induced polarization then radiates scattered light with or without exchanging energy with vibrations in the molecule. The strength of the induced polarization, P , is dependent upon the polarizability, α , and the incident electric field, E :

$$P = \alpha E \quad (1)$$

Polarizability can be regarded as the measure of the flexibility of the electron cloud i.e. the ease with which the electron cloud of the molecule can be deformed or

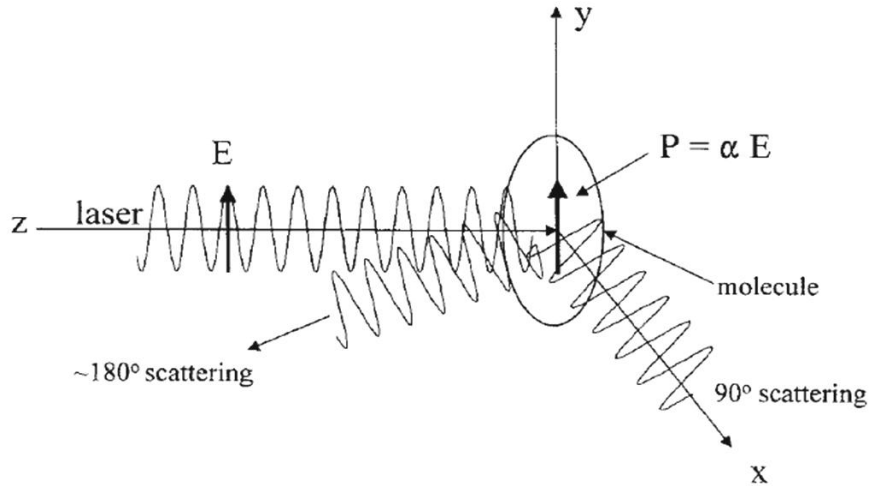


Figure 4.2 Scattering of light by an induced dipole moment due to an incident EM wave. Scattering may be in various directions, but 90° and -180° are shown [Adapted from reference 109]

displaced to produce an electric dipole under the influence of the external electric field. It is a material property that depends on the molecular structure and nature of the bonds. The classical treatment of Raman scattering is based on the effects of molecular vibrations on the polarizability (α). The amplitude of the incident electric field varies according to the following equation:

$$E = E_0 \cos 2 \pi \nu_0 t \quad (2)$$

Where E_0 is the maximum electric field strength, t is the time, ν_0 is the frequency of the laser light (Hz) [$\nu_0 = c / \lambda$].

Substituting Equation (2) into (1) yields the time-dependent induced dipole moment,

$$P = \alpha E_0 \cos (2 \pi \nu_0 t) \quad (3)$$

The vibrational energy of a particular mode is given by:

$$E_{vib} = (v + 1/2) h \nu_{vib} \quad (4)$$

where v is the vibrational quantum number ($v = 0, 1, 2, \dots$, etc), ν_{vib} is the frequency of the vibrational mode, and h is the Planck constant. The physical displacement dQ of

the atoms about their equilibrium position due to the particular vibrational mode may be expressed as:

$$dQ = Q_0 \cos (2 \pi \nu_{\text{vib}} t) \quad (5)$$

where Q_0 is the maximum displacement about the equilibrium position.

Based on the vibrational displacement of equation (5), the polarizability may be given as:

$$\alpha = \alpha_0 + (\alpha_0/\delta Q) Q_0 \cos (2 \pi \nu_{\text{vib}} t) \quad (6)$$

Substituting equation (6) into equation (3) yields equation (7):

$$P = \alpha_0 E_0 \cos (2 \pi \nu_0 t) + (\delta\alpha / \delta Q) Q_0 E_0 \cos (2 \pi \nu_0 t) \cos (2 \pi \nu_{\text{vib}} t) \quad (7)$$

After noting that $\cos a \cos b = [\cos (a + b) + \cos (a - b)] / 2$, equation (7) may be recast as:

$$P = \alpha_0 E_0 \cos (2 \pi \nu_0 t) + \frac{1}{2} (\delta\alpha / \delta Q) Q_0 E_0 \{ \cos [2 \pi (\nu_0 - \nu_{\text{vib}}) t] + \cos [2 \pi (\nu_0 + \nu_{\text{vib}}) t] \} \quad (8)$$

Equation (8) reveals that the induced dipole moment is created at three distinct frequencies, namely ν_0 , $(\nu_0 - \nu_{\text{vib}})$, and $(\nu_0 + \nu_{\text{vib}})$, which results in scattered radiation at these same three frequencies. The first scattered frequency corresponds to the incident frequency, hence it is an elastic scattering (Rayleigh), while the latter two frequencies are shifted to lower or higher frequencies and are therefore inelastic processes. The scattered light in these latter two cases is referred to as Raman scattering, with the down-shifted frequency (longer wavelength) referred to as Stokes scattering, and the up-shifted frequency (shorter wavelength) referred to as anti-Stokes scattering. Also, several conclusions can be made from equation (8). First, the necessary condition for Raman scattering is that the term $\delta\alpha / \delta Q$ must be non-zero. This condition may be physically explained to mean that the vibrational displacement of atoms corresponding to a particular vibrational mode results in a change in the polarizability. This statement is the basis of the primary selection rule for Raman scattering. For example, the polarizability of the C=C bond changes significantly with a vibration associated with the stretch of the C=C bond. So the Raman scattering from a C=C bond is strong,

while that of a C=O bond is relatively weak. In contrast, infrared absorption requires a dipole moment change for a given vibration to be IR active, so the C=C vibration is very weak toward IR absorption and the C=O stretch is strong. Secondly, $\delta\alpha / \delta Q$ may vary significantly for different molecules and for different modes in a given molecule, leading to wide variations in Raman scattering intensity. Thirdly, $\delta\alpha / \delta Q$ is much smaller than α_0 and Raman scattering is therefore much weaker than Rayleigh scattering.

4.2.2 The Quantum theory of Raman scattering ^[70, 110]

According to the principles of quantum mechanics, the energy associated with electronic, vibrational and rotational degrees of freedom of a molecule can assume values only from a discrete set, namely the quantized energy levels corresponding to the possible stationary states of the molecule. These states are characterized by a specific set of quantum numbers describing the level of excitation of each quantized motional degree of freedom. Radiation is absorbed or emitted by the molecule as the result of an upward or downward transition between two energy levels. The radiation absorbed or emitted by the molecule is also quantized, with energy enclosed in discrete photons that can alternatively be viewed as electromagnetic waves. The loss or gain of energy by the molecular system, ΔE , is equivalent to the emitted or absorbed energy of electromagnetic radiation (Figure 4.3). This energy is directly proportional to the frequency or wavenumber of radiation:

$$\Delta E = h\nu = hc\tilde{\nu} \quad (9)$$

Where h is the Planck constant, c is the speed of light, ν is the frequency, and $\tilde{\nu}$ is the wavenumber of the radiation. The relationships between these are given below:

$$\lambda = c / \nu \quad (10)$$

$$\tilde{\nu} = \nu / c = 1 / \lambda \quad (11)$$

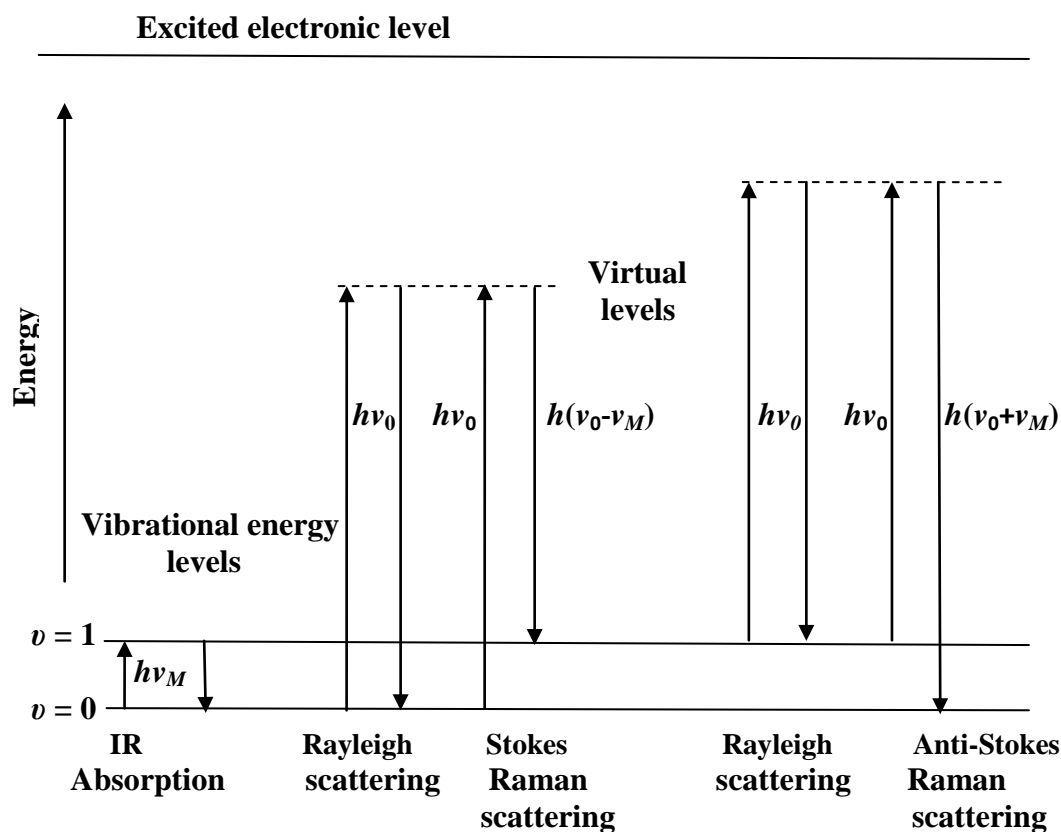


Figure 4.3 Diagram of transitions between vibrational energy levels corresponding to the processes of IR absorption/emission, and Rayleigh and Raman scattering [Adapted from reference 70].

In infrared absorption or emission, there is a direct transition between two vibrational energy levels, most often between the vibrational ground state ($v = 0$) and the first excited state ($v = 1$). These transitions are simple one-photon processes; one photon is absorbed or emitted during the transition. In contrast, Rayleigh and Raman scattering involve two almost simultaneous transitions processing via virtual states in which one photon of the incident radiation is annihilated and another photon, either of the same energy (Rayleigh scattering) or of lower energy (Stokes Raman) or higher energy (anti-stokes Raman) is created (Figure 4.4). The virtual excited state will be extremely short-lived and the energy of the incident photon will be quickly re-radiated. Molecules in the ground state give rise to Stokes Raman scattering at frequencies

$\nu_0 - \nu_M$; where ν_M is the frequency of molecular vibration, given that a change in polarizability occurs during the vibration. If the molecule happens to be in an excited vibrational state when an incident photon is irradiated, the photon may gain energy when scattered giving rise to anti-Stokes Raman scattering at frequencies $\nu_0 + \nu_M$. The differences between the incident frequency of radiation and inelastic scattered frequencies correspond to the frequencies of molecular vibrations. Rayleigh scattering is the most intense form of scattering while Raman scattering is a much rarer event which involves only one in 10^6 of the photons scattered. At room temperature, most molecules are likely to be in the ground vibrational state. Therefore the most intense Raman scattering is normally Stokes Raman scattering. The ratio of the intensities of the Stokes and anti-Stokes scattering is dependent on the number of molecules in the ground and excited vibrational levels. This ratio can be calculated from the Boltzmann distribution equation as follows:

$$\frac{N_n}{N_m} = \frac{g_n}{g_m} \exp \left[\frac{-(E_n - E_m)}{kT} \right] \quad (12)$$

N_n refers to the number of molecules in the excited vibrational energy level (n),

N_m refers to the number of molecules in the ground vibrational energy level (m),

g is the degeneracy of the levels n and m ,

$E_n - E_m$ is the difference in energy between the vibrational energy levels,

k is Boltzmann's constant.

T is the temperature

Some vibrations can occur in more than one way but with the same energy, so that the individual components cannot be separately identified; the number of these components is called the degeneracy (g), i.e. the number of different vibrational states

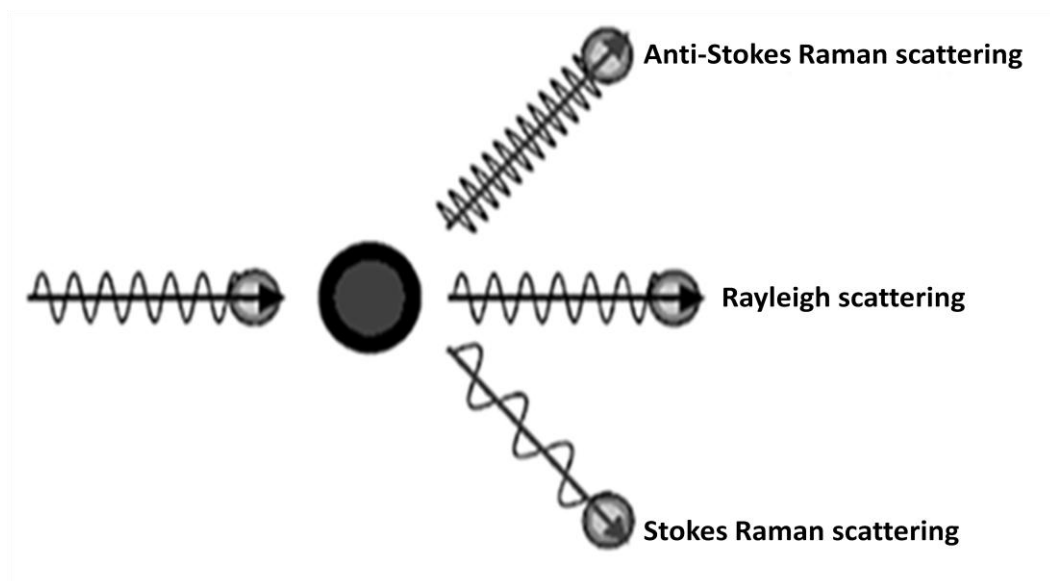


Figure 4.4 Rayleigh and Raman scattering [Adapted from reference 110]

at a particular energy level. For non-degenerate states, g will equal 1 but for degenerate vibrations it can equal 2 or 3. A Raman spectrum is normally represented as a plot of Raman scattering intensity (ordinate) versus wavelength (abscissa). Normally, the abscissa of the spectrum is labelled as the wavenumber shift or Raman shift (cm^{-1}). This is because the energy increase (anti-Stokes) or decrease (Stokes) from the excitation is related to the vibrational energy spacing in the ground electronic state of the molecule and therefore the wavenumbers of the Stokes and anti-Stokes lines are a direct measure of the vibrational energies of the molecule.

4.2.3 Fluorescence emission ^[108]

Fluorescence is caused by the emission of a photon from the lowest vibrational level of an excited electronic state, following a direct absorption of the photon and relaxation of the molecule from its vibrationally excited level of the electronic state back to the lowest vibrational level of the electronic state (Figure 4.5). A fluorescence process typically requires more than 10^{-9} s while a Raman transition is completed within a picosecond or less. Laser-induced fluorescence is the most common source of

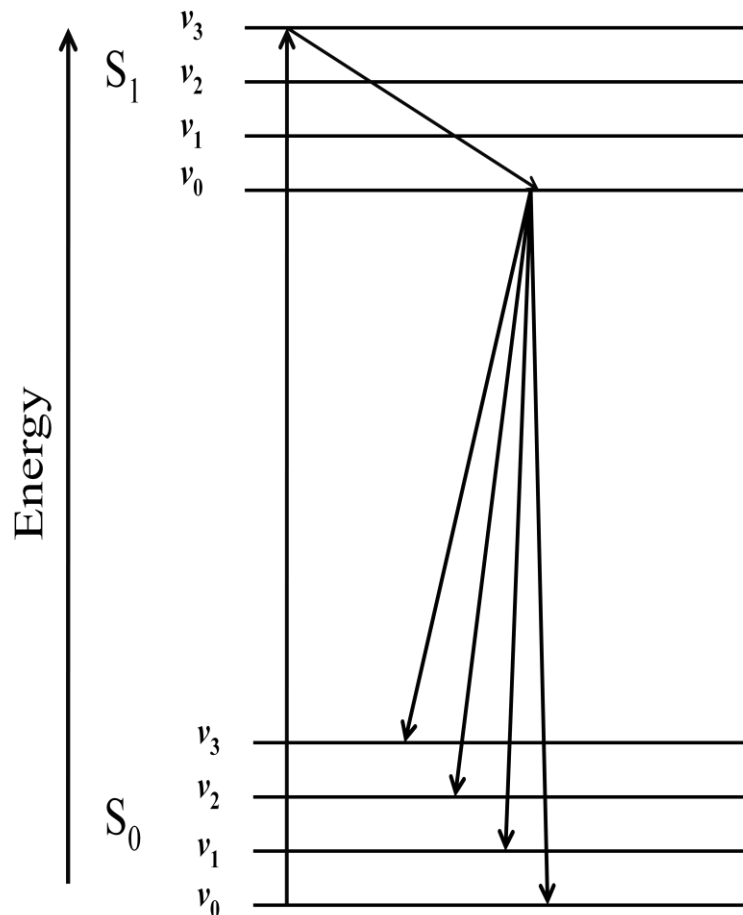


Figure 4.5 Energy level diagram showing fluorescence emission [Adapted from reference 108]

background emission encountered in Raman spectroscopy. Fluorescence spectral features are much broader than Raman bands, and often appear as a slowly changing baseline in a Raman spectrum. When the sample molecules are excited into the first excited electronic singlet state by the absorption of the incident photon, the molecules rapidly relax to the lowest vibrational level of the first excited singlet state. After a period of time (1-10 nanoseconds) the molecules relax back to the ground electronic state by emitting a photon of fluorescence. So the fluorescence photon is lower in energy than the exciting photon. Therefore, the frequency of fluorescence emission may coincide with that of the Stokes Raman radiation. Because fluorescence emission

has a much higher quantum yield than Raman scattering (often of the order of 10^6), so trace levels of fluorescent impurities can lead to the Raman signal being overwhelmed by the fluorescence background. The fluorescence emission is insensitive to the process of creation of the excited singlet state. Therefore, fluorescence can be distinguished from Raman scattering by its invariance in emission wavelength with changing excitation wavelength.

4.2.3.1 Fluorescence quenching methods

There are a number of techniques which have been applied to overcome the problem of fluorescence emission including:

a- The use of near-infrared radiation ^[111]

Because the energy of near infrared radiation is lower than that of the electronic transitions from the ground state in the majority of molecules, therefore the excited state is not populated. Two types of NIR lasers can be used to measure Raman spectra. The first is the diode laser, with the most popular emitting at 785 or 830 nm. Raman spectra generated with NIR diode lasers can be measured using silicon charge-coupled device (CCD) array detectors, which cut off at about 9500 cm^{-1} , limiting the Raman spectral shift to about 3200 cm^{-1} . The other popular NIR laser is the Nd: YAG laser, which emits at 1064 nm; with this excitation source, the fluorescence problem is diminished. CCD detectors lack sensitivity above 1000 nm. Also, the Raman scattering is inherently weaker because the energy of radiation is lower and the intensity of the Raman signal is proportional to $(\nu_0 - \nu_{\text{vib}})^4$. To overcome these problems, Fourier-transform techniques have been invoked for the measurement of weak Raman signals at such long wavelengths.

b- Ultraviolet excitation ^[112]

The absolute frequency of Raman bands varies according to the excitation wavelength

used, whereas fluorescence emission occurs at a constant wavelength which depends on the difference in energy between two electronic states of the molecule. This provides spectral separation of Raman and fluorescence emission bands resulting in high signal-to-noise measurements and low detection limits. In addition, when Raman excitation occurs within an electronic resonance (absorption) band of a material, the scattering cross-section can be improved as much as 10^8 . The resulting Raman spectra are rather different from normal Raman spectra because resonance enhancement occurs only for particular vibrations of the chromophore. Hence, the technique can be used to pick out and identify a molecule in a matrix. However, many compounds absorb UV radiation which means that there is a high risk of sample degradation due to the high energy of the photons in this region.

c- Surface-Enhanced Raman spectroscopy (SERS) ^[113]

Surface Enhanced Raman Spectroscopy is a Raman spectroscopic technique that provides a greatly enhanced Raman signal from Raman-active analyte molecules that have been adsorbed onto certain specially prepared metal surfaces. Increases in the intensity of Raman signal have been observed to the order of 10^4 - 10^6 . The SERS spectra obtained provide highly specific and quantitative information, and are virtually background-free.

d- Photobleaching ^[114]

Photo-bleaching involves irradiating the sample of interest with intense light for a period of time. The laser light source for the photo-bleaching often induces photolytic decomposition, breaking down the fluorescent molecules and reducing the fluorescent background. In many cases the molecule causing the fluorescence is an impurity in the sample. Photo-bleaching modifies the sample by effectively removing the low level contaminant and leaving the species of interest unchanged.

4.2.4 Raman cross section ^[109]

The Raman efficiency of a scatterer is usually characterized by its cross section, σ_j , which depends on $\delta\alpha/\delta Q$. Raman cross section is proportional to the probability of an incident photon being scattered as a Raman-shifted photon with a particular Raman shift and measured in $\text{cm}^2/\text{molecule}$. Although the Raman intensity depends on various experimental parameters such as collection geometry, polarization and wavelength of the incident light, the cross-sections tend to be the major indicator of the intensity of Raman scattering as these parameters are invariant and are determined by the instrument for analytical applications. For a classical treatment, Raman scattering I_R (in watts) can be related to the cross section, with the laser intensity (I_0) in watts,

$$I_R = I_0 \sigma_j D dz \quad (13)$$

Where σ_j refers to the cross section at the wavenumber j , D is the number density of scattering species (molecules per cubic centimetre) and dz is the path length of the laser in the sample. The intensity of Raman scattering is proportional to the cross section, σ_j , with units of square centimetres per molecule. The magnitude of σ_j is related to $\delta\alpha/\delta Q$. Since

$$\sigma_j = \sigma_j^\circ (\nu_0 - \nu_j)^4 \quad (14)$$

where σ_j° is the frequency-independent cross section and $(\nu_0 - \nu_j)$ is the absolute frequency of the scattered light (in reciprocal centimetres), so, I_R will be:

$$I_R = I_0 \sigma_j^\circ (\nu_0 - \nu_j)^4 D dz \quad (15)$$

from equation (15) it can be concluded that the intensity of a Raman band linearly depends on the cross section, density, path length, and the fourth power of the frequency of the scattered radiation. The intensity of the Raman bands depends directly on $(\nu_0 - \nu_j)^4$ which, in turn, depends on the laser frequency. This equation is

based on expressing the power in watts but since modern spectrometers count photons, it is more exact to introduce P_0 and P_R in units of photons per second:

$$P_R = P_0 \sigma_j^\circ D dz \quad (16)$$

where σ_j° now has a different frequency dependence than that of equation (14)

Since $I_R = P_R hc (\nu_0 - \nu_j)$ and $I_0 = P_0 hc \nu_0$

so the final expression for P_R will be :

$$P_R = P_0 \sigma_j^\circ \nu_0 (\nu_0 - \nu_j)^3 D dz \quad (17)$$

Therefore, when P_R is measured as photons per second, the Raman intensity depends on $\nu_0 (\nu_0 - \nu_j)^3$ rather than $(\nu_0 - \nu_j)^4$. Measurement of P_R would require light collection over the solid angle of 4π steradians around the sample. In practice, only a relatively small range of solid angle is observed in one of several scattering directions from the sample; so, it is more useful to define the differential Raman cross section as

$$\beta \text{ (cm}^2 \text{ molecule}^{-1} \text{ sr}^{-1}\text{)}, \quad \beta = d\sigma_j/d\Omega \quad (18)$$

where Ω represents the solid angle of collection.

4.2.4.1 Magnitude of Raman cross section ^[109, 110]

Raman cross sections are determined by quantitatively comparing the Raman signal for an unknown to that for a standard with known cross section. Raman cross sections are nearly always very small compared to other competing processes such as absorption and fluorescence. Raman scattering cross sections are often 6 to 8 orders of magnitude smaller than fluorescence cross sections, leading to the common problem of fluorescence interference. There are several factors affecting the magnitude of Raman cross section (β) including:

1- β is larger for molecules with extended π systems since the electrons are more easily polarized. This can be illustrated by the increase in β for the series benzene, naphthalene, and anthracene.

- 2- Molecules with only single C-H, C-O, and C-C bonds (e.g., glucose) generally have small cross sections. This can be explained by the significant difference in electron affinity and therefore high partial charge and localization of electrons. So these bonds are not likely to be strong Raman scatterers.
- 3- Molecules which contain large or electron-rich atoms, such as sulfur or iodine, often have high β values e.g. the S-S bond stretch in peptides.
- 4- Small molecules without electron-rich atoms, such as H₂, CO, and N₂ have small cross sections.
- 5- Multiple bond stretches generally have high cross section values, which are higher still if they are conjugated with another π system due to the high electron density and mobility of the electrons. These bonds are likely to yield strong Raman bands.
- 6- Raman scattering cross sections strongly increase with delocalization of π electrons. This can be illustrated by the Raman intensity of the ring-stretching band of benzene at 992 cm⁻¹ which is many times weaker than the corresponding band of anthracene. Also, conjugated systems of π electrons have very high Raman cross sections e.g. β -carotene due to resonance effects. Resonance effects can greatly increase the cross section when the incident radiation approaches an electronic absorption band of the sample molecules.
- 7- Vibrations of a molecule as a whole create strong Raman bands e.g. the accordion mode of the saturated hydrocarbon chain (when the hydrocarbon chain as a whole stretches and shrinks).
- 8- Raman intensity of stretching vibrations is normally stronger than that of bending vibrations, because the intensity of Raman scattering is proportional to movements of electron clouds.
- 9- Amplification of Raman signal occurs when a scattering molecule is adsorbed onto

a roughened metal surface e.g. silver or gold; Raman spectra of such molecules are termed surface-enhanced Raman spectra (SERS).

4.2.5 Raman scattering intensity ^[115,122]

The intensity of the signal delivered by the detector of a spectrometer analyzing a given Raman line can be expressed by:

$$S \sim I_0 \sigma_{\lambda} N \Omega T_{\lambda} s_{\lambda} \quad (19)$$

I_0 is the laser irradiance at the sample (watts per unit area), σ_{λ} is the differential cross section for the Raman line analyzed, N is the number of molecules in the probed volume V , Ω is the solid angle of collection of Raman radiation, and T_{λ} and s_{λ} are the throughput of the instrument and the sensitivity of the detector at the wavelength λ , respectively. The Raman scattering intensity is proportional to irradiance of the incident laser (I_0) which can be increased by increasing the laser power or focusing the laser beam into a small sampling area consistent with the survival of the molecular integrity. When a small volume of a sample has to be examined i.e. using microRaman spectroscopy, I_0 and Ω can be modified to compensate for the large reduction in the number of scattering molecules N in the probed volume V . The microscope objectives which are high numerical aperture optics (NA) are able to focus the laser beam into a very small volume and to collect over a wide angle the Raman scattered radiation from this volume. Thus, the significant increase of the local irradiance I_0 and the wide angle of collection Ω compensate for the decrease of the number of molecules N in the probed volume. The number of molecules N in the probed volume is the product of the sample concentration and the laser sampling volume V . So, the Raman scattering intensity is directly proportional to the concentration of the sample. Referring to equations (13, 14 and 15), it can be concluded that the intensity of the Raman scattering is proportional to the fourth

power of the frequency of the Raman scattered radiation $(\nu_0 - \nu_j)^4$. The intensity of the Raman scattered radiation will be affected by the factors determining the magnitude of the Raman cross section mentioned at section (4.2.4.1). Also, single crystals will exhibit different Raman band intensities under different orientations in sample illumination because of the polarization effects which depends on the combination of the incident electric vector and the scattering geometry of the molecular crystal system. This orientation effect is not experienced when examining amorphous or bulk samples because the molecules are randomly oriented. Furthermore, the particle size can affect the intensity of Raman scattering. It was observed that the Raman signal intensity increases as the particle size decreases. ^[116] In a later study, the effect of particle size on Raman intensity has been measured for a number of crystalline solids using fibre-optic Raman spectroscopy. Raman scattering intensity was found to decrease with increasing particle size. ^[117] It was concluded that the overall Raman signal increases because the near-surface Raman signal is increased by diffuse reflectance spreading the exciting beam laterally, generating additional Raman scattering in the region of most efficient acceptance by the collecting fibre.

4.3 Infrared spectroscopy ^[115]

IR radiation does not have enough energy to induce electronic transitions as those seen with UV-VIS spectroscopy. Absorption of IR radiation is restricted to compounds with small energy differences in the possible vibrational and rotational states. For a molecule to absorb IR radiation, the vibrations within a molecule must cause a net change in the dipole moment of the molecule. The alternating electrical field of the incoming radiations interacts with fluctuations in the dipole moment of the molecule and if the frequency of the radiation matches the vibrational frequency of the molecule then radiation will be absorbed, causing a change in the amplitude of the

molecular vibration. The motion of the atoms during vibration is usually described in terms normal coordinate, Q . The molecule is only promoted to the excited state if its dipole moment, μ , changes during the vibration ($\delta\mu / \delta Q \neq 0$) and the intensity of fundamental bands in IR spectra is proportional to $(\delta\mu / \delta Q)^2$. The energy difference for transitions between the ground state ($v_i = 0$) and the first excited state ($v_i = 1$) of most vibrational modes corresponds to the energy of radiation in the MIR spectrum (400–4000 cm^{-1}).

4.4 Selection rules of Raman and IR spectroscopy ^[118]

A vibrational mode will only appear in the Raman spectrum if the displacements in atomic position change the polarizability of the molecule. Conversely, a vibrational mode is IR active when there is a change in the molecular dipole moment during the vibration. Hence, vibrations that give rise to strong Raman bands often weak IR bands and *vice versa*. This characteristic gives the description ‘complementary’ to using Raman and IR spectroscopy together for molecular structural elucidation. When a vibrational mode is allowed under both electric dipole and polarizability selection rules, the observed frequency will be identical. Owing to the different nature of the selection rules, however, the intensities of corresponding bands may exhibit considerable differences. Generally, symmetric vibrations and non-polar groups yield the most intense Raman scattering bands, whereas anti-symmetric vibrations and polar groups yield the most intense IR absorption bands. For example, some of the strongest Raman peaks come from functional groups such as C=C, S-S, C=N, C-H, and C-S which have low polarity and high polarizability. In contrast, the carbonyl vibration (C=O) has a dipole and occurs strongly in IR absorption, whereas although it is active in the Raman spectrum it occurs with weaker intensity. Molecular symmetry can also play a role; for the carbon dioxide molecule, CO_2 , the symmetric stretch of C=O

bonds there is no net dipole moment change and so there is no infrared activity. However, in the asymmetric stretch, the two C=O bonds become of different length and, hence, the molecular vibration generates a dipole. Therefore, the vibration will be infrared-active. Similarly, the O–H stretching vibration is very strong in the IR, but very weak in Raman, because OH bonds are only weakly polarisable. Because of this, water is practically invisible in Raman spectroscopy, while it dominates the IR spectrum.

When the molecule has a centre of symmetry, the Rule of Mutual Exclusion applies which states that, for a molecule with a centre of symmetry, the fundamentals which are active in the Raman spectrum are inactive in the infrared spectrum whereas those active in the infrared spectrum are inactive in the Raman spectrum; that is, the two spectra are mutually exclusive. The definition of the centre of symmetry is that any point in the molecule reflected through the central point will arrive at an identical point on the other side. An example of centrosymmetric molecule is CO₂ for which the symmetric stretch is Raman-active and IR-forbidden; the asymmetric stretch is IR-active and Raman-forbidden.

4.5 Characteristic wavenumbers of Raman-active molecular vibrations ^[115,119]

Some vibrational modes can be attributed to individual functional groups and others to vibrations of the whole molecular structure. Those vibrational modes which can be attributed to individual functional groups (characteristic group vibrations) can be described mathematically if the two bonded atoms are imagined as two vibrating masses connected by a spring. The relationship between the frequency, the masses of the atoms involved in the vibration and the bond strength for a diatomic molecule (AB) is given by Hooke's law:

$$\nu = \frac{1}{2\pi c} \sqrt{\frac{K}{\mu}} \quad (20)$$

where c is the speed of light, K is the force constant of the bond between A and B, and μ is the reduced mass of atoms A and B of masses M_A and M_B ;

$$\mu = \frac{M_A M_B}{M_A + M_B} \quad (21)$$

This law illustrates that the frequency of the vibration depends on the strength of the bond as well as the masses of the vibrating atoms. The lighter the atoms, the higher the frequency will be. Thus C–H vibrations lie at higher frequency than C–I vibrations. The force constant is a measure of bond strength. The stronger the bond, the higher the frequency will be. The frequencies of stretching modes of multiple bonds are higher than those of single bonds between the same atoms i.e. $C\equiv C > C=C > C-C$. Bending modes occur at lower frequencies than stretching modes involving the same functional group as the energies required to bend the bond are lower than those required to stretch them. Also, Raman spectroscopy provides information about the vibrations of functional groups in a molecule, therefore, the functional groups present in a molecule can be deduced from a Raman spectrum. Table (4.1) shows typical wavenumbers of some functional groups. The literature contains exhaustive tabulations of vibrational group wavenumbers which the investigator can use to aid in spectral interpretation. However, some ambiguity will arise in the assignment of molecular vibrations to band wavenumbers in Raman spectra, which occurs because of the overlap of the spectral ranges of these characteristic functional groups. So it is necessary to resort to other spectroscopic information for the clarification of band assignments such as band intensities and the comparison with simplified model spectra.

4.5.1 Effects of adjacent groups on vibrational wavenumbers ^[115, 122]

Examples of the origins and diversity of the observed wavenumbers for important

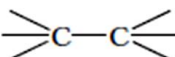
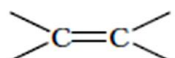
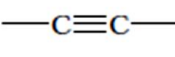
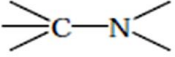
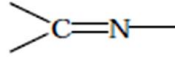
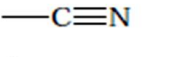
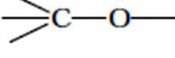
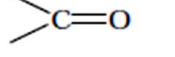
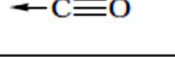
Stretching mode	$\tilde{\nu}$ (cm ⁻¹)
	1150
	1630
	2130
	1090
	1670
	2240
	1060
	1700
	2000

Table (4.1) Typical wavenumbers for stretching modes for C–N, C–O and C–C functionality [Adapted from reference 115].

chemical molecular functionalities are provided by the carbonyl group (C=O). The factors affecting functional group wavenumber position include:

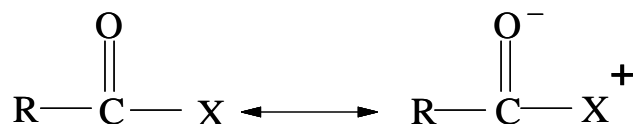
1- Mass effect

The wavenumber of the vibration is independent of the masses of the other atoms on the molecule. This can be exemplified by an aldehyde $\nu(\text{C}=\text{O})$ that occurs at 15 cm⁻¹ higher than the corresponding ketone. The electronic effect is much more important and exemplified by the wavenumber of acid halides $\nu(-\text{C}(\text{Cl})=\text{O})$ in the range 1810-1775 cm⁻¹ while the amide $\nu(-\text{C}(\text{NH}_2)=\text{O})$ occurs in the range 1690-1640 cm⁻¹, despite the fact that the NH₂ group is less than 50% of the mass of Cl atom.

2- Electronic effect

The polarity of the carbonyl group ($\text{X}_2\text{C}^+=\text{O}^-$) causes a decrease in the bond strength and the C=O bond stretching force constant. If the adjacent atom or group X is electron attracting, the polarity of the bond is reduced and the $\nu(\text{C}=\text{O})$ wavenumber is

increased. This can be illustrated by the shift of ν (C=O) in acid chloride (RC(Cl)=O) at about 1800 cm^{-1} to 1715 cm^{-1} in $\text{R}_2\text{C}=\text{O}$. Also, a second electronic effect arises from mesomerism, in which the nonbonding electron of an atom attached to the carbon atom of the carbonyl bond can be donated to the oxygen atom of the carbonyl.



This results in a weakening of the ν (C=O) force constant and a strengthening of the ν (C-X) force constant i.e. decreasing of the wavenumber position of ν (C=O). The proximity of an electron-withdrawing substituent causes an inductive withdrawal of electron density from around the oxygen atom, thereby shortening the bond. This increases the force constant and hence the wavenumber of the vibration. Furthermore, an electronic effect can arise from conjugation in which the double bond character of the C=O is reduced, as with contribution of the type $[\text{O}=\text{C}-\text{C}=\text{C} \longleftrightarrow \overset{-}{\text{O}}-\text{C}=\text{C}-\overset{+}{\text{C}}]$. This results in a shifting of the ν (C=O) to a lower wavenumber.

3- Bond geometry effects

The interaction force constant between the CX and CO bonds changes as the internal bond angle changes consequent upon geometry changes which will affect the ν (C=O) wavenumber. This effect can also be illustrated by the change in wavenumber of the ν (C=C) with local symmetry and conformation changes. Here, the trans conformer is observed at 1662 cm^{-1} while the cis conformer is observed at 1644 cm^{-1} .

4- Hydrogen bonding ^[120]

Compounds containing proton donor groups such as O-H and N-H can be involved intra- or intermolecular hydrogen bonding in the presence of proton acceptors e.g. O,N, halogens, and C=C. The stiffness of the X-H bond is thereby lessened, resulting in a lowering of the stretching wavenumber position, and the band broadens. These

effects are particularly significant in the spectra of alcohols, phenols, carboxylic acids and amides.

4. 6 Raman versus Infrared spectroscopy^[110]

There are several advantages of Raman spectroscopy over IR spectroscopy:

1- Unlike transmission IR spectroscopy, sample preparation is not required and samples can be analysed directly without destroying the sample.

2- Since water is a weak Raman scatterer, Raman spectra of samples in aqueous solution can be obtained without major interference from water vibrations. Thus, Raman spectroscopy is ideal for the studies of biological compounds in aqueous solution. In contrast, IR spectroscopy suffers from the strong absorption of water.

3- Raman spectra of hygroscopic and/or air-sensitive compounds can be obtained by placing the sample in sealed glass tubing. In IR spectroscopy, this is not possible since glass absorbs IR radiation.

4- *In-situ* or in vivo analysis as well as analysis with optical fibres are more easily carried out by Raman spectroscopy which demonstrates the flexibility and versatility of Raman spectroscopy in comparison with IR.

5- Since the diameter of the laser beam is normally 1-2 mm, only a small sample volume is needed to obtain Raman spectra. This is a great advantage over conventional IR spectroscopy when only a small quantity of the sample is available. Also, the spatial resolution of Raman micro-spectroscopy is very high (1 μ) compared with the spatial resolution of IR microscopy which is about 10 mm.

6- Lattice modes which appear below 200 cm^{-1} can be examined using Raman spectroscopy as Raman instruments allow spectral data to be obtained to within 50 cm^{-1} of the incident laser whereas IR data can normally be obtained to approximately 400 cm^{-1} unless special instrumentation is adopted. This gives Raman spectroscopy a

very big advantage over IR spectroscopy where low wavenumber bands can be quite definitive for sample identification and characterization.

7- There is a special type of Raman scattering known as the resonance Raman (RR) effect that has no counterpart in the IR. The resonance Raman effect is an effect in which intensities of Raman bands are significantly increased in cases where the wavelength of the excitation radiation overlaps with an absorption band of the sample molecule. In addition to huge signal enhancement, which significantly increases sensitivity, resonance Raman spectroscopy allows for selective examination of a particular chromophore in the molecule. To the contrary, IR spectroscopy only allows for the acquisition of average spectra of the sample.

4.7 Instrumentation

There are two major instrumental approaches used to collect Raman spectra; Fourier-transform Raman and charge-coupled device (CCD)-based dispersive Raman spectroscopy. Each technique has unique advantages and each is ideally suited to specific analysis. The technologies differ in the laser that is used and the way the Raman scattering is detected and analysed. Recent developmental advances, such as the availability of less expensive and more sensitive charge coupled devices (CCDs), the availability of holographic notch filters and the advent of Fourier transform Raman (FT-Raman) , launched a renaissance of Raman spectroscopy as a routine laboratory technique.

4.7.1 Dispersive Raman spectrometers ^[109, 121]

The basic configuration and components of a dispersive Raman spectrometer are the laser excitation source, sample illumination and collection optics, a spectrometer and a detector (Figure 4.6).

a- Laser

The source of monochromatic radiation is a laser which could be air-cooled argon-ion (488 or 514 nm), doubled continuous wave neodymium yttrium aluminium garnet (Nd: YAG or Nd:Y₃Al₅O₁₂) (532 nm), helium-neon (633 nm), or stabilized diode (785 nm). The stability of the laser radiation is a key attribute of a good spectrometer, and good stability is essential for good function. Frequency stabilization of the laser under standard laboratory conditions (slight temperature fluctuations, vibrational effects, etc.) is required. Laser lifetimes and cost are also considerations of choice to use the laser. The advantage of using shorter wavelength lasers is the enhancement in the Raman signal that occurs at shorter wavelengths. The efficiency of Raman scattering is proportional to $1/\lambda^4$, so there is a strong enhancement as the excitation laser wavelength becomes shorter. One additional consideration associated with laser selection in dispersive Raman systems concerns the use of wavelengths that could potentially generate molecular fluorescence. As the intensity of the Raman scattering is fairly weak, fluorescence emission can be so intense as to mask the scattered Raman photons. Fluorescence occurs when the virtual energy level overlaps real excited electronic level, so as the energy of the laser gets higher (shorter wavelength), the likelihood of fluorescence increases. The phenomenon is excitation wavelength dependent, so a sample that fluoresces at one wavelength may not at another. If fluorescence does not pose a problem for a given sample, shorter wavelength lasers are the excitation source of choice because of the enhanced sensitivity. If fluorescence is a problem or samples can potentially be damaged when using these high-energy sources, then even lower energy sources, such as those used in Fourier-transform Raman spectroscopy, can be used to minimize the fluorescence effects.

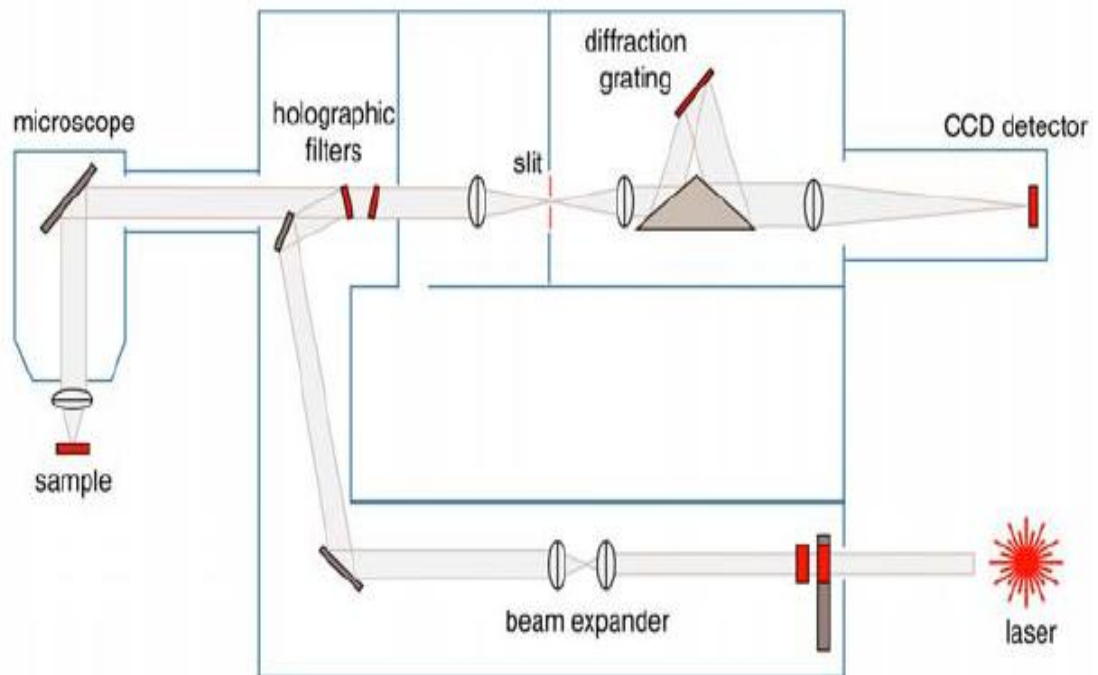


Figure 4.6 Schematic representation of a dispersive Raman spectrometer [Source: Renishaw plc.]

b- Optics

In a dispersive Raman spectrometer, the sample is positioned in the laser beam, and the scattering radiation is collected either in a 180° (the backscattering method) or a 90° (the right-angle method) scattering configuration. Dispersive spectrometers are equipped with efficient light rejection filters to suppress the Rayleigh line and stray light. Frequently used filters are dielectric notch and edge filters, holographic notch filters, and absorption filters. Holographic notch filters have revolutionized Raman spectroscopy by providing excellent attenuation of the Rayleigh line while passing bands as near to it as 50 cm^{-1} . They also exhibit good transmission in both the Stokes and anti-Stokes regions.

c- Spectrometer

The primary function of the spectrometer is to allow for the separation of the scattered radiation according to wavenumbers leading thereby to the appearance of the Raman

spectrum. Dispersion of light by a diffraction grating, shown schematically in Figure 4.7, is the principle of the most common type of dispersive wavelength spectrometers. A spectrometer disperses radiation along a focal plane. A spectrograph with a multichannel detector at the focal plane is a key component in a multichannel spectrometer. If an exit slit is placed at the focal plane, a small range of wavelengths (the band pass) is transmitted, and the device is a monochromator. Gratings have many lines or grooves blazed into the surface, which disperse the incoming light. The higher the number of grooves on the grating, the wider the dispersion angle of the exiting rays. It is necessary to have many grooves (for example, 1800 or 2400 lines/mm) for a high resolution spectrum, in which very closely spaced wavelengths must be distinguished. The higher the dispersion of the exiting rays, the larger the area over which the different wavelengths will lie when they reach the detector surface.

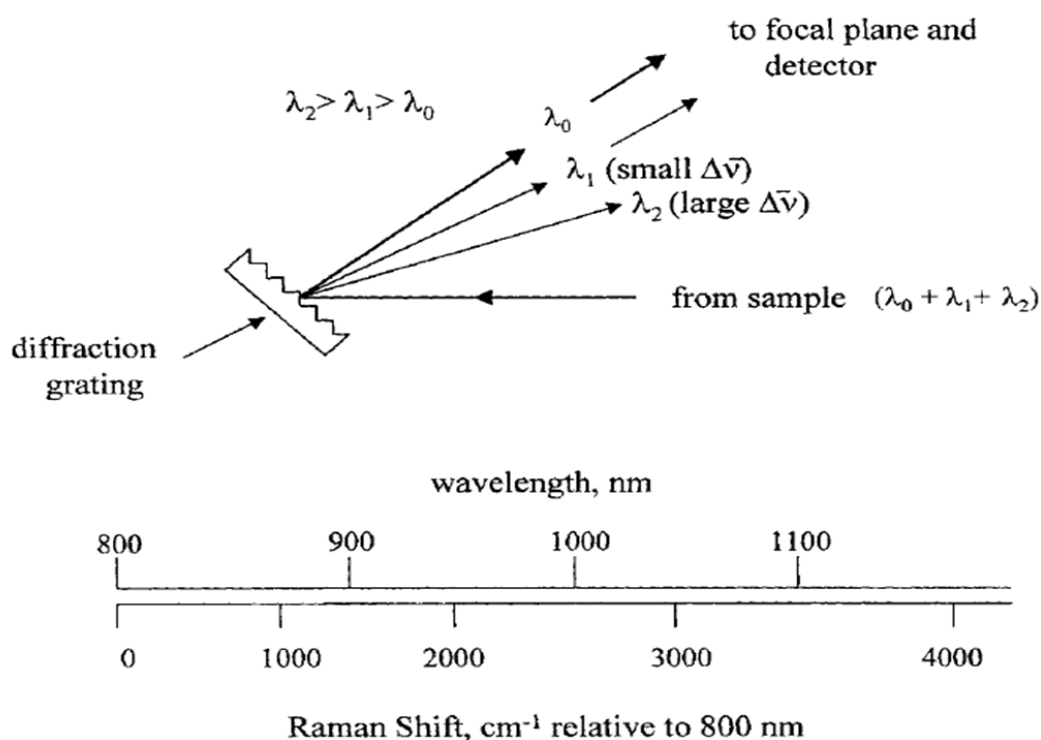


Figure 4.7 Schematic of wavelength dispersion by a diffraction grating [Adapted from reference 109]

With a fixed detector size, there is a point (resolution) beyond which not all of the Raman wavelengths fall on the detector. In cases of higher dispersion (high resolution), it is necessary to move either the grating or the detector to collect sequential regions of the spectrum. Gratings disperse the light according to wavelength, not wavenumber, resulting in a linear spread of wavelengths at the focal plane of the spectrometer. However, if the same range of wavelengths is plotted as Raman shifts, the dispersion is nonlinear. The nonlinear dispersion of Raman shifts is fundamental to wavelength dispersive spectrometers because the physics underlying dispersion is based on wavelength rather than energy. The main consequence of this nonlinear Raman shift dispersion is non-constant spectral resolution i.e. the dispersion becomes greater at higher wavenumbers (cm^{-1}). For this reason, spectral resolution must be stated for a specific wavenumber and will vary across the spectrum and as gratings are blazed for optimum throughput over a relatively narrow wavelength range, they should be selected for the desired resolution and for the correct laser wavelength.

d- Detector

For dispersive systems, a charge-coupled device (CCD) is typically utilized. CCD cameras are commonly produced from silicon and consist of two-dimensional arrays of pixels (e.g., 256 x 1024) that each can be considered as an independent detector. Photons, usually in the 200–1100 nm range, are absorbed by the silicon in the pixel and produce electrons that are stored within it by a system of electrodes. The CCD will accumulate photoelectrons in its array pixels that correspond to particular Raman shifts. Then the CCD is “read out” electronically and the electrons accumulated are converted to a digital value for storage in a computer. The horizontal pixels are calibrated so as to correspond to the wavenumber axis, while the vertical pixels

actually measure the strength of the Raman signal. The image on the CCD is considered as an electronic picture of the Raman signal that is then converted into a spectrum. One of the most important features of a CCD is its quantum efficiency curve that displays the probability of generating a photoelectron versus the energy of radiation. Such curves usually peak at around 600 nm and zero after 1000 nm thus limiting the wavelength range of the lasers that can be used. For a dispersive Raman system with an excitation laser source emitting at 780 nm, the 3000 cm^{-1} response (corresponding to the C-H stretch region of the spectrum) results in 1018 nm radiation. Many common CCDs have very weak responses for the higher wavenumber response of the NIR laser, and going any higher in laser wavelength rapidly disqualifies the CCD as a viable detector.

4.7.1.1 Raman microscopy ^[109, 122]

Raman spectra can be acquired on a small amount of material through the use of a microscope. The use of a microscope allows the operator to view the sample optically, select any part of interest, focus the incident radiation and collect the Raman spectra. However, the optical coupling between the microscope and the spectrometer must be optimized from the sample to the detector and along the optical path. A schematic diagram of the widely adopted laser focusing, sample viewing and light collection geometry is shown in Figure 4.6. Most commercial Raman microscope systems utilize confocal microscopy to increase the axial resolution. In the confocal arrangement (Figure 4.8), the microscope contains a pinhole in its focal plane, which enables only light focussed on the plane containing the sample to be collected efficiently. The pinhole filter stops most other light originating from outside the focal plane since it is not focussed sharply in the plane of the pinhole. Without the use of a pinhole, the same confocal axial discrimination can be achieved if the observed zone

of the sample as well as the entrance slit of the spectrometer is optically conjugated to the array of the pixels of the multichannel charge-coupled device (CCD) detector (Figure 4.6). The microscope objective focuses the laser beam into a very small volume and collect the the light scattered by this volume. There are two volumes that

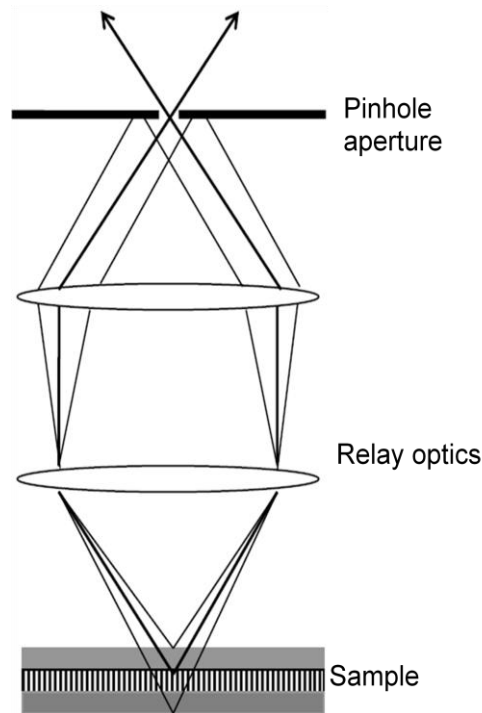


Figure 4.8 Diagram for a confocal Raman set-up [Adapted from reference 109]

are significant: the focal volume defined by the focused laser beam and the scattering volume defined by the collection optics of the Raman microscope. For the highest spatial resolution, without intensity loss, these two volumes should be about the same size and be superimposed. The diameter of the waist (d_l) of the diffraction-limited focus beam can be given by :

$$d_l = 1.27\lambda \left(\frac{f}{D_l} \right) \quad (22)$$

where λ is the laser wavelength, f is the focal length of the lens, and D_l , is the effective beam diameter at the lens. The depth of focus h_l , can be taken as the distance

between the points, either side of the focus, where the intensity of the beam falls to half of its maximum value:

$$h_l = 2.53\lambda \left(\frac{f}{D_l} \right)^2 \quad (23)$$

The focal volume τ_l defined by d_l , and h_l , is thus approximately cylindrical and of magnitude

$$\tau_l = 3.21\lambda^3 \left(\frac{f}{D_l} \right)^4 \quad (24)$$

This volume can be used to estimate approximately the number of molecules being interrogated in the system at any time. The ratio (f / D_l) is closely related to the numerical aperture, which is defined by $NA = n \sin \theta_{\max}$ where n is the refractive index of the medium between the lens and the focus ($n = 1$ in air) and θ_{\max} is the maximum acceptance angle of the objective. So, $\tau_l \propto (NA)^4$.

The main advantages of confocal microscopy is the improvement of both the lateral and axial resolutions (depth discrimination), which allows an “optical sectioning” of transparent specimens. Using a motorized stage, selective maps and images of the sample depicting the distribution of a given molecular species can be obtained by programming it to obtain Raman spectra as a grid over the surface of the sample. Using a judicious selection of non-overlapping Raman bands, the spatial distribution of all the molecular compounds present in the specimen can be mapped out separately. The motorized stage can also be programmed to obtain Raman spectra through the depth of the sample (depth profile) with a maximum depth resolution of 1-2 micrometer in transparent materials. Raman microscopy is advantageous than IR microscopy in this regards, as the limiting spatial resolution is on the order of $1\mu \times 1\mu$ in Raman micro-spectroscopy while it is around $20\mu \times 20\mu$ in infrared microspectroscopy due to the lower wavelengths that can be used.

4.7.1.2 Fibre-optic Raman spectroscopy ^[109, 110]

The versatility of Raman spectroscopy has been extended by the use of fibre-optic probes. Transmission of visible and near-infrared (NIR) light is quite efficient in modern optical fibers, so the spectrometer may be located a significant distance from the sample and Raman spectra can be obtained remotely many metres or even kilometres away from the spectrometer. For example, the sample may be in a pipe in a chemical plant or in a hazardous environment where batch sampling is impractical. Furthermore, a chemical process may be monitored continuously (process monitoring), and the analytical data may be used to control the chemical process (process control). Materials which can not be introduced into the spectrometer due to their physical size or hazardous nature can have the beam brought to the sample surface. Also, the alignment of laser, fibers, and spectrometer may be designed so that sampling requires little or no additional alignment which is advantageous compared to conventional Raman spectrometers. The laser light is carried (Figure 4.9) to the sample by an excitation fiber, and the scattered light is returned to the spectrometer by one or

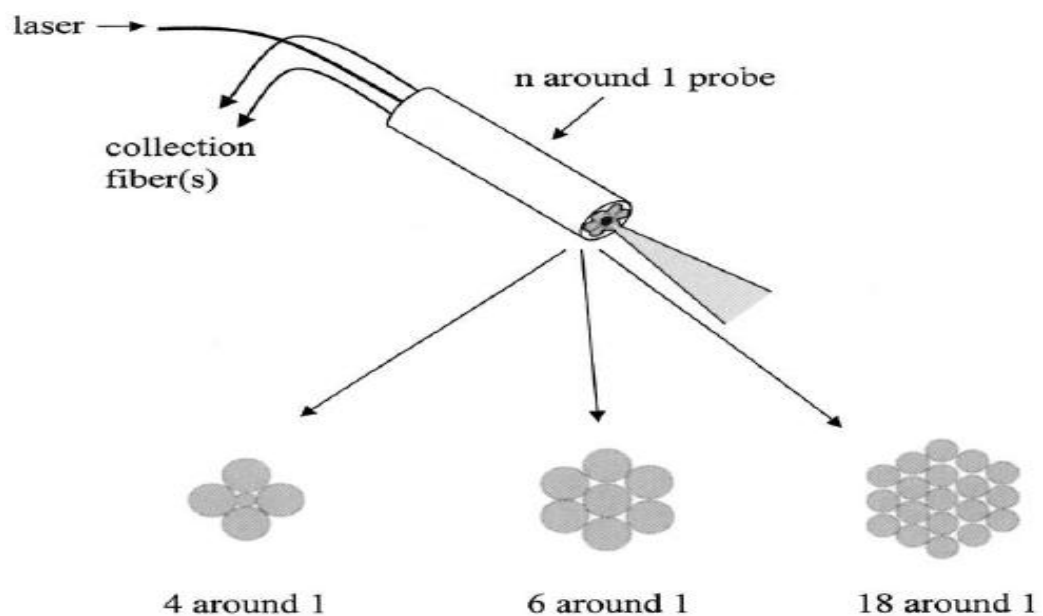


Figure 4.9 Schematic of the n-around-1 fibre-optic probe [Adapted from reference 109].

more collection fibers surrounding the excitation fibre. At the sample, the fibres might be terminated as a simple bundle of parallel fibres, or a more sophisticated probe head containing focusing optics and filters. In probe heads, the fibres are used to convey light from the laser to the probe head and the head to the spectrometer. Lenses, bandpass filters and holographic rejection filters are housed into the probe head to remove the silica background and reject the elastic scattering returning from the sample to the spectrometer. Depending on the probe head configuration, the collection fibers returning scattered light to the spectrometer range from a single fibre of 50 to 200 μm diameter to a bundle of as many as 36 fibres with diameters of 50 to 500 μm . Furthermore, the spectrometer input aperture may be a slit of perhaps 25 to 200 μm width in a dispersive spectrometer or a circular aperture of a few millimetre diameter for an FT-Raman system.

4.7.2 Fourier-transform Raman spectrometer ^[106,109,123]

Many FT-Raman instruments are adaptations of existing FT-IR spectrometer and the components of an FT-Raman spectrometer are shown in figure 4.10. All currently available commercial FT-Raman spectrometers use neodymium: yttrium aluminum garnet (Nd:YAG) lasers operating at 1064 nm. The use of long wavelength is necessary to avoid exciting fluorescence, but long wavelength results in a loss in scattering cross-section since the Raman scattering cross-section is proportional to ν^4 . The laser is directed to the sample either in 180° or 90° geometry. Since an interferometer has a larger aperture than the slit of a dispersive/CCD system, it is not necessary to focus the laser to a small spot. An unfocused or weakly focused laser is advantageous in FT-Raman because it lowers the power density at the sample and relaxes the tolerances on alignment of laser, collection optics, and sample. The scattered radiation from the sample then pass through a filter module which remove

the rayleigh line. Then, the scattered filtered radiation passes through an aperture called a *Jacquinot stop* which permits control of the degree of collimation in the interferometer and excludes severely off-axis radiation. The filtered radiation then passes to an interferometer where it is split by a beamsplitter into two beams of equal intensity. Using moving and fixed mirrors, one beam is subjected to an optical delay, and the two beams are then recombined. When recombined, the two beams interfere producing either a constructive or destructive interference pattern. The modulated radiation leaving the interferometer is directed toward the detector which measures variations in the intensity of the emergent beam as a function of the difference in path length. The interferogram is the sum of the cosine waves for all of the wavelengths

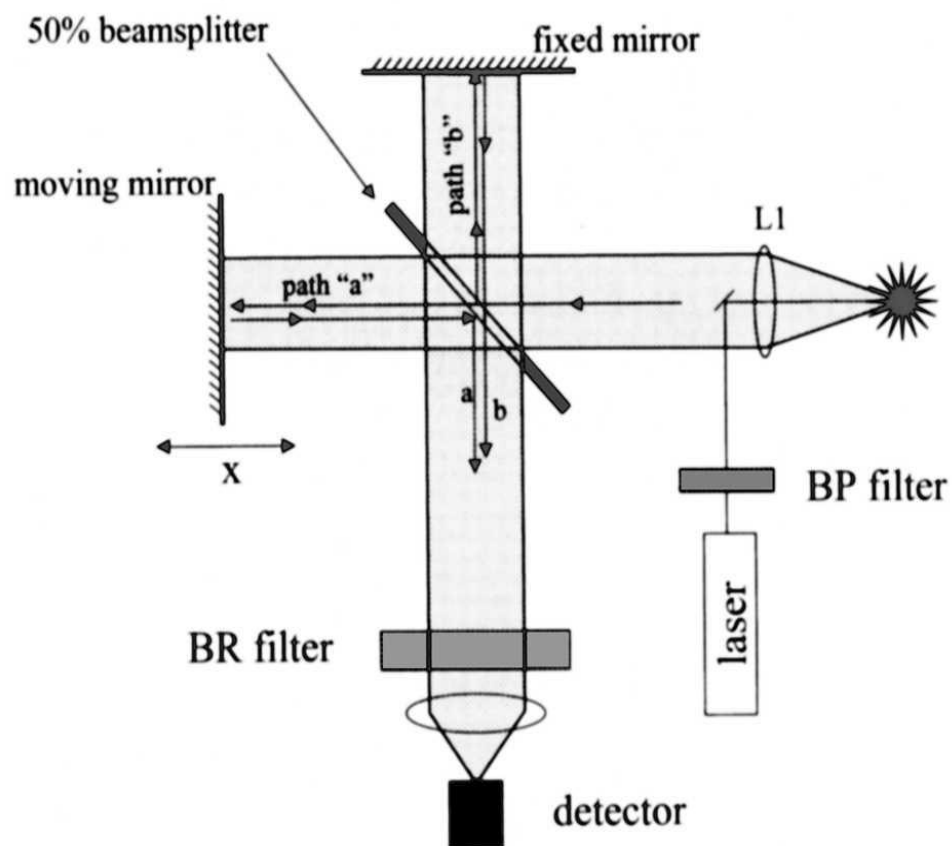


Figure 4.10 Schematic of FT-Raman spectrometer [Adapted from reference 109].

elements in the polychromatic source. The interferogram is then converted into a Raman spectrum of signal intensity against wavenumber by the Fourier-transform operation. Indium gallium arsenide (InGaAs) or liquid nitrogen-cooled germanium (Ge) detectors are usually used for FT-Raman spectroscopy. These detectors are very sensitive, but are noisy and still less sensitive for near-infrared radiation than the silicon CCD is for visible radiation.

4.7.3 Dispersive versus non-dispersive Raman spectrometers ^[124]

1- The use of UV-Visible lasers as excitation sources in dispersive systems increase the Raman scattering intensity (dependent on the ν^4 of the excitation frequency) so short acquisition times are required to obtain the Raman data. It also offers a high sensitivity when coupled with low noise CCD detectors in contrast to the relatively high level noise and low sensitivity of the germanium detector. The scattered radiation is dispersed by the diffraction grating across an array of pixels on the CCD detector and the intensities of the incident light at all frequencies are analysed simultaneously (multi-channel advantage). However, the integrity of the sample may be compromised and fluorescence emission may occur due to the high energy power of these lasers. Moving to the near infrared excitation at 1064 nm inhibits the onset of fluorescence but reduces the Raman scattering intensity due to the relatively low energy power of near-infrared lasers.

2- A grating-based dispersive spectrograph with a CCD at its focal plane (multichannel spectrometer) monitors many wavelengths simultaneously and acquires a spectrum faster than a scanning, single-channel system that must monitor each wavelength in turn. This is called the multichannel advantage. A multiplex spectrometer (FT-Raman) does not separate the different wavelengths scattered by the sample but rather modulates them at frequencies dependent on their wavelengths.

The result is a single beam, detected by a single detector, which contains all wavelengths of interest. Since each wavelength is modulated at a different frequency, a Fourier transform of the multiplex detector output yields a Raman spectrum (multiplex or Fellgett advantage). This difference between multichannel and multiplex approaches has major effects on the characteristics of the Raman spectrum, in terms of resolution, spectral coverage, signal magnitude, and signal/ratio (SNR). For multichannel and multiplex approaches, the simultaneous measurement over the whole spectral range results in an improved S/N ratio. FT-Raman system also offers a constant spectral resolution over the whole spectral range.

3- In dispersive spectrometers, the dispersed light entering a monochromator must enter through a narrow slit so a fraction of the Raman scattering is lost. In addition, reflective losses from gratings and mirrors exacerbate the situation. On the other hand, the entrance of an interferometer is a large circular hole which allows high throughput of scattered radiation to the detector (Jacquinot advantage).

4- In theory, all spectrometers can show an improved S/N ratio if the spectra are averaged. In dispersive Raman systems, frequency precision and accuracy depend on calibration with external standard e.g. silicon and the ability of electromechanical mechanisms to uniformly move gratings and slits during and between the scans. Displacement errors due to mechanical wear may result in band shape distortion and low S/N ratio. Internal calibration of the interferometer against a helium-neon laser provides exceptional wavenumber reproducibility, which facilitates the superposition of spectral data (accumulation) and data subtraction e.g. solvent, background. This is called the Connes advantage.

5- Both dispersive and non-dispersive instruments provide the same spectral information and both offer all the advantages of Raman spectroscopy. However, one

technique is recommended over the other for some situations. Shorter laser wavelengths and more sensitive CCDs make the technique ideal for minor component analysis, offering low detection limits for such applications as impurity analysis in solutions, polymers or environmental sampling. Raman spectroscopy offers the ability to measure vibrational spectra of aqueous samples. aqueous samples, cannot be analyzed using FT-Raman spectroscopy as water has strong interactions in the near-infrared region and therefore, laser radiation and Raman scatter are both susceptible to absorbance by water. Dispersive Raman spectroscopy, with visible laser excitation, is often more sensitive for aqueous samples because water absorbance of the radiation is not present. The confocal approach has been used in dispersive systems and as long as fluorescence is not a problem, the highest spatial resolution can be achieved. FT-Raman spectroscopy is the best choice in situations where samples fluoresce or are likely to contain minor impurities that may fluoresce. This is because of the use of longer excitation wavelengths at the near infrared region (commonly 1064 nm). FT-Raman has experienced great success in forensic analyses through sample containers or evidence bags, negating the need to break the container seal. It has been used to analyze illicit drug substances, clandestine lab samples, explosives and fibres. In particular, street drugs and clandestine lab samples often fluoresce with visible laser excitation but can be analyzed by FT-Raman spectroscopy.

Chapter 5

Raman Spectroscopic Analysis of Drugs of Abuse and Explosives

5.1 Advantages of Raman spectroscopy in forensic science ^[115,122,125]

Raman spectroscopy has been shown to be an effective technique for several forensic applications. Recent technological advances in Raman spectrometers have broadened the use of Raman spectroscopy in forensic applications. Raman spectroscopy produces molecular-specific spectra and, in most cases, sample preparation is minimal, allowing for the non-destructive *in-situ* analysis of tablets, powders, and liquids. This is particularly important with regard to the speed of analysis, prevention of sample contamination and preservation of evidential material. In many cases, FT-IR requires sample preparation, such as a KBr discs and Nujol null. These procedures are time consuming, destructive, or both. In Raman spectroscopic analysis, the preparation of KBr disc is not required which allow non-destructive analysis of the sample. The presence of water in the sample does not interfere with the analysis since water has a very weak Raman scattering. Thus, contrary to infrared spectroscopy, studies by Raman spectroscopy can also be conducted in aqueous solutions. The 1064 nm near-infrared excitation lasers used with Fourier transform Raman systems have enabled the acquisition of Raman spectra from samples that fluoresce with visible laser excitation. Dispersive Raman instruments using laser wavelengths ranging from the visible to the near-infrared region have greater Raman scattering efficiencies. Combined with sensitive charge coupled device (CCD) detectors, these systems have a more general use than FT Raman systems operating at 1064 and have been applied for a wide range of sample analysis. Also, the use of a microscope allows the Raman spectra to be acquired from particulate contaminant and trace amounts of samples which have a considerable interest in forensic science. Most commercial Raman

microscope systems utilize confocal microscopy to increase both axial and spatial resolutions. This makes it possible to examine a surface, such as that from a tablet or fingerprint, to obtain either an image of the surface under the microscope or to map a larger area. Additionally, fibre optic probes are used on dispersive systems to sample non-invasively through containers and plastic bags. The greatest advantage of the use of fibre optics in Raman spectroscopy is the ability to sample remotely without restrictions imposed by sample illuminator geometry. The *in-situ* analysis of drugs and explosives is desirable to avoid evidence contamination or risking operator exposure associated with sample manipulation. Fibre optic probes contribute to the application of small robust Raman instruments designed for field use. The attractive features of portability and ease of sampling included in these instruments allows their use in crime scenes along with other analytical instrumentations where the analysis of potentially hazardous materials is conducted. This enables forensic scientists and law enforcement agents to avoid the risk of transportation of hazardous materials back to the laboratory and minimise the removal of samples from crime scenes.

The following sections will address the applications of different Raman spectroscopic techniques for the forensic analysis of drugs of abuse and explosives.

5.2 Applications of Fourier Transform Raman Spectroscopy

5.2.1 Analysis of drugs of abuse

Fourier-transform Raman spectroscopy has been applied for characterization of pure drugs of abuse namely amphetamine, cocaine hydrochloride, and heroin. The technique was also applied for identification of these drugs in cut samples. Although the pure samples give excellent spectra for identification, some cutting agents were highly fluorescent, so preventing the identification of the drugs. ^[126] FT-Raman spectra were recorded for pure and street illicit drug samples, together with explosives

(Semtex) samples. To overcome the problem of sample alignment, the samples were pressed into a 2 mm cup which was mounted onto a brass rod that could be easily removed, loaded with a new sample and replaced, exactly in its original position. ^[127] Two systematic studies of the vibrational, infrared and Raman, spectra of a series of benzodiazepines were reported. The studied drugs have strong infrared and Raman spectra, which are very rich in spectral features. FT-Raman spectroscopy has proved to be a simple and rapid method for obtaining fluorescence-free spectra of drugs and pharmaceuticals ^[128,129] and has been applied for the identification of methamphetamine and its related compounds such as amphetamine sulphate and ephedrine hydrochloride. ^[130] There were clear differences observed between the Raman spectra which were adequate for the spectral differentiation of the compounds. Also, good quality spectra of methamphetamine could be obtained through plastic packaging without removing the drug from the bag. High quality FT-Raman spectra were measured for 200 standard samples containing controlled substances, related isomers and prescription drugs. Using this relatively long wavelength, almost all samples could be analyzed without the problems of fluorescence associated with conventional dispersive Raman instruments. These spectra were used to create a spectral database, or library, against which unknown samples could be searched and identified. ^[131] Complementary spectroscopic studies of a range of illegal drugs and explosives using Fourier-transform Raman and Terahertz spectroscopies have also been carried out. ^[132]

5.2.2 Analysis of Explosives

FT- Raman spectra were acquired from a wide range of aromatic nitro compounds including explosives ^[133] and identification of the explosives RDX and PETN in three Semtex samples has been reported. ^[134] The technique has been applied to characterize

neat energetic materials and some propellant formulations containing those materials. It was found that only the crystalline components of the propellant formulations are easily observed by FT-Raman spectroscopy. Also, it has been shown that darkly coloured samples are difficult to analyze because they absorb the incident near infrared radiation and pyrolyze or ignite. Furthermore, the technique has been extended to the investigation of crystalline components of propellant formulations during heating.^[135,136] FT-Raman spectra have obtained from 32 explosive materials. The explosives could be distinguished into three classes according to Raman spectra; the nitrate esters containing the (R-O-NO₂) group, the nitroaromatic containing the (Ar-NO₂) group, and the nitramines containing the R-N (NO₂)-R group. Few explosives e.g. Semtex and Teteryl are exceptional because they are either structurally or compositionally different from the majority of the explosives studied.^[137]

5.3 Applications of Raman Microspectroscopy

5.3.1 Analysis of drugs of abuse

Raman micro-spectroscopy has been applied for the identification and characterization of eight barbiturates. All the barbiturates studied could be distinguished from each other by their characteristic Raman spectra.^[138] Raman spectra of cocaine hydrochloride in crystalline and saturated aqueous solutions have been recorded.^[139,140] Vibrational analysis of α -, β -, and γ -hydroxybutyrates using infrared and Raman spectroscopies with an assignment of the fundamental vibrations has been given.^[141] A range of narcotics and explosives was examined using a Raman microscope operating at 244 nm in the UV region. Spectra were obtained from pure and contaminated samples. The relatively shorter wavelength was chosen to exploit the resonance Raman effect, thereby enhancing the band intensities. Also, there was no detectable fluorescence background, even with heavily contaminated samples.

However, UV-Raman is inherently a costly technique and it suffers from the problem of possible sample decomposition caused by the focused UV excitation laser.^[142] Composition profiling of seized ecstasy tablets using Raman microspectroscopy has been reported. The spectra obtained allowed the active drug and excipients used to bulk the tablets to be identified. Although the seized tablets have similar physical characteristics, there was considerable variation in the composition of the tablets with regard to the excipients used to bulk the tablets and the degree of hydration in the MDMA feedstocks used to manufacture them. The highly detailed Raman spectra obtained can be translated into information that is not readily available from other analytical methods and would be useful for the tracing of drug trafficking networks.^[143] Identification of MDMA and related compounds in seized tablets using Raman spectroscopy has been undertaken. Both the drug and the excipients could be identified by their Raman spectra even when more than one compound has been used as the bulking agent and the relative bands intensities of the drug and excipients could be used for quantitative analysis.^[144] In a large study, approximately 1500 ecstasy tablets from different forensic seizures were analyzed by Raman spectroscopy. Although, all the tablets contained MDMA as the active constituent, there were very significant differences in their Raman spectra which were attributable to variation in both the nature and concentration of the excipients used and/or the degree of hydration of the MDMA.^[145] Raman microspectroscopy has been applied for the detection of drugs of abuse in latent fingerprints^[146] and in cyanoacrylate-fumed fingerprints.^[147] The substances studied could be clearly identified using their Raman spectra and were all successfully detected in undeveloped latent and cyanoacrylate-fumed fingerprints. Potentially interfering bands arising from latent fingerprint material and cyanoacrylate polymer were present in the spectra of the drugs but these bands did not prevent the

unambiguous identification of the drugs of abuse. Raman spectroscopy has been applied for the analysis of drugs of abuse in latent fingerprints that had been treated with powders and also subsequently lifted with adhesive tapes. The application of powders to contaminated fingerprints did not interfere with the Raman spectra obtained for the contaminants. Also, interfering Raman bands arising from the lifting tapes could be removed by spectral subtraction or by the selection of specific lifting tapes that have weak Raman bands.^[148,149] Raman spectroscopic detection of drugs of abuse on textile fibres after recovery with adhesive lifters has been reported. Raman spectra from particles of drugs of abuse within fibres following tape lifting were also recorded through evidence bags.^[150] Raman microspectroscopy has also been applied for the identification of single drug crystals on US paper currency. Unfortunately, there was significant fluorescence background emission in the Raman spectra of the drugs especially from dollar bills which had been in circulation relative to those which had come directly from the bank.^[151] In a later study, the authors described two methods for reducing this fluorescence background emission, namely photobleaching and background subtraction.^[152]

5.3.2 Analysis of Explosives

Raman and infrared spectroscopic studies of 1,3,5-triamino-2,4,6-trinitrobenzene (TATB) have been undertaken.^[153] The vibrational properties and structure of pentaerythritol tetranitrate have been studied using Raman and infrared spectroscopies.^[154] Raman microscopy has been applied for the in-situ detection of traces of plastic explosives in fingerprints. Raman spectra and images could be obtained from explosive particles as small as $1\mu\text{m}^3$.^[155]

5.4 Applications of Fibre-optic Raman spectroscopy

5.4.1 Analysis of drugs of abuse

Fibre-optic Raman probes have been applied for the in-situ detection of illicit drugs. It was possible to differentiate cocaine hydrochloride from free base or crack cocaine using their Raman spectra. The fibre-optic probe has also been shown to be useful for measuring the spectra of these drugs after separation by thin layer chromatography (TLC).^[156] Also, a fibre-optic Raman probe has been used for the in-situ identification of cocaine and selected adulterants. The Raman spectra of cocaine hydrochloride and free base cocaine are easily distinguishable from each other and from common cutting agents and impurities such as benzocaine and lidocaine.^[157] Portable Raman spectroscopy has been used for the analysis of seized drugs in an airport environment; the spectra obtained were searched against a constructed library which allowed rapid identification of the samples.^[158] Gamma hydroxybutyric acid (GHB) and its precursor lactone, gamma-butyrolactone (GBL), were analysed using bench-top and portable Raman spectroscopy. It has been demonstrated that the drugs could be detected in a variety of containers including colourless and amber glass vials, plastic vials and polythene bags. Both GBL and GHB could be successfully detected in a range of liquid matrices in drinking glasses simulating actual 'spiked' beverages.^[159]

5.4.2 Analysis of Explosives

A Raman fibre-optic probe has been developed and applied for the detection of traces of explosive materials in fingerprints. Traces of PETN in a fingerprint containing traces of Semtex-H explosive could be detected remotely using a 4 metre long Raman fibre-optic probe.^[160] Raman spectroscopy, with red (632.8 nm) and near-infrared (785 nm) excitation, has been used to obtain the spectra of a wide range of high explosives. The spectra were compared with those obtained using a 1064 nm

FT-Raman spectrometer to choose the best laser wavelength excitation suitable for a field-usable explosive detector. Spectra were obtained for explosives, both neat and in plastic and glass containers. It has been concluded that 785 nm excitation affords an excellent compromise between sensitivity and fluorescence emission suppression.^[161] An acousto-optic Raman spectrometer has been applied for the acquisition of Raman spectra of high explosives.^[162] A blind field test evaluation of Raman spectroscopy as a forensic tool has been described; two portable Raman instruments and two operators have been utilized to analyze a wide range of unknown samples. Spectra of unknowns were searched against a customised hazardous materials reference library. The results have indicated an equivalent performance observed for both the operators and the instruments.^[163] Anti-Stokes Raman spectra of explosive materials were obtained with 1064 nm excitation using a fibre-optic probe and a dispersive spectrograph equipped with a charge-coupled device (CCD) detector. Spectra could be obtained from samples positioned up to twelve metres from the spectrograph.^[164] In a comparison study, Stokes Raman spectra using a fibre-optic probe were measured with 785 and 830 nm excitation, as well as the 1064 nm anti-Stokes Raman spectra of explosive materials. The spectra obtained using the 1064 nm excitation were not of good quality as those achieved using 785 and 830 nm excitations but 830 nm excitation offers slightly better fluorescence rejection than 785 nm. The authors concluded that a laboratory-based FT-Raman spectrometer remains the preferred method for fluorescence-free analysis of these explosives and 830nm excitation is preferred for a field-portable spectrometer.^[165] A portable remote Raman system has been used for the monitoring of hydrocarbon and explosives in the environment. Stand-off spectra of plastic explosives could be measured at 10 metres distance.^[166] A small portable fibre-optic Raman system has been used for stand-off detection of

explosive materials at 50 metres and Raman spectra of RDX, PETN and TNT could be obtained remotely in samples containing up to 8% explosive materials.^[167]

5.5 Applications of Surface enhanced Raman spectroscopy (SERS)

Surface-enhanced Raman spectroscopy (SERS) is a surface sensitive technique that results in the enhancement of Raman scattering by molecules adsorbed on certain rough metal surfaces. Certain roughened metal surfaces, e.g. gold and silver can significantly enhance the Raman scattering observed from adsorbed species. Surface-enhanced Raman spectroscopy gives an enhancement of up to 10^6 in scattering efficiency over normal Raman scattering. This makes it possible to obtain Raman spectra from tiny amounts of material and from weak Raman scatterers.^[168] Certain selection rules are applicable to the interpretation of SERS spectra. Strong peaks in normal Raman scattering can become very weak and new peaks which do not appear in normal Raman scattering can appear in the comparable SERS spectra.^[169] Surface-enhanced Raman spectra of amphetamine and similar stimulant drugs have been recorded on colloidal silver and spectra were also obtained from human urine samples spiked with mixtures of stimulant drugs.^[170] Matrix stabilized silver halides were used as the SERS-active substrate for the acquisition of SERS spectra of different brands of ecstasy tablets and powders containing amphetamine.^[171] Colloidal suspensions and vapour deposited films of both silver and gold were compared for the detection of amphetamine sulfate by SERS. Gold colloid and vapour-deposited films gave lower detection limits than their silver counterparts.^[172] Near-infrared Fourier-transform surface-enhanced Raman spectra of eight benzodiazepines were recorded using gold films over nanospheres as the SERS-active substrates. Identification and discrimination of the drugs could be made from spectra obtained from a few hundred nanograms of analyte.^[173] Surface-enhanced Raman scattering (SERS) from

trinitrotoluene (TNT) adsorbed on colloidal silver and gold has been reported. Different types of surface-enhanced Raman spectra have been observed on these metals, indicating differences in adsorption of the TNT on gold and silver. A sensitivity of less than 1 pg could be achieved for TNT in colloidal gold solutions.^[174] A SERS vapour probe that incorporates a roughened gold substrate, fibre-optic probe, and fan has been used for the vapour phase detection of explosives. TNT, PETN, RDX and other nitro-containing explosives could be detected down to 1-5 pg.^[175] Surface-enhanced Raman spectra of the vapour of explosive material have been recorded from adsorbed molecules on nano-structured gold substrate. The concentration of the adsorbed explosive molecules on the substrate was varied by heating the sample to different temperatures and exposing the substrate to the sample vapour for different lengths of time. The intensities of the Raman bands have been found to increase with the increase in temperature and also with the increase in the duration of exposure for a fixed temperature.^[176]

5.6 Applications of Spatially Offset Raman Spectroscopy (SORS)

The SORS method is based on the collection of Raman spectra from spatially offset regions away from the point of laser focused illumination on the sample surface. These laterally offset Raman spectra contain different relative contributions from sample layers located at different depths. This difference is brought about by a wider lateral diffusion of photons emerging from greater depths. Consequently, the SORS technique effectively suppresses interfering Raman and fluorescence emission signals arising from the surface layer. If a significant background signal is still present then this can be further removed using a scaled subtraction of spectra obtained at different spatial offsets. Instead, the separation of Raman signals originating from different layers in the sample can be achieved using multivariate data analysis chemometrics

applied to a set of spatially offset Raman spectra. ^[177] Spatially offset Raman spectroscopy has been applied for the detection of cocaine concealed inside transparent glass bottles containing alcoholic beverages. A major advantage of the technique is that any interfering Raman and fluorescence contributions originating from the bottle itself are effectively suppressed. ^[178,179] Also, the technique has been applied for the non-invasive detection of liquid and powder explosives concealed within diffusely scattering containers. Raman spectra of these concealed explosives could be acquired through a wide range of plastic containers typically carried by air-travel passengers. ^[180-183]

5.7 Applications of Raman spectroscopy and chemometric methods

Difficulties associated with the complexities of Raman light scattering from materials have limited the use of Raman spectroscopy as a quantitative technique. Poor reproducibility of spectral intensities, problems with high S/N ratios and the presence of fluorescence background have all limited the use of the technique in the past. ^[184] However, advances in instrumentation and the use of multivariate chemometrics techniques have overcome these difficulties. Multivariate analysis techniques are used to correlate statistically observed spectral changes with properties such as concentration and have allowed quantitative analysis to be performed using Raman spectroscopy. Near-infrared Raman spectroscopy and the partial least square (PLS) algorithm have been used to estimate the concentration of cocaine dispersed in glucose. ^[185] Also, Raman spectra obtained from a series of 33 solid mixtures containing cocaine, caffeine and glucose have been analysed using principle component analysis (PCA). Analysis of the data showed that the samples can be classified on the basis of cocaine concentration and discrimination on the basis of the caffeine and glucose concentrations was also possible. ^[186] Raman spectroscopy and

PCA chemometrics have been used for the classification of narcotics in solid mixtures. This method allowed the discrimination between cocaine, MDMA and heroin mixtures even when the Raman spectra are complex or very similar. ^[187,188] Raman spectroscopic data obtained from MDMA in ecstasy tablets have been analysed using PCA and PLS. ^[189] Furthermore, PCA and PLS methods have been applied for the quantitative analysis of amphetamine content in seized street samples. Both methods produced results accurate enough for routine forensic analysis to be possible. ^[190]

5.8 Raman spectroscopy combined with other analytical techniques

Raman spectroscopy has been interfaced with a number of complementary analytical techniques. These interfaced units allow the analytical advantages of the individual technique to be combined into a single integrated system. The complementary nature of the techniques, in terms of information content, practicality and sampling, give a huge advantage over each technique applied individually. Because Raman spectroscopy provides much information about the molecular structure of the compounds investigated, enough evidence can be gathered, in combination with the retention time, mass spectra and UV–Vis spectra, which allows a really unique identification of compound as demanded by forensic investigations. Combined Raman and FT-IR spectroscopy has been used to identify narcotics, cutting agents, narcotic precursors, and explosive materials. ^[191,192] The identification of illicit drugs has been accomplished by a combination of liquid chromatography and surface-enhanced Raman scattering spectroscopy ^[193] ; this has been applied to several illicit solid drugs among which are cocaine, heroin, an ecstasy tablet and amphetamine powder. The HPLC-separated fractions from these samples were collected as microlitre volumes in the wells of a microtitre plate containing a matrix-stabilized silver halide dispersion

which functions as the SERS-active surface. Also, Raman spectroscopy has been interfaced with scanning electron microscopy and energy dispersive X-ray analysis (Raman-SEM/EDX). This system permits the in-situ non-destructive characterization of a sample based on both its elemental and molecular composition. The system has been applied successfully for the characterization of explosive mixtures containing TNT and Tetryl. ^[194]

Chapter 6

Detection of Drugs of Abuse and Explosives on Human Nail Using

Raman Spectroscopy

6.1 Introduction

The analysis of keratinized matrices, such as hair and nails, for drugs of abuse is now recognized as an important tool for forensic toxicologists. Advances in modern analytical instrumentation have enabled the analysis of drugs in these unconventional biological matrices to be accomplished.^[195-199] Several studies in the literature have demonstrated that nail clippings can provide a readily accessible matrix for the post-mortem detection of drugs of abuse; opiates, methamphetamine, cocaine, and cannabis have been successfully detected in the nail clippings of drug abusers.^[200-206] Furthermore, DNA extracted from debris of fingernails of victims of violent or aggressive acts has been used in the identification of the assailants.^[207-209]

Raman spectra of human skin and nail have been recorded using excitation wavelengths in the visible region. Photobleaching has been applied to reduce the strong fluorescent background observed in the spectra.^[210] With the use of excitation sources in the near infrared, Raman spectroscopy could be applied for the characterization of molecular structure of sensitive biomaterials such as skin, callus, hair, and nail.^[211] A comparative study of the FT-Raman spectra of mammalian and avian keratotic biopolymers (stratum corneum, human nail, feather, and bull's horn) was carried out by Akhtar and Edwards.^[212] Raman spectroscopy and multivariate classification techniques have been applied for the differentiation of fingernails and toenails.^[213] Recently, a novel method for human gender classification using Raman spectroscopy of fingernail clippings has been reported.^[214]

The ability to identify visually obscured particles of forensic relevance affords

significant advantages to the investigator. Manual handling, packaging or transportation of drugs of abuse and explosive substances may result in contamination of the nail by these substances. Detection of drug particles on nail and other articles related to an individual, such as hair or clothing, could be of evidential value to identify this individual as a drug user or drug dealer. Also, the detection of explosives residues on nail can be used as an evidence to establish a link between these materials and individuals involved in terrorist activities. An added difficulty in the analytical procedure is afforded by the presence of a nail varnish coating which has been applied; although obscuring the particulate material to preliminary visual observation this will actually trap the particulate matter between the coating and the nail. The discrimination of confocal Raman microscopy for the detection of drugs of abuse, explosive and explosive precursor substances on uncoated nail and also under a coating of nail varnish is demonstrated. Exploiting the high axial resolution of the confocal arrangement, interference-free spectra of drugs of abuse and explosives could be acquired from particles visually masked by the nail varnish. Furthermore, the application of Raman mapping techniques allows visualization of particle morphology in obscured settings and obtaining the spatial distribution of a given compound within a heterogeneous specimen. This investigation establishes the utility of these Raman spectroscopic techniques in this context for the first time and establishes the technique of *in-situ* Raman mapping as a useful tool for forensic investigation

6.2 Experimental

6.2.1. Samples

a- Drugs of Abuse

Pure samples of cocaine hydrochloride, N-methyl-3,4-methylenedioxy-amphetamine

HCl (MDMA-HCl), amphetamine, nitrazepam and flunitrazepam were supplied by Sigma-Aldrich Company Ltd., United Kingdom. Seized street samples of cocaine hydrochloride, MDMA and amphetamine were supplied by the Home Office Scientific Development Branch.

b- Explosive samples

Pentaerythritol tetranitrate (PETN), trinitrotoluene (TNT) and ammonium nitrate samples were also supplied by the Home Office Scientific Development Branch. Hexamethylenetetramine (HMTA) and pentaerythritol used in this study were supplied by the Sigma-Aldrich Company Ltd., United Kingdom; they are used in the manufacture of high explosives such as RDX and PETN. [22, 215]

Finger nail clipping samples were collected and stored in clean containers prior to the analysis. A red nail varnish (GC, Procter & Gamble, ‘‘Nail Slicks Well Red 141, Rouge Expert’’) was purchased from a local store. The nail clippings were doped with few crystals of the drugs of abuse and explosive substances. Raman spectra were collected from individual crystals of dimensions in the range of 5–10 μm on the surface of the nail. A single layer of the nail varnish was then applied to the doped nails and spectra of the crystals of the drugs of abuse and explosives under the nail varnish coating were collected.

6.2.2. Raman spectroscopy

Reference Raman spectra of drugs of abuse and explosive samples, nail and nail varnish were obtained to be used for comparison with the spectra of the drugs and explosive particles on the surface of the nail and under nail varnish. Raman spectra were collected using a Renishaw InVia Reflex dispersive Raman microscope (Wotton-under-Edge, UK). The Raman scattering was excited with a 785 nm near-infrared diode laser (Renishaw HPNIR laser (Renishaw, Wotton-under-Edge, UK) and a 50x

objective lens giving a laser spot diameter of 5 μm . Spectra were obtained at 2 cm^{-1} resolution for a 10s exposure of the CCD detector in the wavenumber region 100-3200 cm^{-1} using the extended scanning mode of the instrument. With 90.8 mW laser power at the sample, one accumulation was collected for the drugs of abuse and explosive samples and five accumulations for both the nail and nail varnish. Spectral acquisition, presentation, and analysis were performed with the Renishaw WIRE (service pack 9) and GRAMS[®]AI version 8 (Thermo Electron Corp, Waltham, MA, USA) softwares.

Raman point maps ($\sim 40 \times 40 \mu\text{m}$ map area) were acquired for crystals of pure and street cocaine hydrochloride under the nail varnish. Using a 50x objective, Raman maps were obtained by collecting spectra with 10s exposure time and subsequently moving the sample in a raster pattern with a step size of 3 μm . The laser intensity at the sample was reduced to 25% (10.8 mW) to avoid burning of the sample. Data acquisition covered the spectral range 1800-100 cm^{-1} with a spectral resolution of 2 cm^{-1} with each exposure of the CCD detector. The total acquisition time for the Raman map experiment was approximately about 12 hours. Also, a Raman point map ($\sim 30 \times 30 \mu\text{m}$ map area) was acquired for a PETN crystal under the nail varnish. Using a 50x objective, Raman map was obtained by collecting spectra with 10s exposure time and subsequently moving the sample in a raster pattern with a step size of 2 μm . Data acquisition covered the spectral range 100-1800 cm^{-1} with a spectral resolution of 2 cm^{-1} with each exposure of the CCD detector. The laser intensity at the sample was reduced to 10.8 mW to avoid burning of the sample. The total acquisition time for the Raman map experiment was approximately 10 hours. A depth profile was obtained from a PETN particle coated by the nail varnish. Spectra were collected from the nail varnish coating ($Z = 0 \mu\text{m}$) and by incrementally moving the laser focus by 20

μm intervals through the PETN particle to the nail substrate using the graduated fine focus adjust of the microscope.

6.3 Results and Discussion

6.3.1 Detection of pure drugs of abuse on human nail

Raman spectroscopy provides a unique spectral ‘fingerprint’ of any molecule, so each spectrum is molecularly specific and contains key signature bands that can be used for unambiguous identification. The Raman spectra of cocaine hydrochloride, MDMA, amphetamine, nitrazepam, and flunitrazepam in the spectral wavenumber region $1800\text{-}100\text{ cm}^{-1}$ are shown in Figure 6.1. Also, Table (6.1) lists the Raman shifts and vibrational assignments of the principal characteristic bands in the spectra of the drugs of abuse, which can be used to identify them. Figure (6.2 C) shows the Raman spectrum of human nail and vibrational assignments of the main bands are listed in table (6.2). The spectra obtained from pure cocaine hydrochloride, MDMA and amphetamine sulphate crystals on human nail are shown in figures (6.2), (6.3) and (6.4), respectively. Comparison of these spectra with the reference spectra of the drugs showed that the drugs could be easily identified using their Raman spectra. The Raman spectrum of cocaine hydrochloride has several characteristic features that can be used to identify the drug, such as the benzoate ester (C=O) stretch at 1711 cm^{-1} , the aromatic ring (C=C) stretch at 1594 cm^{-1} , ring breathing mode at 998 cm^{-1} , pyrrolidine ring (C-C) stretch at 866 cm^{-1} , and the piperidine ring (C-C) stretch at 784 cm^{-1} , respectively. Also, the characteristic Raman bands of MDMA could be identified such as those at 807 , 769 and 712 cm^{-1} . These MDMA characteristic bands were tentatively assigned to the δ (OCCO)_{symm} (sub. catechol) mode, the aryl C–H wag mode, and the δ (C-C-C) mode, respectively. It can also be observed that the Raman spectrum obtained from a crystal of amphetamine sulphate on the surface of the nail

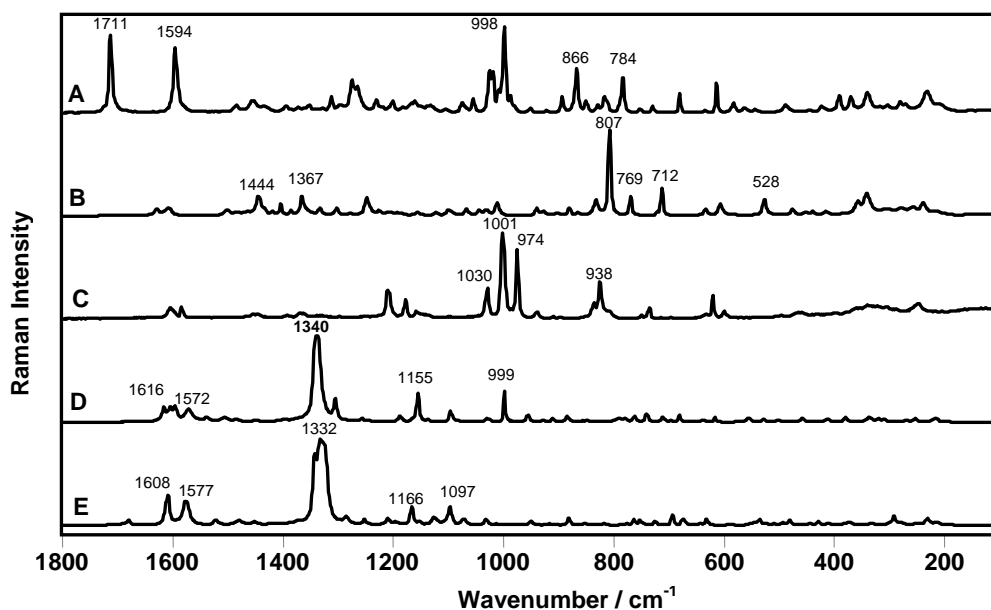


Figure 6.1 Reference Raman spectra of drugs of abuse

A: Cocaine hydrochloride

B: MDMA

C: Amphetamine sulphate

D: Nitrazepam

E: Flunitrazepam

785 nm, 90.8 mW, 10 second exposure, 1 accumulation for A-E

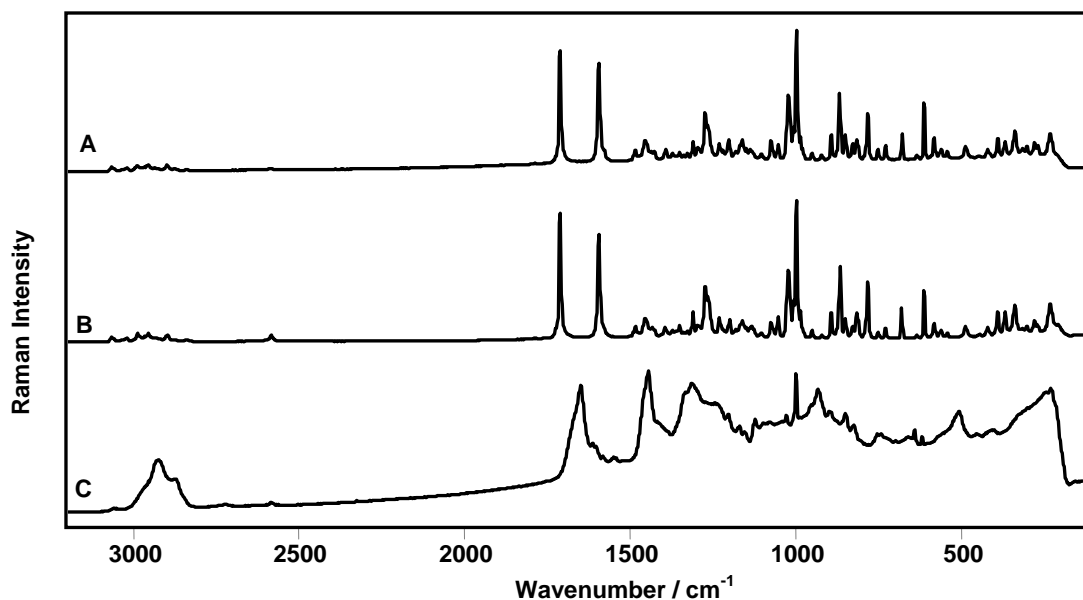


Figure 6.2 Raman spectra of

A: Cocaine hydrochloride on human nail

B: Reference cocaine hydrochloride

C: Human nail

785 nm, 90.8 mW, 10s exposure, 1 accumulation for A & B, 5 accumulations for C

Drugs of Abuse	Raman shift / cm^{-1} , Vibrational assignment	Reference
Cocaine hydrochloride	1711 cm^{-1} ; benzoate ester (C=O) stretch	140
	1594 cm^{-1} ; aromatic ring (C=C) stretch	
	998 cm^{-1} ; ring breathing mode	
	866 cm^{-1} ; pyrrolidine ring (C-C) stretch	
	784 cm^{-1} ; piperidine ring (C-C) stretch	
MDMA	1444 cm^{-1} ; $\delta_{\text{asym}}(\text{CH}_3)$ / $\delta(\text{CH}_2)_{\text{scissors}}$	158
	1367 cm^{-1} ; $\delta_{\text{sym}}(\text{CH}_3)$	
	807 cm^{-1} ; $\delta(\text{OCCO})_{\text{symm}}$ (sub. catechol)	
	769 cm^{-1} ; Aryl C-H wag	
	712 cm^{-1} ; $\delta(\text{C-C-C})$ mode	
	528 cm^{-1} ; $\delta(\text{C-C-C})_{\text{ring}}$	
Amphetamine	1030 cm^{-1} ; $\nu(\text{C-C})$ aromatic ring vibration	158
	1001 cm^{-1} ; Monosubstituted aromatic ring breathing mode	
	974 cm^{-1} ; $\nu(\text{SO}_4^{2-})_{\text{asym}}$	
	938 cm^{-1} ; $\rho(\text{CH}_3)$	
Nitrazepam	1616 cm^{-1} ; C=N stretch	129
	1572 cm^{-1} ; C=C stretch	
	1340 cm^{-1} ; symm. NO_2 stretch	
	1155 cm^{-1} ; C-C-N stretch (diazepine ring)	
	999 cm^{-1} ; aromatic ring breathing	
Flunitrazepam	1608 cm^{-1} ; C=N stretch	129
	1577 cm^{-1} ; C=C stretch	
	1332 cm^{-1} ; symm. NO_2 stretch	
	1166 cm^{-1} ; C-C-N stretch (diazepine ring)	
	1097 cm^{-1} ; aromatic in-plane CH deformation	

Table 6.1 Raman shifts and vibrational assignments of the principal characteristic bands in the spectra of the drugs of abuse.

Wavenumber / cm^{-1}	Assignment
2930	ν (CH_3) symmetric
2873	ν (CH_2) asymmetric
1650	amide I ν ($\text{C}=\text{O}$)
1445	δ (CH_2) scissoring
1315	δ (CH_2)
1001	ν (CC) aromatic ring
934	ρ (CH_3) terminal
850	δ (CCH) aromatic
509	ν (SS)

Table 6.2 Raman shifts and vibrational assignments of the main bands of human nail (References 212, 216)

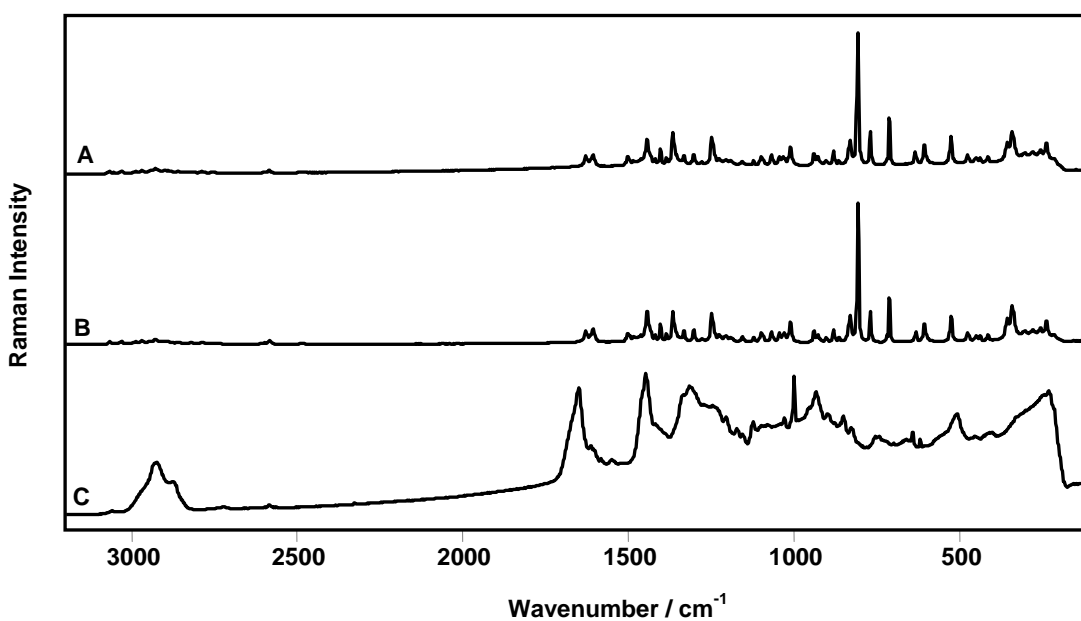


Figure 6.3 Raman spectra of
A: MDMA on human nail
B: Reference MDMA
C: Human nail
785 nm, 90.8 mW, 10s exposure, 1 accumulation for A & B, 5 accumulations for C

(Figure 6.4) contains some bands assigned to the nail substrate; the ν (CH_3) at 2930 cm^{-1} , the amide I ($\text{C}=\text{O}$) at 1650 cm^{-1} and the δ (CH_2) mode at 1445 cm^{-1} . [212, 216] These bands do not interfere with the identification of amphetamine which can be established by the diagnostic features at 1030 cm^{-1} [$\nu(\text{C}-\text{C})$], 1001 cm^{-1} [monosubstituted aromatic ring breathing], and 974 cm^{-1} [$\nu(\text{SO}_4)^{2-}$ asym]. Similarly, the confocal spectra obtained from flunitrazepam (Figure 6.5) and nitrazepam crystals (Figure 6.6) on human nail show the key signature bands of these drugs (Table 6.1) and no significant bands can be assigned to the nail substrate.

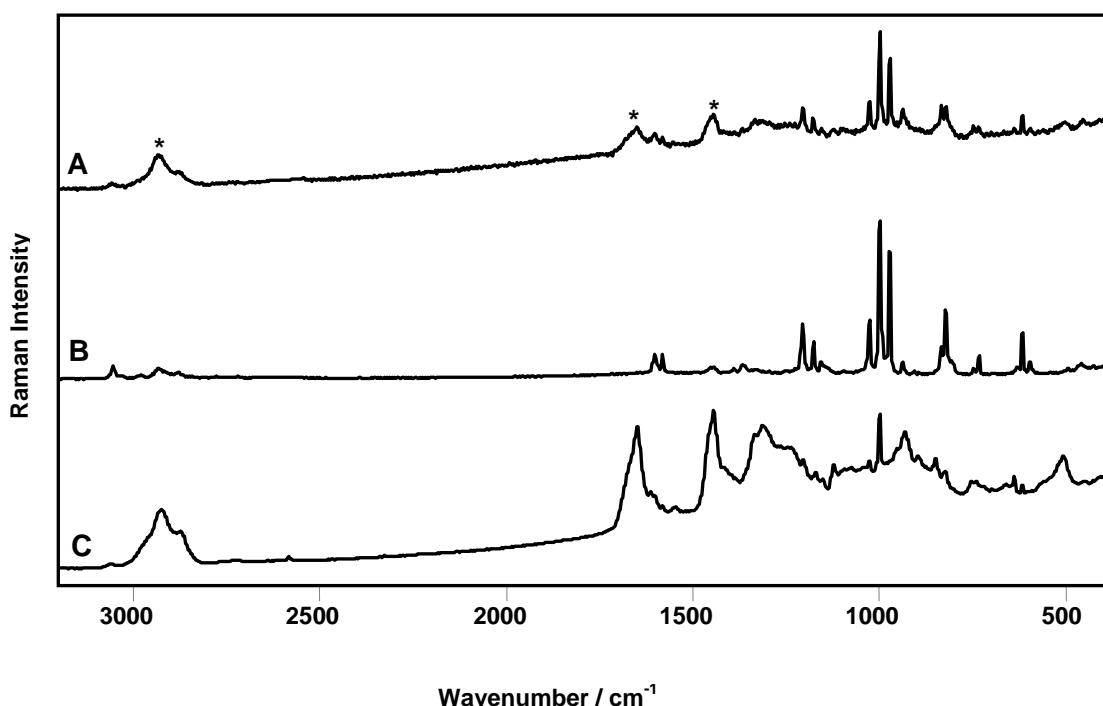


Figure 6.4 Raman spectra of
 A: Amphetamine on human nail (Asterisks indicate nail bands)
 B: Reference amphetamine
 C: Human nail
 785 nm, 90.8 mW, 10s exposure, 1 accumulation for A & B, 5 accumulations for C

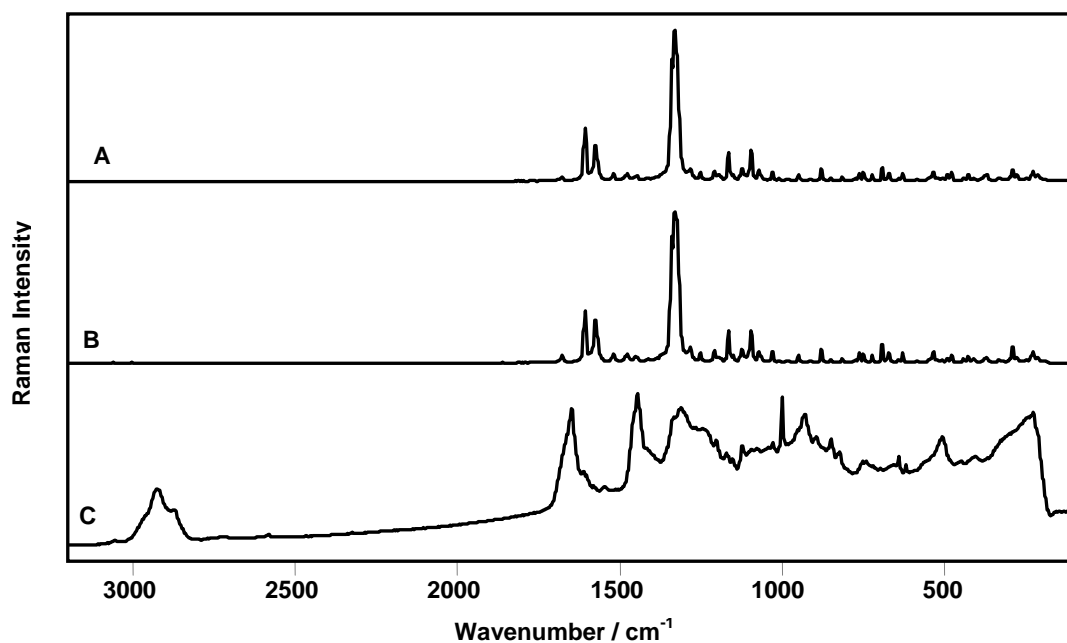


Figure 6.5 Raman spectra of
 A: Flunitrazepam on human nail
 B: Reference flunitrazepam
 C: Human nail
 785 nm, 90.8 mW, 10s exposure, 1 accumulation for A &B, 5 accumulations for C

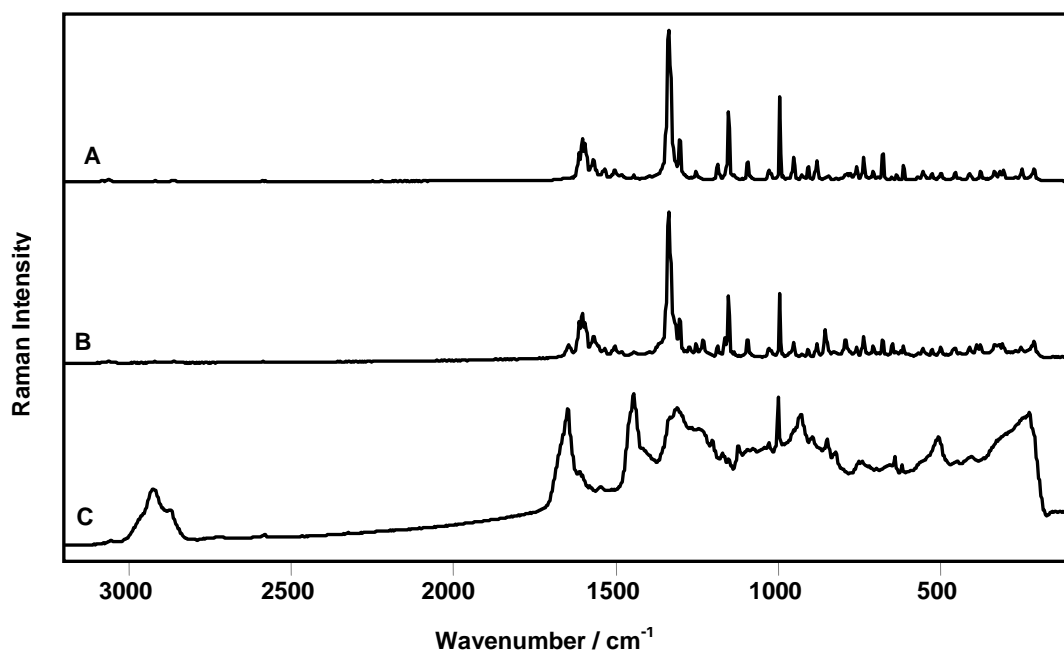


Figure 6.6 Raman spectra of
 A: Nitrazepam on human nail
 B: Reference nitrazepam
 C: Human nail
 785 nm, 90.8 mW, 10s exposure, 1 accumulation for A &B, 5 accumulations for C

6.3.2 Detection of seized drugs of abuse on human nail

Illegal drugs are generally mixed with a variety of materials (cutting agents) which may complicate the detection of the drugs on the nail. Fluorescence emission arising from these substances may overwhelm the Raman signal from the drugs of abuse. In addition, the Raman bands of the cutting agents may overlap with the characteristic bands of the drugs. Nail clippings were doped with few crystals of seized street samples of drugs of abuse namely cocaine hydrochloride, MDMA and amphetamine from which confocal Raman spectra were obtained. Although these spectra contain some bands arising from the nail substrate and/or the excipients, the major bands of the drugs of abuse are still very clear and are not obscured by spectral bands due to excipients in the street samples (Figures 6.7- 6.9). It can also observe that there is some fluorescence background in the spectra of the drugs which may arise from the cutting agents.

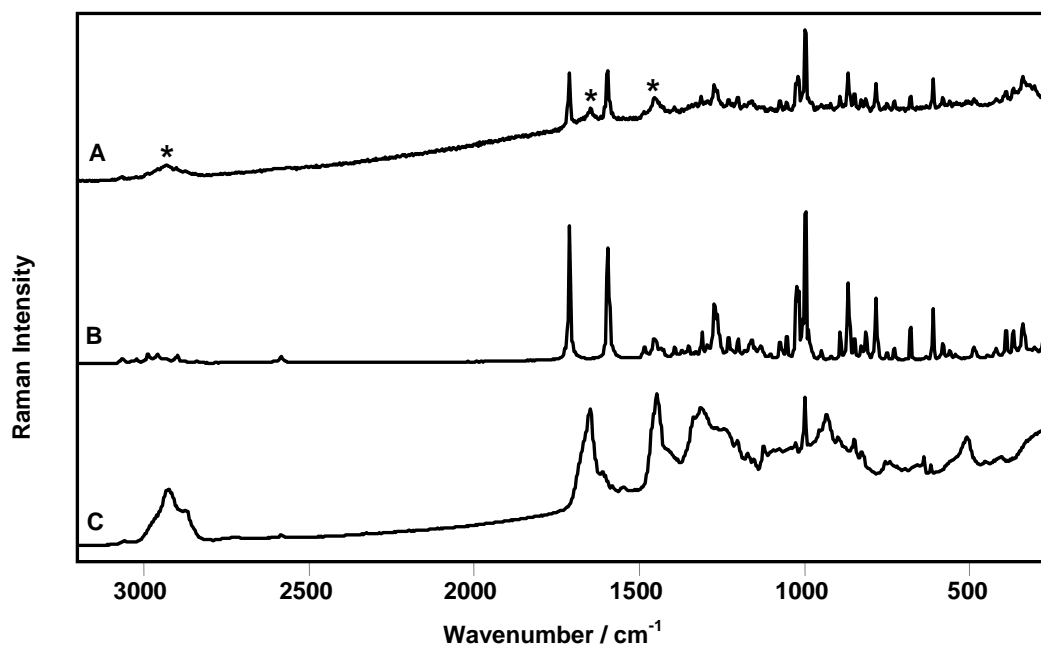


Figure 6.7 Raman spectra of

A: Street cocaine hydrochloride on human nail (Asterisks indicate nail bands)

B: Reference cocaine hydrochloride

C: Human nail

785 nm, 90.8 mW, 10s exposure, 1 accumulation for A &B, 5 accumulations for C

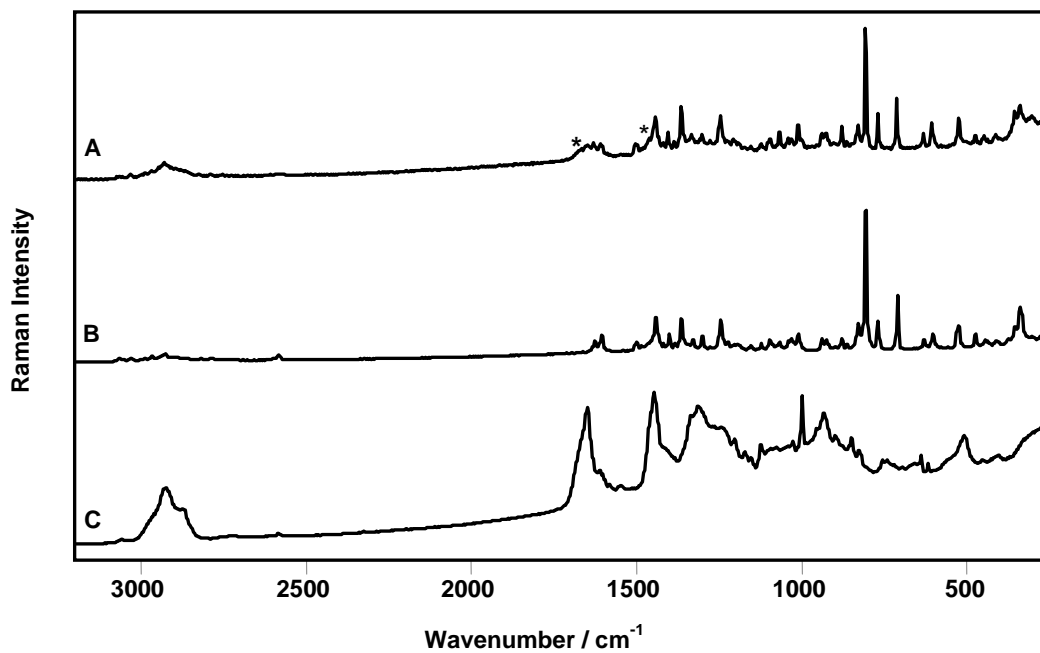


Figure 6.8 Raman spectra of

A: Street MDMA on human nail (Asterisks indicate nail bands)

B: Reference MDMA

C: Human nail

785 nm, 90.8 mW, 10s exposure, 1 accumulation for A & B, 5 accumulations for C

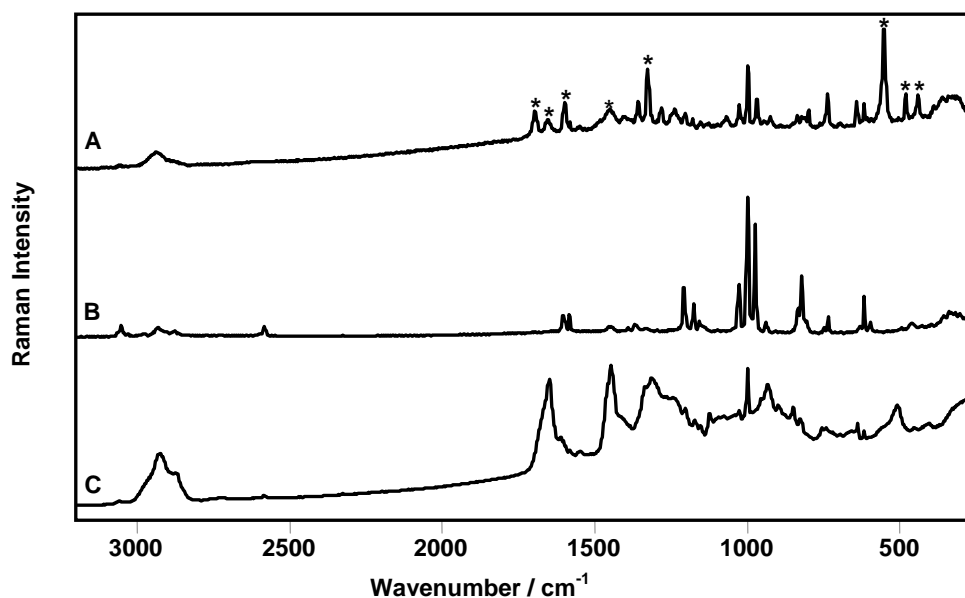


Figure 6.9 Raman spectra of

A: Street amphetamine on human nail (Asterisks indicate bands from nail & excipients)

B: Reference amphetamine

C: Human nail

785 nm, 90.8 mW, 10s exposure, 1 accumulation for A & B, 5 accumulations for C

6.3.3 Detection of drugs of abuse under nail varnish

The incident laser radiation was focused with the microscope objective to record the Raman spectra from crystals of drugs of abuse coated with a nail varnish. It can be observed that a significant fluorescence emission is present in the Raman spectrum of the nail varnish (Figure 6.10A). The diagnostic Raman bands of cocaine hydrochloride can be clearly identified in the spectrum obtained from a crystal of the drug masked by the nail varnish (Figure 6.10). Although the drug crystal is sandwiched between the highly fluorescent nail varnish and the nail substrate, the Raman spectrum could be obtained without interference from these highly fluorescent matrices. Also, the spectrum obtained from an MDMA crystal coated with a nail varnish (Figure 6.11) shows the characteristic Raman bands of the drugs. Despite the presence of some bands assignable to the nail varnish (marked with asterisks at figure 6.11B), these

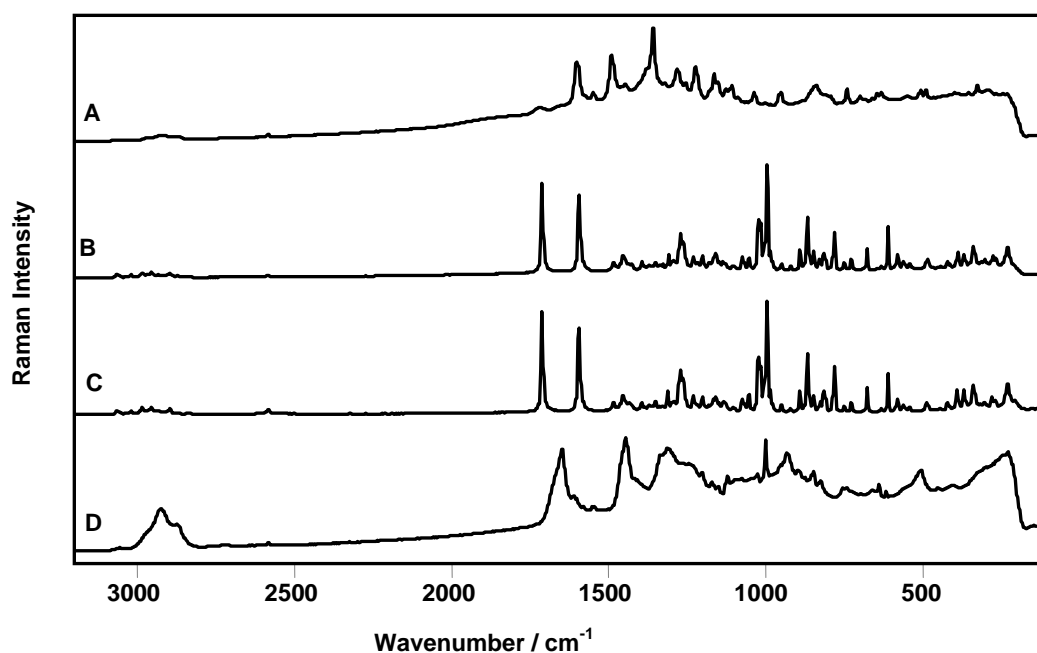


Figure 6.10 Raman spectra of:

A: Nail varnish

B: Pure cocaine.HCl crystal under nail varnish

C: Reference cocaine hydrochloride

D: Nail

785 nm, 90.8 mW, 10s exposure, 1 accumulation for B & C, 5 accumulations for A & D

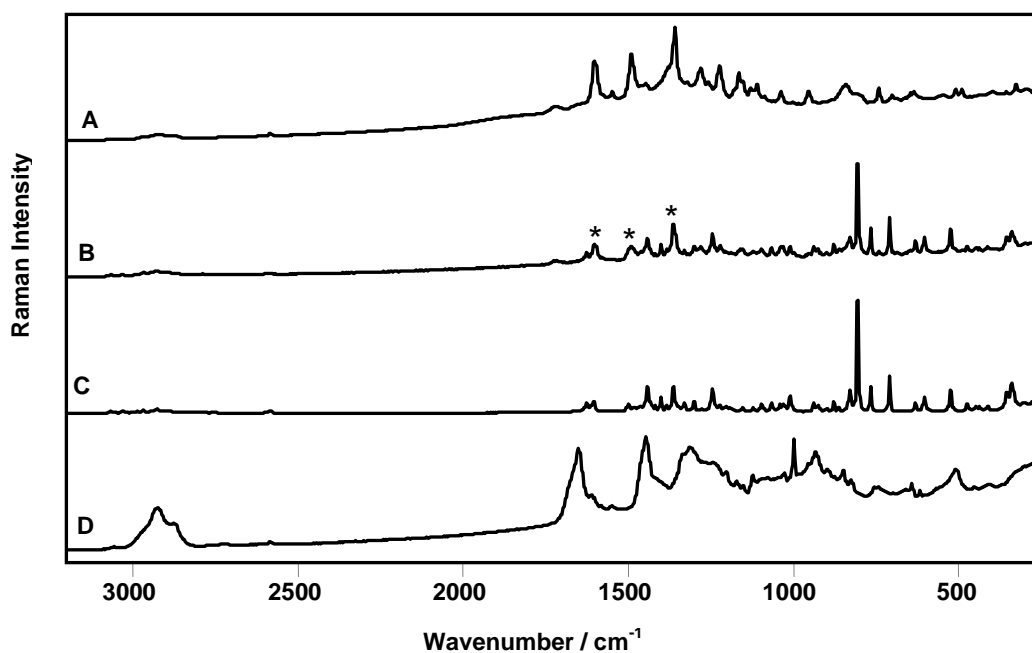


Figure 6.11 Raman spectra of:

A: Nail varnish

B: MDMA crystal under nail varnish (asterisks indicate nail varnish bands)

C: Reference MDMA

D: Nail

785 nm, 90.8 mW, 10s exposure, 1 accumulation for B & C, 5 accumulations for A&D

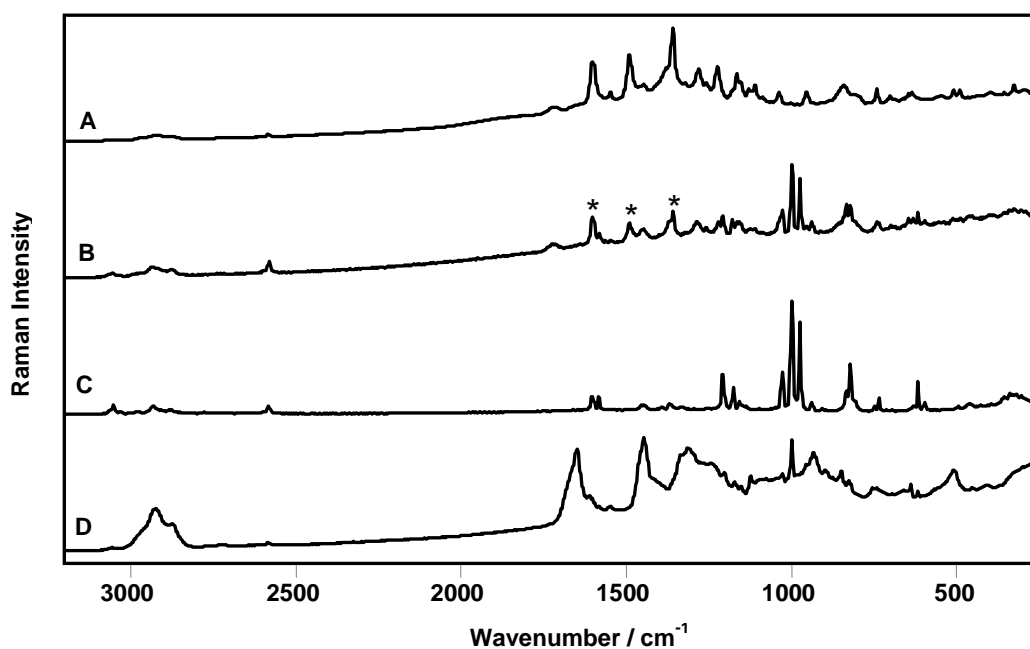


Figure 6.12 Raman spectra of:

A: Nail varnish

B: Amphetamine crystal under nail varnish (asterisks indicate nail varnish bands)

C: Reference amphetamine

D: Human nail

785 nm, 90.8 mW, 10s exposure, 1 accumulation for B & C, 5 accumulations for A&D

bands do not interfere with the identification of the drug. Similarly, the confocal Raman spectrum acquired from an amphetamine crystal (Figure 6.12) masked by the nail varnish comprises three bands arising from the nail varnish. These bands do not prevent identification of the drug as they do not overlap with the key bands of amphetamine sulphate. Figures 6.13 and 6.14 show the Raman spectra acquired from flunitrazepam and nitrazepam crystals under a nail varnish coating, respectively, in which the characteristic bands of the drugs can be unambiguously identified. There are no significant bands in the spectra which can be assigned to either the nail substrate or the nail varnish coating.

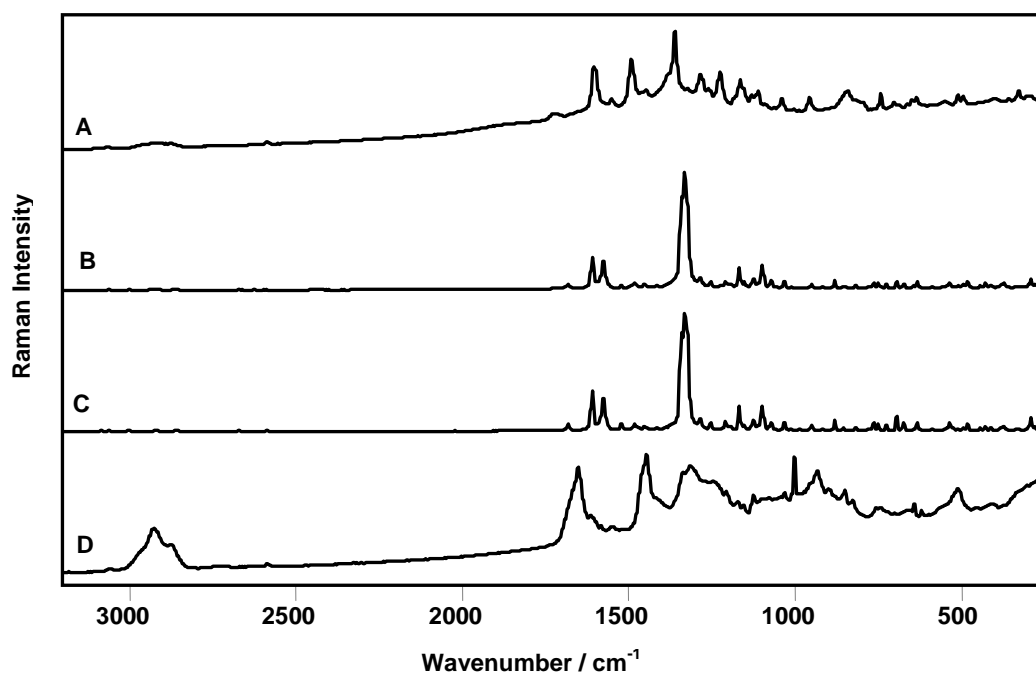


Figure 6.13 Raman spectra of:

A: Nail varnish

B: flunitrazepam crystal under nail varnish

C: Reference flunitrazepam

D: Nail

785 nm, 90.8 mW, 10s exposure, 1 accumulation for B & C, 5 accumulations for A&D

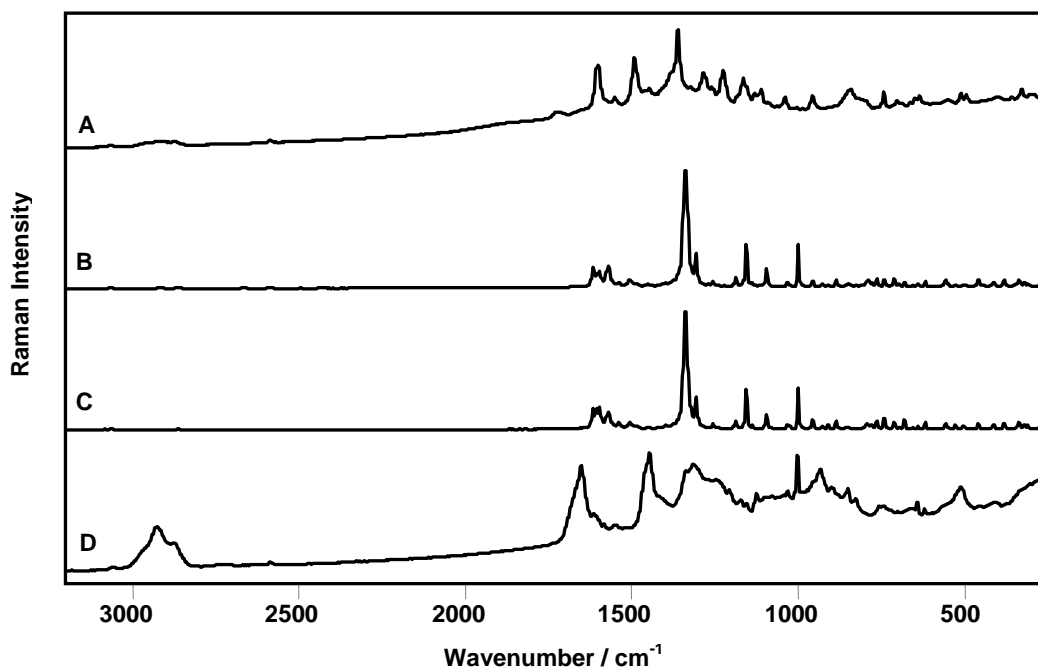


Figure 6.14 Raman spectra of:

A: Nail varnish

B: Nitrazepam crystal under nail varnish

C: Reference nitrazepam

D: Nail

785 nm, 90.8 mW, 10s exposure, 1 accumulation for B & C, 5 accumulations for A&D

6.3.4 Detection of explosives on human nail

In this section, the feasibility of using confocal Raman microscopy for the detection of explosives and their precursors on the surface of human nail has been investigated.

The Raman spectra of the explosives PETN, TNT, ammonium nitrate, and of the explosive precursors HMTA and pentaerythritol are shown in figure 6.15. Also, table (6.3) lists the Raman shifts and vibrational assignments of the principal characteristic bands in the spectra of the explosives, which can be used to identify each substance within the group of explosives studied. It has been observed that the spectra obtained from the explosive particles on the surface of the nail contain some bands arising from the nail substrate. In each case the strongest bands arising from the nail substrate did not interfere with the identification of the explosives as these bands do not overlap

with the characteristic Raman bands of the explosive substances. Figure (6.16) shows an image of a PETN crystal of several microns in size on the surface of the nail and the Raman spectrum obtained from this crystal is shown in figure (6.17A). Comparison of this spectrum with the reference spectrum showed that PETN could be easily identified by its Raman spectrum which comprises strong sharp features in the fingerprint region of the spectrum. The Raman spectrum of PETN has several characteristic features of nitrate ester explosives which can be used to identify it; the symmetric (NO_2) stretching mode at 1290 cm^{-1} , the (O-N) stretch mode at 871 cm^{-1} , and the (CCC) deformation mode at 622 cm^{-1} . PETN could be identified from these strong bands and, through careful confocal sampling, no significant peaks in the spectrum appear from the nail substrate.



Figure 6.16 PETN crystal on the surface of human nail

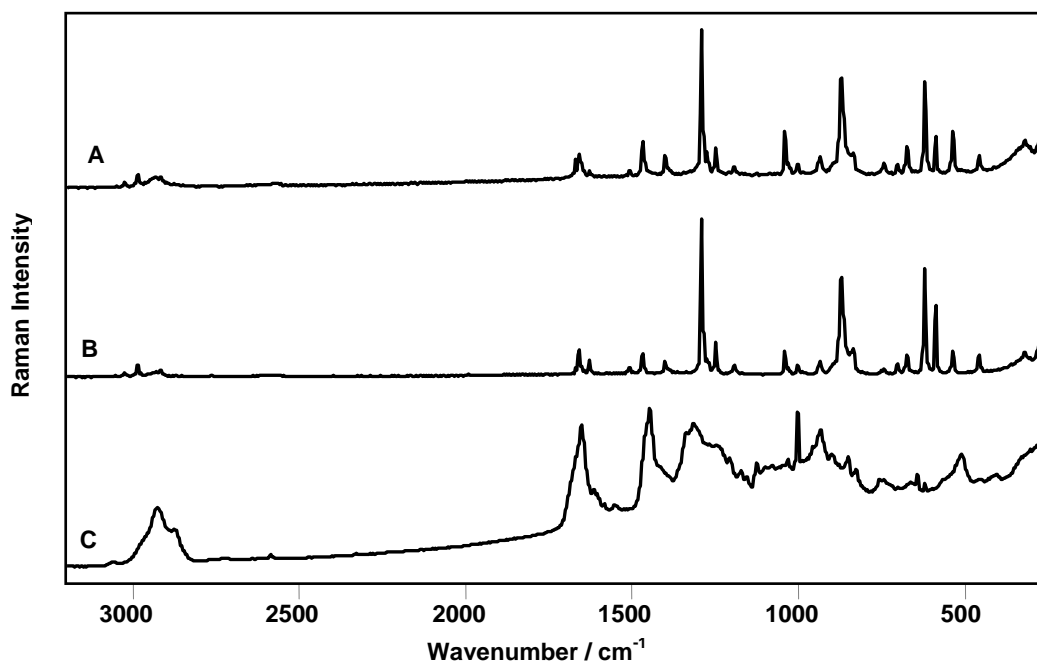


Figure 6.17 Raman spectra of:

A: PETN on the surface of the nail

B: Reference PETN

C: Human Nail

785 nm, 90.8 mW, 10s exposure, 1 accumulation for A & B, 5 accumulations for C

A confocal spectrum obtained from a TNT crystal on the surface of the nail (Figure 6.18) shows that the explosive could be readily identified. The Raman spectrum of TNT contains several diagnostic features such as the $\nu_{\text{as}}(\text{NO}_2)$ at 1532 cm^{-1} , the $\nu_{\text{s}}(\text{NO}_2)$ at 1357 cm^{-1} and the (NO_2) scissoring mode at 822 cm^{-1} . Despite that TNT spectrum contains two very weak bands arising from the nail; the amide I (C=O) at 1650 cm^{-1} and the $\delta(\text{CH}_2)$ mode at 1445 cm^{-1} , these nail bands do not overlap with the explosive characteristic bands. Also, a spectrum obtained from an ammonium nitrate crystal embedded on the surface of the nail (Figure 6.19) contains some bands arising from the nail; the amide I (C=O) at 1650 cm^{-1} and the $\delta(\text{CH}_2)$ mode at 1445 cm^{-1} . The presence of these nail bands did not prevent identification of ammonium nitrate which could be identified by its very strong $(\text{NO}_3)^-$ stretching mode at 1040 cm^{-1} and the $(\text{NO}_3)^-$ bending mode at 712 cm^{-1} .

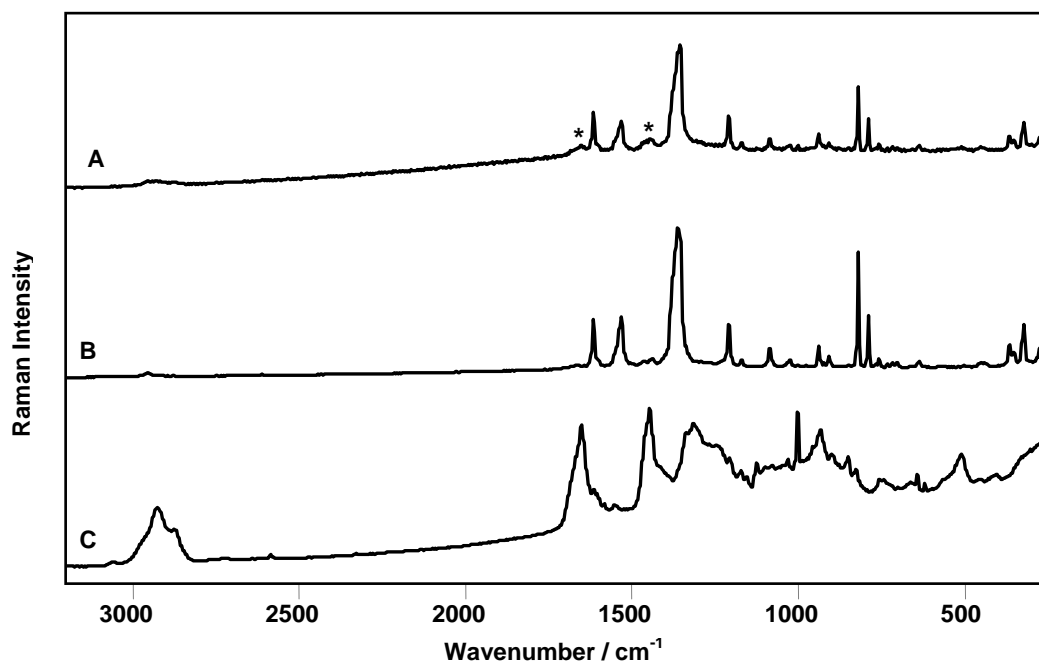


Figure 6.18 Raman spectra of:

A: TNT on the surface of the nail

B: Reference TNT

C: Human Nail

785 nm, 90.8 mW, 10s exposure, 1 accumulation for A &B, 5 accumulations for C

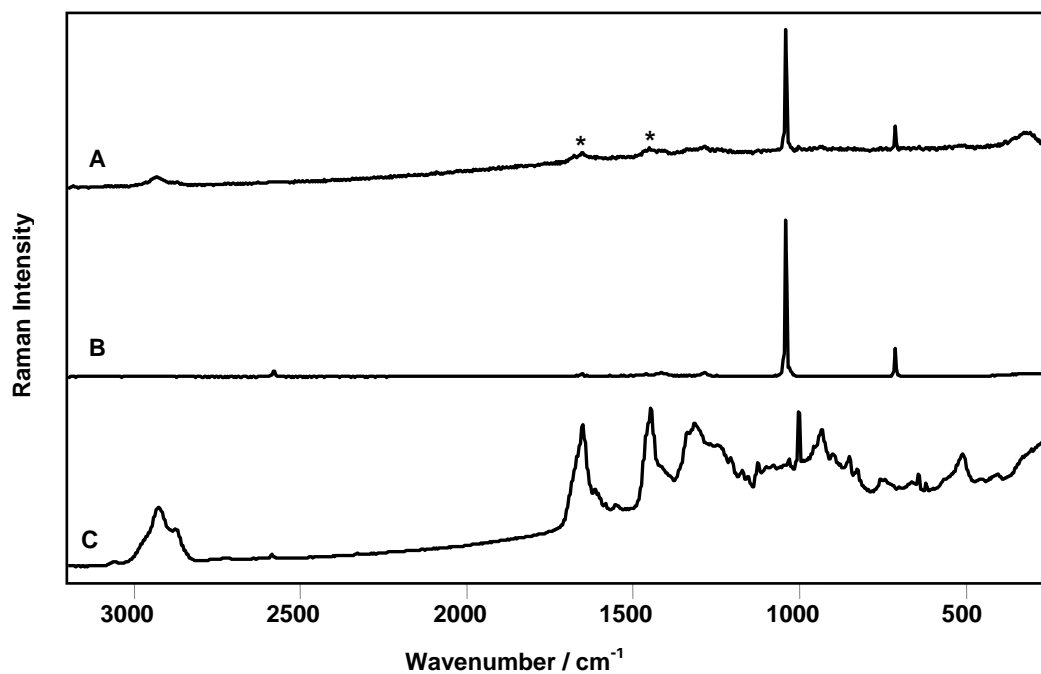


Figure 6.19 Raman spectra of:

A: Ammonium nitrate on the surface of the nail

B: Reference ammonium nitrate

C: Human Nail

785 nm, 90.8 mW, 10s exposure, 1 accumulation for A &B, 5 accumulations for C

The Raman spectrum obtained from an HMTA crystal on the surface of the nail is shown in Figure (6.20). It is observed that the amide I (C=O) mode assigned to the nail substrate appears as a broad weak band at 1650 cm^{-1} . The presence of this band did not interfere with the identification of the explosive precursor HMTA which can be easily identified by several characteristic signature bands such as the strong (N-C-N) bending modes at 1040 and 462 cm^{-1} , and the very strong (N-C) stretching mode at 777 cm^{-1} . Similarly, the amide I (C=O) band appears at 1650 cm^{-1} in the Raman spectrum collected from a pentaerythritol particle on the surface of the nail (Figure 6.21). The identity of the explosive precursor can be established by the key Raman bands at 439 cm^{-1} [δ (C-C-C)], 873 and 810 cm^{-1} [δ (CH_2)_{rock}] and 1071 cm^{-1} [ν (C-O)].

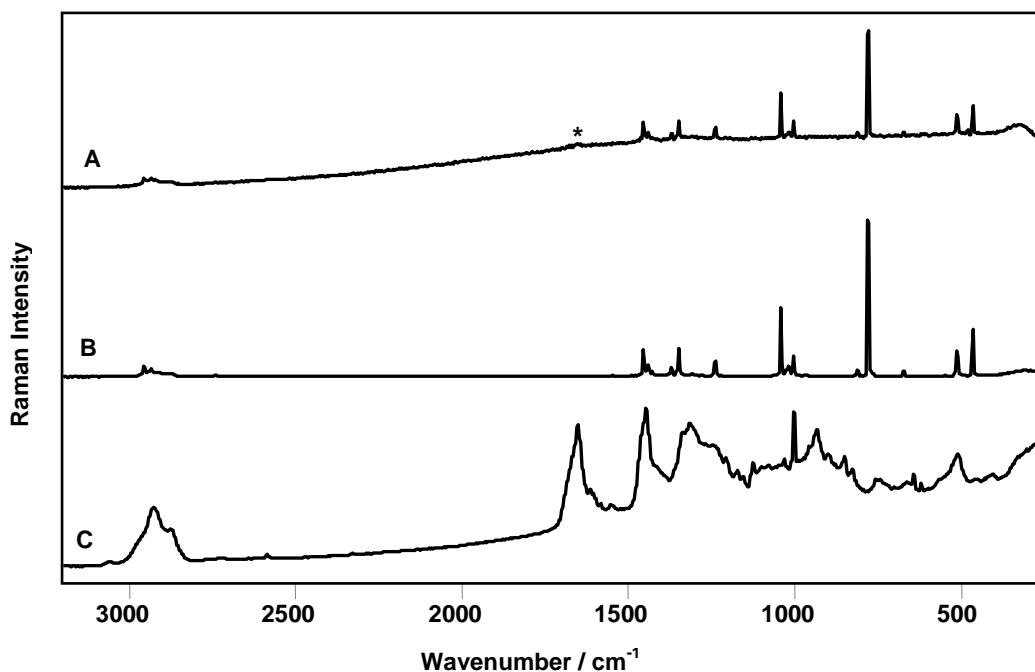


Figure 6.20 Raman spectra of:

A: HMTA on the surface of the nail

B: Reference HMTA

C: Human Nail

785 nm, 90.8 mW, 10s exposure, 1 accumulation for A & B, 5 accumulations for C

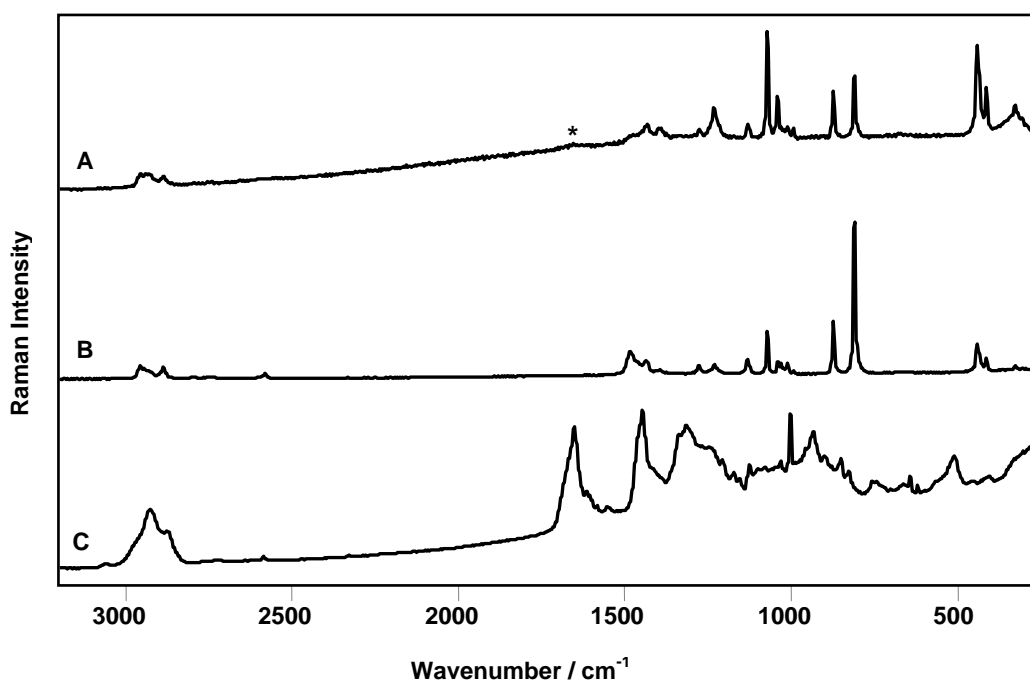


Figure 6.21 Raman spectra of:

A: Pentaerythritol on the surface of the nail

B: Reference Pentaerythritol

C: Human Nail

785 nm, 90.8 mW, 10s exposure, 1 accumulation for A & B, 5 accumulations for C

6.3.5 Detection of explosives under nail varnish

Figure (6.22) shows an image of a PETN crystal obscured by nail varnish. The incident laser radiation was focused with the microscope objective onto this crystal, and the collected Raman spectrum is displayed in Figure (6.23A). Comparing the spectrum of PETN under the nail varnish with the reference spectrum, it is clearly observed that PETN can be identified, and there are no significant peaks in the spectrum that are clearly attributable to either the nail or nail varnish. Although the crystal of the explosive is sandwiched between the highly fluorescent nail varnish and the nail substrate, the Raman spectrum could be obtained without interference from these fluorescent matrices. Also, the spectra obtained from TNT (Figure 6.23B) and ammonium nitrate (Figure 6.23C) crystals under the nail varnish show the characteristic Raman bands of the explosives and no significant band can be assigned

to either the nail varnish coating or the nail substrate. Coating of the explosive particles with the nail varnish presented no difficulty in determining the identity of the explosive substances. Further illustrations of the applicability of this approach were obtained from HMTA and pentaerythritol particles covered by nail varnish (Figure 6.24). These spectra are of good S/N ratio, with no detectable background fluorescence. Although these spectra contain two bands assignable to the nail varnish, the characteristic bands of the explosive precursors can be clearly identified.

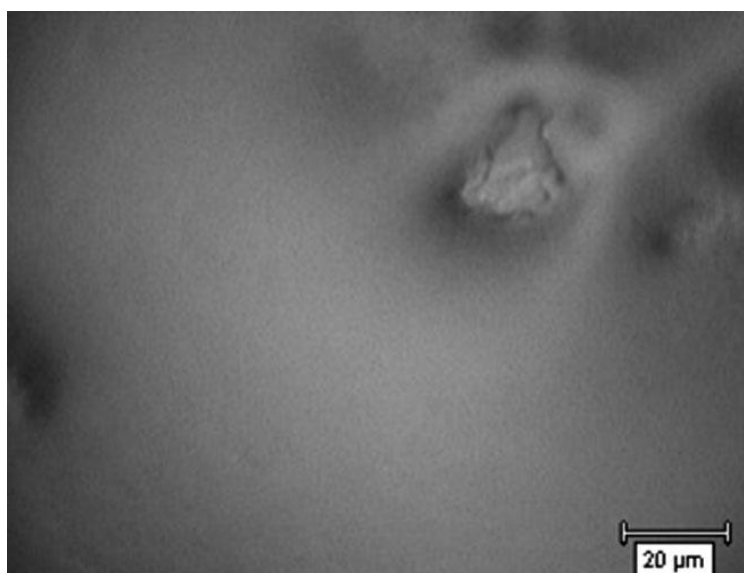


Figure 6.22 PETN crystal under nail varnish.

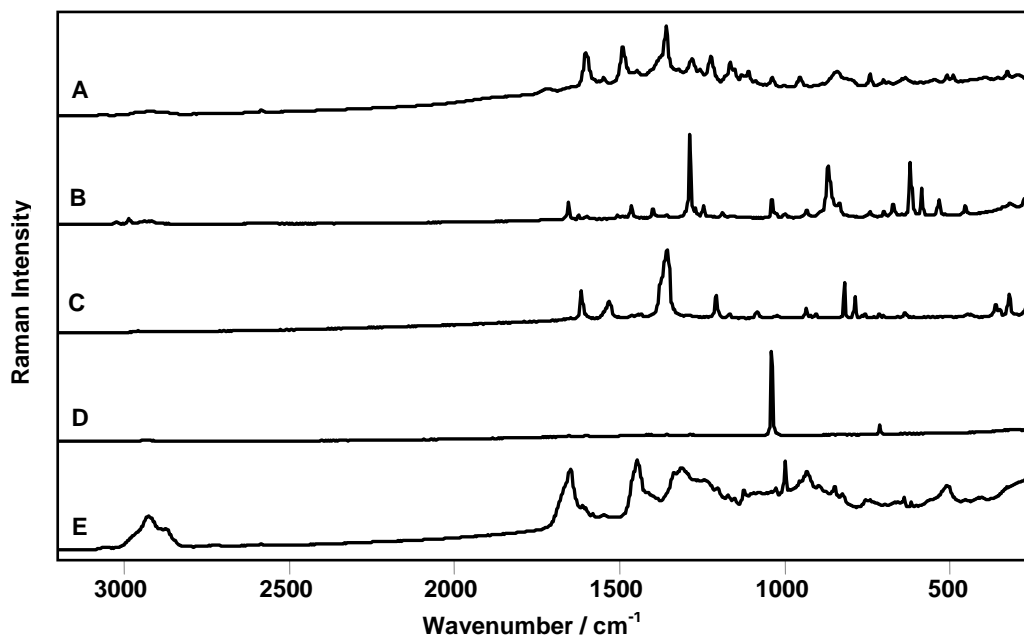


Figure 6.23 Raman spectra of:

A: Nail varnish

B: PETN crystal under nail varnish

C: TNT crystal under nail varnish

D: Ammonium nitrate crystal under nail varnish

E: Human Nail

785 nm, 90.8 mW, 10s exposure, 1 accumulation for B-D, 5 accumulations for A&E

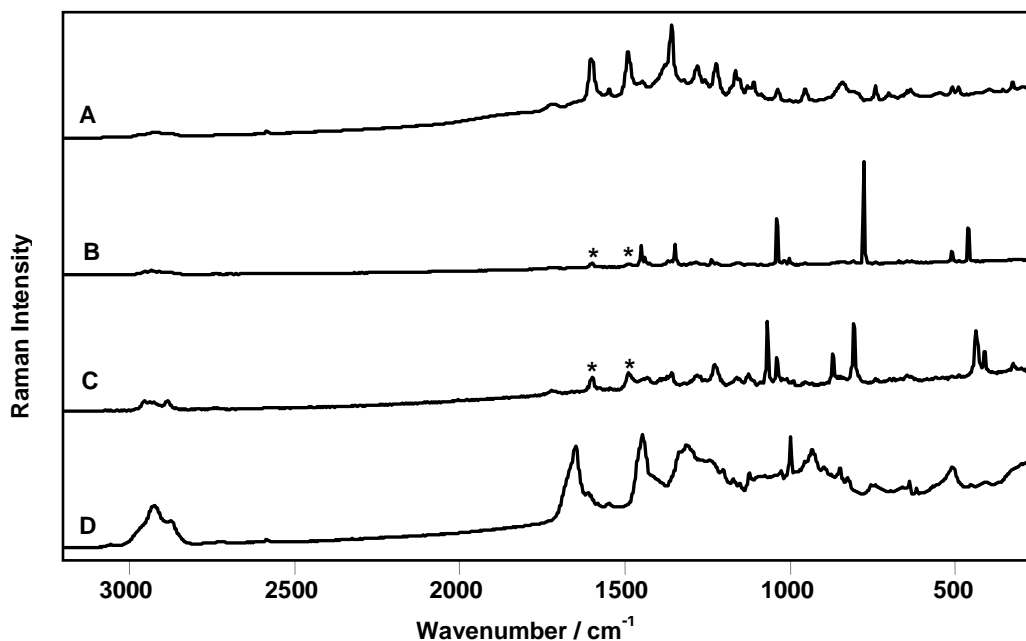


Figure 6.24 Raman spectra of:

A: Nail varnish

B: HMTA crystal under nail varnish

C: Pentaerythritol crystal under nail varnish

D: Human Nail

785 nm, 90.8 mW, 10s exposure, 1 accumulation for B&C, 5 accumulations for A&D

To summarize the previous results, table 6.4 lists the characteristic Raman bands of each drug of abuse and explosives that have been identified in the spectra obtained from particles of these substances on the surface of human nail.

Drugs of abuse and Explosives on nail	Detected bands (cm ⁻¹)
Cocaine hydrochloride	1711(s),1594(s),998(s),866 (m) ,784 (m)
MDMA	1444(m),1367(m) ,807(s) ,769(m) ,712(m) , 528(m)
Amphetamine sulphate	1030(m) ,1001(s) ,974(s) ,938(m)
Flunitrazepam	1608 (m),1577 (m),1332 (vs), 1166 (m), 1097 (m)
Nitrazepam	1616 (m), 1572(m) ,1340 (vs), 1155 (m), 999(m)
PETN	1290 (vs), 871(s),622(s)
TNT	1532 (m),1357 (vs),822 (m)
Ammonium nitrate	1040 (vs) ,712 (m)
hexamethylenetetramine	1040(m) ,777(s), 462(m)
pentaerythritol	1071(vs),873(m) , 810(m) ,439(s)

Table 6.4 characteristic Raman bands of drugs of abuse and explosives identified in the spectra obtained from their particles on the surface of the nail

Raman spectra could be acquired from drugs of abuse and explosive particles on the surface of the nail with dimensions in the range 5–10 µm. The spectra are of high quality with a good signal/noise (S/N) ratio, and there was no appreciable background due to fluorescence. Spectra of the drugs of abuse and explosives could be readily obtained non-destructively within three minutes with little or no sample preparation. Confocal Raman microscopy was applied to focus the laser beam and collect the Raman scattering from particulate matter on the surface of the nail. Interference from

the nail and nail varnish was overcome by carefully focusing the confocal beam, and the resulting spectra allowed ready differentiation of interference from bands of the nail substrate and nail varnish coating. In addition, the NIR laser at 785 nm gave excellent spectra of the drugs and explosives and there was no detectable background fluorescence. This high discrimination power of the confocal microscope is attributed to the ability of such a system to isolate the light originating from a small region of the sample coincident with the focal point, which efficiently eliminates the contribution from out-of-focus zones, thereby making their Raman signals negligible.

6.3.6 Raman mapping [222 , 223]

Raman mapping is a non-invasive technique capable of probing the chemical composition of materials at micrometre-to-submicrometre scales with little or no sample preparation. Selective maps of the sample depicting the distribution of a given molecular species can be obtained. Point and line Raman mapping involve either a laser spot or a laser line sample illumination. In point mapping, the laser beam is focused by the microscope objective on the surface of the sample that is placed on a motorized microscope stage driven by a computer. The automatic step-by-step displacement of the stage in both the x and y directions allows any selected area of the sample to be scanned. All information is acquired sequentially during the scanning of the surface of the sample. For each position of the sample, a complete Raman spectrum is recorded. Then the computer can build up maps of the sample by retrieving in its memory, for each location, any spectroscopic information of interest (e.g. band position, band intensity, band area, half band width, etc.). Also, the improved axial resolution on the confocal Raman microscopy allows non-destructive depth profiling by acquiring spectra as the laser focus is moved incrementally deeper into a transparent sample. This approach often is termed “optical sectioning” as

opposed to mechanically cutting a cross-section and scanning the laser beam laterally across the section.

Raman mapping was carried out for crystals of pure cocaine hydrochloride, street cocaine hydrochloride ($\sim 40 \times 40 \mu\text{m}$ map area) and a PETN particle ($\sim 30 \times 30 \mu\text{m}$ map area) obscured by the nail varnish. Using the WIRE 2 software, Data were collected in an XY raster pattern and processed using band intensity, position, area, etc. In this case, a band from the analyte (998 cm^{-1} for cocaine hydrochloride and 1290 cm^{-1} for PETN) was chosen that was not affected by other species in the matrix. This band was curve-fitted using WIRE 2, and the mapping data was processed with this curve-fit to give false colour images of cocaine hydrochloride (Figures 6.25 and 6.26) and PETN (Figure 6.27) particles. The Raman point maps show that the particles could be clearly located under the nail varnish. Though time consuming ($\sim 10\text{-}12 \text{ h}$), the technique provides an overview of the spatial distribution of the particles of the drugs of abuse and explosives under nail varnish.

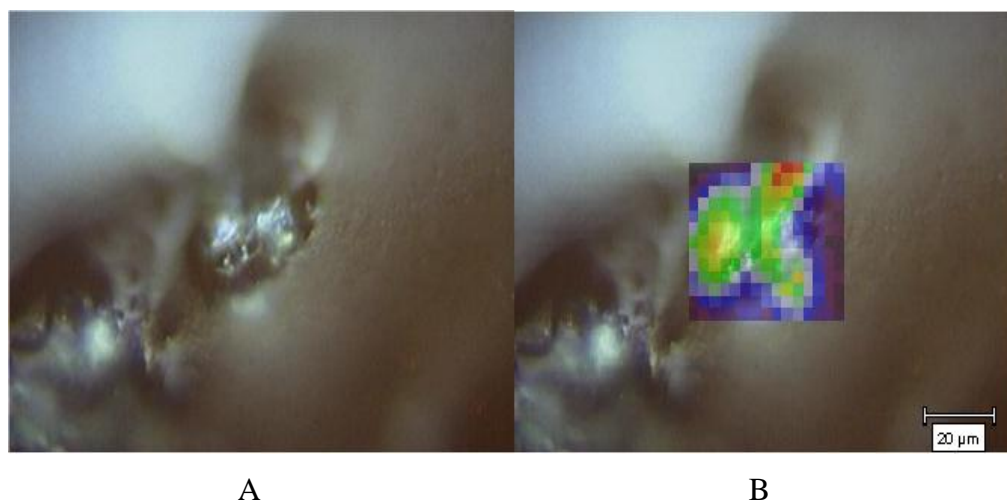


Figure 6.25

A: Video image of a pure cocaine.HCl crystal under nail varnish.

B: Raman point map of a pure cocaine.HCl crystal under nail varnish (Acquired using 998 cm^{-1} peak area) low peak area in blue, high peak area in red

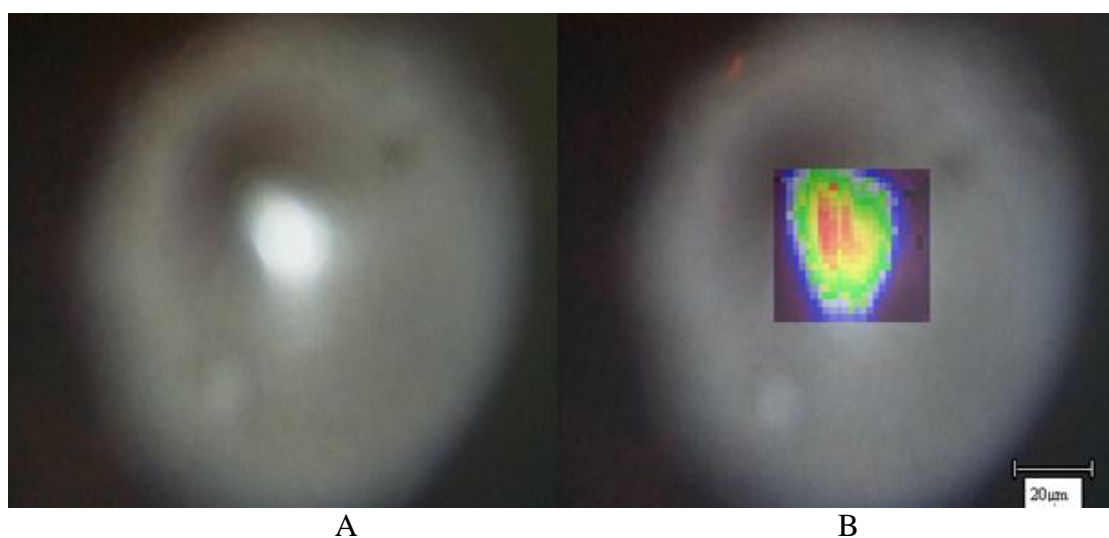


Figure 6.26

A: Video image of a street cocaine.HCl crystal under nail varnish

B: Raman point map of a street cocaine.HCl crystal under nail varnish (Acquired using 998 cm^{-1} peak area) low peak area in blue, high peak area in red

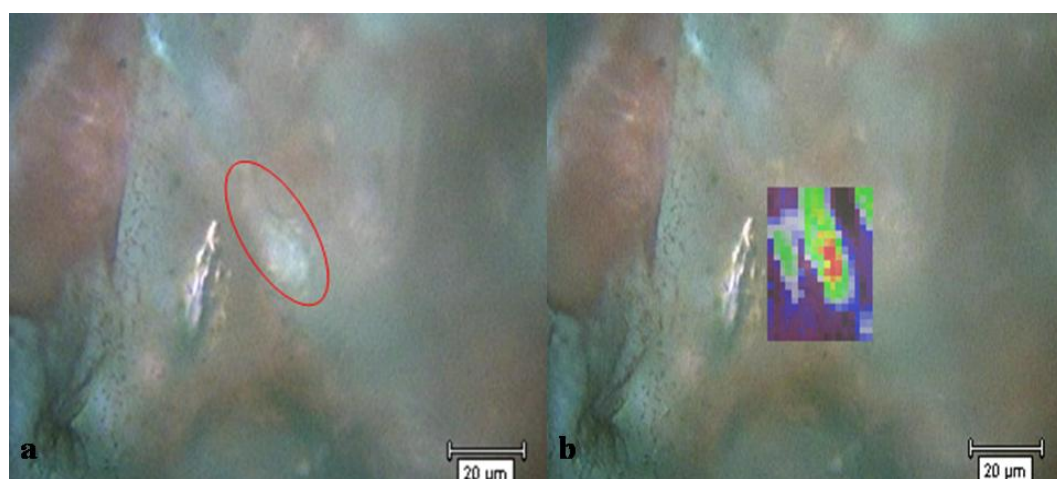


Figure 6.27

(a) Video image of a PETN crystal under nail varnish

(b) Point Raman map of PETN crystal under nail varnish (acquired using 1290 cm^{-1} peak area): low peak area in blue, high peak area in red.

Further illustrations of the depth discrimination capability of the confocal approach are demonstrated in Figure 6.28, where a PETN particle under a nail varnish coating was depth-profiled. Spectra were collected from the nail varnish coating ($Z = 0 \mu\text{m}$) and then at $20\text{-}\mu\text{m}$ intervals through the PETN particle down to the nail substrate using the graduated fine-focus adjustment of the microscope. These spectra show that the three layers are clearly distinguishable and distinctive spectra could be obtained from the nail varnish coating, the explosive contaminant and nail substrate. This investigation establishes the utility of these Raman spectroscopic techniques in this context for the first time and establishes the technique of in situ Raman mapping as a useful tool for forensic investigation.

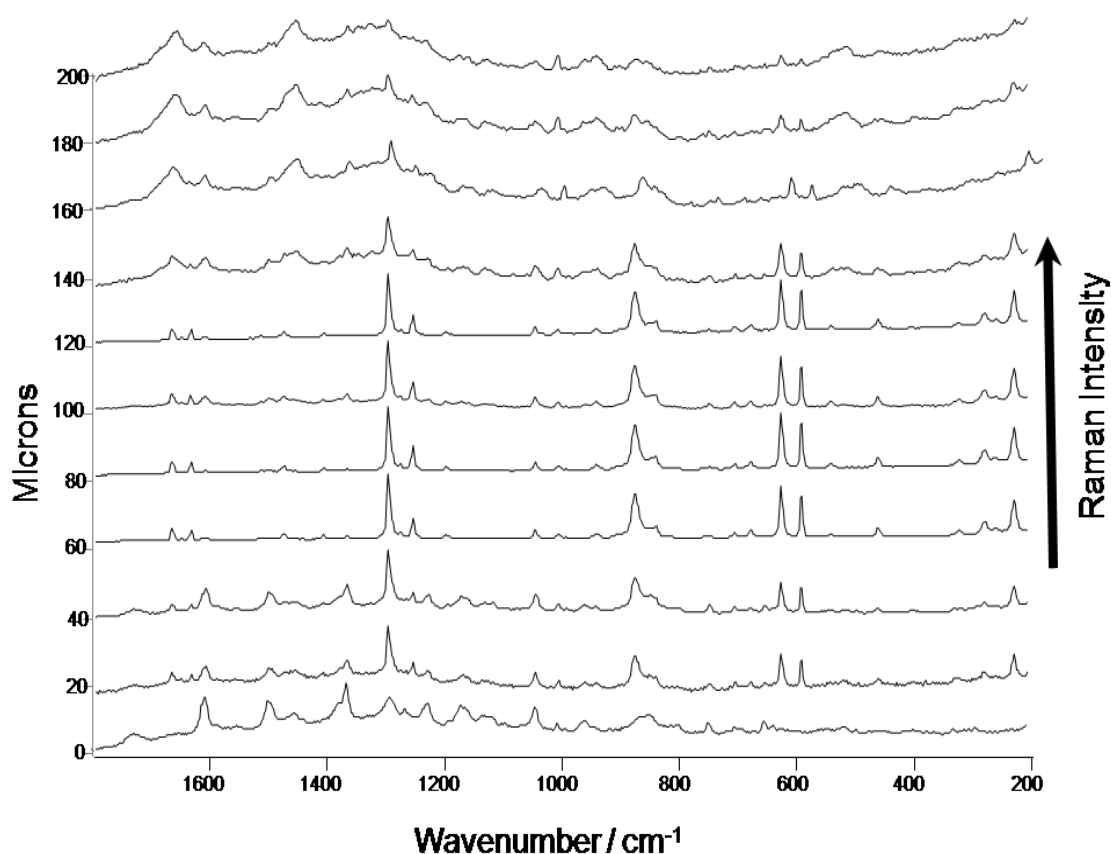


Figure 6.28 Confocal depth profile of a PETN particle coated with nail varnish. Spectra were collected from the nail varnish coating ($Z = 0 \mu\text{m}$) and at $20\text{-}\mu\text{m}$ intervals through the PETN particle down to the nail substrate.

These results confirm that the detection of drug particles on nail and other articles related to an individual, such as hair or clothing, could be of evidential value to identify this individual as a drug user or drug dealer. Also, the detection of explosives on nails can be used for security purposes or as a strong evidence to establish a link between these hazardous substances and individuals involved in possible terrorist activities.

Chapter 7

***In-situ* detection of drugs-of-abuse and explosives on clothing using confocal Raman microscopy**

7.1 Introduction

The examination of clothes represents an important step in forensic evidential investigations, especially in serious crimes such as those involving firearms related offences. ^[224-226] Clothing damage analysis is an integral part of the examinations carried out in sexual assault cases. ^[227] Trace DNA is often detected from blood or semen stains on clothes examined in forensic laboratories. ^[228,229] Moreover, drugs-of-abuse and their metabolites have been detected in garments belonging to known abusers, generally involving destructive chemical analytical procedures. ^[95,230, 231] Residues of illicit drugs on clothing can provide useful information. The transportation, re-packaging, sale and use of these materials will almost inevitably cause contamination of the clothing and other possessions of persons involved in these activities. Money contaminated with drugs can be directly associated with the drug-related crimes; a limited number of studies have demonstrated the use of Raman microscopy for the detection and identification of illicit drugs and related substances on paper currency. ^[151,152]

Two surveys of high explosives traces in public places were carried out in a number of major cities of the United Kingdom. Samples were collected from taxis, trains, buses, airports, police stations, private houses, privately owned vehicles, and clothing. The results of the surveys indicate that it is unlikely that someone in public areas could accidentally become significantly contaminated with explosives. ^[232, 233] There have been several high-profile cases in the public domain where the identification of minute amounts of particulate matter has formed a significant part of the forensic evidence.

So, the detection of explosive residues on clothing can be used as a strong evidence to establish a link between these materials and individuals involved in terrorist activities, because handling, packaging, and transportation of these materials will almost inevitably cause contamination of the premises, clothing, and other possessions of these persons. [234]

In this section, the application of confocal Raman microscopy to the in situ identification of drugs-of-abuse and explosives particulates on a variety of fibres and textiles contaminated with these materials has been investigated. Clothing of persons involved in drug-related activities will be inevitably contaminated with these drugs. Also, transportation, packaging, handling or processing of explosive substances will leave the clothing and other possessions of the involved persons contaminated with these substances. The contamination of clothing results from microscopic particles of the drugs and explosives physically trapped between the fibres of the specimens. In such situations, confocal Raman microscopy can be effectively applied for acquisition of spectra of drugs-of-abuse and explosives without significant interference from the substrate matrices. This is achieved by correlating the sampling volume with the dimensions of analyte particle. Spatial-resolution of the sample probe in this way effectively increases the sensitivity of the technique and allows molecular information to be obtained in conjunction with microscopic evaluation of evidential materials. Importantly, the separation of matrix and analyte spectra is highly desirable for automated (search-match) database-recognition procedures, a consideration that may become important in future application with 'non-expert' evaluation of data. Confocal Raman microscopy offers an alternative direct technique with advantageous attributes over other methods for explosives analysis. The technique has the ability to provide both speed and specificity for trace identification of particulate matter on undyed and

dyed clothing. Also, in-situ analysis of drugs and explosives particles from contaminated surfaces without sample handling or preparation is desirable to avoid sample loss or cross-contamination associated with sample manipulation. Furthermore, the non-destructive and non-contact character of the technique offers a special role for Raman spectroscopy in the first-pass evaluation screening of materials of forensic relevance.

7.2 Experimental

7.2.1. Samples

See section 6.2.1

Fibres and textiles

A set of natural and synthetic fibres was used in this study in an attempt to cover the wide range of textile materials used in real life. Natural fibres included wool, silk, and cotton. Polyester fibres were used as a representative of synthetic fibres. Also, pieces of blue denim and an orange-coloured T-shirt were used in this study as examples of commonly encountered dyed clothing. A bundle of fibres, each about 1 cm in length, and textile pieces ($\sim 2 \times 2$ cm) were contaminated with few crystals from each drug and explosive and then presented to the spectrometer. Trapping of the particles between the clothing fibres was achieved by pressing small quantities against the fibre bundles and textile pieces and removing the surface excess of the explosive by gentle brushing.

7.2.2. Raman spectroscopy

Raman spectra were collected using a Renishaw *InVia* Reflex dispersive Raman microscope with a 785 nm near-infrared diode laser (Renishaw, Wotton-under-Edge, UK) and a 50 \times objective lens giving a laser spot diameter of 5 μ m. Spectra were obtained at 2 cm^{-1} resolution for a 10 second exposure of the CCD detector in the

wavenumber region 100-1800 cm^{-1} . This wavenumber range was chosen as it contains the spectroscopic fingerprint region of the drugs of abuse and explosive substances. Raman spectra were collected from particles with edge dimensions in the range 5–10 μm . With 90.8 mW laser power at the sample, one accumulation was collected for the drugs and explosives reference spectra and for confocal experiments with contaminated textiles. Reference spectra for the textile samples were collected with five accumulations. With these parameters, the total acquisition time of the spectra of the drugs of abuse and explosives on fibres was about 90 seconds. Spectral acquisition, presentation, and analysis were performed with the Renishaw WIRE (service pack 9) and GRAMS AI version 8 (Thermo Electron Corp, Waltham, MA, USA) software.

7.3 Results and Discussion

7.3.1 Detection of pure drugs of abuse on clothing

Table 7.1 lists the Raman shifts and vibrational assignments of the Raman bands of the fibre substrates studied in this work. This will help to identify these bands if they appear in the Raman spectra of the drugs of abuse and explosives and give an idea about the bands which may interfere with their identification.

7.3.1.1 Drugs on undyed natural fibres

The Raman spectra obtained from cocaine hydrochloride, MDMA and amphetamine crystals trapped between cotton fibres are shown in figure (7.1). It can be observed that the characteristic bands of the drugs of abuse can be clearly identified. The identity of each drug can be unambiguously established and through careful confocal sampling, no significant peaks in the spectra appear from the cotton fibres. Similarly, the confocal Raman spectra obtained from crystal of the benzodiazepines flunitrazepam and nitrazepam trapped between cotton fibres show the diagnostic

Fibre	Wavenumber/ cm ⁻¹	Vibrational assignment	Reference
Cotton	1477	δ (CH ₂) scissor	235
	1378	δ (CH ₂)	
	1120	ν (COC) symmetric	
	1094	ν (COC) asymmetric	
	456	ν (CCO) ring	
	433	ν (CCO) ring	
	378	δ (CCC) ring , symmetric	
Silk	1664	ν (CO) amide I	236
	1446	δ (CH ₂) scissoring	
	1227	ν (CN)	
	1081	ν (CC) skeletal	
	1001	ν (CC) aromatic	
Wool	1654	amide I ν (C=O)	216, 239
	1445	δ (CH ₂)	
	1312	δ (CH ₂)	
	1001	Phe ν (C=C) symmetric	
	933	ν (CC) skeletal	
Polyester	1725	ν (C= O)	237, 238
	1610	ν (C=C)	
	1285	δ (COH)	
	854	γ (CCC)	
	629	in- plane ring bend	

Table 7.1 Wavenumbers and vibrational assignments of the fibre substrates

Raman features of the drugs (Figure 7.2) and there is no band in the spectra that can be assigned to the cotton substrate. Further illustrations of the applicability of this approach were obtained from particles of the drugs of abuse trapped between the fibres of silk and wool specimens. The spectra obtained from drug particles trapped between silk and wool fibres contain several bands arising from the fibre substrate. In each case the strongest bands arising from the substrate did not interfere with the identification of the drugs of abuse. The confocal spectra obtained from crystals of cocaine hydrochloride, MDMA and amphetamine sulphate on silk fibres (Figure 7.3) show the characteristic bands of the drugs. Despite the Raman spectrum obtained from an MDMA crystal between silk fibres (Figure 7.3 B) contains two bands arising from

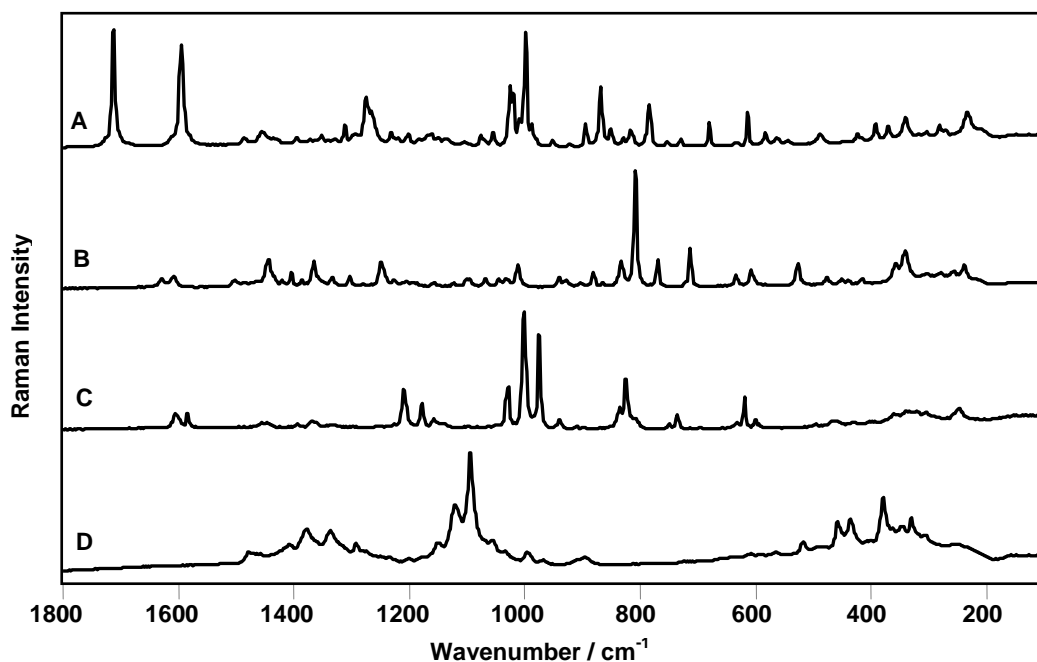


Figure 7.1 Raman spectra of
 A: Cocaine hydrochloride on cotton
 B: MDMA on cotton
 C: Amphetamine sulphate on cotton
 D: Cotton fibres
 785 nm, 90.8 mW, 10s exposure, 1 accumulation for A-C, 5 accumulations for D.

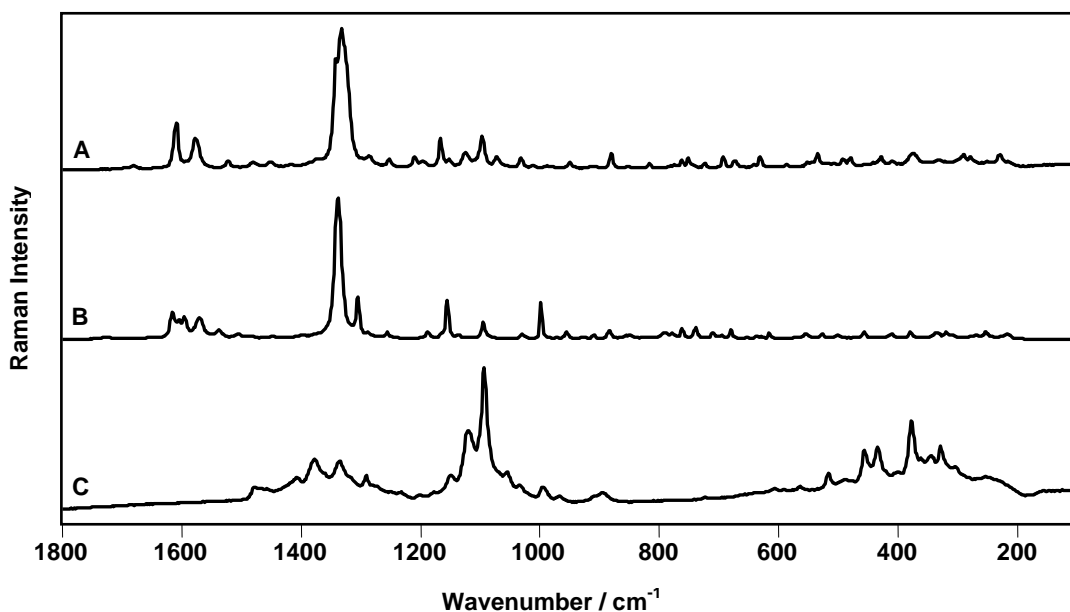


Figure 7.2 Raman spectra of
 A: Flunitrazepam on cotton
 B: Nitrazepam on cotton
 C: Cotton fibres
 785 nm, 90.8 mW, 10s exposure, 1 accumulation for A&B, 5 accumulations for C.

the silk substrate; the amide I (C=O) stretch at 1664cm^{-1} , the (CN) stretch at 1227cm^{-1} . [236] The presence of these bands in the drug spectrum did not prevent identification of the drug which can be identified by its signature characteristic bands at 807 , 769 and 712cm^{-1} . Also, the spectra obtained from flunitrazepam and nitrazepam particles on silk fibres contain two bands arising from the silk substrate (marked with asterisks in figure 7.4). These bands did not interfere with the identification of the drugs as they do not overlap with the characteristic Raman bands of the benzodiazepine drugs. Also, the spectra obtained from cocaine hydrochloride, MDMA and amphetamine particles (Figure 7.5) and flunitrazepam and nitrazepam (Figure 7.6) trapped between wool fibres show the diagnostic Raman features of the drugs of abuse and no bands in the spectra can be assigned to the wool fibre substrate.

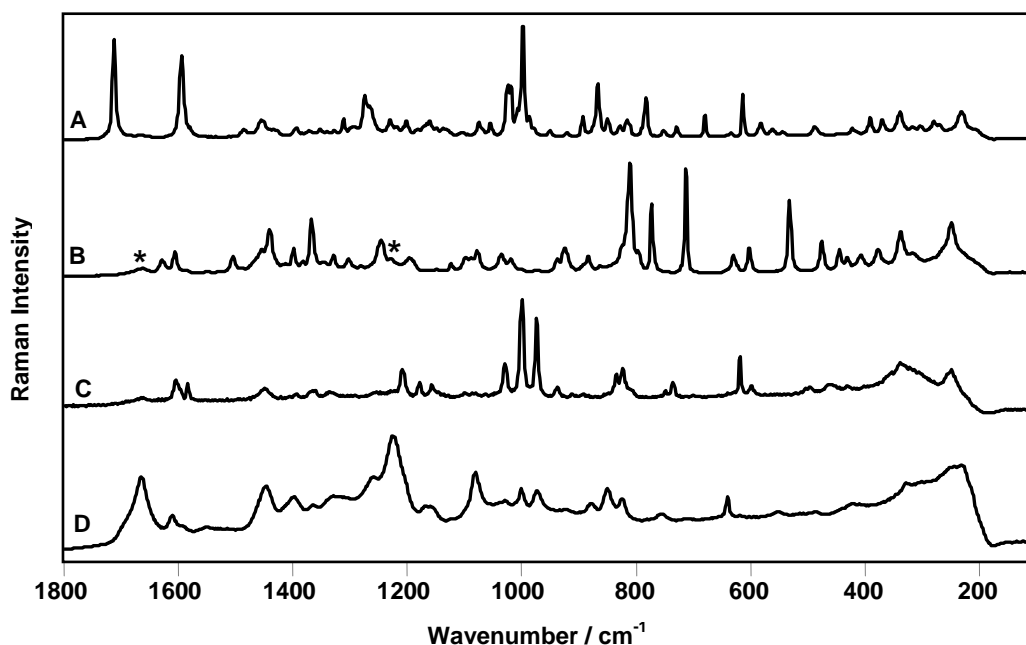


Figure 7.3 Raman spectra of
A: Cocaine hydrochloride on silk
B: MDMA on silk
C: Amphetamine sulphate on silk
D: Silk fibres

785 nm, 90.8 mW, 10s exposure, 1 accumulation for A-C, 5 accumulations for D.

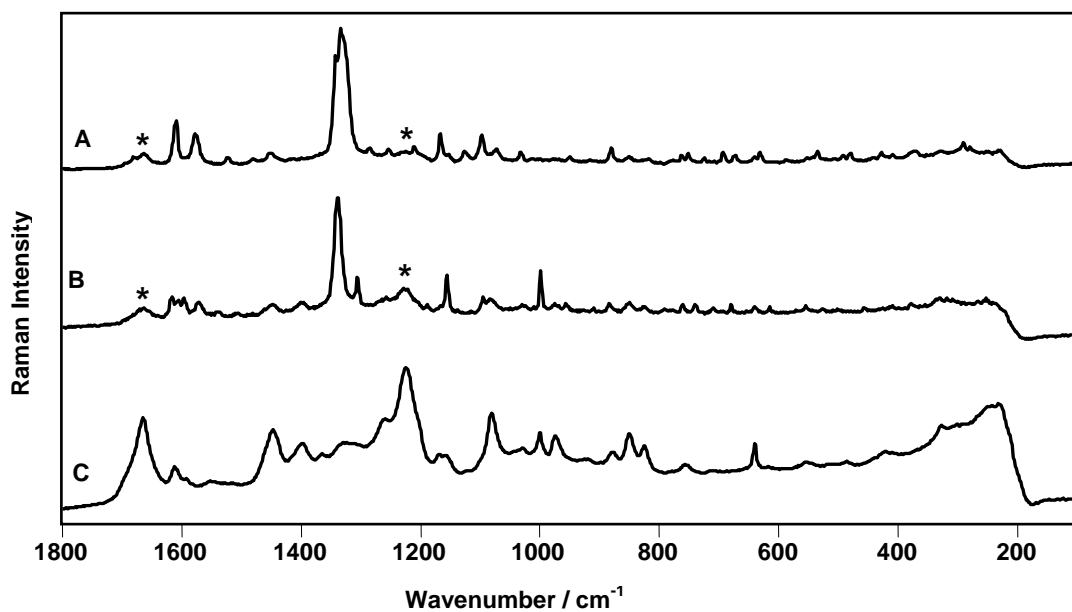


Figure 7.4 Raman spectra of

A: Flunitrazepam on silk

B: Nitrazepam on silk

C: Silk fibres

785 nm , 90.8 mW, 10s exposure, 1 accumulation for A&B, 5 accumulations for C.

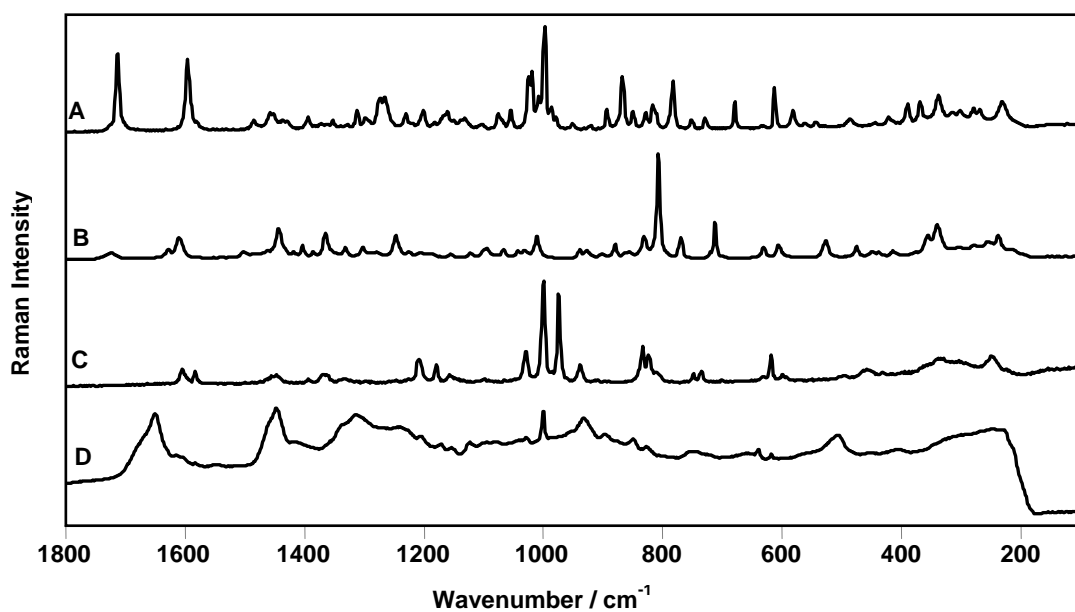


Figure 7.5 Raman spectra of:

A: Cocaine hydrochloride on wool

B: MDMA on wool

C: Amphetamine on wool

D: Wool

785 nm, 90.8 mW, 10s exposure, 1 accumulation for A-C, 5 accumulations for D

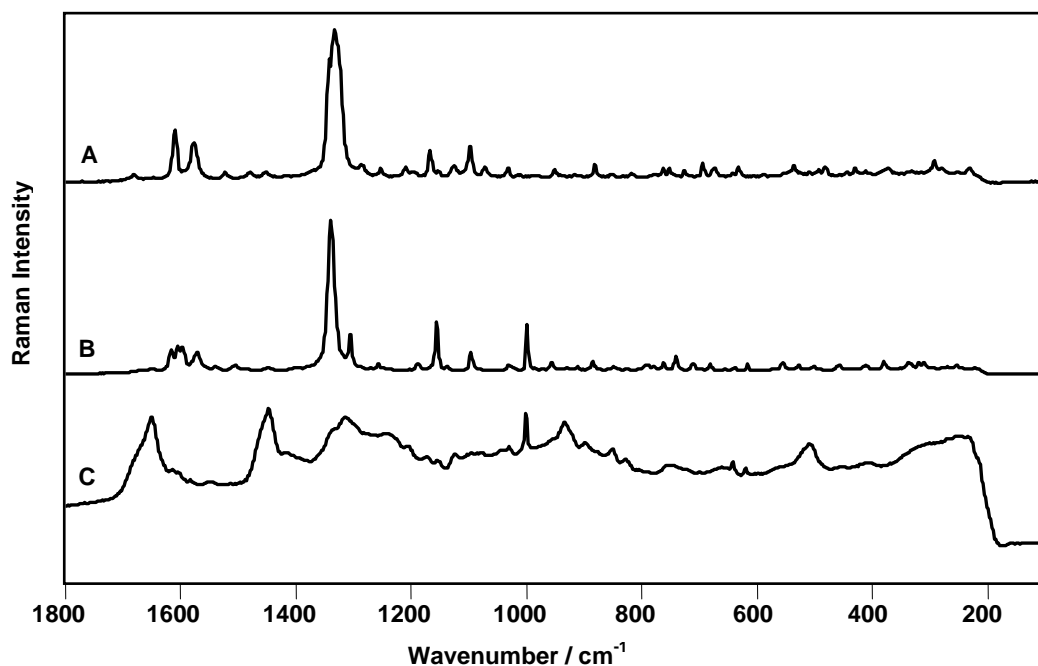


Figure 7.6 Raman spectra of:

A: Flunitrazepam on wool

B: Nitrazepam on wool

C: Wool fibres

785 nm, 90.8 mW, 10s exposure, 1 accumulation for A&B, 5 accumulations for C.

7.3.1.2 Drugs on undyed synthetic fibres

Figure 7.7 shows an image of a single cocaine hydrochloride particle trapped between polyester fibres, the spectrum of which is shown in Figure 7.8. In addition to the bands arising from the drug, the resulting spectrum also contains several peaks assigned to polyester fibre (marked with asterisks in Figure 7.8a): these appear at 1725cm^{-1} [ν (C=O)], 1610cm^{-1} (aromatic ring stretch), 1285cm^{-1} [δ (COH)] and 854cm^{-1} [γ (CCC)].^[237,238] The polyester bands at 1725 and 1610cm^{-1} overlap with the drug bands at 1711 and 1594cm^{-1} , respectively. While the overlapped bands at *ca.* 1600cm^{-1} are clearly resolved, the polyester feature at 1725cm^{-1} appears as a shoulder at higher wavenumber on the cocaine benzoate ester band at 1711cm^{-1} . However, spectral subtraction can be applied to the data to give a difference spectrum (Figure 7.8b) that agrees well with the reference spectrum of pure cocaine hydrochloride.



Figure 7.7 Cocaine HCl crystal trapped between polyester fibres.

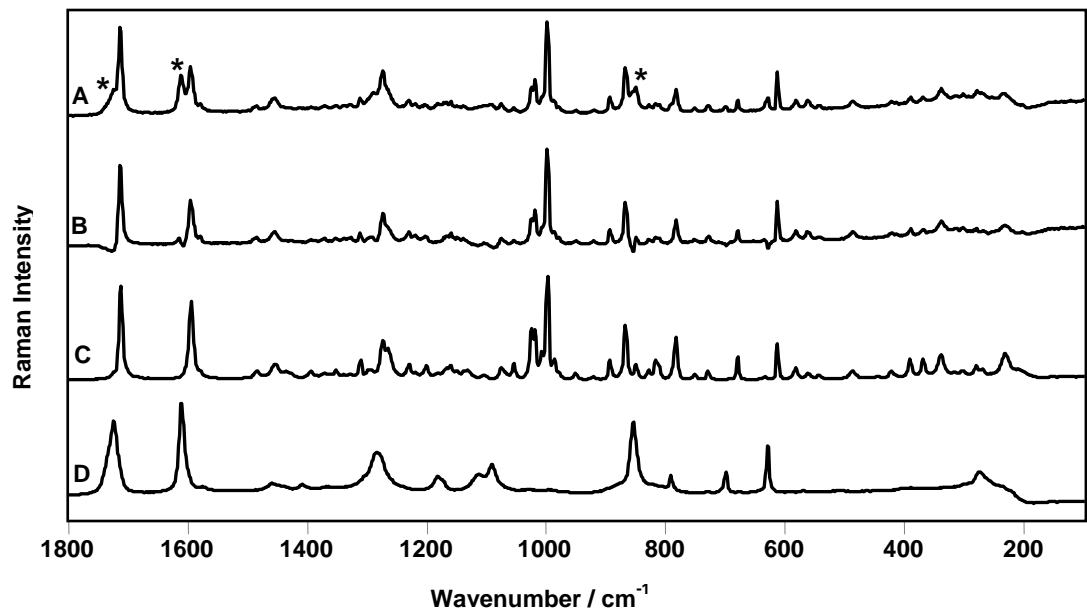


Figure 7.8 Raman spectra of:

A: Cocaine hydrochloride on polyester fibres (Asterisks indicate polyester bands)

B: Subtract spectrum (A-D)

C: Reference cocaine hydrochloride

D: Polyester fibres

785 nm, 90.8 mW, 10s exposure, 1 accumulation for A&C, 5 accumulations for D

Figure 7.9 shows the Raman spectrum obtained from a crystal of MDMA trapped between polyester fibres in which the characteristic bands of the drug are clearly observed. Although the drug spectrum has two bands assigned to the polyester substrate, these bands do not overlap with the drug characteristic bands and the identity of the drug can be unambiguously established. Also, the spectrum obtained from an amphetamine sulphate particle trapped between polyester fibres (Figure 7.10) contain several bands arising from the fibre substrate. The strongest bands arising from the substrate did not interfere with the identification of the drug as the drug characteristic features can be clearly observed. Similarly, flunitrazepam and nitrazepam can be identified in the spectra acquired from particles of the drugs on polyester fibres (Figure 7.11) as the strongest bands arising from the fibres do not overlap with the key signature bands of the drugs.

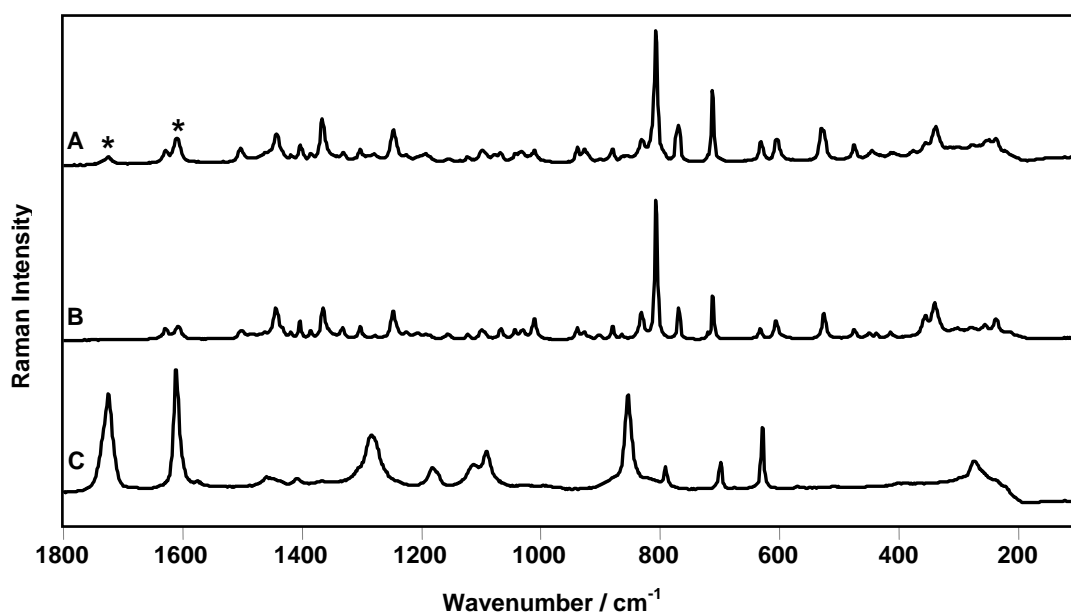


Figure 7.9 Raman spectra of:

A: MDMA on polyester fibres (Asterisks indicate polyester bands)

B: Reference MDMA

C: Polyester fibres

785 nm, 90.8 mW, 10s exposure, 1 accumulation for A&B, 5 accumulations for C

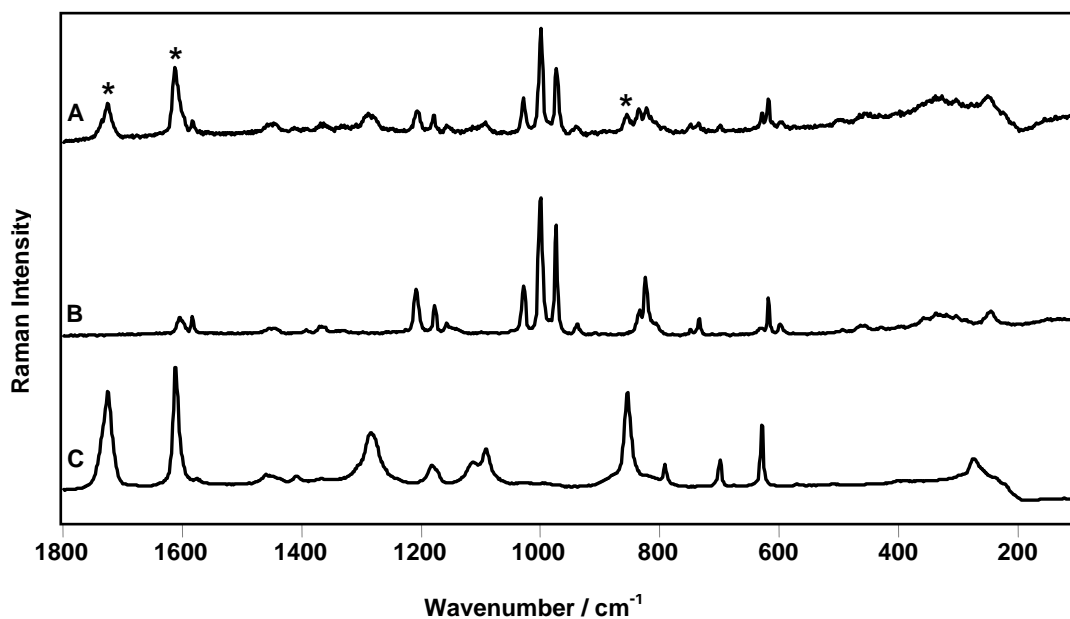


Figure 7.10 Raman spectra of:

A: Amphetamine on polyester fibres (Asterisks indicate polyester bands)

B: Reference amphetamine

C: Polyester fibres

785 nm, 90.8 mW, 10s exposure, 1 accumulation for A&B, 5 accumulations for C

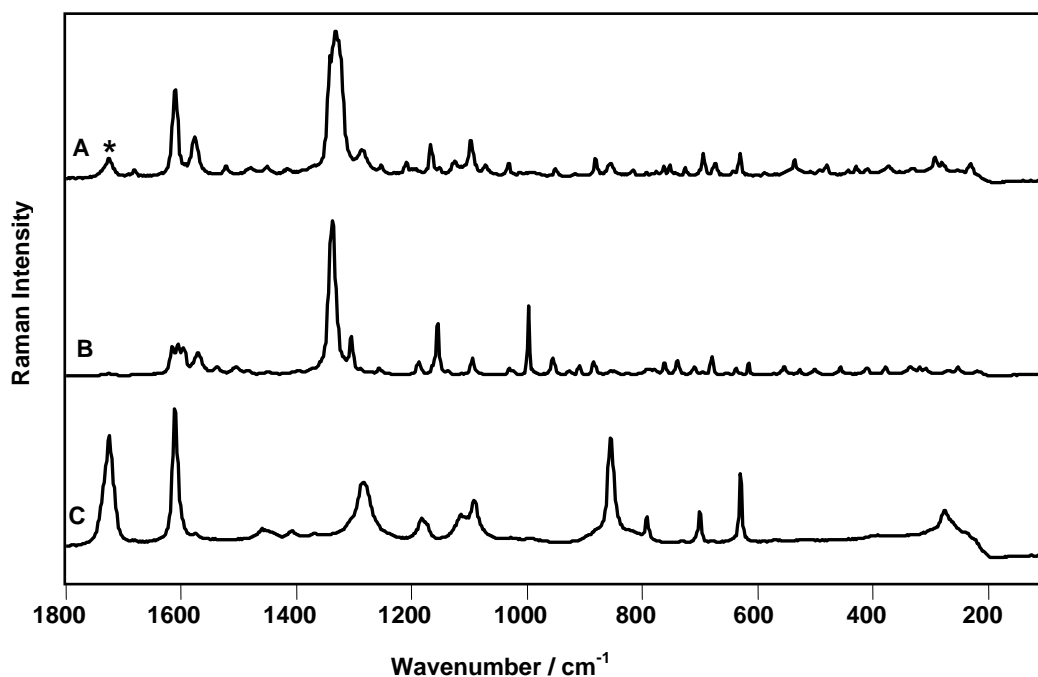


Figure 7.11 Raman spectra of:

A: Flunitrazepam on polyester fibres (Asterisks indicate polyester bands)

B: Nitrazepam on polyester fibres

C: Polyester fibres

785 nm, 90.8 mW, 10s exposure, 1 accumulation for A&B, 5 accumulations for C

7.3.1.3 Drugs on dyed textiles

The previous results were acquired from drug particles trapped between fibres of undyed natural and synthetic fibres. Of course, many real samples are dyed and it is necessary to determine how this will affect the Raman spectra of the drug particles trapped between fibres of dyed textiles specimens. In particular, the presence of dye on the fibres can create fluorescent background problems for Raman spectroscopy and the functional group features, arising from the dye molecules, may interfere with the identification of drugs. The spectra obtained from drugs of abuse particles trapped between blue-dyed denim fibres again shows the characteristic Raman features of the drugs of abuse (Figures 7.12 and 7.13). While a band corresponding with the strongest band in the Raman spectrum of the denim substrate (attributable to blue indigo dye) at 1570 cm^{-1} is also present in the spectra of cocaine hydrochloride and MDMA, this band did not interfere with the identification of the drug contaminants.

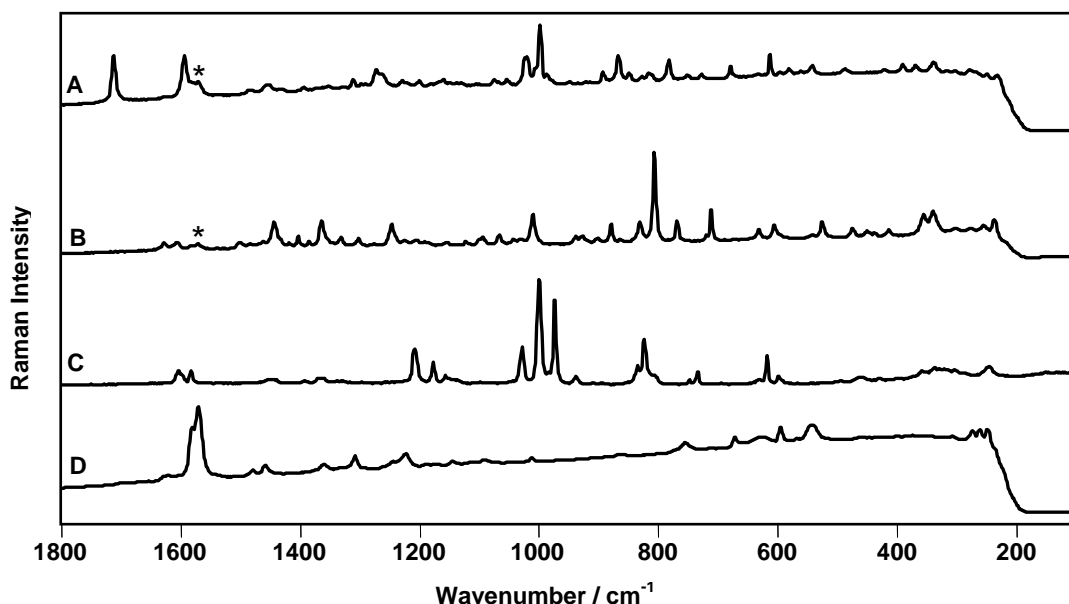


Figure 7.12 Raman spectra of:

A: Cocaine HCl between blue denim fibres (asterisks indicate denim bands)

B: MDMA between blue denim fibres (asterisks indicate denim bands)

C: Amphetamine between blue denim fibres

D: Blue denim spectrum.

785 nm, 90.8 mW, 10s exposure, 1 accumulation for A-C, 5 accumulations for D

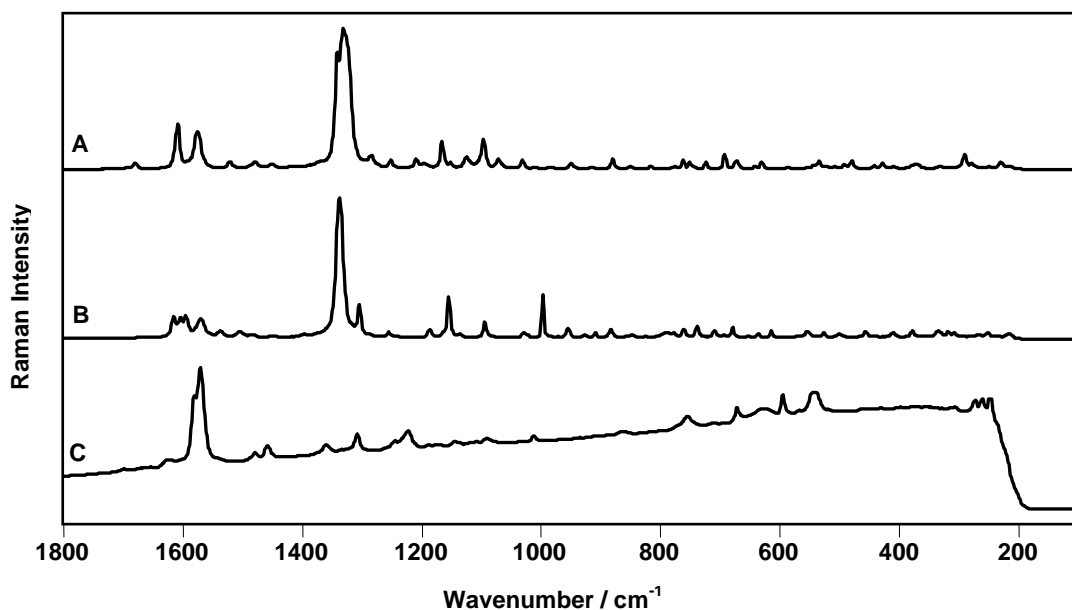


Figure 7.13 Raman spectra of:

A: Flunitrazepam between blue denim fibres

B: Nitrazepam between blue denim fibres

C: Blue denim spectrum.

785 nm, 90.8 mW, 10s exposure, 1 accumulation for A&B, 5 accumulations for C

Figures 7.14 and 7.15 show the spectra collected from crystals of drugs of abuse trapped between fibres of an orange-coloured T-shirt, respectively. It is clear that the Raman spectrum of the orange-coloured T-shirt contains few cotton bands superimposed on a significant fluorescence background which may swamp Raman signal from the drugs. It is observed that a broad fluorescence background could be seen in the spectra of the drugs, but the Raman spectra were usually clearly visible above the background and the characteristic drug bands are clearly observed. The major advantage of confocal Raman microscopy, namely the ability to focus the incident laser radiation onto and collection of Raman scattering from small specimens even when embedded within the interior of a larger highly fluorescent media, is clearly demonstrated in this experiment.

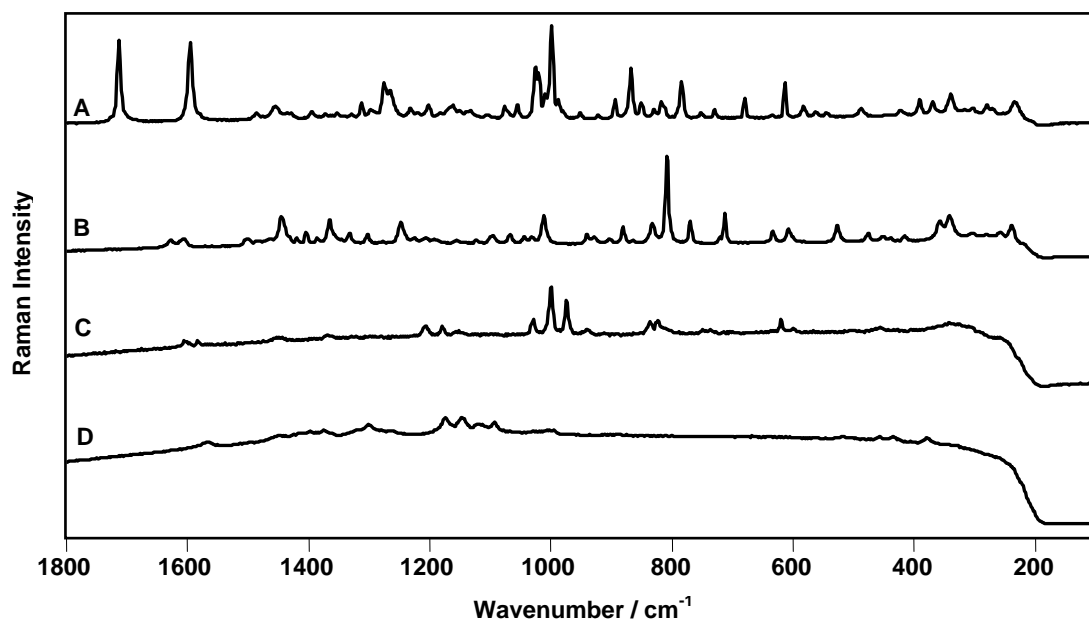


Figure 7.14 Raman spectra of:

A: Cocaine HCl between orange T-shirt fibres

B: MDMA between orange T-shirt fibres

C: Amphetamine between orange T-shirt fibres

D: Orange T-shirt fibres

785 nm, 90.8 mW, 10s exposure, 1 accumulation for A-C, 5 accumulations for D

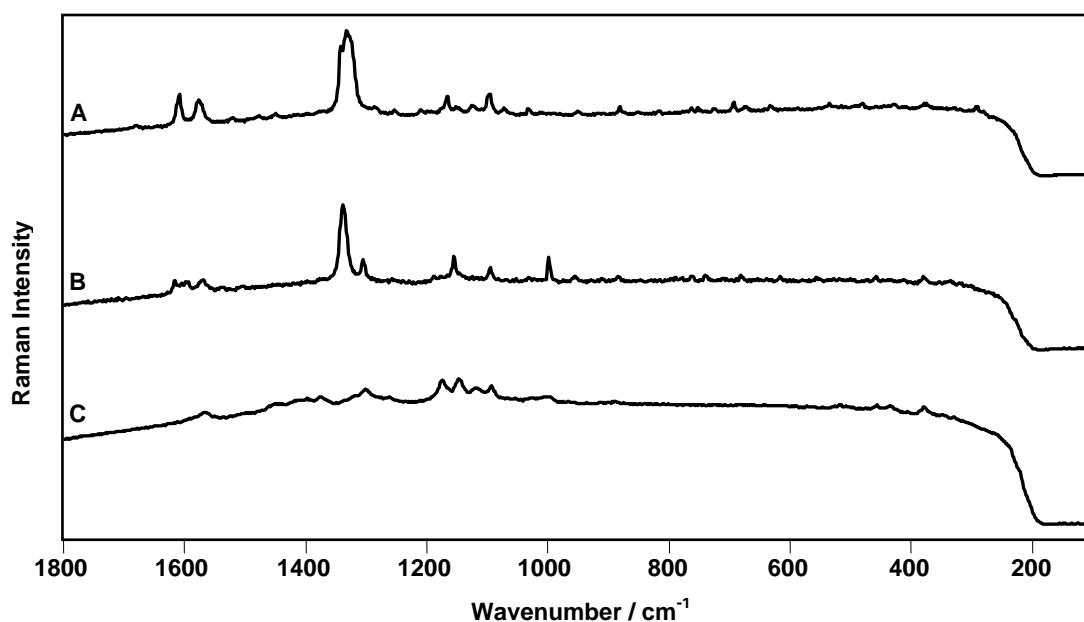


Figure 7.15 Raman spectra of:

A: Flunitrazepam between orange T-shirt fibres

B: Nitrazepam between orange T-shirt fibres

C: Orange T-shirt fibres

785 nm, 90.8 mW, 10s exposure, 1 accumulation for A&B, 5 accumulations for C

7.3.2 Detection of seized drugs of abuse on clothing

Illegal drugs are generally mixed with a variety of materials to increase the bulk of the sample prior to distribution. In such situations, the identification of drugs of abuse by Raman spectroscopy may be difficult due to several complications arising from the diluent matrix. The primary major complication is overlapping of the Raman bands of the excipients and the drugs of abuse which may impede the identification of the drugs. The second major complication lies in the presence of fluorescent contaminants that can conceal the Raman signal through background emission, thus making identification of the drugs difficult or impossible. Furthermore, Raman spectral bands or background fluorescence which may arise from the fibre polymers or dyed textiles can exacerbate the problem of identification. In this section, the application of confocal Raman microscopy to the detection of traces of street samples of drugs of abuse on a similar range of textile substrates has been investigated.

7.3.2.1 Detection of seized drugs of abuse on undyed natural fibres

The Raman spectra obtained from crystals of seized street samples of cocaine, MDMA and amphetamine on cotton fibres are shown in figure 7.16. In figure 7.16A, the additional small band adjacent to the aromatic ring (C=C) stretch at 1594 cm^{-1} is due to an adulterant present in the sample. This adulterant presented no difficulty in determining the identity of cocaine hydrochloride. It is also observed that no band in the spectrum can be assigned to the cotton fibre substrate. Also, the Raman spectrum acquired from a crystal of seized MDMA sample between cotton fibres (Figure 7.16B) shows the principle diagnostic bands of MDMA. No significant band can be attributable to the excipients or the fibre substrate. Despite that the spectrum obtained from a crystal of street amphetamine sample has two bands arising from the cutting agents (marked with asterisks in figure 7.16C), these bands do not overlap with the

principal bands of amphetamine sulphate. In Figure 7.17, the spectra obtained from drugs particles trapped between silk fibres contain some bands arising from the silk substrate and the cutting agents in the samples. The presence of these bands does not prevent the identification of the drugs of abuse which can be readily identified by their diagnostic bands. Similarly, the spectra obtained from drug particles trapped between wool fibres (Figure 7.18) contain some bands attributable to the cutting agents. Again, these bands do not overlap with the diagnostic bands of the drugs and presented no difficulty in determining the identity of the drug. It is also noted that no significant band can be assigned to the cutting agents in the spectrum collected from street MDMA on wool (Figure 7.18C) .This arises because of the microscopic collection of data has facilitated the acquisition of selective Raman spectra from individual drug crystals in heterogeneous sample.

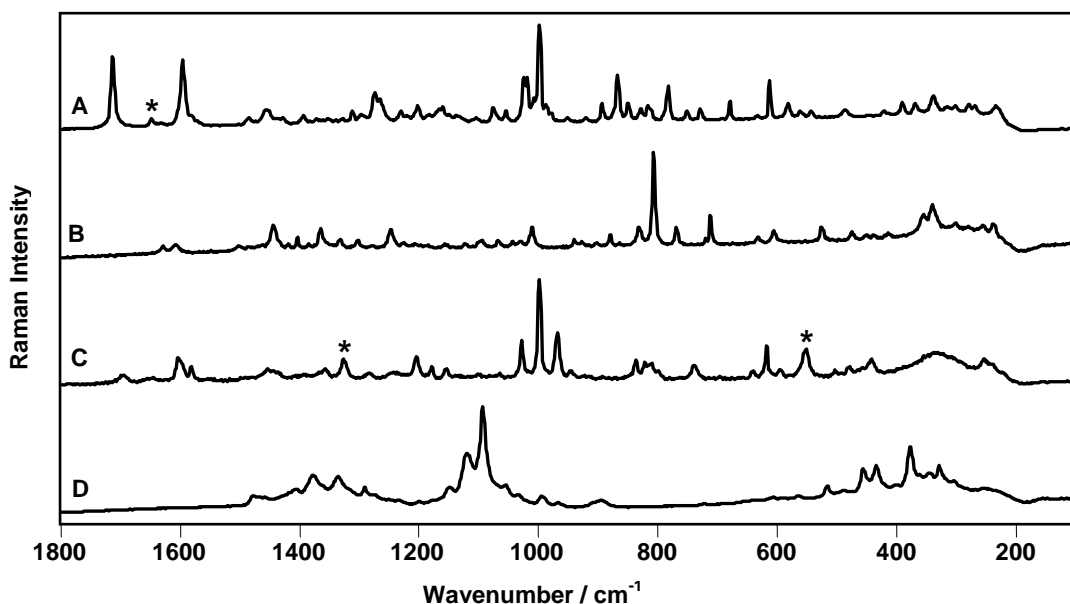


Figure 7.16 Raman spectra of:

A: Street cocaine HCl between cotton fibres (asterisks indicate exipient bands)

B: Street MDMA between cotton fibres

C: Amphetamine between cotton fibres (asterisks indicate exipient bands)

D: Cotton fibres

785 nm, 90.8 mW, 10s exposure, 1 accumulation for A-C, 5 accumulations for D

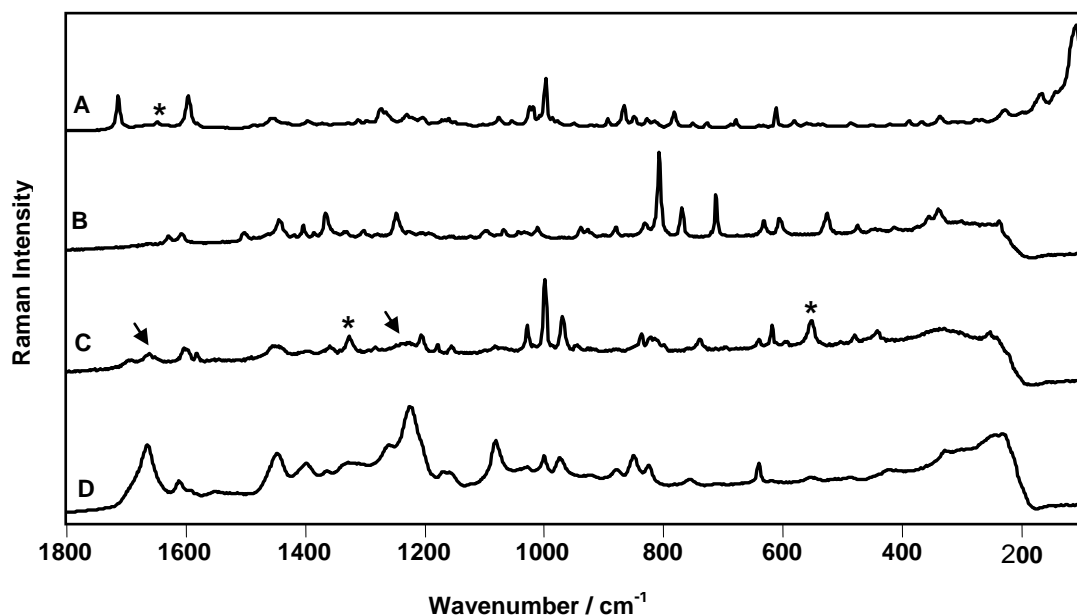


Figure 7.17 Raman spectra of

A: Street cocaine hydrochloride on silk (asterisks indicate exipient bands)

B: Street MDMA on silk

C: Street Amphetamine on silk (asterisks indicate exipient bands and arrows indicate silk bands)

D: Silk fibres

785 nm, 90.8 mW, 10s exposure, 1 accumulation for A-C, 5 accumulations for D.

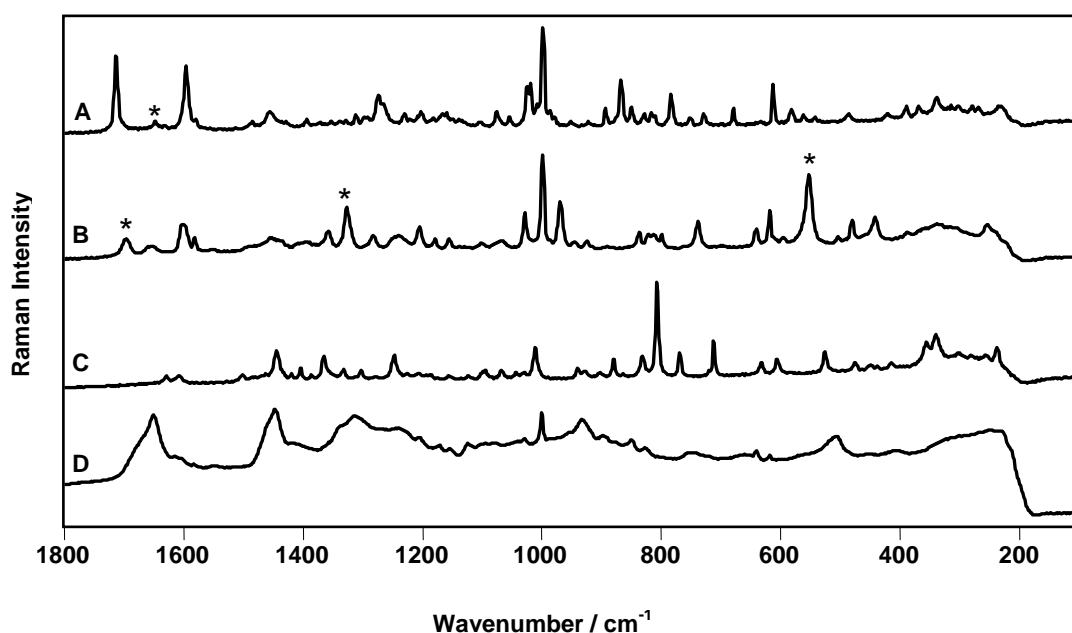


Figure 7.18 Raman spectra of

A: Street cocaine hydrochloride on wool (asterisks indicate exipient bands)

B: : Street Amphetamine on wool (asterisks indicate exipient bands)

C: Street MDMA on wool

D: Wool fibres

785 nm, 90.8 mW, 10s exposure, 1 accumulation for A-C, 5 accumulations for D.

7.3.2.2 Detection of seized drugs of abuse on undyed synthetic fibres

Figure 7.19 shows the Raman spectrum acquired from a crystal of street sample of cocaine hydrochloride in which the polyester bands at 1725 and 1610 cm^{-1} overlap with the drug bands at 1711 and 1594 cm^{-1} , respectively. Spectral subtraction has been applied to the data to give a difference spectrum (Figure 7.19B) that agrees well with the reference spectrum of cocaine hydrochloride (Figure 7.19C). Although this spectrum comprises a band arising from the excipients, the characteristic bands of cocaine hydrochloride still identified. The spectra obtained from particles of street MDMA and amphetamine (Figure 7.20) between polyester fibres contain some bands arising from the fibre substrate. In each case the strongest bands arising from the polyester substrate did not interfere with the identification of the drug as they appear in the 1800–1500 cm^{-1} spectral region away from the drug characteristic features which are clearly observed in the spectra.

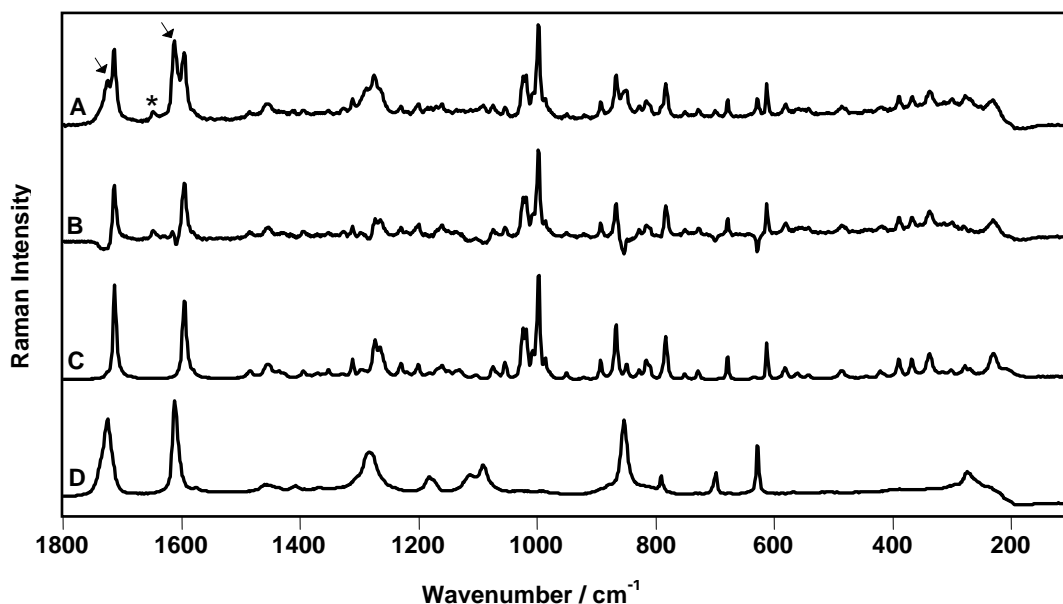


Figure 7.19 Raman spectra of:

A: Street Cocaine hydrochloride on polyester fibres (Asterisks indicate excipients bands and arrows indicate polyester bands)

B: Subtract spectrum (A-D)

C: Reference cocaine hydrochloride

D: Polyester fibres

785 nm, 90.8 mW, 10s exposure, 1 accumulation for A&C, 5 accumulations for D

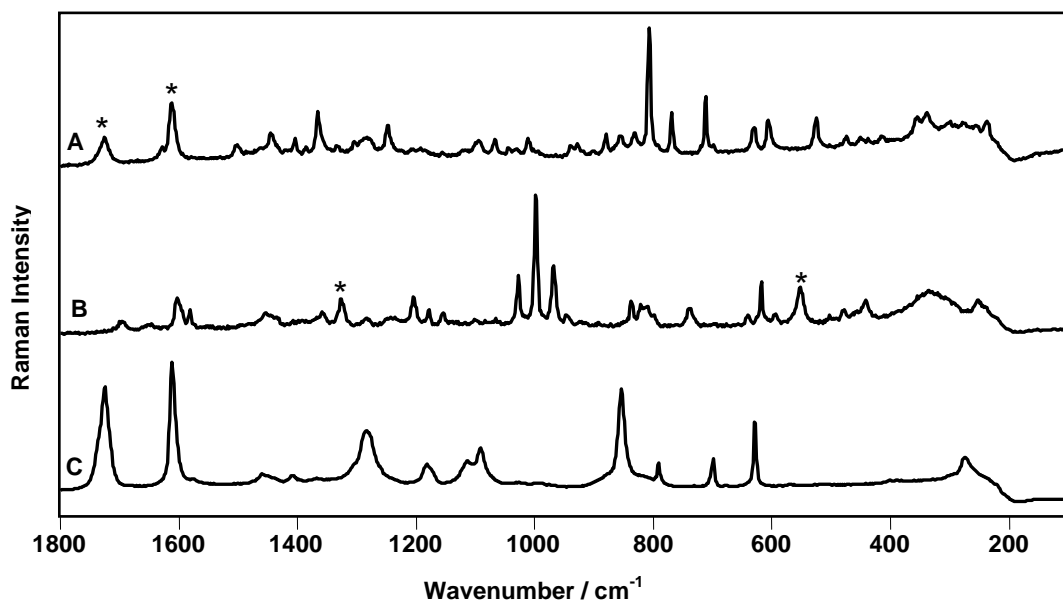


Figure 7.20 Raman spectra of:
 A: Street MDMA on polyester fibres (Asterisks indicate polyester bands)
 B: Amphetamine on polyester bands (Asterisks indicate excipient bands)
 C: Polyester fibres
 785 nm, 90.8 mW, 10s exposure, 1 accumulation for A&B, 5 accumulations for C

7.3.2.3 Detection of seized drugs of abuse on dyed textiles

The spectra acquired from drug particles between blue denim fibres contain some bands arising from the cutting agents (Figure 7.21). In addition to these bands, the strongest denim band at 1570 cm^{-1} appears at the cocaine hydrochloride and amphetamine spectra. In each case the identity of the drug contaminant can be established. Also figures (7.22) shows the spectra obtained from particles of seized cocaine hydrochloride and MDMA and amphetamine trapped between the fibres of an orange-dyed T-shirt, respectively. A broad fluorescence background can be seen in the spectra of the drugs. However, despite this the Raman spectra of the drugs are clearly visible above the background and the characteristic Raman bands of the drugs are clearly observed.

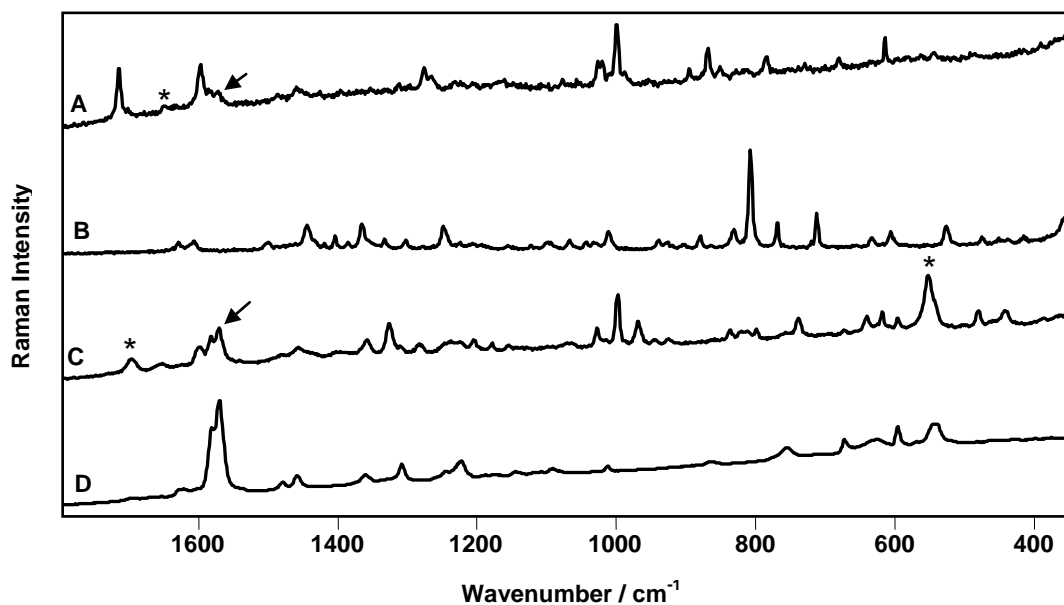


Figure 7.21 Raman spectra of:

A: Street cocaine HCl between blue denim fibres (asterisks indicate excipient bands and arrows indicate denim band)

B: Street MDMA between blue denim fibres

C: Street amphetamine between blue denim fibres (asterisks indicate excipient bands and arrows indicate denim band)

D: Blue denim spectrum.

785 nm, 90.8 mW, 10s exposure, 1 accumulation for A-C, 5 accumulations for D

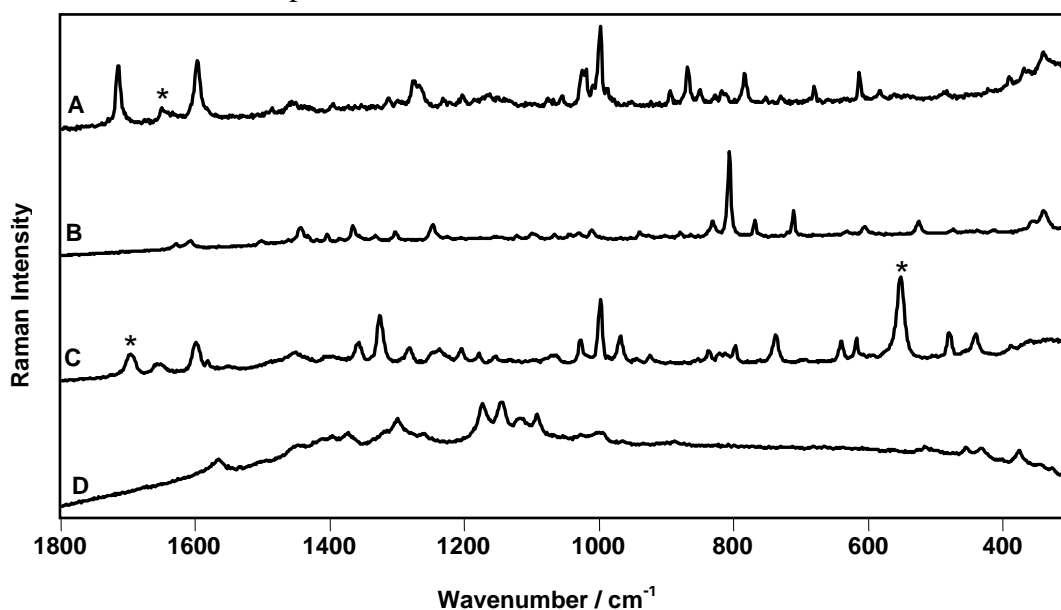


Figure 7.22 Raman spectra of:

A: Street cocaine HCl between orange T-shirt fibres (asterisks indicate excipient bands)

B: Street MDMA between orange T-shirt fibres

C: Street Amphetamine between orange T-shirt fibres (asterisks indicate excipient bands)

D: Orange T-shirt fibres

785 nm, 90.8 mW, 10s exposure, 1 accumulation for A-C, 5 accumulations for D

7.3.3 Detection of explosives and explosive precursors on clothing

7.3.3.1 Explosives on undyed natural fibres

The Raman spectra obtained from PETN, TNT, ammonium nitrate, hexamethylenetetramine (HMTA), and pentaerythritol particles trapped between cotton fibres are shown in Figure 7.23. Comparison of these spectra with the reference spectra of the explosives showed that the explosives could be easily identified by their Raman spectra, which comprise strong sharp features throughout the spectral wavenumber region 100–1800 cm^{-1} . The characteristic Raman bands of the explosives can be clearly identified, and no significant bands in the spectra appear from the cotton fibres.

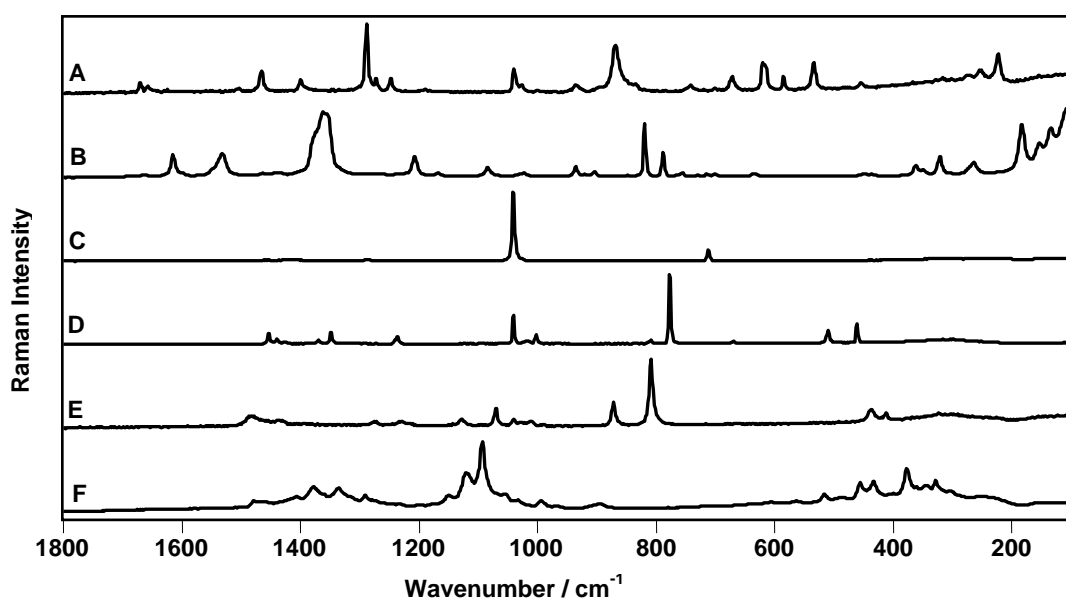


Figure 7.23 Raman spectra of

A: PETN particle on cotton fibres

B: TNT particle on cotton fibres

C: Ammonium nitrate particle on cotton fibres

D: HMTA particle on cotton fibres

E: Pentaerythritol particle on cotton fibres

F: Cotton fibres

785 nm, 90.8 mW, 10 s exposure, 1 accumulation for (A-E), 5 accumulations for (F).

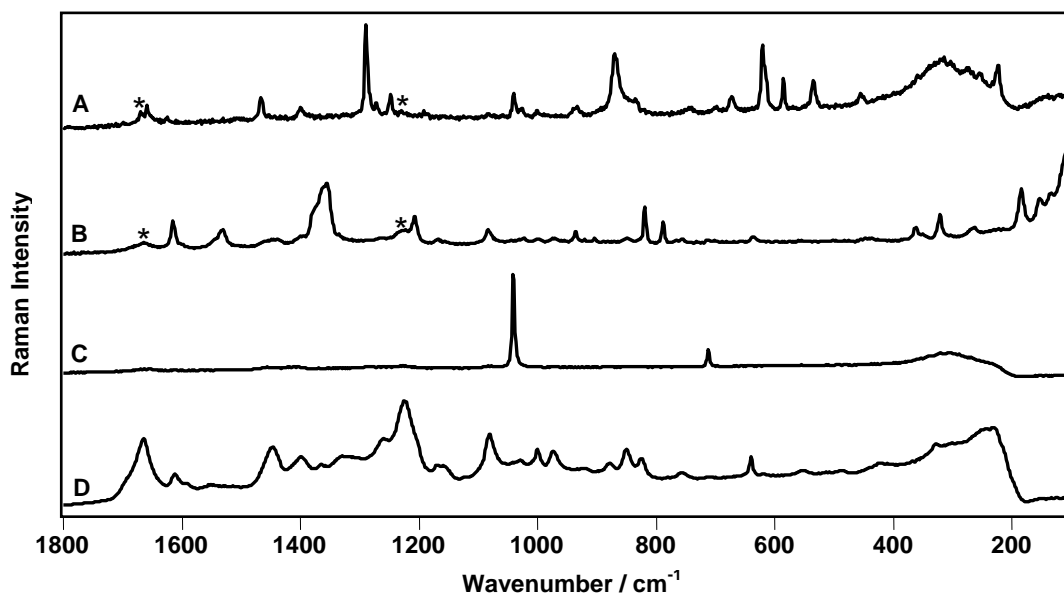


Figure 7.24 Raman spectra of:
 A: PETN particle on silk fibres
 B: TNT particle on silk fibres
 C: Ammonium nitrate particle on silk fibres
 D: Silk fibres (asterisks indicate silk bands)
 785nm, 90.8 mW, 10s exposure, 1 accumulation for A-C, 5 accumulations for D.

The Raman spectra obtained from the explosives PETN, TNT, and ammonium nitrate and from the explosive precursors particles trapped between silk fibres contain some bands attributable to the silk substrate (marked with asterisks in figures 7.24 and 7.25); these are the amide I ν (C=O) stretch at 1664 cm^{-1} and the (CN) stretch at 1227 cm^{-1} .^[236] The presence of these bands in the spectra of the explosives does not interfere with the identification of the explosives, which can be identified by their characteristic bands. Similarly, the spectra obtained from the explosives and explosive precursors trapped between wool fibres contain some bands (marked with asterisks in figures 7.26 and 7.27, respectively) assignable to the wool substrate; the amide I ν (C=O) mode at 1654 cm^{-1} , and the δ (CH₂) mode at 1445 cm^{-1} .^[216,239] These bands do not overlap with characteristic features of the explosives, allowing the explosives and the explosive precursors to be readily identified.

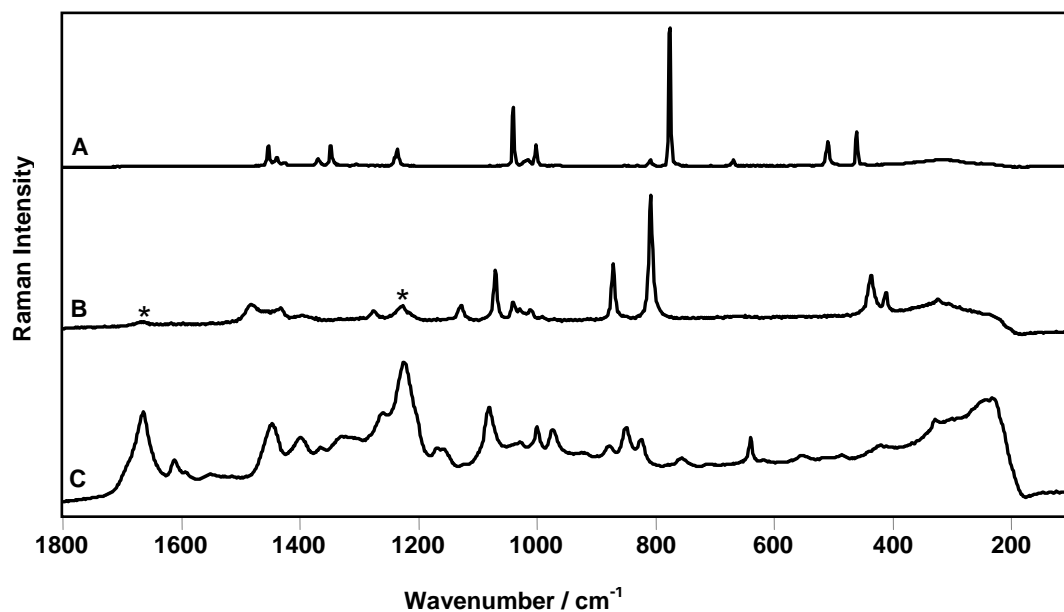


Figure 7.25 Raman spectra of:
 A: HMTA particle on silk fibres
 B: Pentaerythritol particle on silk fibres
 C: Silk fibres (asterisks indicate silk bands)
 785nm, 90.8 mW, 10s exposure, 1 accumulation for A&B, 5 accumulations for C.

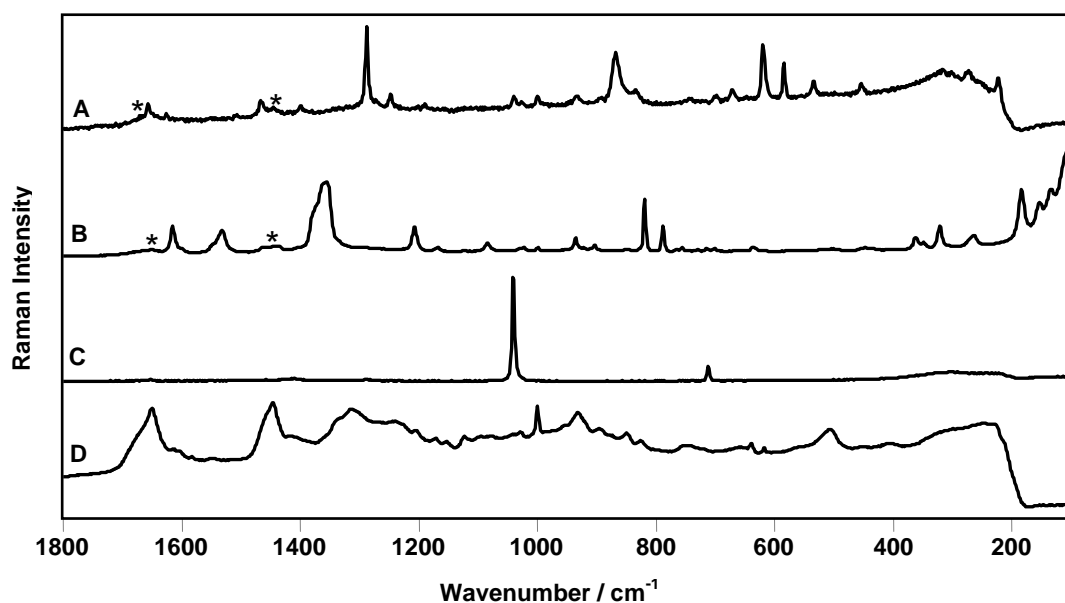


Figure 7.26 Raman spectra of:
 A: PETN particle on wool fibres
 B: TNT particle on wool fibres
 C: Ammonium nitrate particle on wool fibres
 D: Wool fibres (asterisks indicate wool bands)
 785nm, 90.8 mW, 10s exposure, 1 accumulation for A-C, 5 accumulations for D.

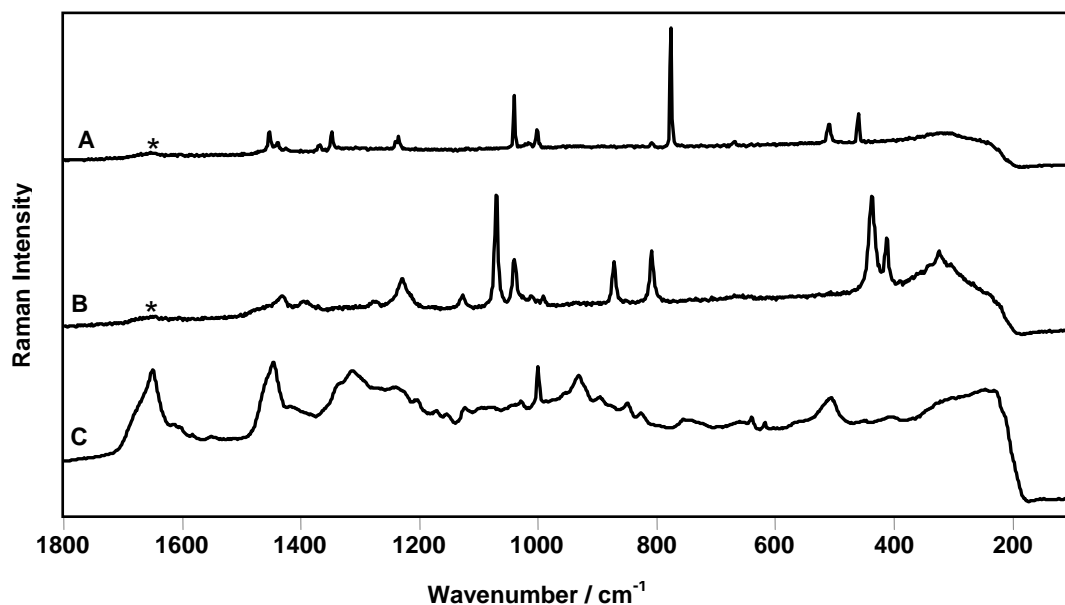


Figure 7.27 Raman spectra of:
 A: HMTA particle on wool fibres
 B: Pentaerythritol particle on wool fibres
 C: Wool fibres (asterisks indicate wool bands)
 785nm, 90.8 mW, 10s exposure, 1 accumulation for A&B, 5 accumulations for C

7.3.3.2 Explosives on undyed synthetic fibres

The spectra collected from the explosives PETN, TNT, ammonium nitrate, and from the explosive precursors HMTA and pentaerythritol particles trapped between polyester fibres are shown in figure 7.28, which also allows the presence of the explosive contaminant to be readily established. In addition to the explosives diagnostic bands (*vide supra*), the resulting spectra also contains several peaks assigned to polyester fibre (marked with dashed lines in Figure 7.28): these appear at 1725 cm^{-1} ν (C=O), 1610 cm^{-1} (aromatic ring stretch), and 854 cm^{-1} [γ (CCC)].^[237,238] In each case, the strongest bands arising from the polyester fibres do not overlap with the characteristic features of the explosives which can be clearly observed.

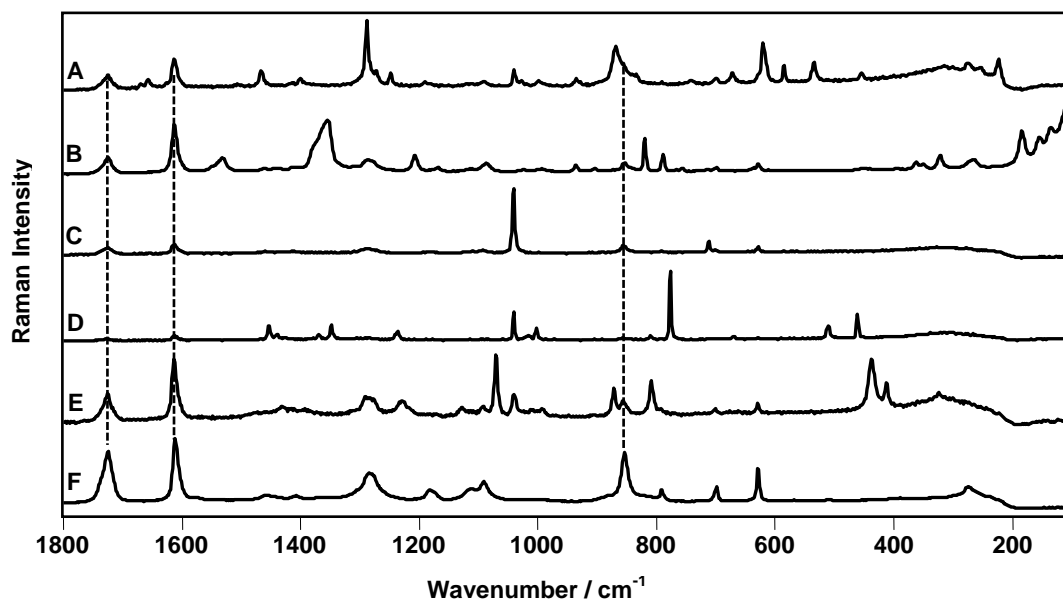


Figure 7.28 Raman spectra of
 A: PETN particle on polyester fibres
 B: TNT particle on polyester fibres
 C: Ammonium nitrate particle on polyester fibres
 D HMTA particle on polyester fibres
 E: Pentaerythritol particle on polyester fibres
 F: Polyester fibres (dashed lines indicate polyester bands)
 785 nm, 90.8 mW, 10 s exposure, 1 accumulation for A-E, 5 accumulations for F

7.3.3.3 Explosives on dyed textiles

The spectra obtained from explosives and the explosive precursor particles trapped between blue-dyed denim fibres again show the characteristic Raman features of the explosives and their precursors. While a band corresponding with the strongest band in the Raman spectrum of the denim substrate (attributable to blue indigo dye) at 1570 cm^{-1} is also present in the spectra, this band did not interfere with the identification of the explosives (Figure 7.29). Raman spectra were successfully collected from the explosives PETN, TNT, and ammonium nitrate as well as from the explosive precursors HMTA and pentaerythritol particles trapped between the fibres of an orange-coloured T-shirt. Fluorescence emission from the T-shirt fibres has given rise to a slight fluorescence background in the spectra of the explosives. However, the

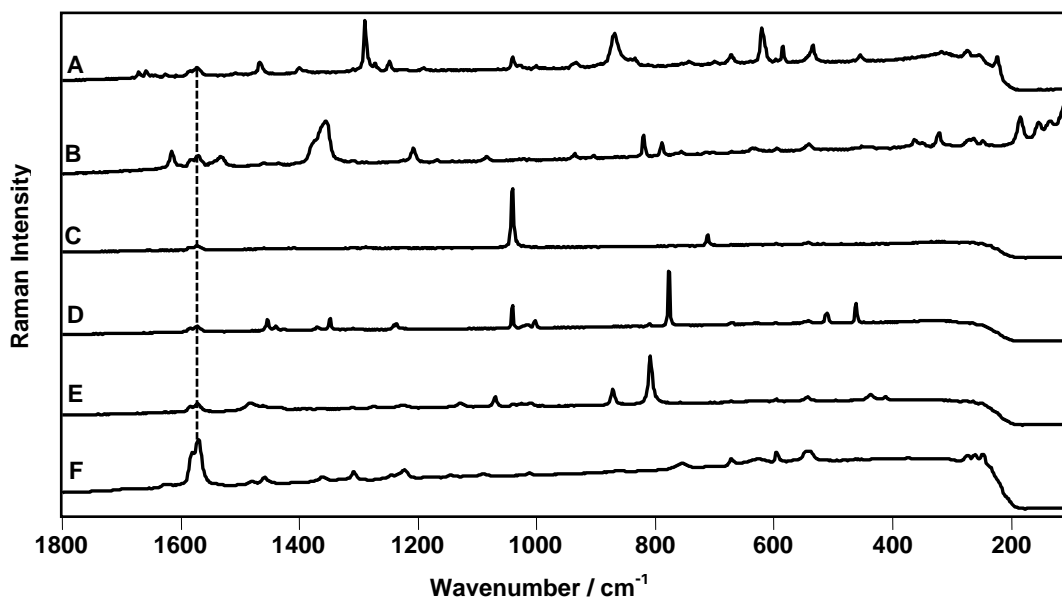


Figure 7.29 Raman spectra of

- A: PETN particle on denim fibres
- B: TNT particle on denim fibres
- C: Ammonium nitrate particle on denim fibres
- D: HMTA particle on denim fibres
- E: Pentaerythritol particle on denim fibres
- F: Denim fibres

785 nm, 90.8 mW, 10 s exposure, 1 accumulation for A-E, 5 accumulations for F

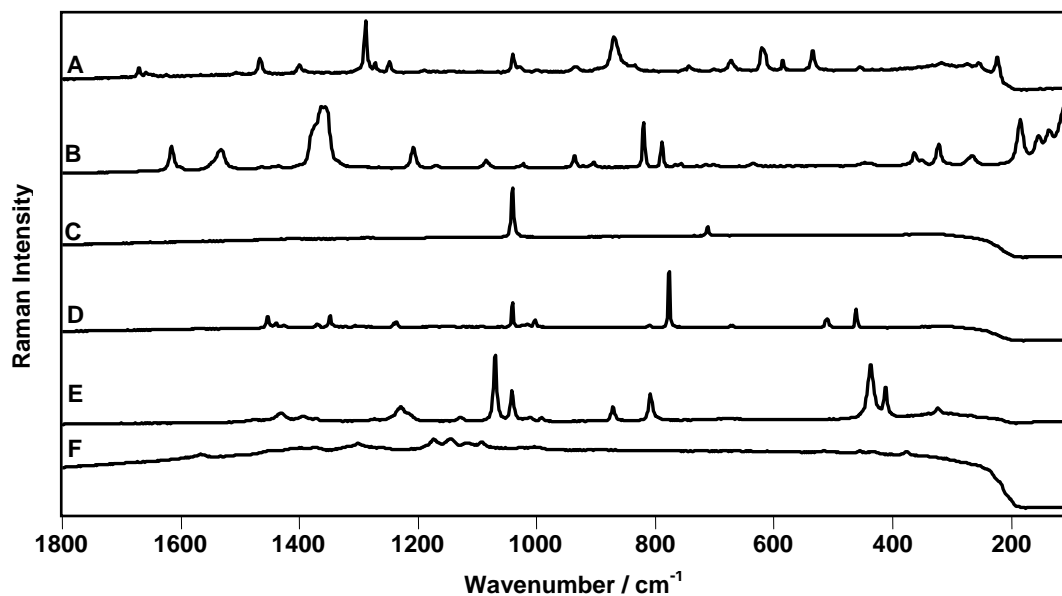


Figure 7.30 Raman spectra of

- A: PETN particle between orange T-shirt fibres
- B: TNT particle between orange T-shirt fibres
- C: Ammonium nitrate particle between orange T-shirt fibres
- D: HMTA particle between orange T-shirt fibres
- E: Pentaerythritol particle between orange T-shirt fibres
- F: Orange T-shirt fibres

785 nm, 90.8mW, 10 s exposure, 1 accumulation for A-E, 5 accumulations for F

Raman spectral bands of the explosives are clearly identifiable above the background and in all cases the presence of the contaminants were easily recognised (Figure 7.30).

These results confirm the applicability of the discrimination of confocal Raman microscopy for drugs-of-abuse and explosives trapped between fibres of various textiles. Raman spectra could be obtained from particles of an average size in the range 5-10 μm . This ability for discrimination could be attributed to the ability of the confocal system to focus the incident laser radiation to obtain data non-destructively from the drugs and explosive crystals embedded between the fibres of the specimens. Consequently, the resulting Raman spectra contain Raman signal almost exclusively from the focal point of the laser. The presence of some spectral bands arising from the fibre polymers and/or dyes did not interfere with the identification of the drugs which could be clearly identified by their characteristic Raman bands. If necessary, interfering bands could be successfully removed by spectral subtraction. Also, Raman spectra could be acquired from drug particles embedded within highly fluorescent specimens. The likelihood of generation of fluorescence is much reduced due to the use of near-infrared laser as an excitation source. Raman spectra of the explosive, explosive precursor substances and the drugs of abuse could be readily obtained in situ non-destructively, within 90 s and without sample preparation. These results confirm that the detection of drugs-of-abuse on clothing could be of evidential value to establish a link between these substances and individuals involved in activities related to drug trade or drug abuse. Also, the detection of explosive residues on clothing can be used as a strong evidence to establish a link between these materials and individuals involved in terrorist activities.

These results show that with the application of confocal techniques, interpretable Raman spectra can be obtained directly from particles as small as $5 \mu\text{m}^3$ - approximately 180 pg in mass- and hence the technique has a sensitivity comparable to ionisation desorption mass spectrometric techniques. [54, 98, 240-243] In addition, this approach leaves the particle unaltered and in its original environment. Thus, a clear application of the confocal Raman experiment is as a screening method for identification of particulates during initial inspections of clothing prior to further examination. Furthermore, the rapid acquisition of Raman spectra of explosives in situ allows forensic scientists and police agencies to screen the potential of particulates as evidential material during initial inspections of clothing. The technique provides an alternative or complementary method to pre-existing technology for the direct rapid forensic analysis of samples such as clothing without their destruction and /or lengthy extractive and chromatographic separation.

Chapter 8

***In situ* detection of drugs of abuse in clothing impregnated with the drugs using benchtop and portable Raman spectroscopy**

8.1 Introduction

Drug trafficking and smuggling is an ongoing battle facing law enforcement agencies. Cocaine smuggling is a high-value pursuit for smugglers and has been attempted by a wide diversity of concealment methods including the use of bottled liquids,^[244] canned milk,^[245] wax and book bindings,^[246] wicker baskets and bamboo sticks^[247] and suspensions in cans of beer.^[248] Smuggling of illicit drugs ‘starched’ into cloth^[246] and dissolved in rubber-like material has also been identified,^[249] and, in particular, traffickers have used clothing impregnated with cocaine for smuggling. These materials are prepared by pouring cocaine solutions onto the clothing and allowing the solvent to evaporate.^[250,251] The main laboratory procedures used for identifying the drugs of abuse in these cases included gas chromatography with flame ionization detection (GC-FID),^[245] gas chromatography mass spectrometry (GC-MS)^[246] and Fourier-transform infrared-attenuated total reflectance (FT-IR-ATR).^[247] These analytical techniques require preparation steps in which the sample to be analysed is extracted into an organic solvent before injection into the GC. Also, each of these approaches requires isolation and/or destruction of the analyte and these techniques therefore alter or destroy the evidential material during analysis. On the contrary, Raman spectroscopy is a non-destructive technique, produces molecular-specific spectra and sample preparation or pre-treatment is not required. This is particularly important with regard to the speed of analysis, prevention of sample contamination and preservation of evidential material. Raman spectroscopic instrumentation has been traditionally restricted to the laboratory due to the

sophistication required to analyse the inherently weak scattering process. However, recent advances have allowed the production of compact and field portable Raman systems that are commercially available. Principal developments allowing this technological advance are the advent of compact, powerful, stable and reliable near-infrared solid-state laser sources along with the use of high-resolution charge coupled device (CCD) detectors.^[252] These developments in addition to spectral identification software have facilitated the commercial availability of portable fibre-optic Raman probes for in-field applications. In this section, the application of fibre-optic Raman spectroscopy to the *in-situ* identification of drugs of abuse, namely cocaine hydrochloride, MDMA and amphetamine sulphate, on a variety of fibres and textiles impregnated with the drugs has been investigated. In such situations, it has been demonstrated that fibre-optic Raman spectroscopy can be applied effectively for the acquisition of Raman spectra of the drugs of abuse. The spectra were readily obtained *in-situ* non-destructively without necessitating sample extraction or pre-treatment. The spectra obtained were identified by searching against an identification library, which is desirable for automated database recognition algorithms; an important consideration for future applications involving non-expert evaluation of data. Furthermore, the non-destructive and non-contact character of the technique offers a special role for Raman spectroscopy in the first-pass evaluation screening of materials.

8.2 Experimental

8.2.1 Samples

a- Drugs of abuse

Pure cocaine hydrochloride, MDMA and amphetamine sulphate were obtained from Sigma-Aldrich and were used without further purification. A saturated solution was prepared for each drug by dissolving 450 mg of cocaine.HCl, 20 mg of MDMA, and

35 mg of amphetamine sulphate in 1 ml of an ethanol/water mixture.

b- Fibres and textiles

A set of natural and synthetic fibres was used in this study in an attempt to cover the wide range of textile materials found in real life. Natural fibres included wool, silk and cotton. Polyester fibres were used as a representative of synthetic fibres. Also, pieces of blue denim and an orange-coloured T-shirt were used in this study as representatives of dyed clothing commonly found on an everyday basis. A bundle of fibres and textile pieces about 0.5 cm in length were soaked with the solutions of the drugs. Then the fibre bundles and textile pieces were left overnight to dry by evaporation of ethanol prior to spectroscopic examination.

8.2.2 Spectroscopic instrumentation

Raman spectra were collected from the drugs-impregnated fibre bundles and textile pieces using three different spectrometers; one benchtop spectrometer, a Renishaw *InVia* Reflex dispersive spectrometer, and two portable spectrometers namely, a Renishaw RX210 ‘Raman-in-a-suitcase’ (RIAS) portable Raman analyser and a Delta Nu Inspector Raman FSX instrument.

a- Renishaw InVia reflex spectrometer

Raman spectra were obtained using a Renishaw *InVia* Reflex spectrometer (Wotton-under-Edge, UK), operating with a high power NIR diode laser emitting at 785 nm and thermoelectrically cooled CCD (400×575 pixels) detector, coupled to a Renishaw compact fibre-optic probe with a 25-mm focal length lens. The diffraction grating ($1200 \text{ lines mm}^{-1}$) gave the spectral range $3200\text{--}100 \text{ cm}^{-1}$ with a spectral resolution of 2 cm^{-1} . Daily calibration of the wavenumber axis was achieved by recording the Raman spectrum of a silicon wafer (1 accumulation, 10 s) in static

mode. If necessary, an offset correction is performed to ensure that the position of the silicon band is calibrated at $520.5 \pm 0.1 \text{ cm}^{-1}$. Spectra were recorded from drugs-impregnated clothing with the accumulation of one scan, 10-s exposure and 28-mW laser power at the sample. The spectrometer was controlled by PC with instrument control software (Renishaw WiRE 2 Service Pack 9). Using the instrument in the microscopic mode (Renishaw *InVia* dispersive Raman microscope), reference Raman spectra of pure drugs, fibres and textiles were obtained to be compared with the spectra collected from the three spectrometers. The Raman scattering was excited with a 785-nm near-infrared diode laser and a 50x objective lens giving a laser spot diameter of 5 μm . Spectra were obtained for a 10-s exposure of the CCD detector in the wavenumber region $100\text{--}3200 \text{ cm}^{-1}$ using the extended scanning mode of the instrument. With 110 mW laser power, one accumulation was collected for the drugs and five accumulations were collected for the fibres and textiles.

b- Renishaw portable Raman analyser RX210 'RIAS'

The RIAS (Wotton-under-Edge, UK) was equipped with a diode laser emitting at 785 nm and a thermoelectrically cooled (400×575 pixels) CCD detector, with a coupled Renishaw compact fibre optic probe, equipped with a 20 \times (NA 0.35) Olympus objective lens. The diffraction grating (1000 lines/mm) afforded the spectral range $2100\text{--}100 \text{ cm}^{-1}$ with a spectral resolution of 10 cm^{-1} . The power of the diode laser was 49 mW at the sample. Daily calibration of the wavenumber axis was achieved by recording the Raman spectrum of a silicon wafer (one accumulation, 10-s exposure) for static modes. If necessary, an offset correction is performed to ensure that the position of the silicon band is $520.5 \pm 0.1 \text{ cm}^{-1}$. Spectra were recorded with the accumulation of one scan, 10-s exposure. The spectrometer was controlled by a portable PC with instrument control software (Renishaw WiRE 2 Service pack 8).

c- Delta Nu inspector Raman FSX

The Inspector Raman instrument (Laramie, WY, USA) was equipped with a diode laser emitting at 785 nm and a thermoelectrically (1×1024 pixels) CCD detector and a custom 25-mm-focal-length nose piece. The spectral range was $2000\text{--}200\text{ cm}^{-1}$ with a spectral resolution of 8 cm^{-1} . The laser power at the sample was 37 mW. Daily calibration of the wavenumber axis was achieved by recording the Raman spectrum of polystyrene within the calibration routine built into the software. Spectra were recorded with the accumulation of one scan, 10-s exposure. The spectrometer was controlled by a portable PC with instrument control software (Nu Spec Version 4.75).

8.3 Results and Discussion

For these studies, drug-impregnated clothing was simulated by treating a piece of denim with a methanolic solution of cocaine hydrochloride. After the cloth was left to dry, a scanning electron micrograph (Quanta 400, FEI Ltd, Cambridge, UK) was taken (Figure 8.1). The image clearly shows that microcrystals of the drug molecules form between the denim fibres.

8.3.1 Cocaine hydrochloride-impregnated clothing

a- Cocaine hydrochloride-impregnated undyed natural fibres

Raman spectra were collected from the cocaine hydrochloride-impregnated cotton bundle using the three spectrometers (Figure 8.2). Comparison of these spectra with the reference spectrum of cocaine hydrochloride showed that the drug could be easily identified by its Raman spectrum. The characteristic Raman bands of cocaine hydrochloride can be identified, such as those at 1711 , 1594 , 998 , 866 and 784 cm^{-1} . These key signature bands are clearly observed in the spectra collected from the three spectrometers and the results compare favourably with the reference cocaine hydrochloride. The total acquisition times were 25, 20 and 60 s for data collected from

the Delta Nu Inspector Raman FSX, the RIAS portable spectrometer and the Renishaw *InVia* Reflex Spectrometer coupled to a fibre-optic probe respectively. Also, the spectra collected from cocaine impregnated wool show the characteristic features of cocaine hydrochloride (Figure 8.3). Although the spectrum obtained from cocaine-impregnated wool using the Delta Nu Inspector Raman FSX instrument contains two bands assigned to the wool; the amide I ν (C=O) mode at 1654 cm^{-1} and the δ (CH₂) mode at 1445 cm^{-1} (marked with asterisks in Figure 8.3 A).^[216,239] The presence of these bands did not prevent the identification of the characteristic signature bands of the drug. Similarly, the characteristic Raman features of cocaine hydrochloride could be clearly observed in the Raman spectra collected from cocaine-impregnated silk (Figure 8.4). The spectra are of a high quality with a good signal/noise ratio and no appreciable background due to fluorescence. The NIR laser at 785 nm gave excellent spectra for the drug and there was no detectable background fluorescence. There were no significant bands that could be assigned to the fibre substrate; the Raman scattering from the drug is usually relatively intense compared to that from the fibres allowing ready differentiation from interference from the fibres substrate bands.

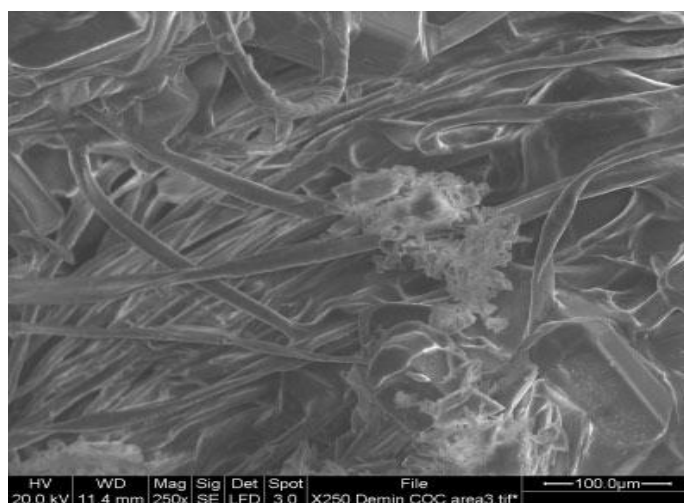


Figure 8.1 Scanning electron micrograph of a piece of denim impregnated with cocaine hydrochloride

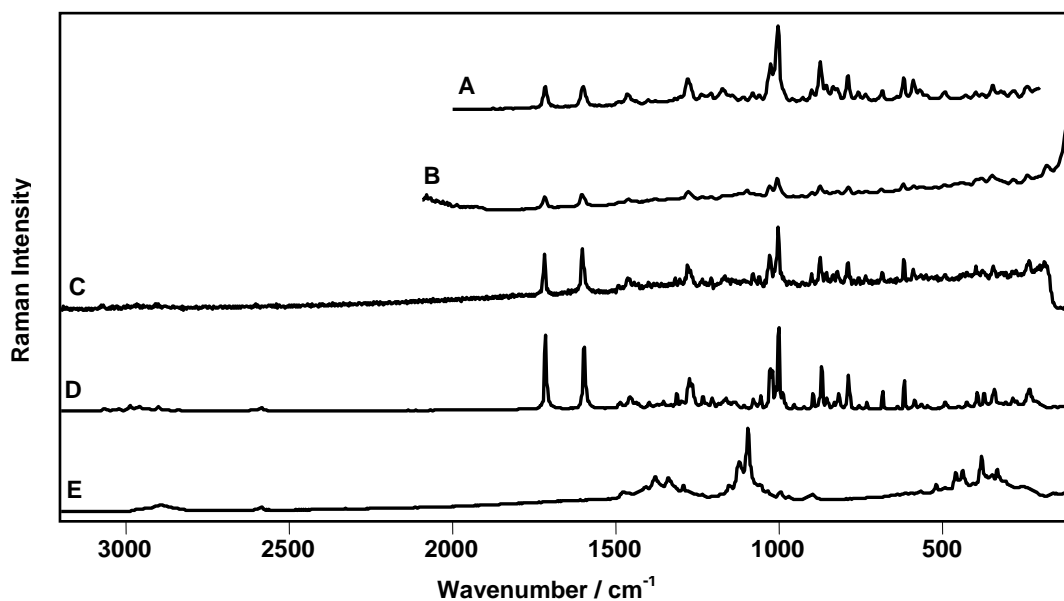


Figure 8.2 Raman spectra of cocaine-impregnated cotton collected using
 A: Delta Nu portable
 B: RIAS portable
 C: Benchtop Renishaw InVia Reflex dispersive spectrometer coupled to a fibre optic probe
 D: Reference cocaine.HCl
 E: Reference cotton fibres

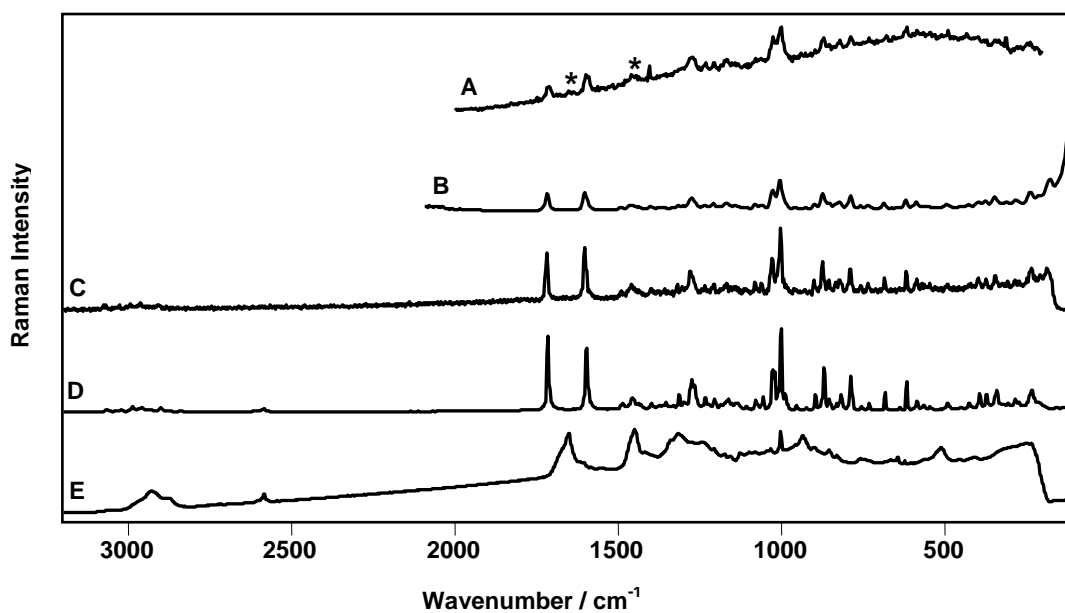


Figure 8.3 Raman spectra of cocaine-impregnated wool collected using
 A: Delta Nu portable (Asterisks indicate wool bands)
 B: RIAS portable
 C: Benchtop Renishaw *InVia* reflex dispersive spectrometer coupled to a fibre optic probe
 D: Reference cocaine.HCl and
 E: Reference wool fibres

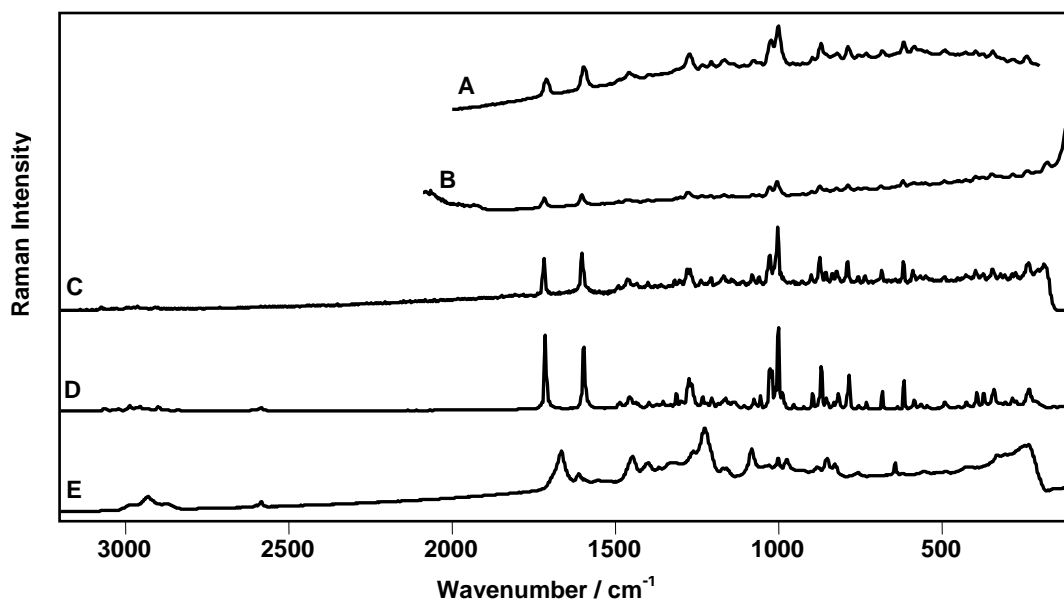


Figure 8.4 Raman spectra of cocaine-impregnated silk collected using
 A: Delta Nu portable
 B: RIAS portable
 C: Benchtop Renishaw *InVia* reflex dispersive spectrometer coupled to a fibre optic probe
 D: Reference cocaine.HCl and
 E: Reference silk fibres

b- Cocaine hydrochloride–impregnated undyed synthetic fibres

Figure 8.5 shows the spectra obtained from cocaine hydrochloride– impregnated polyester fibres. In addition to the bands arising from the drug, the resulting spectra also contain several peaks assigned to the polyester fibres (marked with dashed lines in Figure 8.5): these appear at 1725 cm^{-1} [$\nu(\text{C}=\text{O})$], 1610 cm^{-1} (aromatic ring stretch) and 854 cm^{-1} [$\gamma(\text{CCC})$].^[237,238] The polyester bands at 1725 and 1610 cm^{-1} overlap with the drug bands at 1711 and 1594 cm^{-1} respectively. While the overlapped bands at ca. 1600 cm^{-1} are clearly resolved, the polyester feature at 1725 cm^{-1} appears as a shoulder at a higher wavenumber on the cocaine benzoate ester band at 1711 cm^{-1} . However, in each case, the identity of cocaine hydrochloride was readily established and the drug characteristic features at 1711 , 1594 , 998 , 866 and 784 cm^{-1} could be clearly identified.

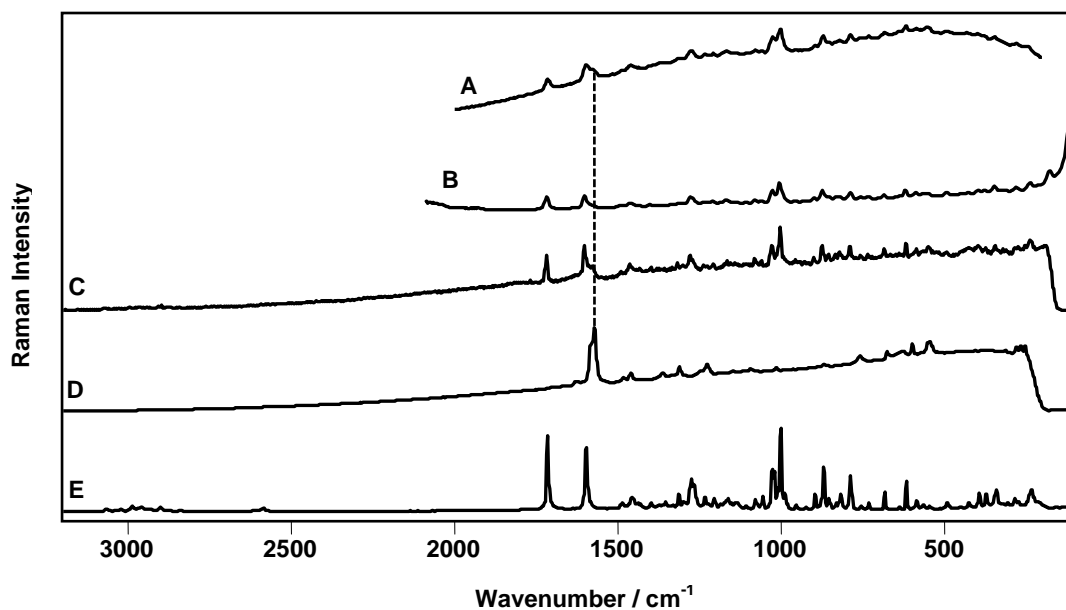


Figure 8.6 Raman spectra of cocaine-impregnated denim collected using
 A: Delta Nu portable
 B: RIAS portable
 C: Benchtop Renishaw *InVia* Reflex dispersive spectrometer coupled to a fibre optic probe
 D: Reference denim fibres (dashed line indicates denim band)
 E: Reference cocaine.HCl

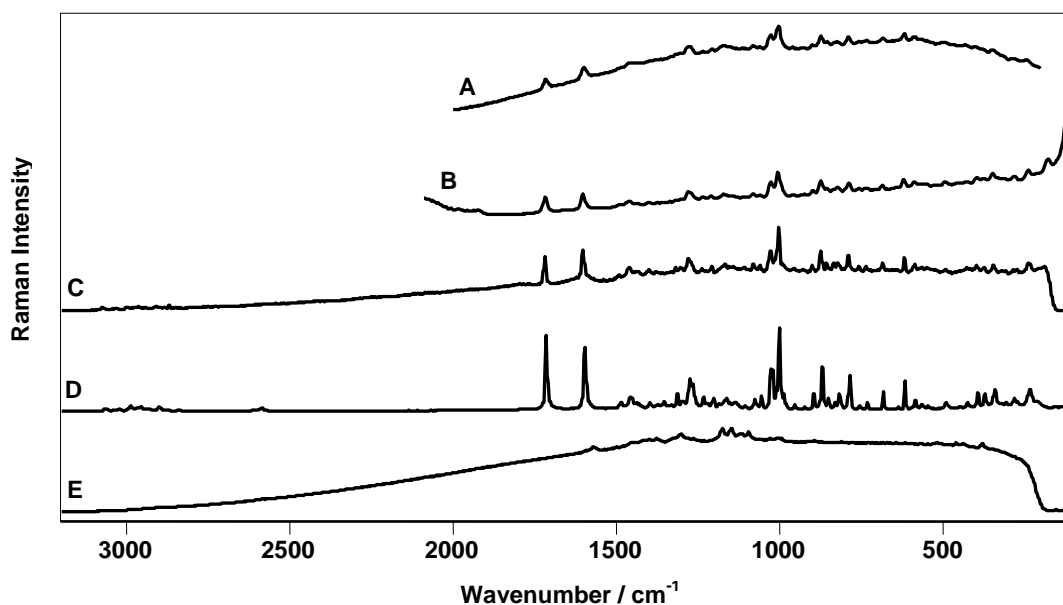


Figure 8.7 Raman spectra of cocaine-impregnated T-shirt collected using
 A: Delta Nu portable
 B: RIAS portable
 C: Benchtop Renishaw *InVia* reflex dispersive spectrometer coupled to a fibre optic probe
 D: Reference cocaine.HCl
 E: Reference T-shirt fibres

Further illustrations of the applicability of this approach were obtained from MDMA and amphetamine sulphate-impregnated clothing. The Raman spectra were collected using the two portable instruments; the Renishaw portable Raman analyser RX210 ‘RIAS’ and Delta Nu inspector Raman FSX.

8.3.2 MDMA-impregnated clothing

a- MDMA-impregnated undyed natural fibres

Comparing the spectra collected from MDMA-impregnated cotton fibres using the two portable instruments with the reference spectrum of MDMA showed that the drug can be identified. The characteristic Raman bands of MDMA can be identified such as those at 807, 769 and 712 cm^{-1} . There is no significant band in the spectra attributable to the cotton fibres (Figure 8.8). Similar results were obtained from MDMA-impregnated-wool and silk fibres (Figures 8.9 and 8.10, respectively). The characteristic features of MDMA can be clearly observed in the spectra.

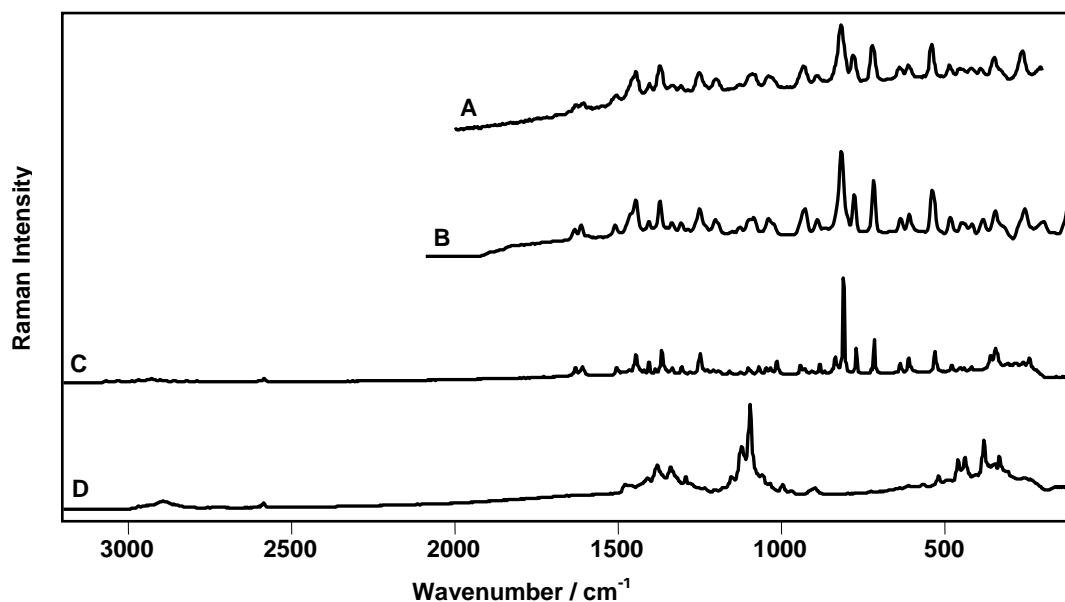


Figure 8.8 Raman spectra of MDMA-impregnated cotton collected using
A: Delta Nu portable
B: RIAS portable
C: Reference MDMA
D: Reference cotton fibres

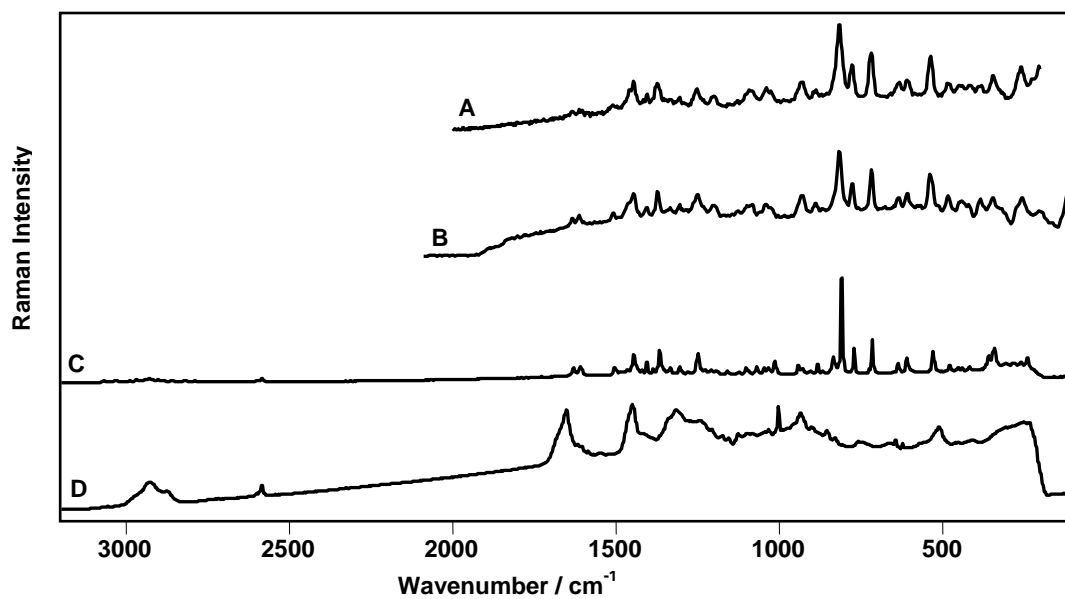


Figure 8.9 Raman spectra of MDMA-impregnated wool collected using
 A: Delta Nu portable
 B: RIAS portable
 C: Reference MDMA
 D: Reference wool fibres

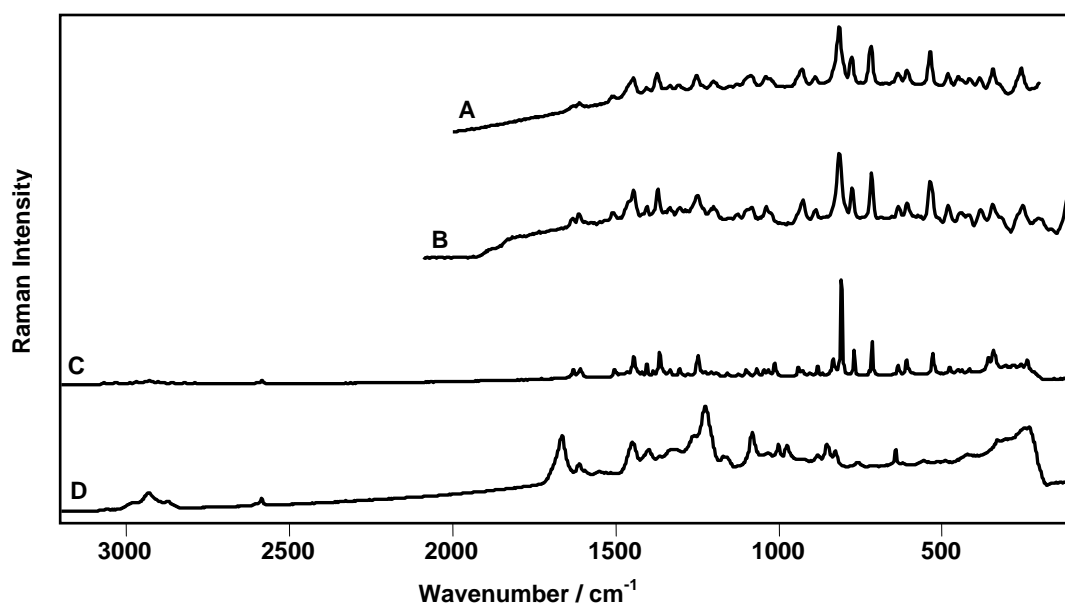


Figure 8.10 Raman spectra of MDMA-impregnated silk collected using
 A: Delta Nu portable
 B: RIAS portable
 C: Reference MDMA
 D: Reference silk fibres

b- MDMA-impregnated undyed synthetic fibres

Figure 8.11 shows the spectra obtained from MDMA-impregnated polyester fibres in which the key signature bands of MDMA can be unambiguously identified. Although the strongest band of polyester fibres appears in the Raman spectrum acquired using the RIAS portable; this does not prevent the identification of MDMA.

c- MDMA-impregnated dyed textiles

The spectra obtained from MDMA impregnated-denim and orange-coloured T-shirt show the characteristic Raman features of MDMA (Figures 8.12 and 8.13, respectively). A broad fluorescent background can be seen in these spectra but the diagnostic Raman features of MDMA are clearly visible above the background and the characteristic drug bands are clearly observed.

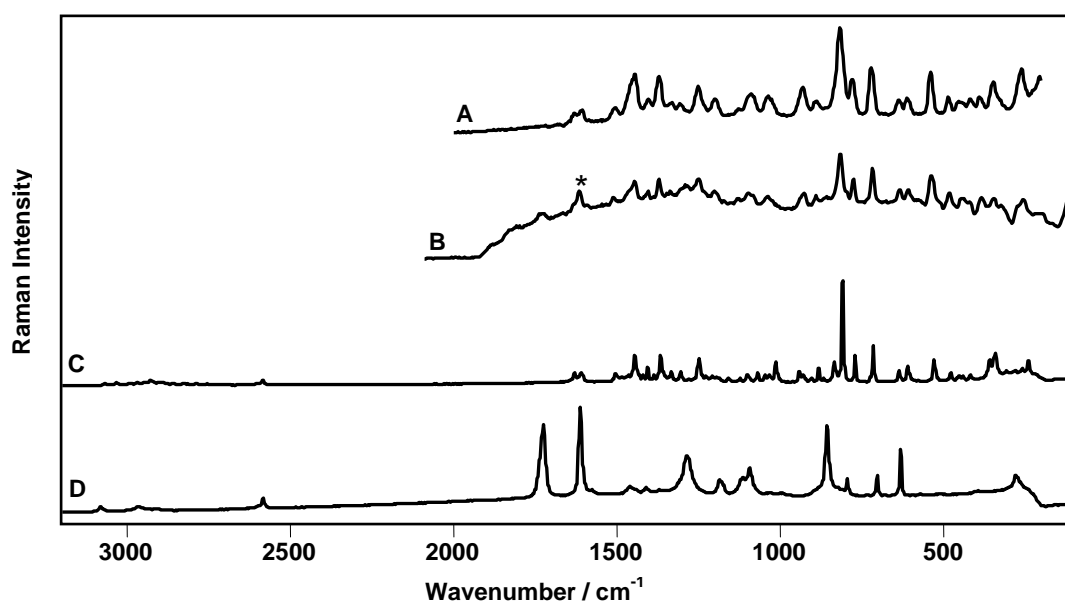


Figure 8.11 Raman spectra of MDMA-impregnated polyester collected using
A: Delta Nu portable
B: RIAS portable
C: Reference MDMA
D: Reference polyester fibres

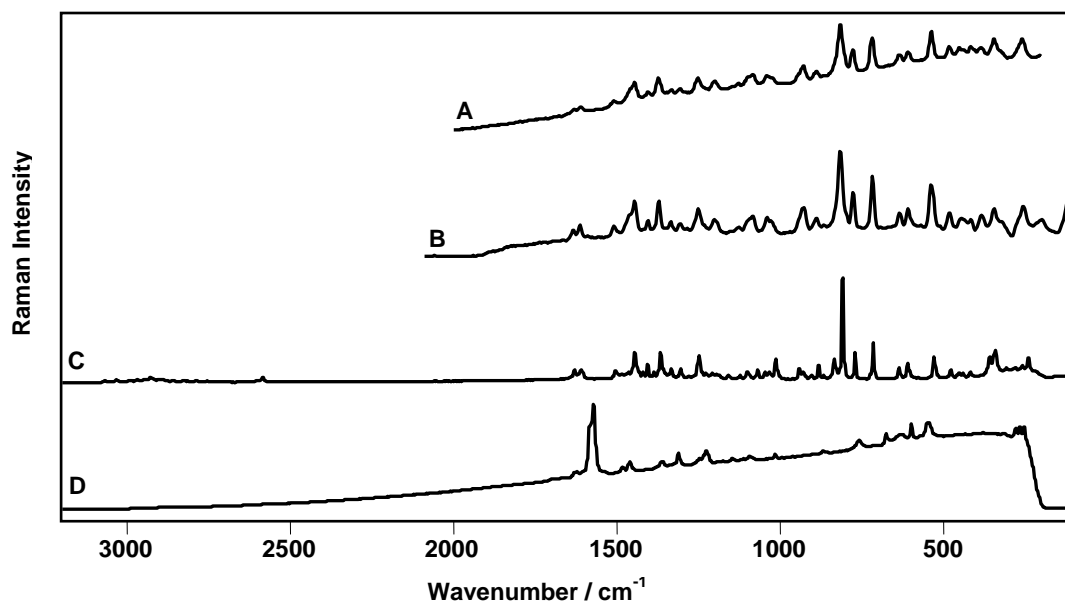


Figure 8.12 Raman spectra of MDMA-impregnated denim collected using
 A: Delta Nu portable
 B: RIAS portable
 C: Reference MDMA
 D: Reference denim fibres

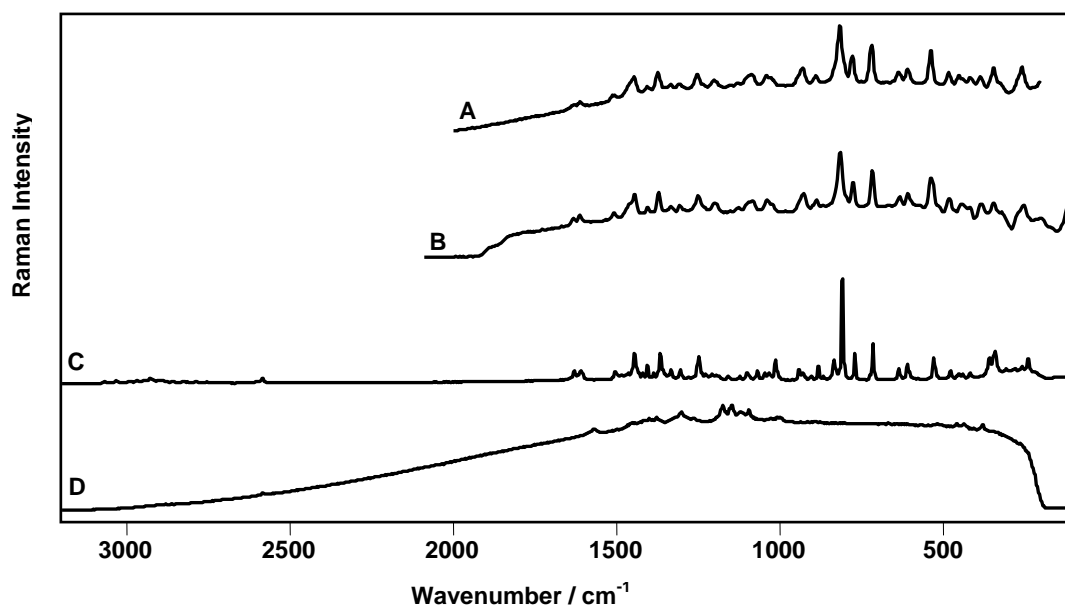


Figure 8.13 Raman spectra of MDMA-impregnated T-shirt collected using
 A: Delta Nu portable
 B: RIAS portable
 C: Reference MDMA
 D: Reference T-shirt fibres

8.3.3 Amphetamine sulphate-impregnated clothing

a- Amphetamine sulphate-impregnated undyed natural fibres

The characteristic bands of amphetamine sulphate i.e. those at 1030, 1001, 974 cm^{-1} can be identified at the spectra obtained from amphetamine-impregnated cotton fibres (Figure 8.14). There is no significant band can be assigned to the cotton substrate. Also, the Raman spectra acquired from amphetamine sulphate-impregnated wool and silk fibres (Figures 8.15 and 8.16, respectively) show these key signatures bands of the drug.

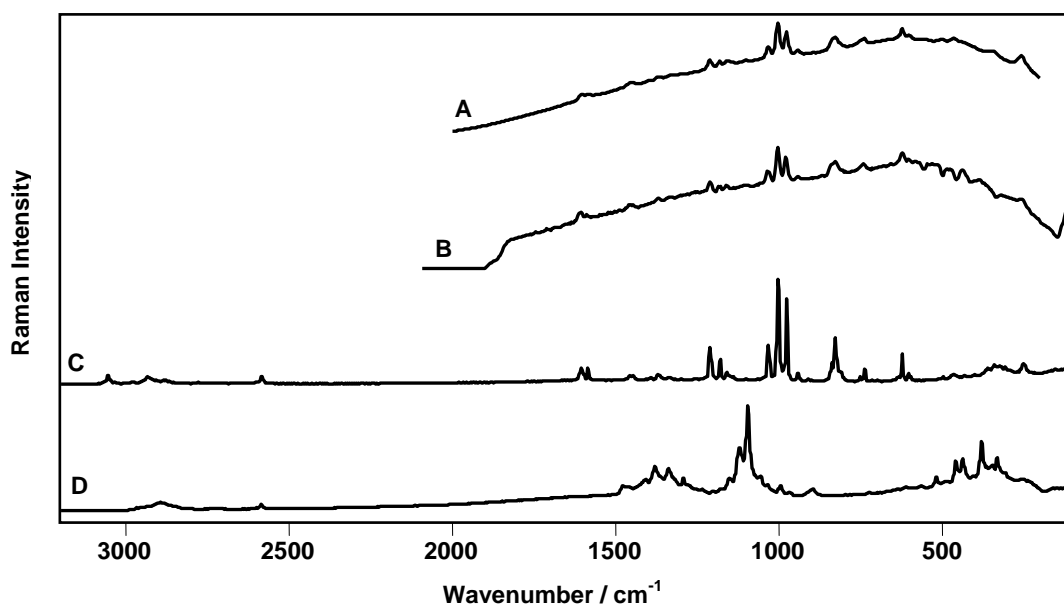


Figure 8.14 Raman spectra of amphetamine-impregnated cotton collected using
A: Delta Nu portable
B: RIAS portable
C: Reference amphetamine sulphate
D: Reference cotton fibres

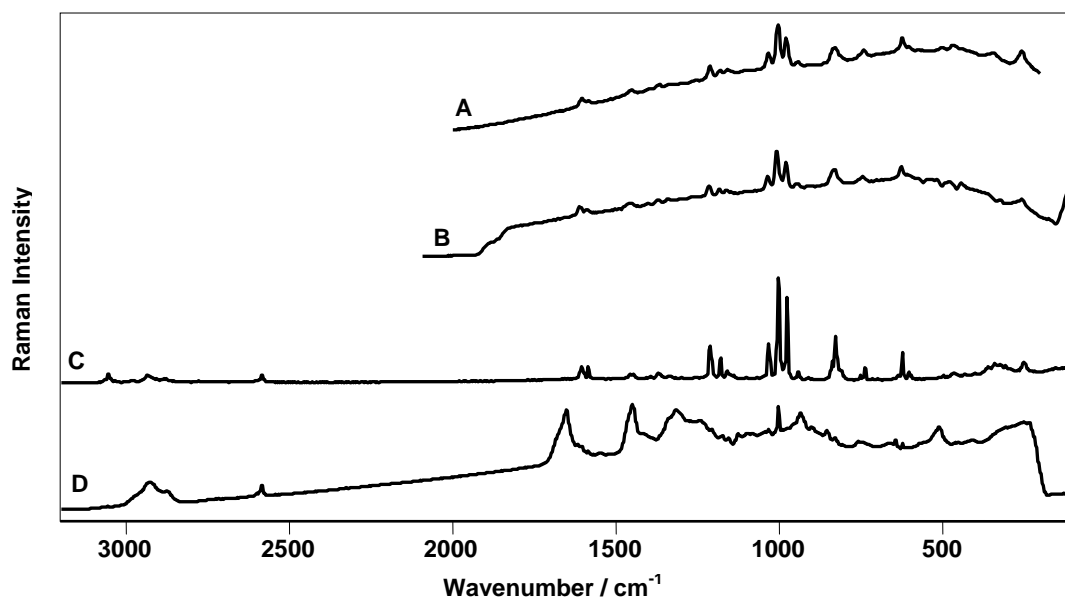


Figure 8.15 Raman spectra of amphetamine-impregnated wool collected using
 A: Delta Nu portable
 B: RIAS portable
 C: Reference amphetamine sulphate
 D: Reference wool fibres

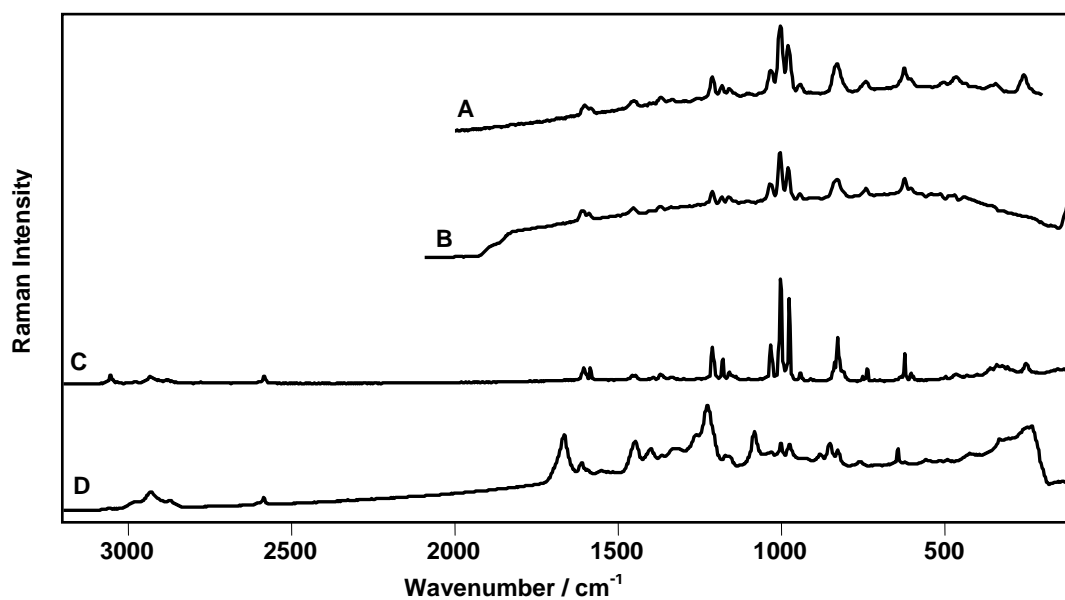


Figure 8.16 Raman spectra of amphetamine-impregnated silk collected using
 A: Delta Nu portable
 B: RIAS portable
 C: Reference amphetamine sulphate
 D: Reference silk fibres

b- Amphetamine sulphate–impregnated undyed synthetic fibres

Figure 8.17 shows the spectra obtained from amphetamine–impregnated polyester fibres. The identity of amphetamine sulphate is readily established and the drug characteristic features can be clearly identified.

c- Amphetamine sulphate–impregnated dyed textiles

The spectra obtained from cocaine-impregnated denim show the characteristic Raman features of amphetamine sulphate (Figure 8.18). Also, Figure 8.19 shows the Raman spectra collected from amphetamine sulphate–impregnated orange-coloured T-shirt specimens. A broad fluorescent background can be seen in the spectra collected from the two spectrometers but in all cases the diagnostic Raman features of amphetamine are clearly visible above the background.

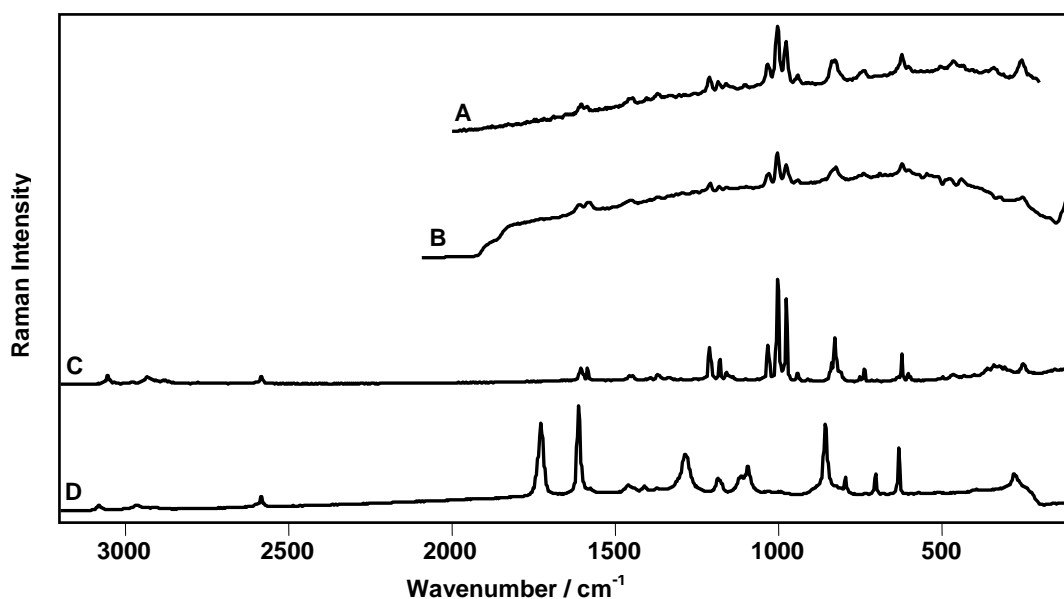


Figure 8.17 Raman spectra of amphetamine-impregnated polyester collected using
A: Delta Nu portable
B: RIAS portable
C: Reference amphetamine sulphate
D: Reference polyester fibres

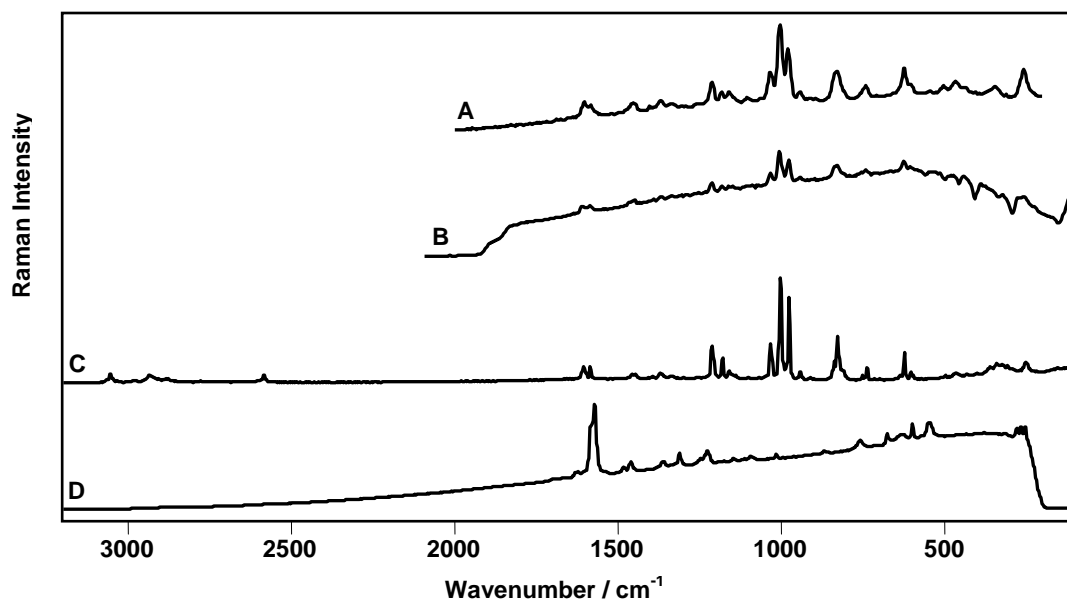


Figure 8.18 Raman spectra of amphetamine-impregnated denim collected using
 A: Delta Nu portable
 B: RIAS portable
 C: Reference amphetamine sulphate
 D: Reference denim fibres

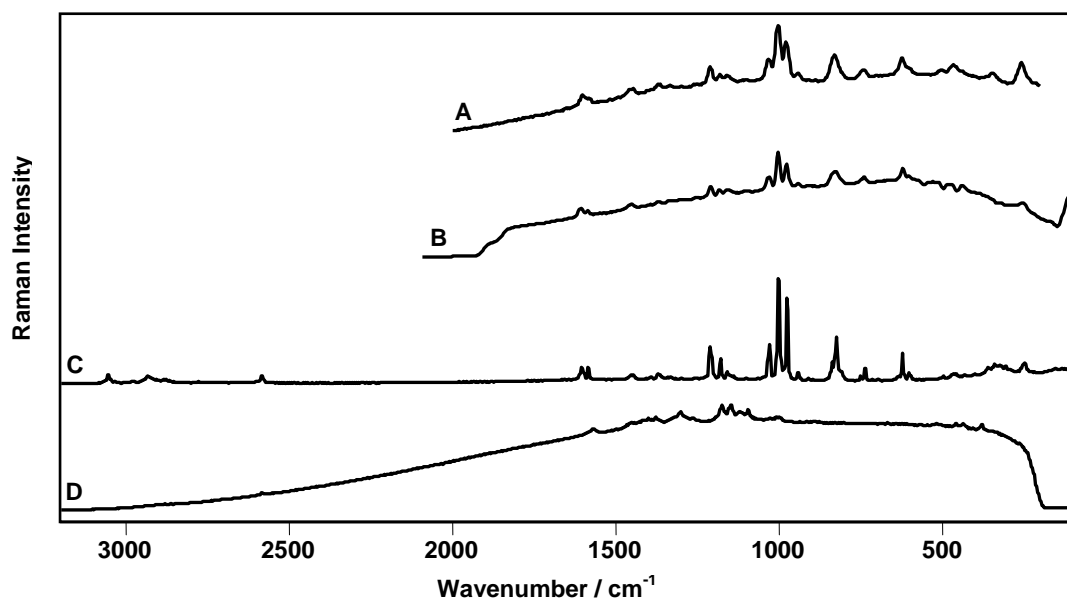


Figure 8.19 Raman spectra of amphetamine-impregnated T-shirt collected using
 A: Delta Nu portable
 B: RIAS portable
 C: Reference amphetamine sulphate
 D: Reference T-shirt fibres

8.3 Data comparison and library searching

Raman spectra from all instruments were exported to the Galactic^{*}.SPC format. Spectra were then compared using GRAMS AI (Version 8.0, Thermo Electron Corp, Waltham, MA, USA); the Raman spectra were not subjected to any data manipulation or processing techniques and are reported as collected. We have used the spectral ID function of GRAMS AI to construct instrument specific libraries, which contain spectra of a range of narcotics and explosives. This allows the user to rapidly identify unknown compounds by searching a database held on the spectrometer computer. Once the spectral data have been collected from each spectrometer, a library search was carried out. The search algorithm provided by GRAMS AI software involves using double-sided peak matching (with shoulder detection), non-baseline corrected, 32-bit data construction and using the first derivative least squares. Essentially, the software compares the peak position search data with data in the constructed libraries for the highest number of peak position matches. Tables 8.1-8.3 present the percentage matches for peaks searches of the constructed libraries. The data show that in all the cases a positive identification can be made, with the highest match being assigned to the drug of interest in all the cases.

These results show a clear application of portable Raman spectroscopy as a primary screening technique for drugs-of-abuse in live situations. Data could be obtained rapidly and, using a library search, unambiguous identification of unknown contaminants could be made. Identification can be readily obtained, for example, in a port of entry using the portable spectrometers and, on taking the sample to the laboratory, identification can be confirmed using the benchtop Raman spectrometer coupled to a fibre-optic probe or other hyphenated analytical techniques. In addition, our approach leaves the drug unaltered and in its original environment without risking

operator exposure or evidence contamination. Furthermore, the rapid acquisition of Raman spectra in situ in the field offer a reliable method for forensic scientists and police agencies that has the potential for rapidly identifying unknown samples.

Instrument Cocaine-impregnated Sample	Renishaw <i>InVia</i> Library match %	RIAS Match%	Delta Nu Match%
Cotton	77	92	89
Wool	82	98	79
Silk	74	93	74
Polyester	80	97	76
Denim	67	94	78
T-shirt	67	89	79

Table 8.1 Library searching matches of the spectra obtained from the cocaine hydrochloride- impregnated clothing using three spectrometers

Instrument MDMA-impregnated Sample	RIAS Match%	Delta Nu Match%
Cotton	90	72
Wool	91	73
Silk	94	78
Polyester	89	69
Denim	95	79
T-shirt	87	74

Table 8.2 Library searching matches of the spectra obtained from the MDMA-impregnated clothing using two portable spectrometers

Instrument Amphetamine- impregnated Sample	RIAS Match%	Delta Nu Match%
Cotton	93	90
Wool	95	82
Silk	90	80
Polyester	96	79
Denim	97	83
T-shirt	91	92

Table 8.3 Library searching matches of the spectra obtained from the amphetamine sulphate-impregnated clothing using two portable spectrometers

Chapter 9

Detection of drugs of abuse and explosives on skin using confocal Raman spectroscopy

9.1 Introduction

Vibrational spectroscopy has been applied to characterize the molecular nature of human and animal skin and have shown that FT-Raman spectroscopy is a powerful technique for probing the structure of the *stratum corneum*, which is the outermost layer of the skin and which provides the main barrier to the ingress of most drugs and environmental contaminants.^[253-255] The advent of excitation sources of lower energy in the near infrared, has enabled the recording of Raman spectra from sensitive biomaterials such as skin, nail, hair, and bone^[211] and the study of human skin in vitro and in vivo.^[256, 257] FT-Raman spectroscopy has been applied for the characterization of mummified human skin and nail^[258-261] and for the study of molecular alterations in skin cancer.^[262] Ambient ionization mass spectrometry has been applied successfully for the detection of explosives on skin.^[263] This section addresses the detection of traces of drugs of abuse and explosives on human skin. Confocal Raman microscopy has been applied for the identification of particulate matter contaminant on human skin. The spectra were readily acquired non-invasively without sample preparation. With the use of a lower energy laser excitation operating at 785 nm wavelength, the drugs and explosives contaminants can be obtained without alteration of the analyte or affecting the integrity of the skin substrate.

9.2 Experimental

9.2.1. Samples: See section 6.2.1

- Skin samples

Human skin samples were kindly provided by the Department of Biomedical Sciences

and cut into small pieces (1x1 cm). Skin samples were doped with a few crystals of the drugs of abuse and explosives and then placed on the stage of the microscope prior to analysis.

9.2.2. Raman spectroscopy

Raman spectra were collected using a Renishaw *InVia* Reflex dispersive Raman microscope with a 785 nm near-infrared diode laser (Renishaw, Wotton-under-Edge, UK) and a 50×objective lens giving a laser spot diameter of 5 μm . Spectra were obtained at 2 cm^{-1} resolution for a 10 second exposure of the CCD detector in the wavenumber region 100–1800 cm^{-1} using the extended scanning mode of the instrument. Raman spectra were collected from particles with edge dimensions in the range 5–10 μm . With 90 mW laser power at the sample, one accumulation was collected for the drugs and explosives reference spectra and for confocal experiments with contaminated skin samples. Reference spectrum for the human skin was collected with five accumulations. With these parameters, the total acquisition time of the spectra of the drugs of abuse and explosives on skin was about 90 seconds. Spectral acquisition, presentation, and analysis were performed with the Renishaw WIRE (service pack 9) and GRAMS AI version 8 (Thermo Electron Corp, Waltham, MA, USA) software.

9.3 Results and Discussion

9.3.1 Detection of pure drugs of abuse on human skin

Table 9.1 lists the Raman shifts and vibrational assignments of the strongest bands of human skin. This can help in identifying these bands if they appear in the Raman spectra obtained from particles of drugs of abuse and explosives on the surface of human skin. Figure 9.1 shows the confocal Raman spectrum acquired from a crystal of cocaine hydrochloride on skin. The principal Raman features of cocaine

Wavenumber	Vibrational assignment
1651	ν (C=O) amide I
1440	δ (CH ₂) (CH ₃)
1338	δ (CH ₂)
1127	ν (CN)
1001	ν (C=C) symmetric
937	ν (CC)

Table 9.1 Wavenumber and vibrational band assignments of human skin

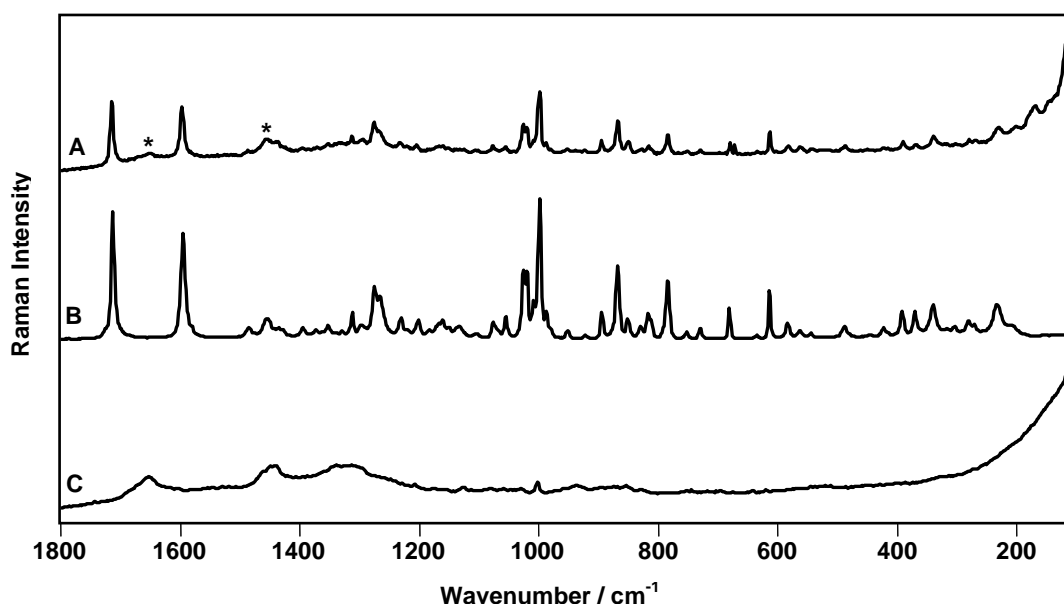


Figure 9.1 Raman spectra of
A: Cocaine hydrochloride on human skin
B: Reference cocaine hydrochloride
C: Human skin
785 nm, 90.8 mW, 10s exposure, 1 accumulation for A &B, 5 accumulations for C

hydrochloride can be identified in this spectrum, such as those at 1711, 1594, 998, 866 and 784 cm^{-1} . Although the presence of two bands arising from the skin ^[253,255] substrate can be observed in the spectrum; those at 1651 cm^{-1} [ν (C=O) amide I] and 1440 cm^{-1} [δ (CH₂) scissoring], the drug can be identified by its characteristic Raman bands described above. Figure 9.2 shows the Raman spectrum obtained from an

MDMA crystal on human skin. It can be observed that the characteristic Raman bands of MDMA are clearly identified (bands at 807,769 and 712 cm^{-1}) and that there is no significant band attributable to the skin substrate. Also, the confocal Raman spectrum acquired from an amphetamine sulphate crystal on the surface of human skin (Figure 9.3) shows the characteristic Raman bands of the drug and, although the strongest bands arising from the skin at 1651 cm^{-1} and 1440 cm^{-1} appear in the spectrum of the drug, these bands do not overlap with the key signature bands of amphetamine sulphate. Similarly, the Raman spectra acquired from the benzodiazepines , flunitrazepam and nitrazepam , (Figures 9.4 and 9.5, respectively) crystals on human skin show the characteristic Raman features of the drugs and compare favourably with the reference Raman spectra of the drugs. No significant bands in these spectra can be assigned to the skin substrate.

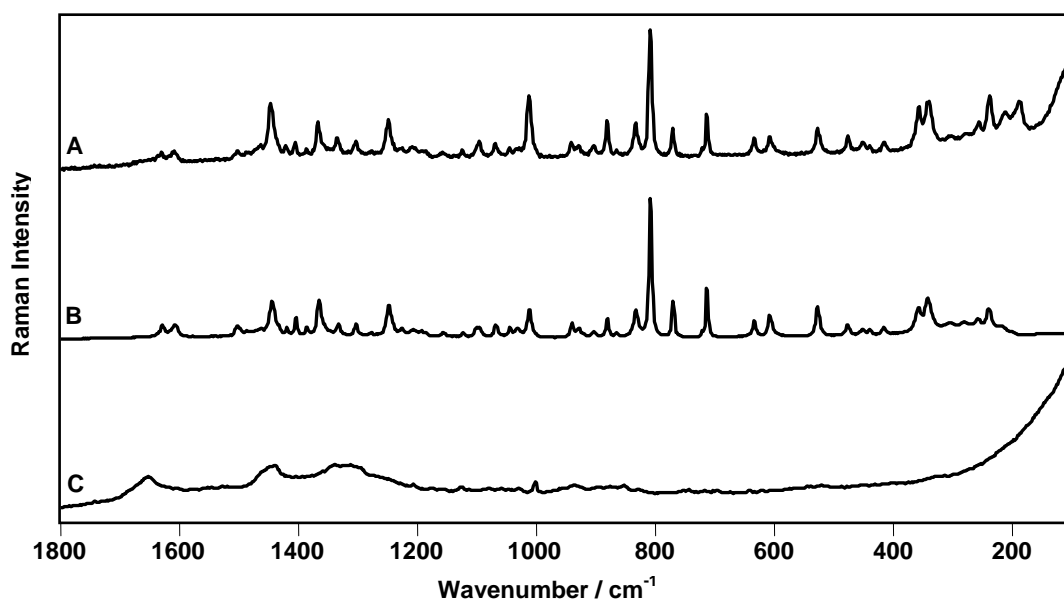


Figure 9.2 Raman spectra of

A: MDMA on human skin

B: Reference MDMA

C: Human skin

785 nm, 90.8 mW, 10s exposure, 1 accumulation for A &B, 5 accumulations for C

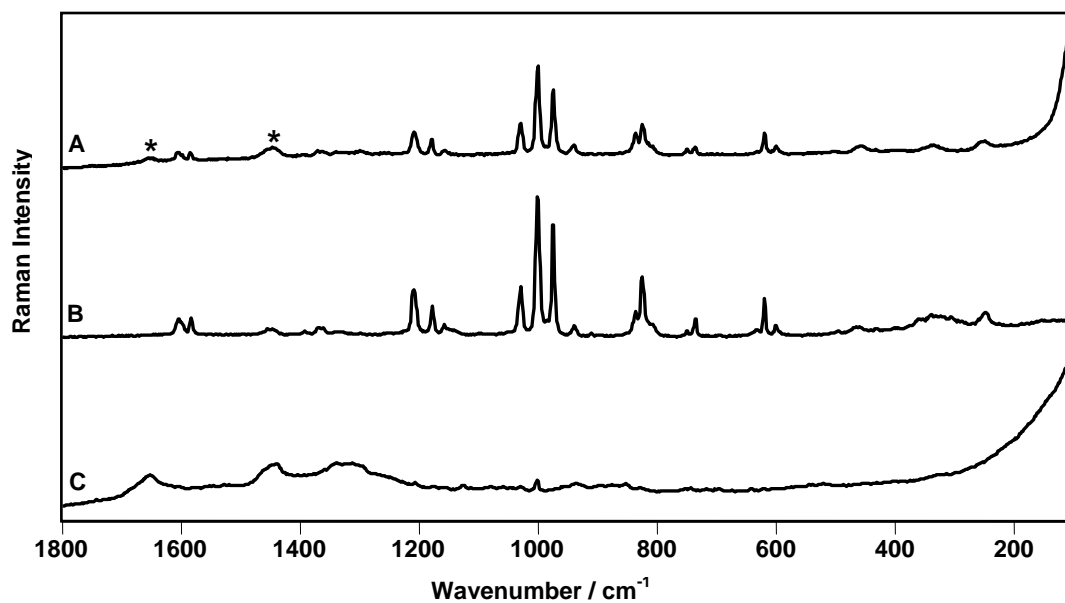


Figure 9.3 Raman spectra of
 A: Amphetamine sulphate on human skin
 B: Reference Amphetamine sulphate
 C: Human skin
 785 nm, 90.8 mW, 10s exposure, 1 accumulation for A &B, 5 accumulations for C

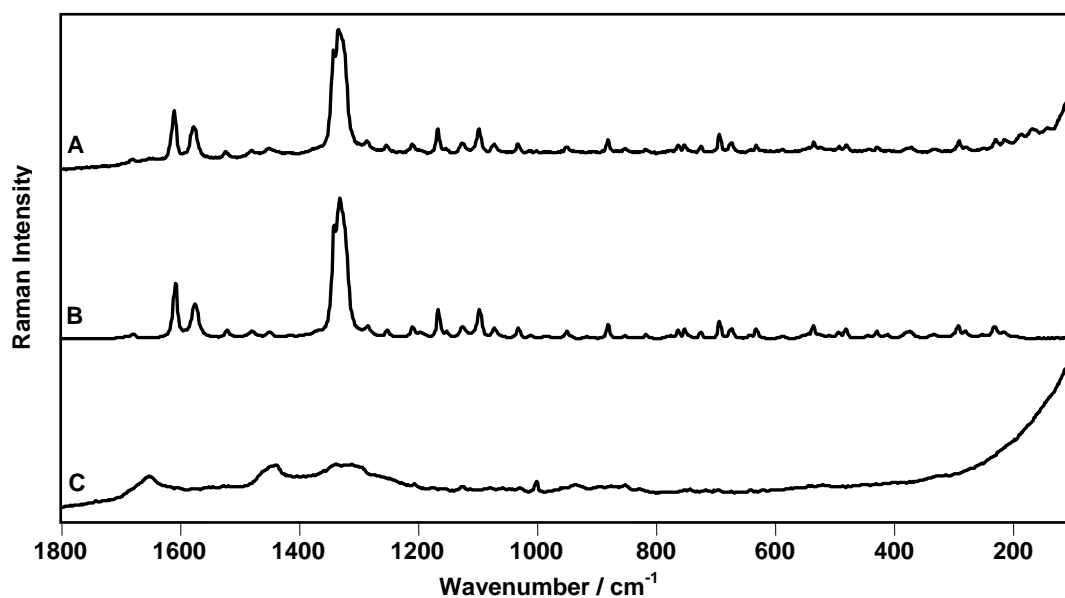


Figure 9.4 Raman spectra of
 A: Flunitrazepam on human skin
 B: Reference Flunitrazepam
 C: Human skin
 785 nm, 90.8 mW, 10s exposure, 1 accumulation for A &B, 5 accumulations for C

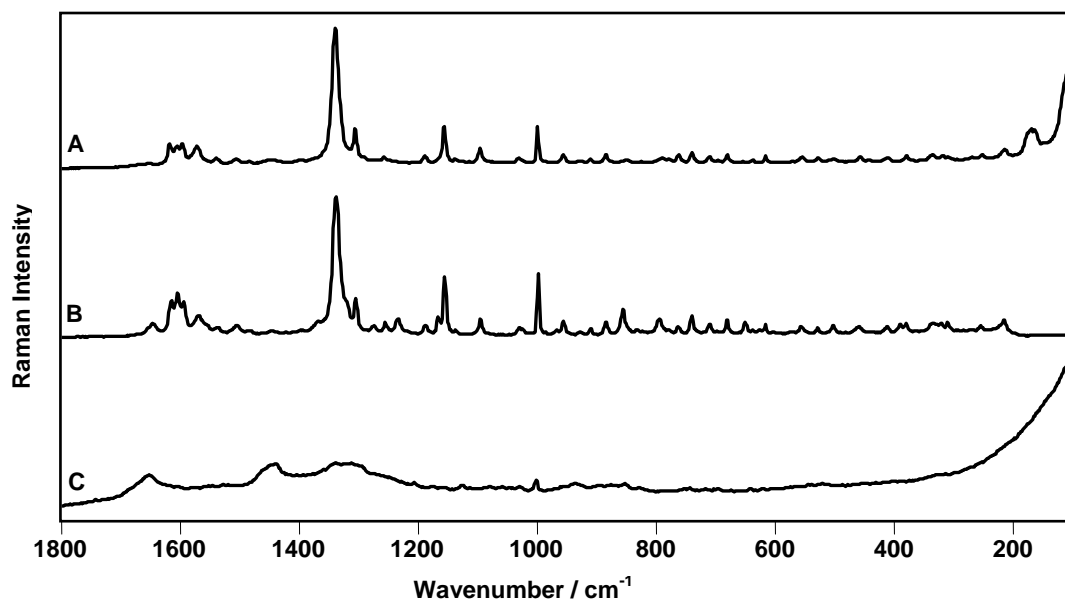


Figure 9.5 Raman spectra of
 A: Nitrazepam on human skin
 B: Reference nitrazepam
 C: Human skin
 785 nm, 90.8 mW, 10s exposure, 1 accumulation for A &B, 5 accumulations for C

9.3.2 Detection of street drugs of abuse on human skin

The cutting agents that may be used to bulk the street samples of the drugs of abuse may complicate the spectroscopic detection of these drugs on the skin. Fluorescence emission arising from these substances may overwhelm the Raman signal from the drugs of abuse and the Raman bands of the cutting agents may additionally overlap with the characteristic bands of the drugs. Confocal Raman spectra were obtained from skin crystals of seized street samples of the drugs of abuse, namely cocaine hydrochloride, MDMA and amphetamine sulphate, on human skin. The characteristic bands of cocaine hydrochloride can be seen in the Raman spectrum acquired from a crystal of the drug on skin (Figure 9.6). In addition to these bands there are just one band arising from the cutting agent (at $\sim 832 \text{ cm}^{-1}$) and two further bands arising from the skin at 1651 and 1440 cm^{-1} . Also, MDMA can be identified from the confocal spectrum obtained from a crystal of a street sample of the drug on the surface of skin

(Figure 9.7). The principal bands of MDMA can be clearly observed and no significant features can be assigned to the cutting agent. Although the strongest two bands arising from the skin substrate (marked with asterisks in figure 9.7A) appear in the spectrum, these bands do not overlap with the characteristic bands of the drug as they appear in the spectral region $1650\text{-}1300\text{ cm}^{-1}$, away from the characteristic Raman bands of MDMA. Similarly, the spectrum collected from a particle of seized sample of amphetamine sulphate shows the characteristic bands of the drug (Figure 9.8). In addition to the strongest bands arising from the skin substrate (marked with asterisks in figure 9.8A), there are two bands at 1360 and 555 cm^{-1} arising from the excipients (marked with arrows in figure 9.8A). Despite the presence of these interfering bands, the major bands of amphetamine sulphate are still observable and can be clearly identified.

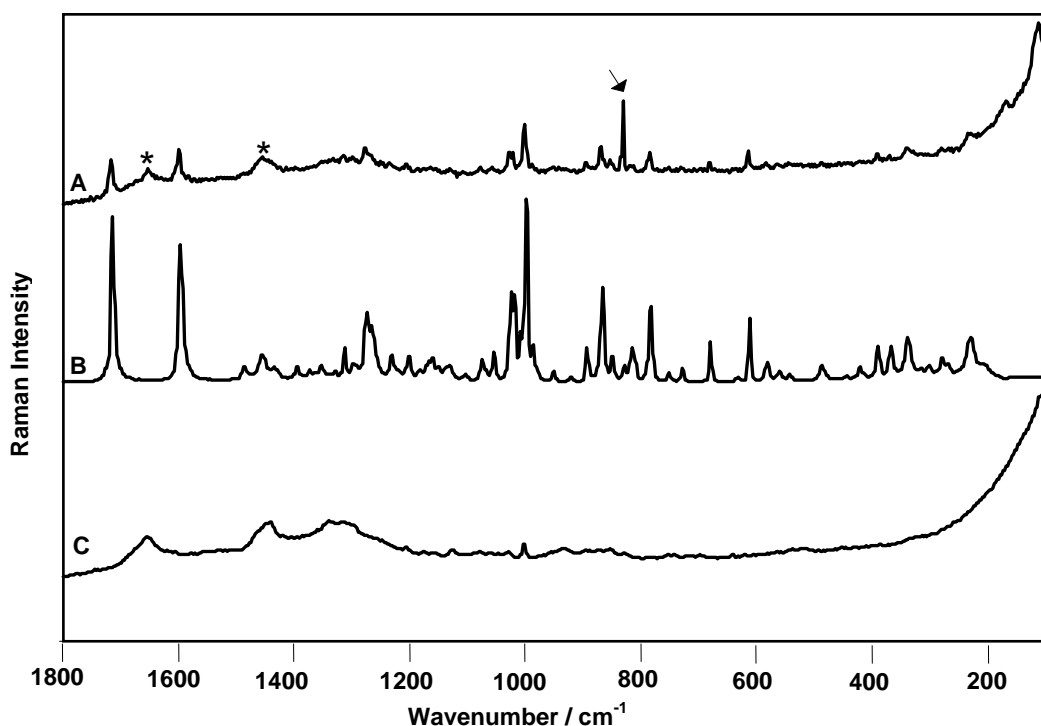


Figure 9.6 Raman spectra of

A: Street cocaine hydrochloride on human skin (Asterisks indicate skin bands & arrows indicate excipient bands)

B: Reference cocaine hydrochloride

C: Human skin

785 nm, 90.8 mW, 10s exposure, 1 accumulation for A &B, 5 accumulations for C

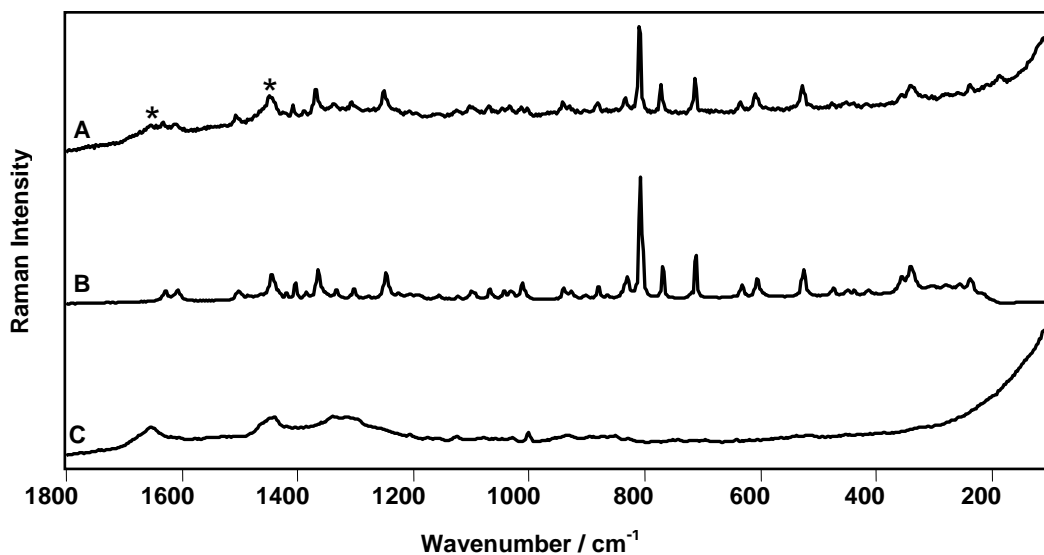


Figure 9.7 Raman spectra of
 A: Street MDMA on human skin (Asterisks indicate skin bands)
 B: Reference cocaine hydrochloride
 C: Human skin
 785 nm, 90.8 mW, 10s exposure, 1 accumulation for A &B, 5 accumulations for C

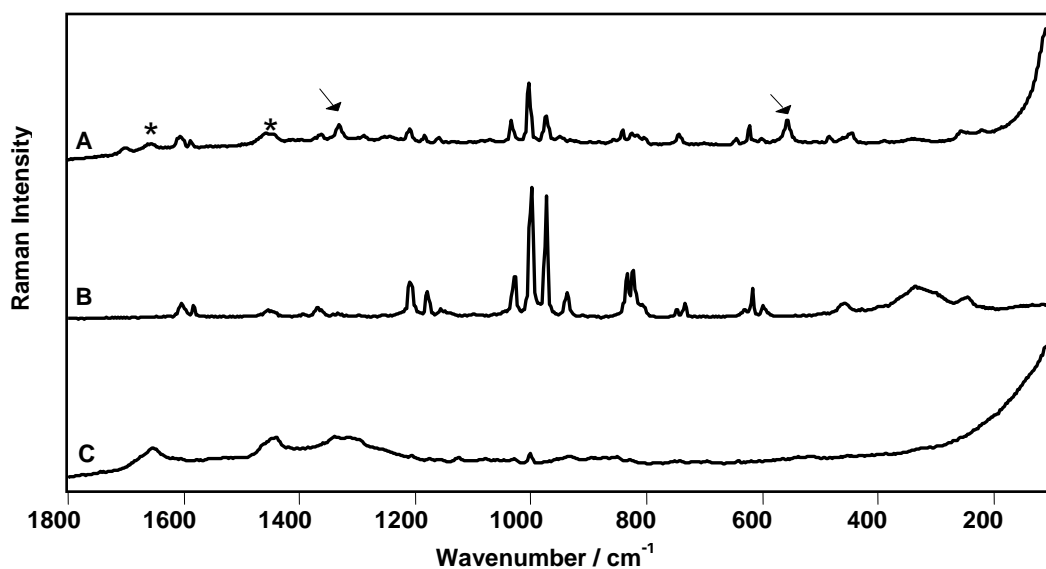


Figure 9.8 Raman spectra of
 A: Street amphetamine sulphate on human skin (Asterisks indicate skin bands & arrows indicate excipient bands)
 B: Reference amphetamine sulphate
 C: Human skin
 785 nm, 90.8 mW, 10s exposure, 1 accumulation for A &B, 5 accumulations for C

9.3.3 Detection of explosives on human skin

Figure (9.9) shows an image of a PETN crystal on human skin and the Raman spectrum obtained from this crystal is shown in figure (9.10A). The characteristic Raman features of the explosive PETN can be clearly identified. Two bands arising from the skin substrate appear in the spectrum of the explosive; the amide I at 1651 cm^{-1} , which appears as a shoulder on the PETN band at 1656 cm^{-1} , and the δ (CH_2) scissoring mode at 1440 cm^{-1} . The presence of these skin bands do not interfere with the identification of PETN. The confocal Raman spectrum obtained from a particle of TNT on human skin shows the characteristic bands of the explosive (Figure 9.11) and no significant band can be attributable to the skin substrate. Also, the spectrum obtained from an ammonium nitrate particle on human skin shows the key signature bands of the explosive (Figure 9.12). Despite the presence of two bands arising from the skin, the explosive can be identified by its characteristic bands.



Figure 9.9 PETN crystal on the surface of human skin

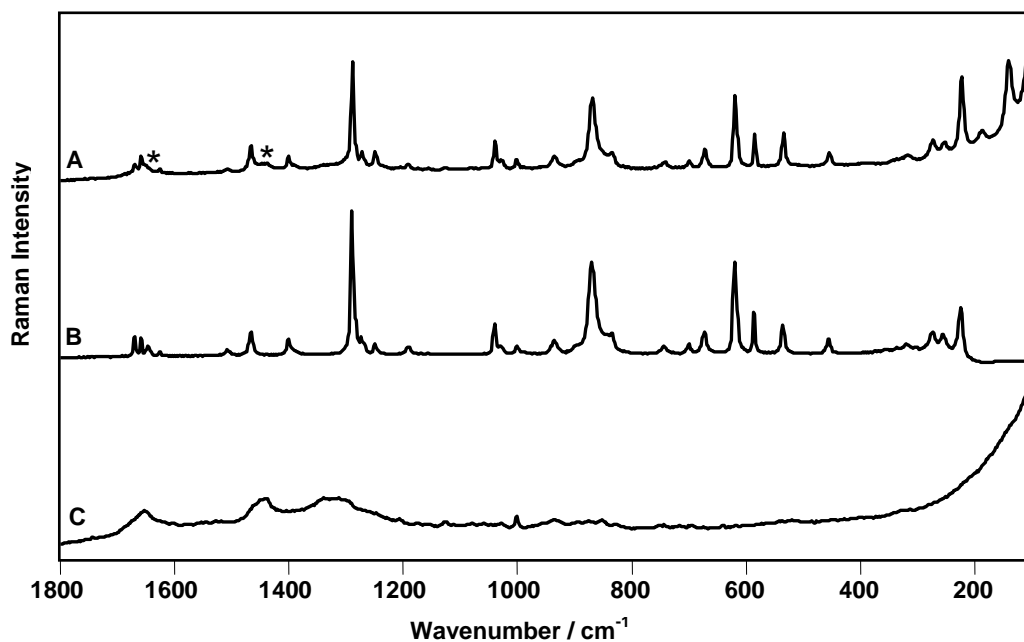


Figure 9.10 Raman spectra of
 A: PETN on human skin (Asterisks indicate skin bands)
 B: Reference PETN
 C: Human skin
 785 nm, 90.8 mW, 10s exposure, 1 accumulation for A &B, 5 accumulations for C

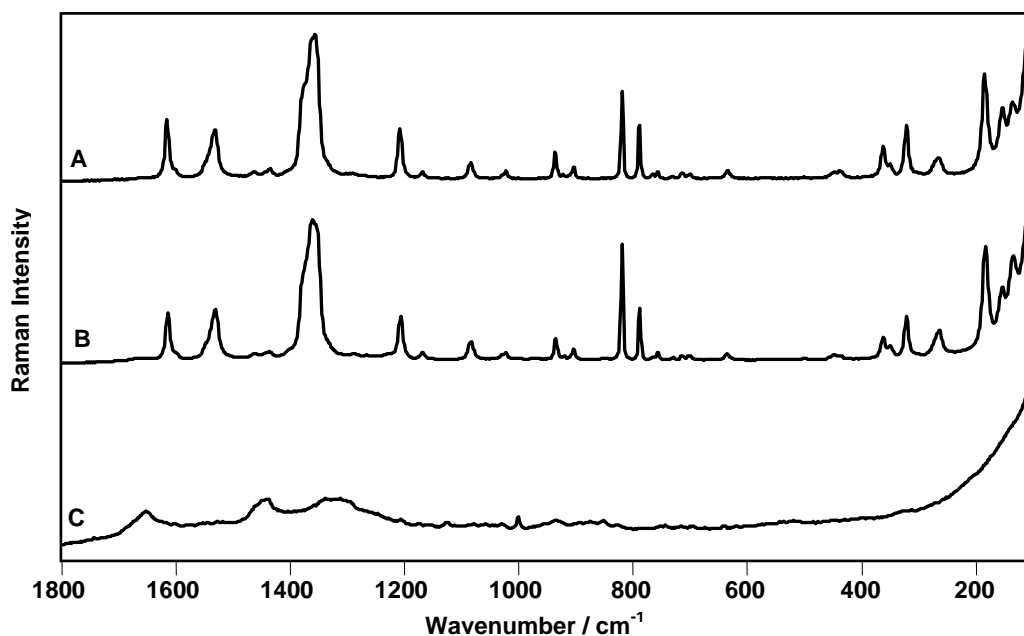


Figure 9.11 Raman spectra of
 A: TNT on human skin
 B: Reference TNT
 C: Human skin
 785 nm, 90.8 mW, 10s exposure, 1 accumulation for A &B, 5 accumulations for C

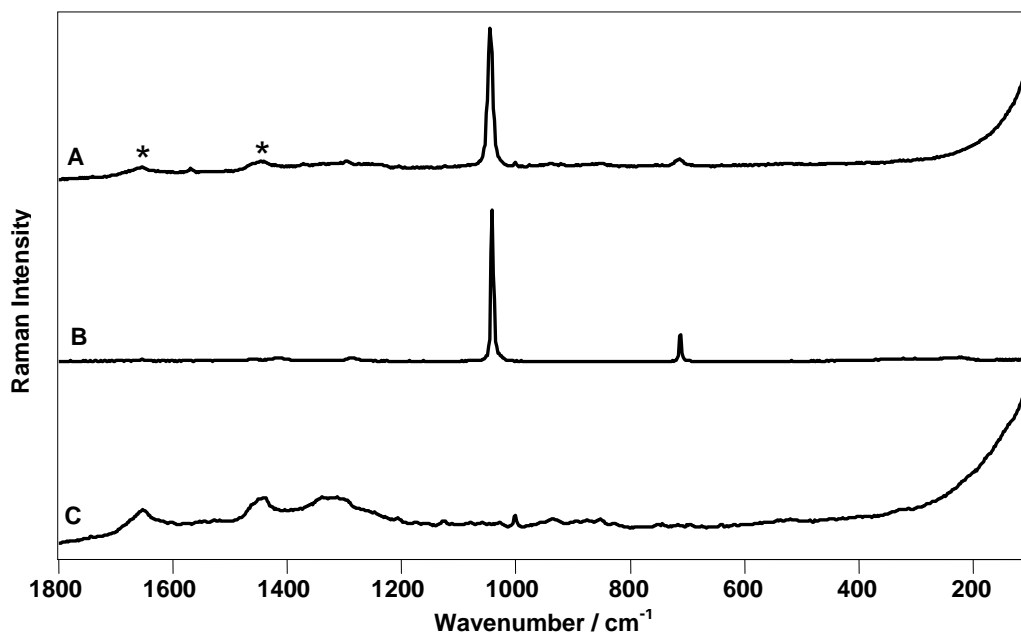


Figure 9.12 Raman spectra of

A: Ammonium nitrate on human skin (Asterisks indicate skin bands)

B: Reference ammonium nitrate

C: Human skin

785 nm, 90.8 mW, 10s exposure, 1 accumulation for A & B, 5 accumulations for C

The Raman spectrum obtained from an HMTA crystal on the surface of the skin is shown in Figure (9.13). It is observed that the amide I assigned to the skin substrate appears as a broad weak band at 1651 cm^{-1} . The presence of this band did not interfere with the identification of the explosive precursor HMTA which can be easily identified by several characteristic signature bands such as the strong (N-C-N) bending modes at 1040 and 462 cm^{-1} , and the very strong (N-C) stretching mode at 777 cm^{-1} . Similarly, the amide I (C=O) mode appears at 1651 cm^{-1} in the Raman spectrum collected from a pentaerythritol particle on the surface of the skin (Figure 9.14). The identity of the explosive precursor can be established from the key Raman bands at 1071 , 873 , 810 and 439 cm^{-1} .

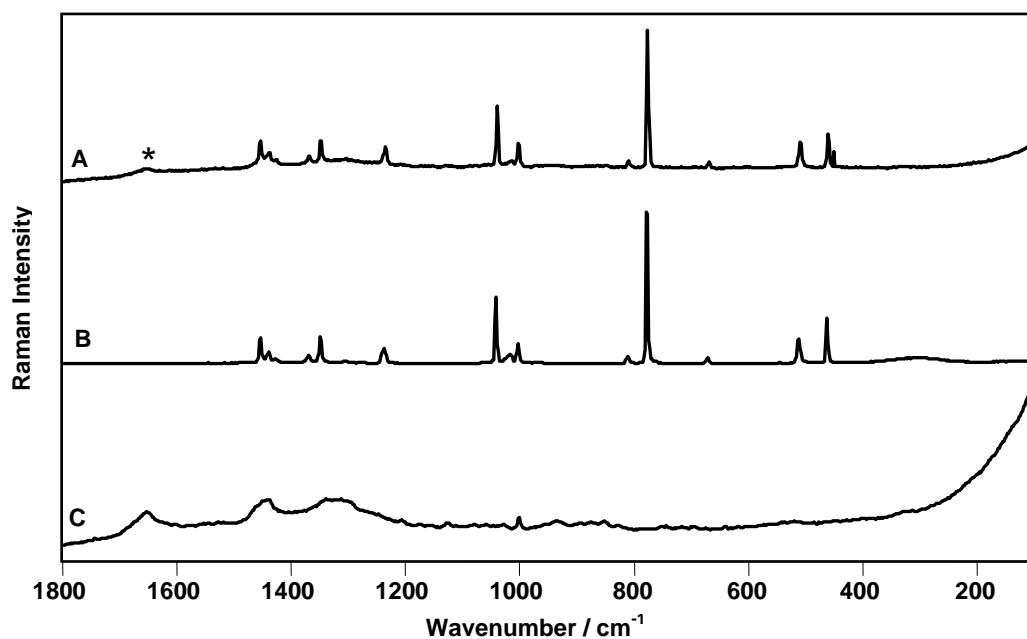


Figure 9.13 Raman spectra of
 A: Hexamethylenetetramine (HMTA) on human skin (Asterisks indicate skin bands)
 B: Reference hexamethylenetetramine
 C: Human skin
 785 nm, 90.8 mW, 10s exposure, 1 accumulation for A &B, 5 accumulations for C

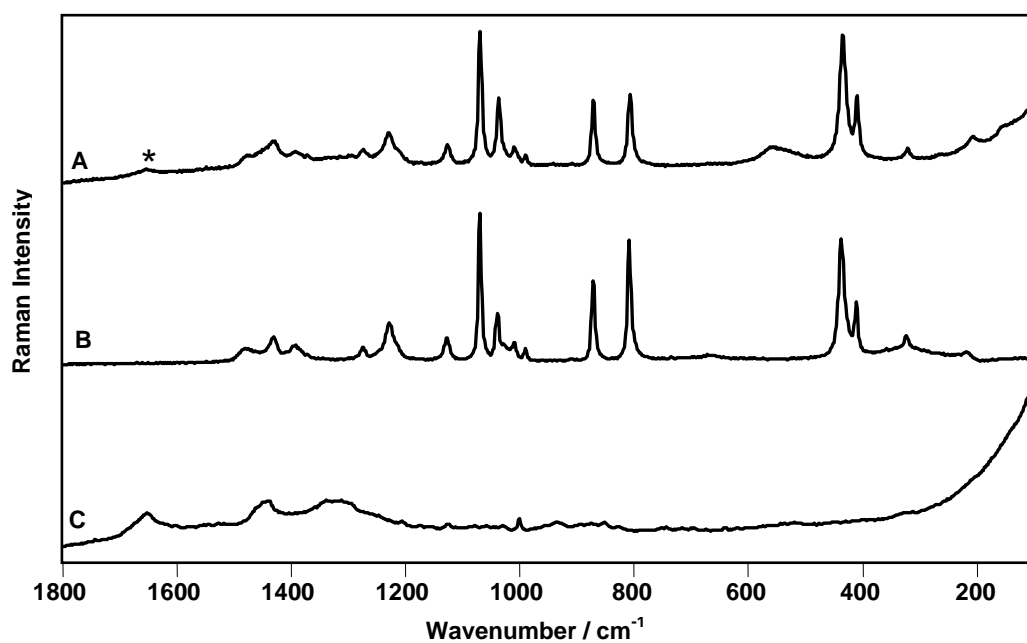


Figure 9.14 Raman spectra of
 A: Pentaerythritol on human skin (Asterisks indicate skin bands)
 B: Reference pentaerythritol
 C: Human skin
 785 nm, 90.8 mW, 10s exposure, 1 accumulation for A &B, 5 accumulations for C

The previous results demonstrate that Raman spectroscopy is a rapid non-destructive technique that can be used for the detection and identification of drugs of abuse and explosives on skin. The presence of the particles on a complex matrix such as the skin did not prevent the detection of drugs of abuse and explosives. The spectra of the drugs of abuse and explosives could be readily obtained *in-situ* non-destructively, within 90 second and without sample preparation or alteration of the analyte of interest. Raman spectra were collected from particles with dimensions in the range 5–10 μm . The acquired spectra are of high quality with a good S/N ratio. Interfering bands arising from the skin substrate did not prevent identification of the skin contaminant. In all cases, the Raman spectra could be acquired without affecting the integrity of the skin substrate. The detection of drugs of abuse on skin can be of evidential value in cases of intentional or accidental drug overdose. Raman spectroscopy has been shown to be a rapid non-destructive technique that can be used for the *in-situ* identification of drugs of abuse in forensic toxicology cases, to provide structural information of the drugs, and to correlate the analytical toxicological data. Also, the results demonstrate that despite the complex background of human skin, Raman spectroscopy has the ability to provide both the speed and specificity for the detection of the explosive materials. Detection of traces of explosives on skin or clothing or other possessions could help to identify passengers who are potential security risks and allow the deduction of the source of explosion after an incident. Another area of potential interest is the application to the detection of harmful chemicals on skin after the intentional or accidental exposure to these chemicals.

Chapter 10

A new portable Raman spectrometer equipped with 1064nm excitation: feasibility for the identification of drugs of abuse and explosives

10.1- Introduction

A major challenging task confronting hazardous materials response teams involves the accurate and rapid detection and identification of potentially hazardous chemicals outside the classical laboratory environment and under potentially dangerous conditions. The analysis of unknown compounds requires extreme care because of the possible instability of samples. Many chemicals can be sensitive to shock, heat, or light and can react violently by deflagration or explosion. Another concern facing the forensic investigator is the collection of evidence from clandestine laboratories. These containers are usually unlabelled and may cause significant hazards if opened. Hence the ability to analyze the samples without the need to open the containers is significantly important. Raman spectroscopy is an attractive technique for identifying materials of forensic relevance because of the ease with which fibre-optic probes can be interfaced with small rugged spectrometers that can be used in the field.^[109] The main obstacle in using Raman spectroscopy for the analysis of drugs of abuse and explosives is sample fluorescence.^[161] Over the last two decades, the feasibility of adoption of portable Raman spectrometers for the identification of drugs of abuse and explosive materials has been investigated by several research groups in an attempt to build up an instrument that affords a good compromise between sensitivity and fluorescence rejection.

Explosives have been analyzed by both FT- and CCD-Raman spectroscopy in order to determine an appropriate wavelength for constructing a field-usable explosives analyzer.^[161] The authors concluded that 1064 nm excitation eliminates the majority

of fluorescence although longer data acquisition times are required to attain the desired SNR. Also, 785 nm excitation showed a benefit over that at 633 nm for most of the explosives studied, although several samples (e.g. Semtex) suffered from similar fluorescence levels with 785 nm and 633 nm excitations. A fibre-optic probe equipped with a 633 nm laser has been applied for the detection of traces of explosives in fingerprints. Using a four metre fibre-optic probe, it was possible to locate and identify traces of explosive in fingerprints.^[160] A fibre-optic Raman probe equipped with a 532 nm laser has been applied for the *in-situ* detection of illicit drugs. It was possible to differentiate cocaine hydrochloride from free base or crack cocaine using their Raman spectra.^[156] Also, a fibre-optic Raman probe has been used for the *in-situ* identification of cocaine and selected adulterants. The Raman spectra of cocaine hydrochloride and free base cocaine are easily distinguishable from each other and from common cutting agents and impurities such as benzocaine and lidocaine.^[157] A blind field test evaluation of Raman spectroscopy as a forensic tool has been described; two portable Raman instruments equipped with 785 nm lasers and two different operators have been utilized to analyze a wide range of unknown samples. Spectra of the unknown samples were searched against a customised hazardous materials reference library. The results have indicated an equivalent performance observed for both the operators and the instruments.^[163] A standoff Raman system equipped with a 532 nm laser for detecting high explosives at distances up to 50 metres in ambient light conditions has been demonstrated.^[167] A portable Raman system has been used to monitor hydrocarbons and explosives in the environment.^[166] Illicit drugs have been analyzed using a portable Raman analyzer equipped with a diode laser emitting at 785 nm and a thermoelectrically cooled CCD detector.^[158,159] One of the approaches used to minimize fluorescence is to increase the laser

wavelength and the most common long wavelength used is the 1064 nm Nd:YAG laser. However, Stokes Raman spectra cannot be normally measured with a CCD Raman spectrometer operating at this wavelength because CCD detectors cut off about this wavelength. Anti-Stokes Raman spectra of explosive materials have been obtained with 1064 nm excitation using a fibre-optic probe sampling and a charge – coupled device (CCD) detector. ^[164] An Anti-Stokes correction routine has been used which allowed the anti-Stokes spectra measured with 1064 nm excitation to be searched against libraries of Stokes spectra obtained using FT-Raman spectrometry. In a later study, the anti-Stokes Raman spectra of the selected explosives were compared with Stokes Raman spectra obtained using a fibre-optic probe equipped with 830 nm and 785 nm excitation lasers and a CCD detector. ^[165] It was concluded that the anti-Stokes Raman spectra measured with 1064 nm and CCD detection is not the optimal approach for the analysis of these explosives .The decreased fluorescence background is offset by the decrease in signal intensity caused by the longer excitation wavelength , the decreased Raman scattering intensity caused by the Boltzmann distribution of molecules , and the concomitant increase in the data acquisition times; 830 nm excitation was found to offer a slightly better fluorescence rejection than 785 nm particularly for the analysis of fluorescent samples , such as Semtex.

An alternative approach to using dispersive spectrometers based on CCD-detectors is to use a longer excitation wavelength coupled to Ge or InGaAs detectors. A dispersive Raman spectrometer with a germanium detector and a 1064 nm laser has been applied to measure the Stokes Raman spectra of the explosives. ^[264] This instrument did not offer any advantage over either 830 nm Stokes or 1064 nm anti-Stokes measurement made with a CCD detector. Thus, the device did not show a wide applicability for forensic applications of Raman spectroscopy due to the high cost of the detector, the

need for liquid nitrogen cooling, the low signal-to-noise ratio of the data obtained due to the detector noise characteristics and the decreased sensitivity related to the ν^4 dependence of the near-infrared excitation. A dispersive portable Raman spectrometer based on a thermoelectrically cooled InGaAs detector and operating at 1064 nm excitation wavelength has been demonstrated. [265,266]

In this section a portable prototype Raman spectrometer (DeltaNu Advantage 1064) equipped with 1064 nm laser excitation (Figure 9.1A) has been evaluated for the analysis of drugs of abuse and explosives. The feasibility of the instrument for the analysis of the samples both as pure materials and contained in plastic and glass containers has been investigated. The advantages, disadvantages and the analytical potential of the instrument are assessed based on a comparison with a portable Raman spectrometer operating with 785 nm excitation.

10.2- Experimental

10.2.1. Samples

a- Drugs of Abuse

Pure samples of cocaine hydrochloride, free base cocaine “crack” , N-methyl-3,4-methylenedioxy-amphetamine HCl (MDMA-HCl), amphetamine sulphate , gamma-hydroxybutyric acid (GHB), nitrazepam and flunitrazepam were supplied by Sigma-Aldrich Company Ltd., United Kingdom. Seized street samples of cocaine hydrochloride, MDMA, amphetamine, heroin and cannabis resin were supplied by the Home Office Scientific Development Branch.

b- Explosives samples

Samples of pentaerythritol tetranitrate (PETN), cyclotrimethylenetrinitramine (RDX), trinitrotoluene (TNT), and ammonium nitrate and five plastic explosive samples were supplied by the Home Office Scientific Development Branch. The explosive

precursors hexamethylenetetramine (HMTA) and pentaerythritol used in this study were supplied by the Sigma-Aldrich Company Ltd., United Kingdom.

10.2.2 Raman spectroscopic instrumentation

The Advantage 1064 is a prototype ^[267] compact Raman spectrometer supplied by DeltaNu (Laramie, WY, U.S.A.) .This system measures 12 x 8 x 4 inches (LWH) and weighs 9 kg (Figure 10.1 A). It is equipped with a 1064 nm diode laser giving a maximum laser power of 1000 mW at source. This is a dispersive reflective grating system giving Raman spectra in the wavenumber range 200-2000 cm^{-1} . The output optics provides a laser spot size of approximately 100 microns. The detector is an Intevac Photonics MOSIR 950 camera based on transfer electron (TE) photocathode and electron bombardment (EB) gain technology. ^[268] Electron-bombardment CCD is a technique that improves the sensitivity and spectral range of a CCD detector. The photons are detected by an InGaAs photocathode placed in front of the CCD detector (Figure 10.2). The photocathode then releases electrons that are accelerated across a gap and focused onto the CCD detector. These energetic electrons generate multiple charges in the CCD detector, resulting in a modest gain of a few hundred times. The camera has a working range from 950 to 1650 nm and is thermoelectrically cooled to -40 C°. A knee-shaped optical head attached to the instrument allows for the flexible positioning of the sample relative to the instrument (Figure 10.1B) .The instrument is equipped with NuSpec software which permits the selection of three steps of operable spectral resolution from 15 to 20 cm^{-1} . The DeltaNu software allows a five-step set-up of adjustable laser power from 800mW to 30 mW. The spectral integration time and the number of accumulations are under the full control of the operator. Raman spectra were acquired from the drugs of abuse and explosives samples both as neat materials and in plastic and glass containers to investigate the penetration power of the laser.

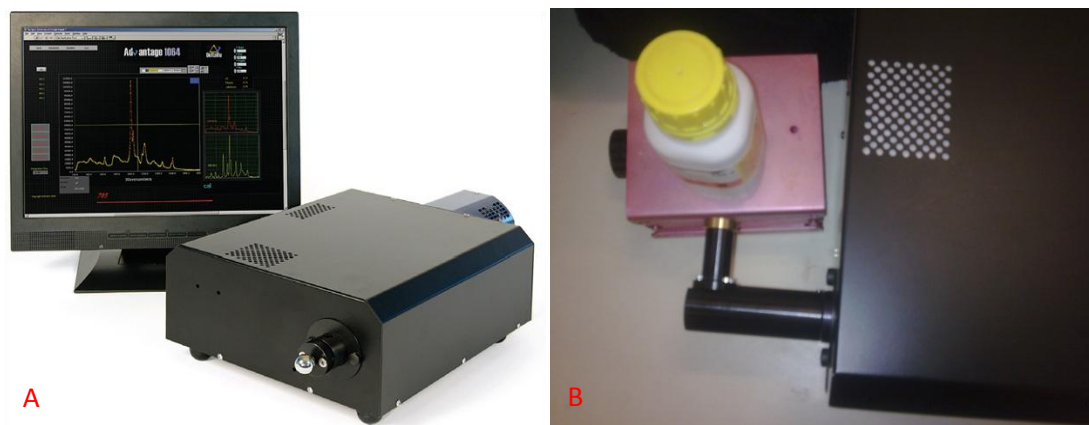


Figure 10.1 A: Advantage 1064 system [Adapted from reference 267]

B: Knee-shaped optical head

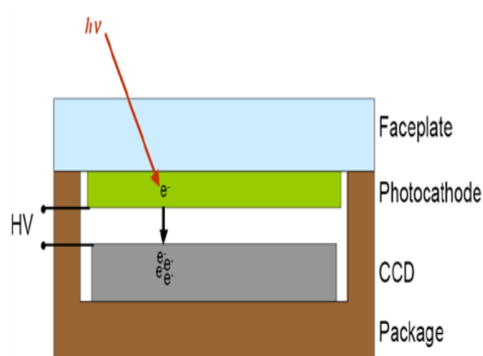


Figure 10.2 Electron-bombarded CCD : NIR light is absorbed by the photocathode, electrons are emitted through the photocathode, voltage accelerated and impact a back illuminated CCD [Adapted from reference 269]

To compare the results obtained from the 1064 Advantage system, corresponding measurements on another portable instrument using 785 nm laser wavelength as an excitation source have been performed. Delta Nu Inspector Raman instrument (Laramie, WY, USA) is equipped with a diode laser emitting at 785 nm , a thermoelectrically cooled (1×1024 pixels) CCD detector and a custom 25-mm-focal-length nose-piece. The spectral range is $2000\text{--}200\text{ cm}^{-1}$ with a spectral resolution of 8 cm^{-1} . The laser power at the sample was 37 mW. Daily calibration of the wavenumber axis was achieved by recording the Raman spectrum of polystyrene within the calibration routine built into the software. Spectra were recorded with the accumulation of one scan, 10-s exposure. The spectrometer was controlled by a

portable PC with instrument control software (Nu Spec Version 4.75). Reference spectra of the drugs of abuse were obtained using a benchtop Renishaw *In Via* Reflex spectrometer (Renishaw, Wotton-under-Edge, UK) coupled with 785 nm diode laser to be compared with the spectra collected using the 1064 Advantage system. Also, a benchtop Bruker IFS66 FT-Raman instrument operating with 1064 nm excitation (Nd³⁺/YAG laser) was also employed for comparison purposes; Raman spectra were observed over a wavenumber range from 50-4000 cm⁻¹.

10.3- Results and Discussion

10.3.1 Analysis of pure samples of drugs of abuse

Figure (10.3) shows the 1064 Advantage Raman spectra acquired from cocaine hydrochloride and MDMA samples. The wavenumber region of 2000-200 cm⁻¹ displayed provides a sufficient number of spectral peaks to afford unambiguous identification of the drugs concerned. The key signature bands of the drugs are clearly observed in the spectra and the results compare favourably with the reference spectra recorded using a laboratory benchtop Renishaw InVia Reflex spectrometer. The band wavenumber positions are within 1-3 cm⁻¹ of the reference spectra. The spectra are of high quality with a good signal/noise (S/N) ratio and there was no appreciable background observed due to fluorescence emission. On comparison with the spectra recorded using 785 nm excitation, it is observed that the S/N ratio has been increased for the same integration time and number of scans. The spectra obtained can also differentiate between the two forms of cocaine; cocaine hydrochloride and “crack” cocaine (Figure 10.4). Significant differences occur in the 850-900 cm⁻¹ spectral region where a very prominent band dominates at 870 cm⁻¹ with two much weaker adjacent bands at 850 and 895 cm⁻¹ in the cocaine.HCl Raman spectrum (Figure 10.4 A).

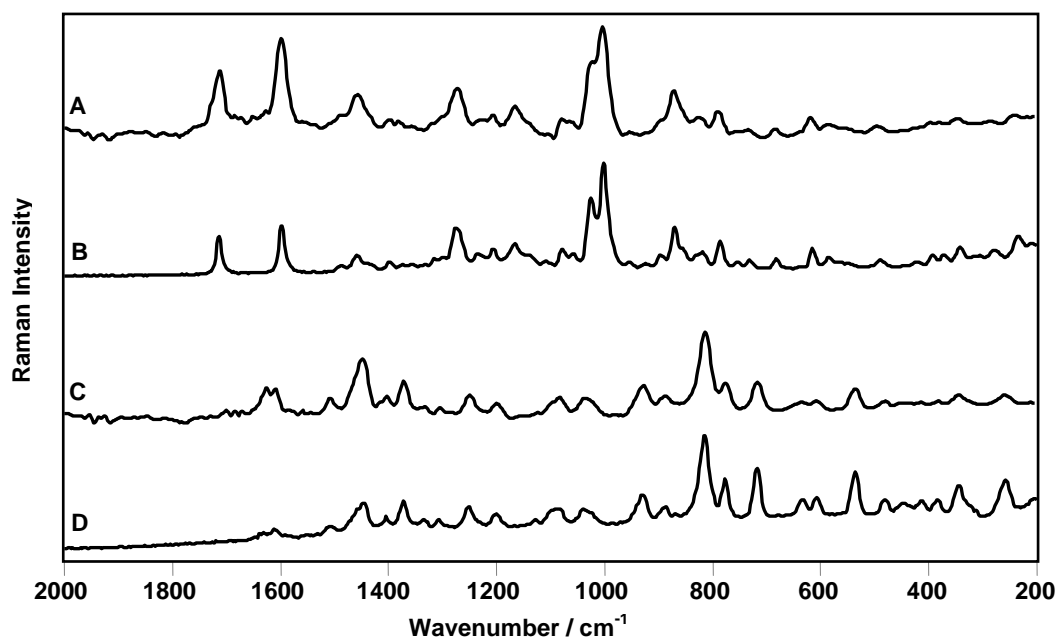


Figure 10.3 Raman spectra of drugs of abuse

A: Cocaine HCl , Advantage 1064 nm, 10 second exposure, 1 accumulation

B: Cocaine HCl , DeltaNu, 785 nm, 10 second exposure, 1 accumulation

C: MDMA , Advantage 1064 nm, 10 second exposure, 1 accumulation

D: MDMA , DeltaNu, 785 nm, 10 second exposure, 1 accumulation

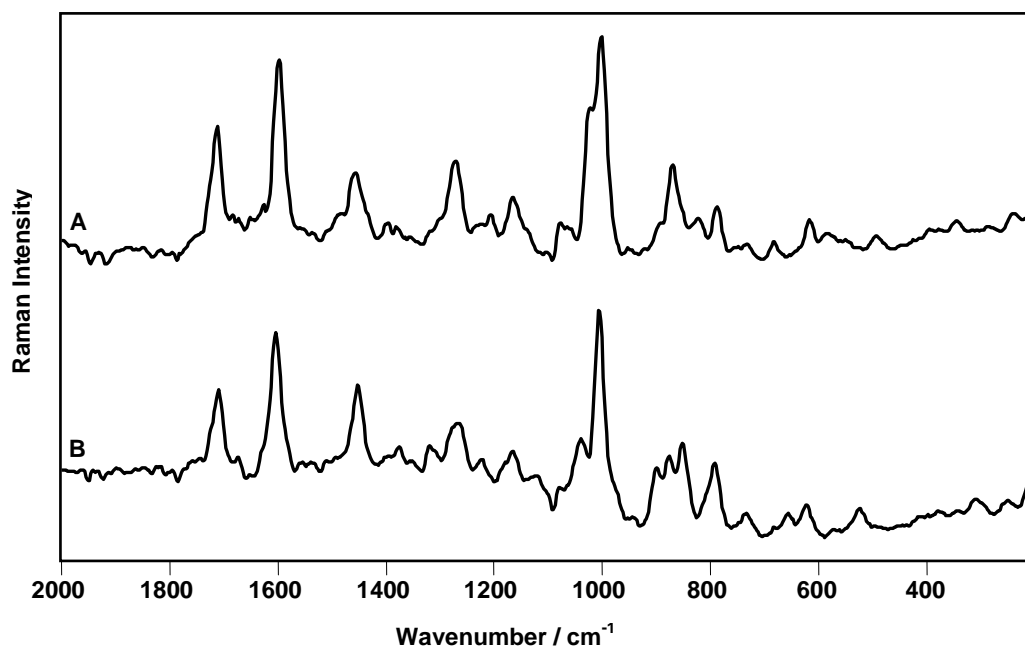


Figure 10.4 Raman spectra of drugs of abuse

A: Cocaine HCl, Advantage 1064 nm, 10 second exposure, 1 accumulation

B: Cocaine free base , Advantage 1064 nm, 10 second exposure, 1 accumulation

The corresponding region in the freebase cocaine Raman spectrum (Figure 10.4B) also shows three bands of similar intensity at approximately 850, 870, and 895 cm^{-1} . The aromatic ring breathing modes of the benzoic acid of cocaine occur in the region from about 1000 to 1035 cm^{-1} and also contain key distinguishing features. Although the symmetric stretch of the benzoic acid aromatic ring breathing mode at 1000 cm^{-1} is similar for both drugs, the asymmetric stretch is different for the two forms of cocaine. The band observed at 1025 cm^{-1} for cocaine.HCl is shifted 10 cm^{-1} relative to the corresponding band at 1035 cm^{-1} for freebase cocaine. The Raman spectra acquired from pure samples of amphetamine sulphate and heroin (Figure 10.5) shows the characteristic bands of the drugs and the S/N ratio is significantly improved when compared with the data collected using the 785 nm excitation (lower spectrum). Also, the spectra obtained from flunitrazepam and nitrazepam (Figure 10.6) are very rich in spectral features that can be used to identify the individual drugs and to discriminate between the closely related benzodiazepines.

The key signature bands of the drugs are clearly observed in the spectra and the results compare favourably with the reference spectra recorded using a laboratory benchtop Renishaw InVia Reflex spectrometer. The band wavenumber positions are within 1-3 cm^{-1} of the reference spectra. The wavenumber region of 2000-200 cm^{-1} displayed provides a sufficient number of spectral peaks to afford unambiguous identification. The unprocessed spectra can clearly differentiate between different drug types, allowing the *in-situ* identification to be made. The spectra are of a high quality with a good signal/noise (S/N) ratio and there was no appreciable background observed due to fluorescence emission. The spectra collected using the Advantage 1064 nm (upper spectra) are of much improved S/N compared with the spectra collected using 785 nm excitation (lower spectra).

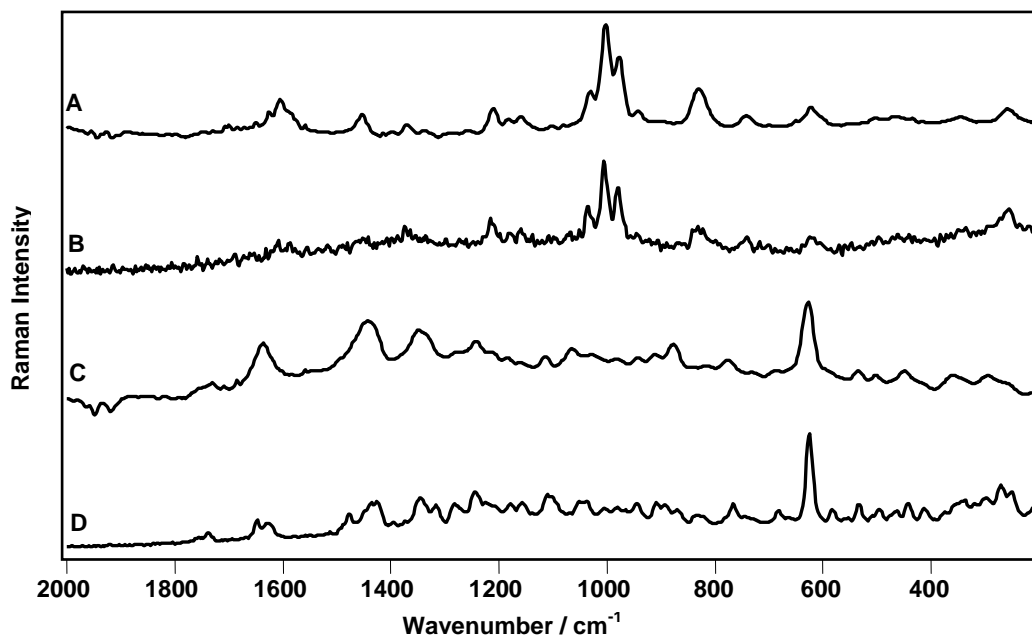


Figure 10.5 Raman spectra of drugs of abuse

A: Amphetamine sulphate, Advantage 1064 nm, 10 second exposure, 1 accumulation

B: Amphetamine sulphate, DeltaNu, 785 nm, 10 second exposure, 1 accumulation

C: Heroin, Advantage 1064 nm, 10 second exposure, 1 accumulation

D: Heroin, DeltaNu, 785 nm, 10 second exposure, 1 accumulation

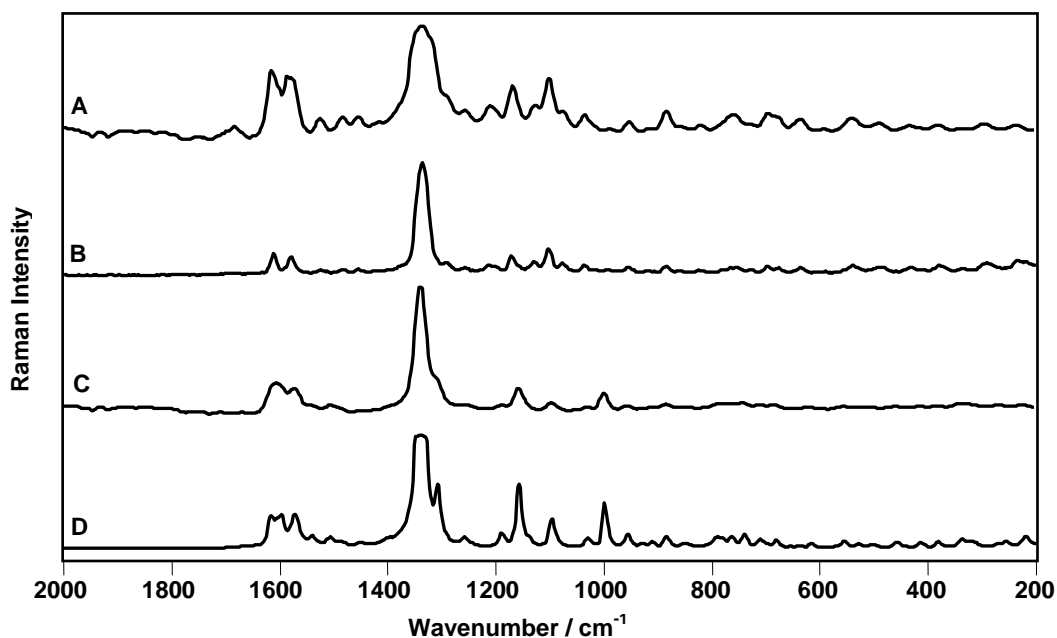


Figure 10.6 Raman spectra of drugs of abuse

A: Flunitrazepam, Advantage 1064 nm, 10 second exposure, 1 accumulation

B: Flunitrazepam, DeltaNu, 785 nm, 10 second exposure, 1 accumulation

C: Nitrazepam, Advantage 1064 nm, 10 second exposure, 1 accumulation

D: Nitrazepam, DeltaNu, 785 nm, 10 second exposure, 1 accumulation

10.3.2 Analysis of seized samples of drugs of abuse

Illicit drugs are usually diluted or cut at various levels with other drugs or common household products that exhibit significant fluorescence even under conditions of 785 nm laser excitation. Such excipient compounds include paracetamol, caffeine, aspirin, flour, talc, etc. These cutting agents may complicate the Raman spectrum, making the identification of individual components very difficult. Figure 10.7 and figure 10.8 compare the 1064 nm and 785 nm spectra for street-grade cocaine hydrochloride and an MDMA tablet, respectively. Despite the presence of some bands attributable to the cutting agent(s), the characteristic bands of cocaine hydrochloride and MDMA can be easily identified and compare favourably with the spectra obtained with benchtop spectrometer. It is observed that shifting to the 1064 nm wavelength has resulted in a damping of the fluorescence background emission compared with the spectra achieved

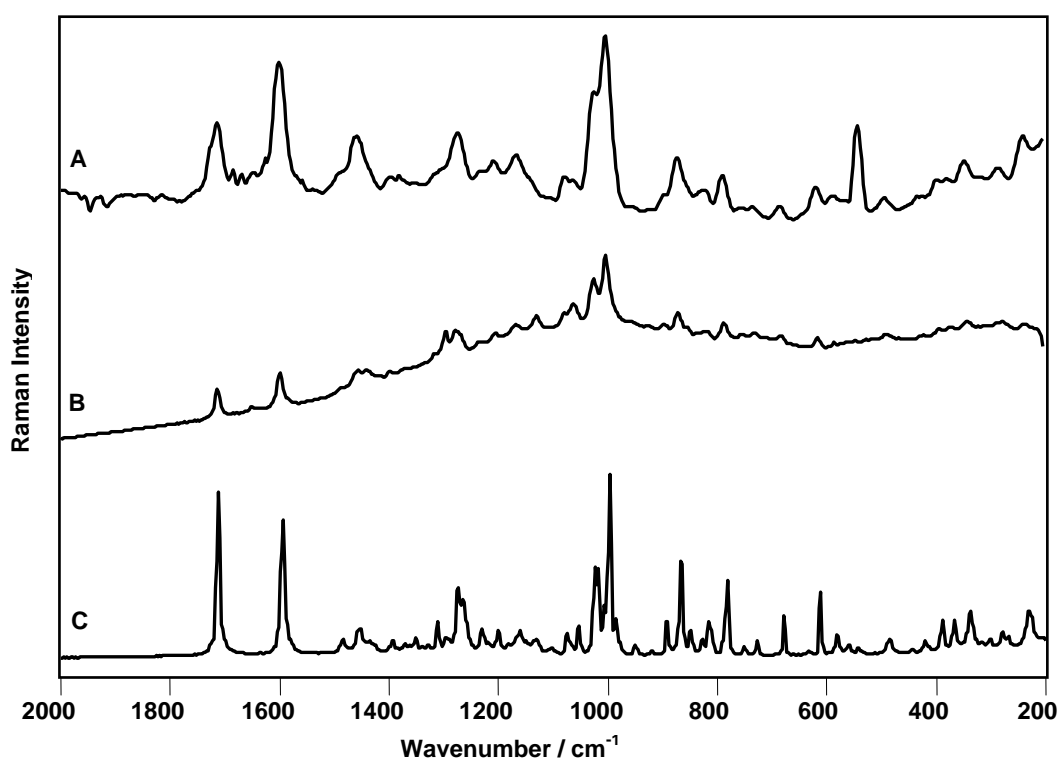


Figure 10.7 Raman spectra of seized cocaine.HCl

A: Advantage 1064 nm, 10 second exposure, 1 accumulation

B: DeltaNu, 785 nm, 10 second exposure, 1 accumulation

C: Reference cocaine HCl, benchtop Invia Reflex Raman microscope, 785 nm

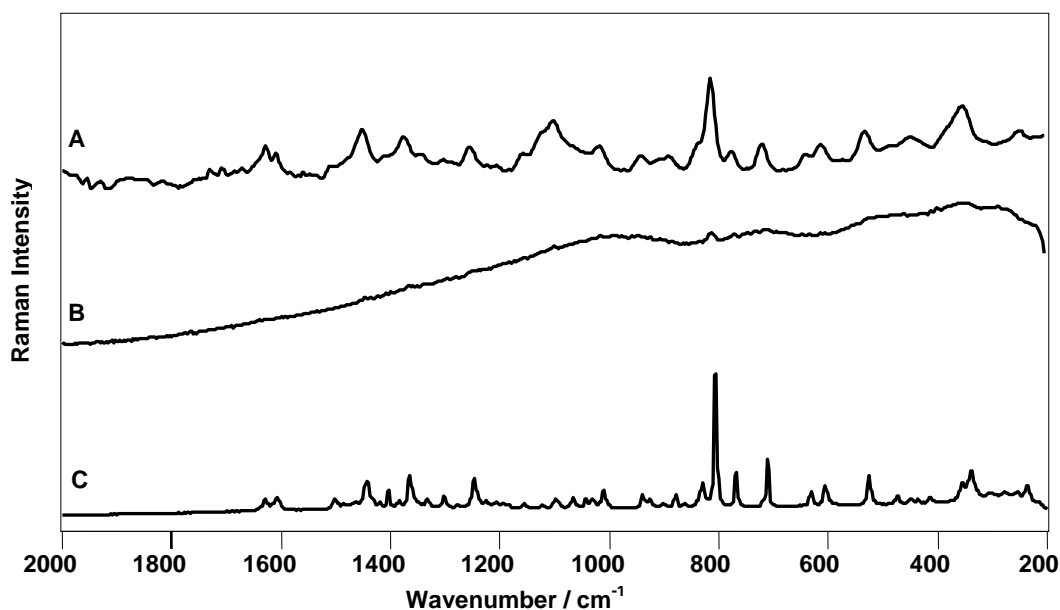


Figure 10.8 Raman spectra of seized MDMA

A: Advantage 1064 nm, 10 second exposure, 1 accumulation

B: DeltaNu, 785 nm, 10 second exposure, 1 accumulation

C: Reference MDMA, benchtop Invia Reflex Raman microscope, 785 nm

with 785nm excitation. This can also be seen in the spectra obtained from another two street samples of cocaine hydrochloride and MDMA (Figure 10.9). Shifting to 1064 nm excitation wavelength has resulted in a significant damping of the fluorescence emission. Similar results were obtained from two seized samples of amphetamine (Figure 10.10). With the 785 nm excitation, significant fluorescence background can be seen in the Raman spectra of both samples (Figure 10.10 B and D) whereas with the 1064 nm excitation, fluorescence-free spectra can be obtained and the characteristic Raman features of amphetamine can be clearly observed. It can also observe that the spectra contain few bands attributable to the cutting agents and this did not therefore prevent the identification of amphetamine as the active drug constituent of both samples. Further illustration of the applicability of this prototype instrument was demonstrated by the identification of seized heroin samples. Figure (10.11A) shows the Raman spectrum acquired from a seized heroin sample in which

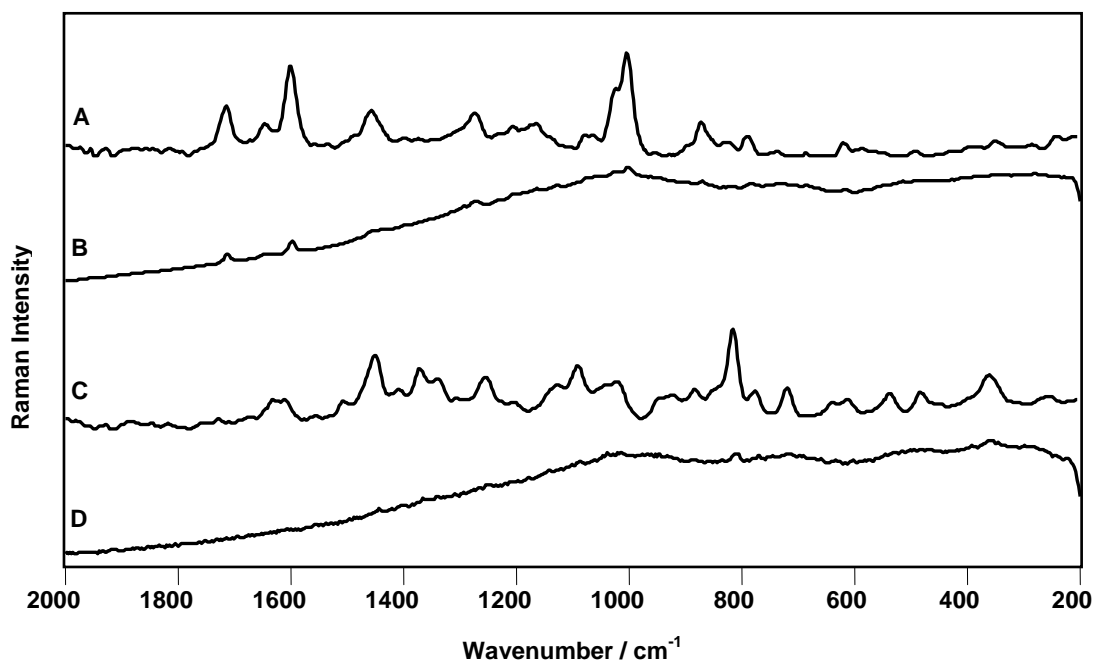


Figure 10.9 Raman spectra of seized drugs of abuse

- A: Cocaine HCl, Advantage 1064 nm, 10 second exposure, 1 accumulation
- B: Cocaine HCl, DeltaNu, 785 nm, 10 second exposure, 1 accumulation
- C: MDMA, Advantage 1064 nm, 10 second exposure, 1 accumulation
- D: MDMA, DeltaNu, 785 nm, 10 second exposure, 1 accumulation

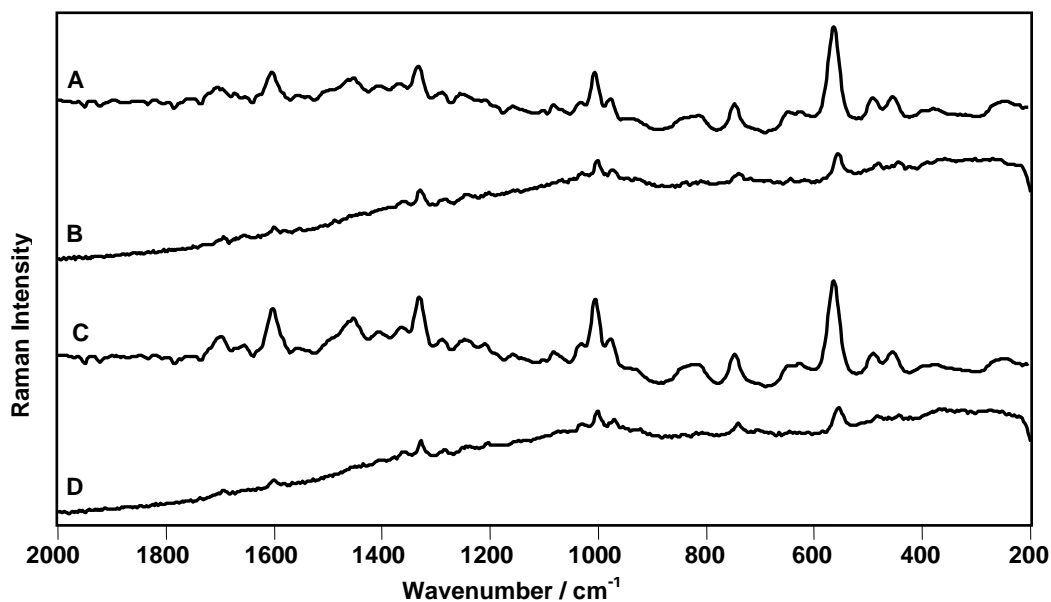


Figure 10.10 Raman spectra of seized amphetamines

- A: Sample 1, Advantage 1064 nm, 10 second exposure, 1 accumulation
- B: Sample 1, DeltaNu, 785 nm, 10 second exposure, 1 accumulation
- C: Sample 2, Advantage 1064 nm, 10 second exposure, 1 accumulation
- D: Sample 2, DeltaNu, 785 nm, 10 second exposure, 1 accumulation

the characteristic Raman bands of heroin can be clearly identified and agree well with the reference spectrum of heroin (Figure 10.11C). It can also observe that with the 785 nm excitation, the Raman spectrum of heroin is completely masked by the fluorescence emission arising from the cutting agents. In neither of the above cases does the cutting agent fluoresce appreciably but in other cases this may be problematic despite the use of the longer laser wavelength. Figure 10.12 shows the Raman spectra of seized heroin and cannabis resin collected using the 1064 Advantage system (upper spectrum) and FT-Raman spectra (lower spectrum). The larger spectral backgrounds observed in both these spectra is due to the fluorescence from the cutting agents. Although the longer excitation wavelength may suppress fluorescence in the majority of cases, it is apparent that some cutting agents may significantly fluoresce and so render the identification of the drug difficult, if not impossible.

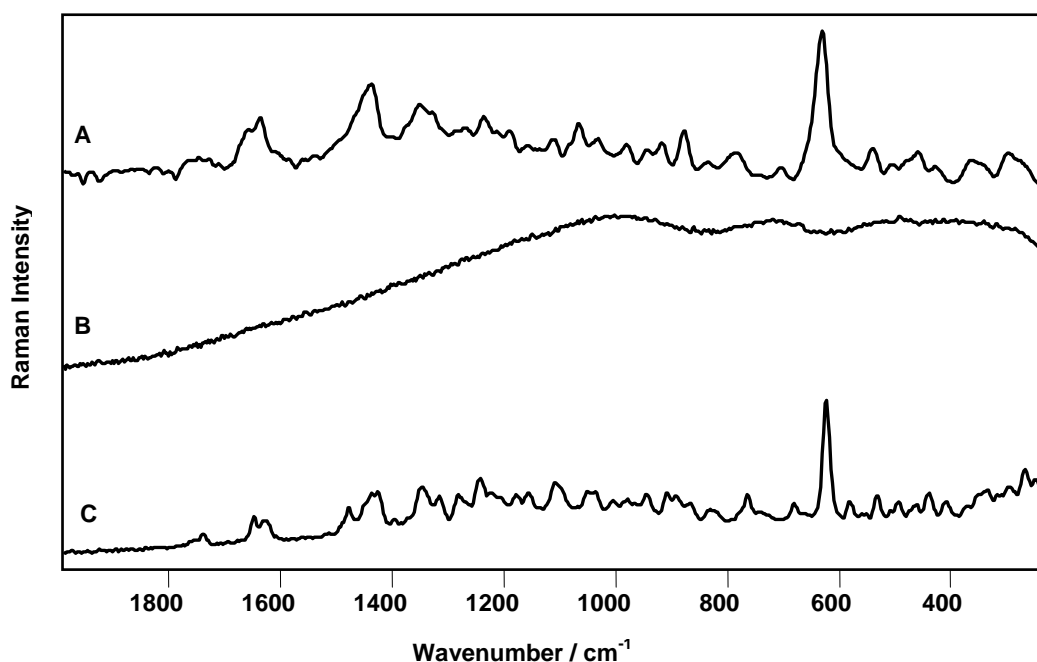


Figure 10.11 Raman spectra of seized heroin

A: Advantage 1064 nm, 10 second exposure, 1 accumulation

B: DeltaNu, 785 nm, 10 second exposure, 1 accumulation

C: Reference heroin, DeltaNu, 785 nm, 10 second exposure, 1 accumulation

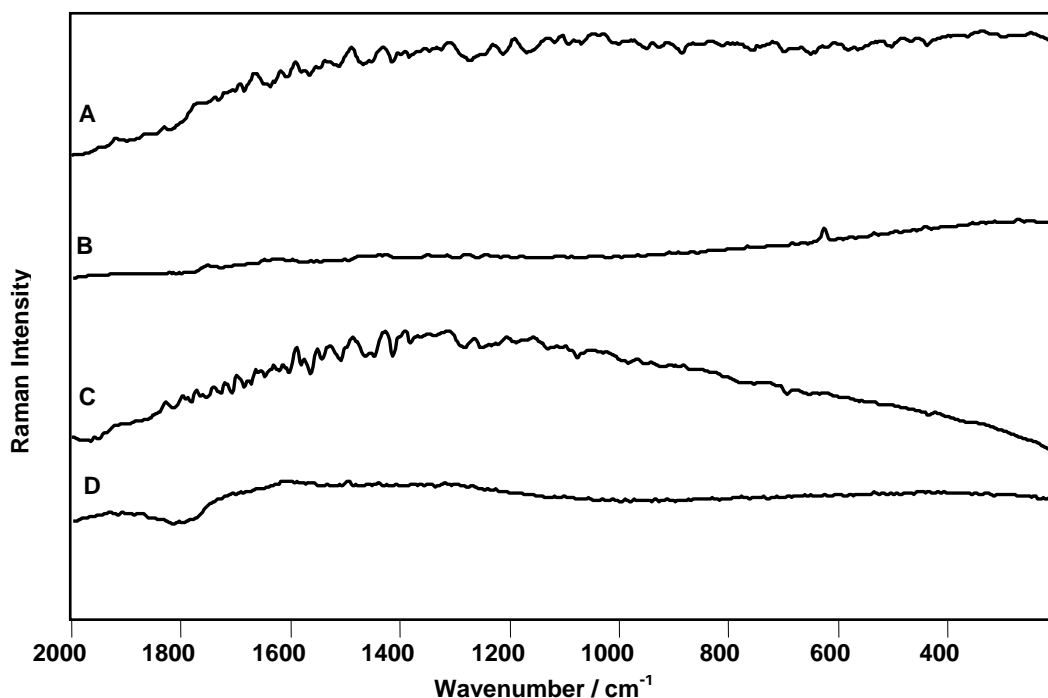


Figure 10.12 Raman spectra

- A: Seized heroin, Advantage 1064 nm, 10 second exposure, 1 accumulation
 B: Seized heroin, FT-spectrometer, 200scans, 4 cm^{-1} resolution, 200 mW laser power
 C: Seized cannabis, Advantage 1064 nm, 10 second exposure, 1 accumulation
 D: Seized cannabis, FT-spectrometer, 200scans, 4 cm^{-1} resolution, 200 mW laser power

10.3.3 Analysis of samples of drugs of abuse inside plastic bags

The feasibility of the instrument for sampling drugs of abuse which are contained in transparent containers, such as clear plastic bags, that are used by crime scene investigators to store drug evidence and to maintain the chain of custody, has also been investigated here. Pure and street samples of drugs of abuse were analyzed without removing them from their plastic containers. Figure (10.13) shows the Raman spectra collected from cocaine hydrochloride and MDMA samples inside clear plastic bags. On comparison with the reference spectra, it can be concluded that the drugs can be identified and the containers presented no difficulty in obtaining the spectra of the drugs. Also, figure (10.14) shows the spectra recorded from amphetamine sulphate

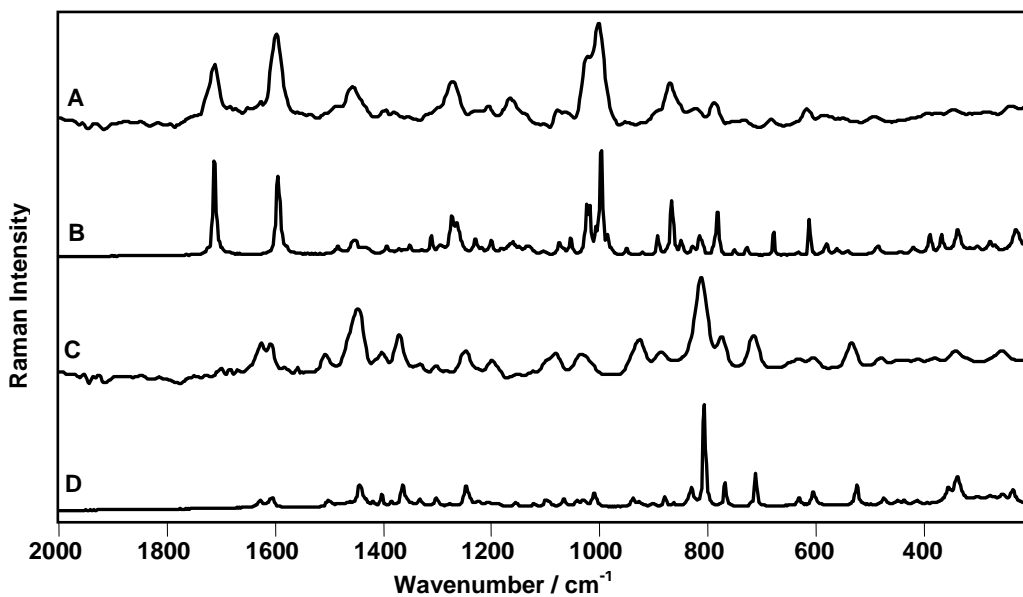


Figure 10.13 Raman spectra of drugs of abuse inside plastic bags
 A: Cocaine.HCl, Advantage 1064 nm, 10 second exposure, 1 accumulation
 B: Reference cocaine.HCl
 C: MDMA, Advantage 1064 nm, 10 second exposure, 1 accumulation
 D: Reference MDMA

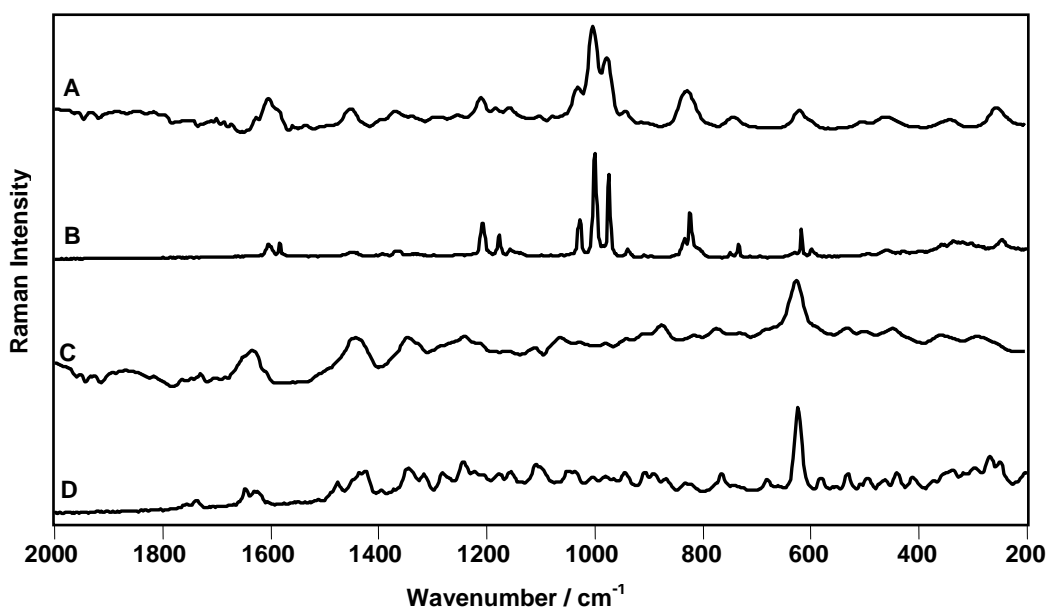


Figure 10.14 Raman spectra of drugs of abuse inside plastic bags
 A: Amphetamine, Advantage 1064 nm, 10 second exposure, 1 accumulation
 B: Reference amphetamine
 C: Heroin, Advantage 1064 nm, 10 second exposure, 1 accumulation
 D: Reference Heroin

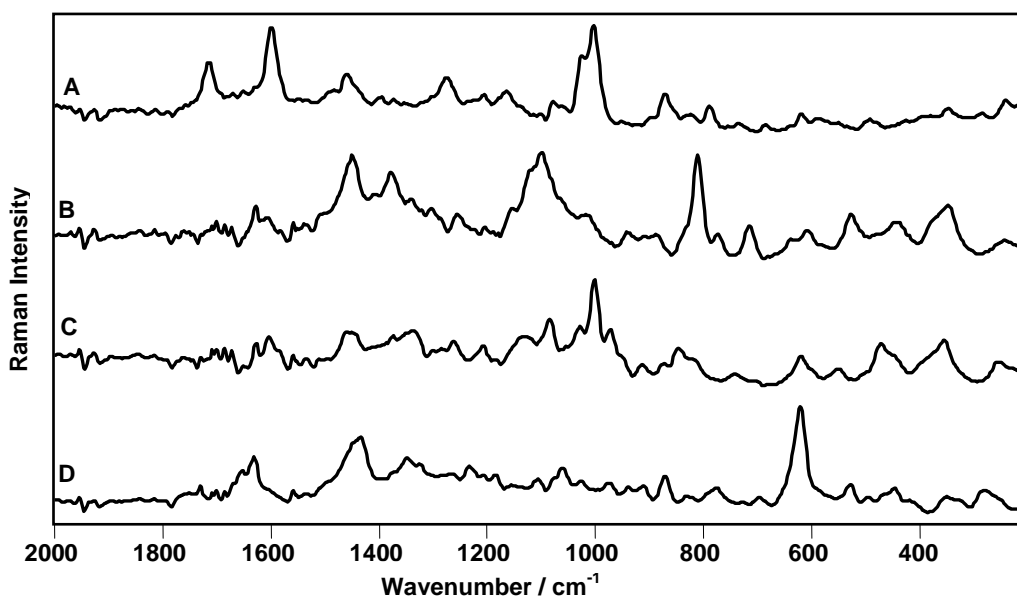


Figure 10.15 Raman spectra of seized drugs of abuse inside plastic bags
A: Cocaine hydrochloride
B: MDMA tablet
C: Amphetamine
D: Heroin

and heroin samples inside their plastic bag containers. The spectra of the drug samples can be acquired without interference from the plastic containers and no significant band in the spectra obtained can be assigned to the plastic container. Also, Raman spectra were obtained from seized samples of drugs of abuse namely, cocaine hydrochloride, an MDMA tablet, amphetamine and heroin. The samples were analysed inside their sealed plastic containers as received from the Home Office Scientific Development Branch. The principal characteristic bands of the drugs can be clearly observed (Figure 10.15) in all cases and the plastic containers did not prevent the identification of the drugs. The increased spectral background is attributed to the cutting agents present in the seized samples.

10.3.4 Analysis of samples of drugs of abuse inside glass containers

After investigating drugs of abuse as neat powders and inside their plastic containers, the drugs were analysed whilst held in glass (clear and coloured glass) and polymer containers.

10.3.4.1 Analysis of samples of drugs of abuse inside clear glass vials

The Raman spectra acquired from samples of drugs of abuse inside clear glass containers (Figure 10.16) shows the characteristic bands of the drugs which can then be accurately identified. This clearly demonstrates the ability of this instrument to sampling the drugs inside their containers which is of significant importance for field analysis. This can be attributed to the drugs of abuse being relatively good Raman scatterers whereas the glass container is a much poorer Raman scatterer.

10.3.4.2 Analysis of samples of drugs of abuse inside green-coloured vials

Raman spectra were obtained from drug samples held in coloured glass containers as the drugs may be smuggled in coloured containers (such as wine bottles). Coloured containers usually fluoresce under visible excitation, which may mask the Raman signal from the drugs of abuse. It can be observed that the characteristic features of the drugs are clearly identified and the coloured glass did not significantly attenuate the illumination laser or prevent the detection of the Raman signals from the drugs (Figure 10.17).

10.3.4.3 Analysis of samples of drugs of abuse inside amber yellow vials

Figure 10.18 shows the Raman spectra collected from drugs of abuse samples inside amber yellow vials, from which the identity of the drugs can be readily established and no glass background can be seen in the spectra.

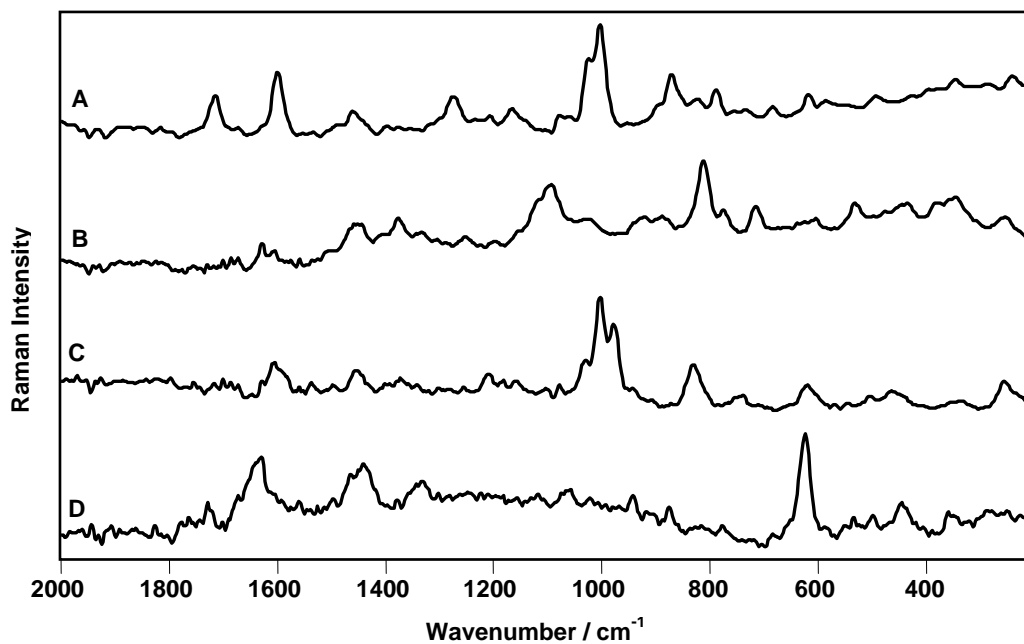


Figure 10.16 Raman spectra of drugs of abuse inside clear glass containers
 A: Cocaine hydrochloride
 B: MDMA tablet
 C: Amphetamine
 D: Heroin

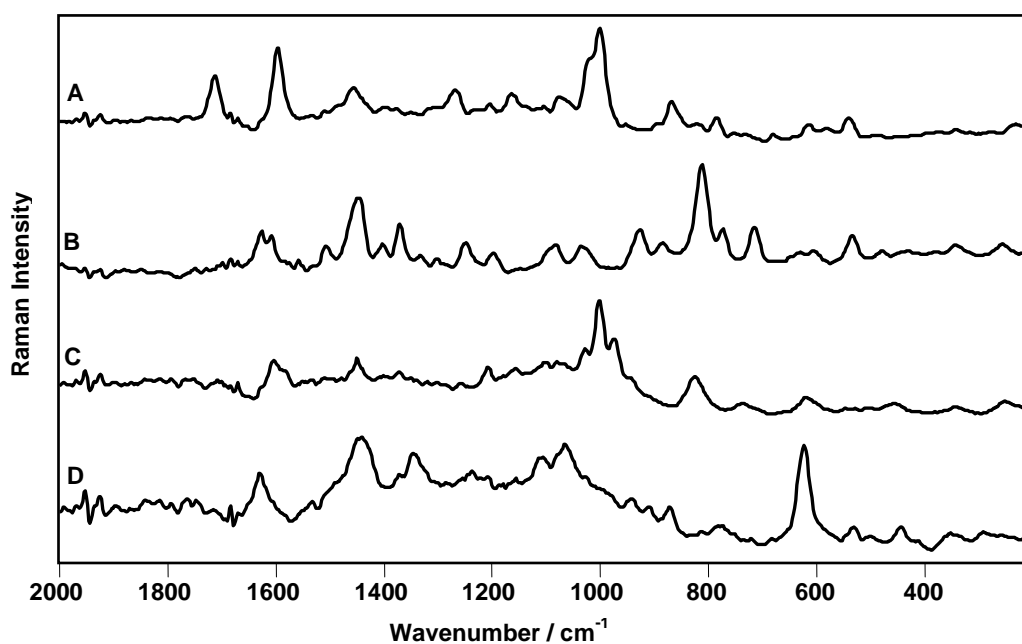


Figure 10.17 Raman spectra of drugs of abuse inside green-coloured glass containers
 A: Cocaine hydrochloride
 B: MDMA
 C: Amphetamine
 D: Heroin

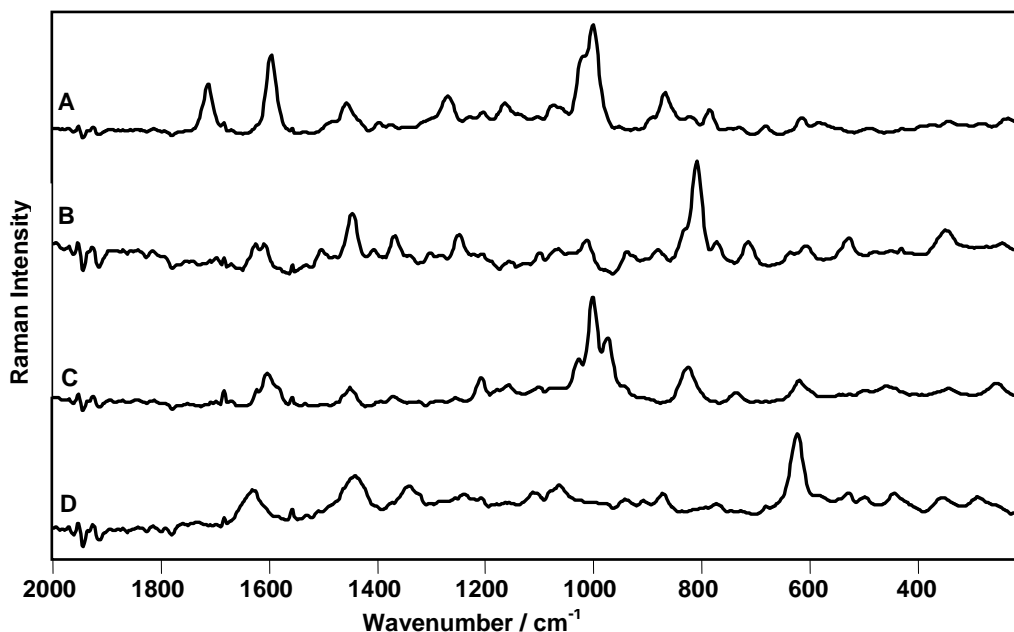


Figure 10.18 Raman spectra of drugs of abuse inside amber yellow glass containers
 A: Cocaine hydrochloride
 B: MDMA
 C: Amphetamine
 D: Heroin

10.3.4.4 Analysis of samples of drugs of abuse inside brown containers

Significant backgrounds can be observed in the Raman spectra collected from cocaine hydrochloride and amphetamine sulphate samples inside a brown container (figure 10.19 and figure 10.20, respectively). Spectral subtraction of the glass background has been applied, giving subtracted spectra that agree well with the reference spectra of cocaine hydrochloride and amphetamine sulphate, respectively. However, in other cases, the drugs of abuse cannot be identified because of the significant glass background observed (Figure 10.21). The drugs of abuse, namely cocaine hydrochloride and MDMA, cannot be identified even after subtraction of the glass background and similar results were obtained when sampling the drugs either through the sides or the bottom of the drug containers. This can be attributed to the colour of the glass and laser absorption.

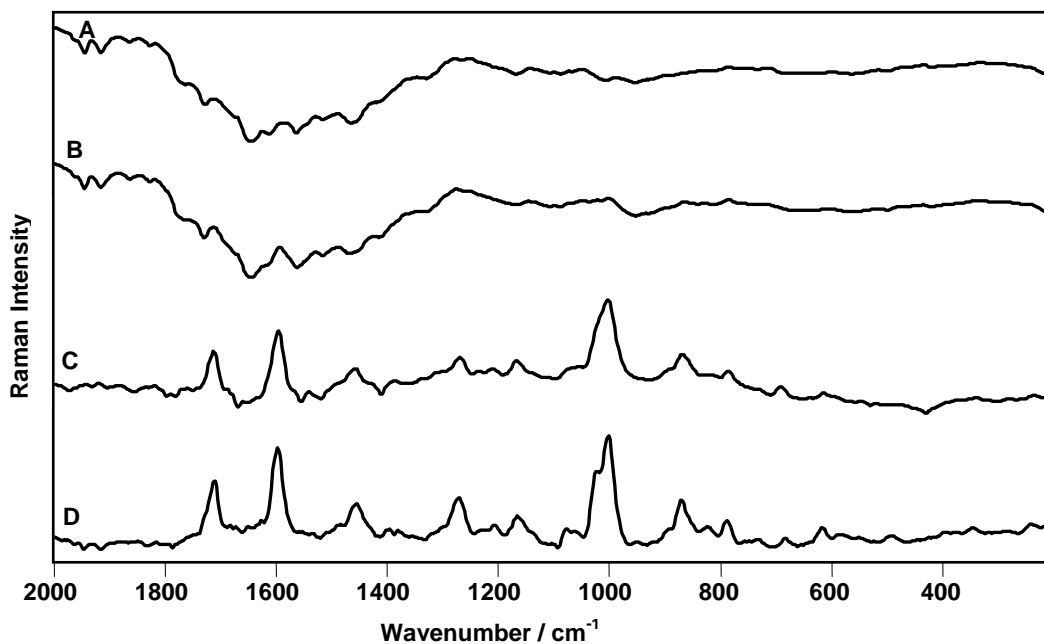


Figure 10.19 Raman spectra of cocaine hydrochloride inside brown glass containers
 A: Brown glass
 B: cocaine hydrochloride inside brown glass container
 C: Subtract spectrum (B-A)
 D: Reference cocaine hydrochloride

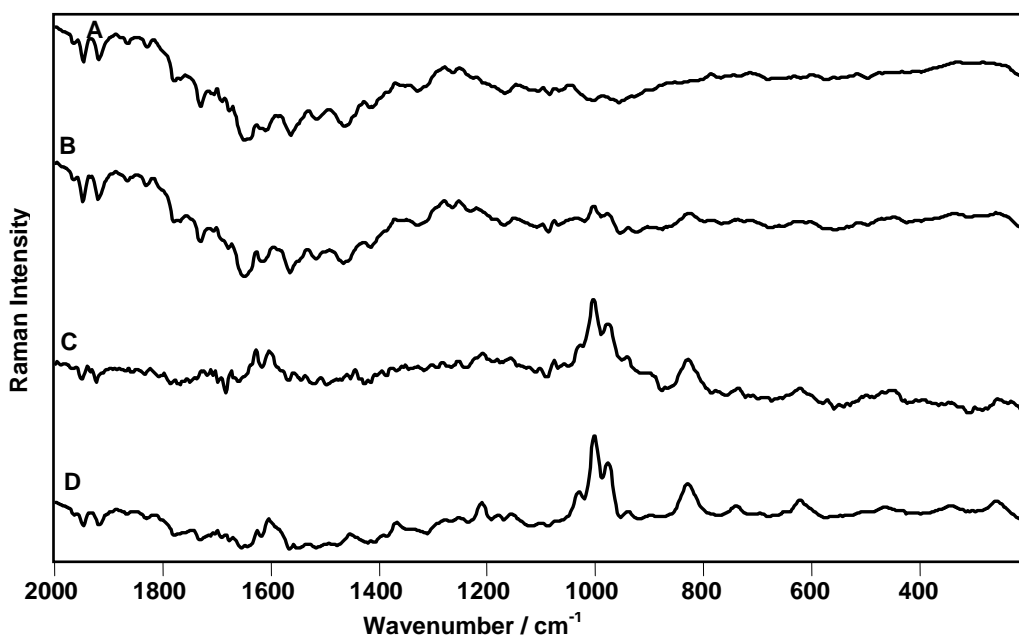


Figure 10.20 Raman spectra of amphetamine sulphate inside brown glass containers
 A: Brown glass
 B: Amphetamine sulphate inside brown glass container
 C: Subtract spectrum (B-A)
 D: Reference amphetamine sulphate

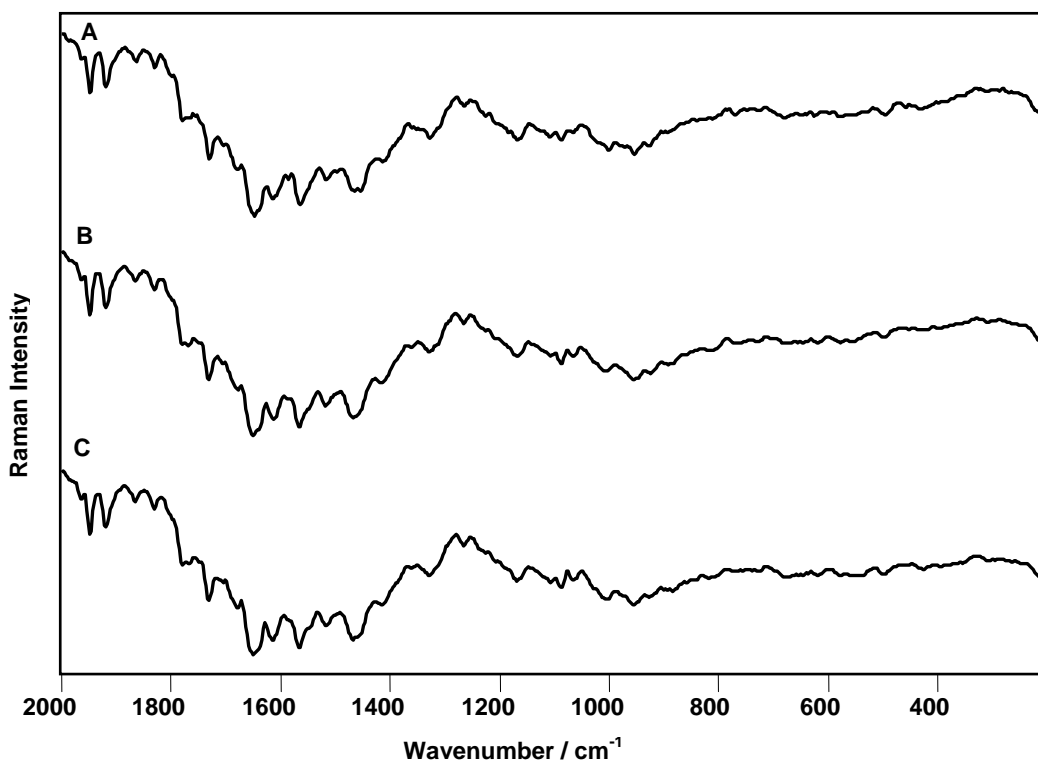


Figure 10.21 Raman spectra of drugs of abuse inside brown glass containers
 A: Brown glass
 B: Cocaine.HCl
 C: MDMA

10.3.5 Analysis of explosives and explosive precursors

The feasibility of the instrument for the analysis of the explosives and explosive precursors was also investigated. Figure (10.22) shows the Raman spectra collected from RDX and PETN, TNT and ammonium nitrate explosives using the 1064 system. All of the explosive compounds studied here exhibit strong Raman scattering; there is no fluorescence emission background and the majority of the vibrational bands can be clearly identified. The band wavenumber positions are observed within 1-3 cm^{-1} of the reference spectra obtained with a laboratory benchtop Renishaw Invia Reflex microscope. Also, the spectra obtained from the explosives precursors hexamethylenetetramine (HMTA) and pentaerythritol (Figure 10.23) are very rich in vibrational bands that can afford sufficient identification and the band wavenumber positions are within 1-3 cm^{-1} of the reference spectra. Plastic explosives usually

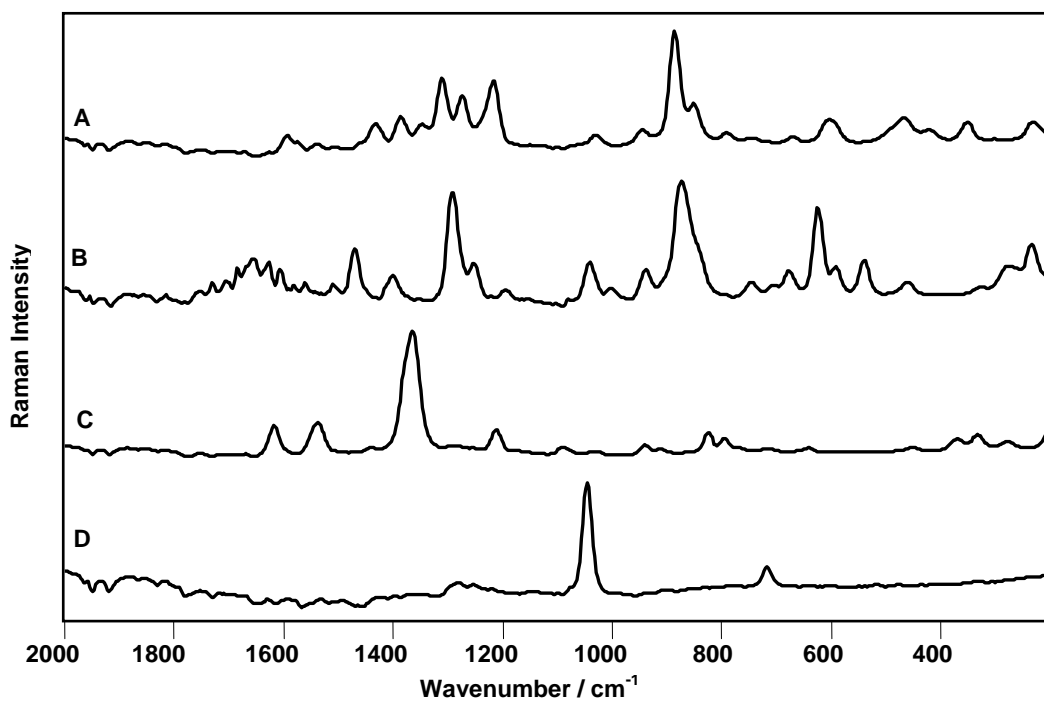


Figure 10.22 Raman spectra of the explosives

A: RDX

B: PETN

C: TNT

D: Ammonium nitrate

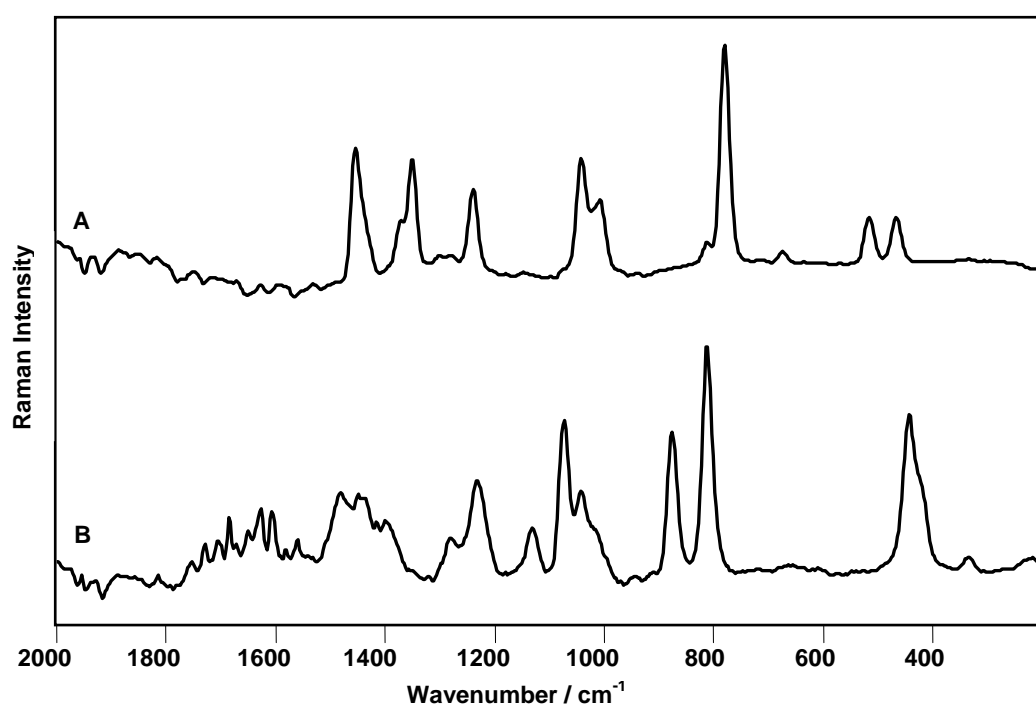


Figure 10.23 Raman spectra of the explosive precursors

A: Hexamethylenetetramine (HMTA)

B: Pentaerythritol

exhibit strong fluorescence emission even with the near infrared excitation at 785 nm. Raman spectra were obtained from four samples of Semtex explosive and the spectra were compared with the spectra obtained for the same samples with 785 nm excitation. The spectra obtained from the first two samples are shown in figure 10.24 which clearly show the advantage of shifting to the 1064 nm laser wavelength. These samples are highly fluorescent and using 785 nm excitation resulted in the Raman signal being completely masked by the fluorescence background. At 1064 nm laser excitation, the fluorescence background is significantly reduced and the characteristic bands of the explosives can be clearly identified. On comparison of the spectra of these two samples with the reference spectra of RDX and PETN (Figure 10.25) , it can be concluded that both samples are a mixture of RDX and PETN but sample one is mainly PETN while sample two is mainly RDX. Similar results were obtained from the other two samples of plastic explosives subjected for analysis (Figure 10.26).With the 785 nm laser, the fluorescence background overwhelms the Raman signal from the explosives, while shifting to 1064 nm excitation has resulted in a damping of the fluorescence background emission and the characteristic bands of the explosives are clearly observed. Again, on comparison of the Raman spectra of these two samples with the reference spectra of RDX and PETN (Figure 10.27), sample three can be identified as PETN while sample four is identified as RDX.

10.3.6 Analysis of explosives and explosive precursors inside plastic bags

The Raman spectra acquired from explosives powders through clear plastic packaging are shown in figure (10.28). All the samples can be identified and the packaging did not interfere with the detection of the explosives. There is no significant band in the spectra that can be assigned to the plastic container neither can any fluorescence background be seen in the spectra. This is significantly important as the ability to

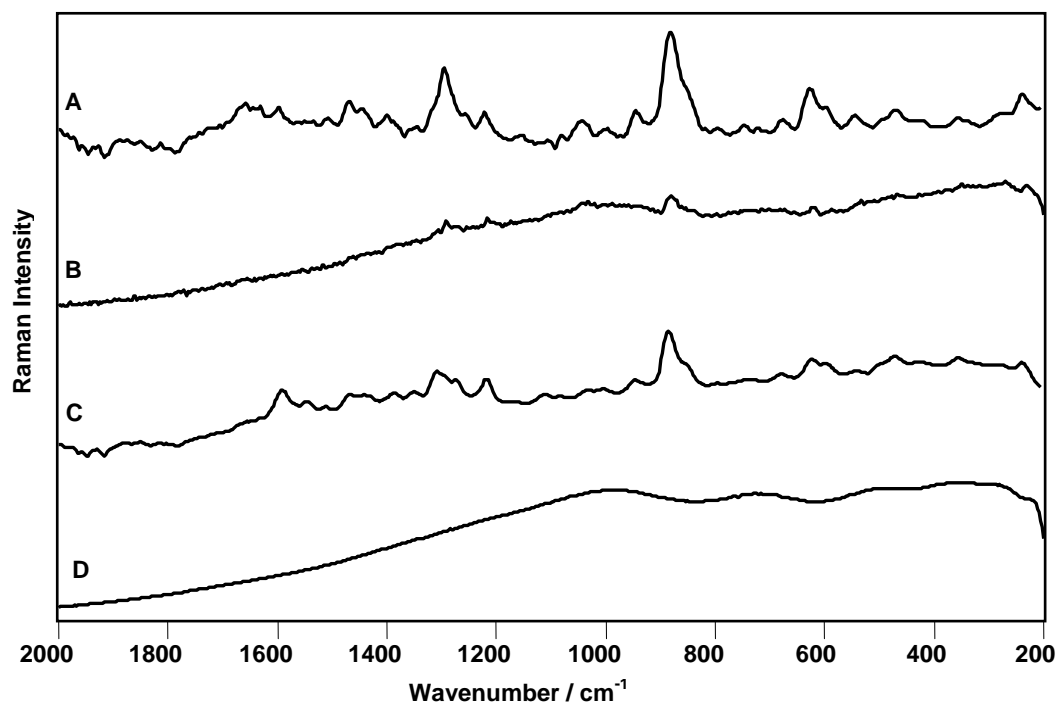


Figure 10.24 Raman spectra of the plastic explosives

- A: Semtex (sample 1), Advantage 1064 nm , 10 second exposure, 1 accumulation
- B: Semtex(sample 1), DeltaNu, 785 nm, 10 second exposure, 1 accumulation
- C: Semtex (sample 2), Advantage 1064 nm , 10 second exposure, 1 accumulation
- D: Semtex(sample 2), DeltaNu, 785 nm, 10 second exposure, 1 accumulation

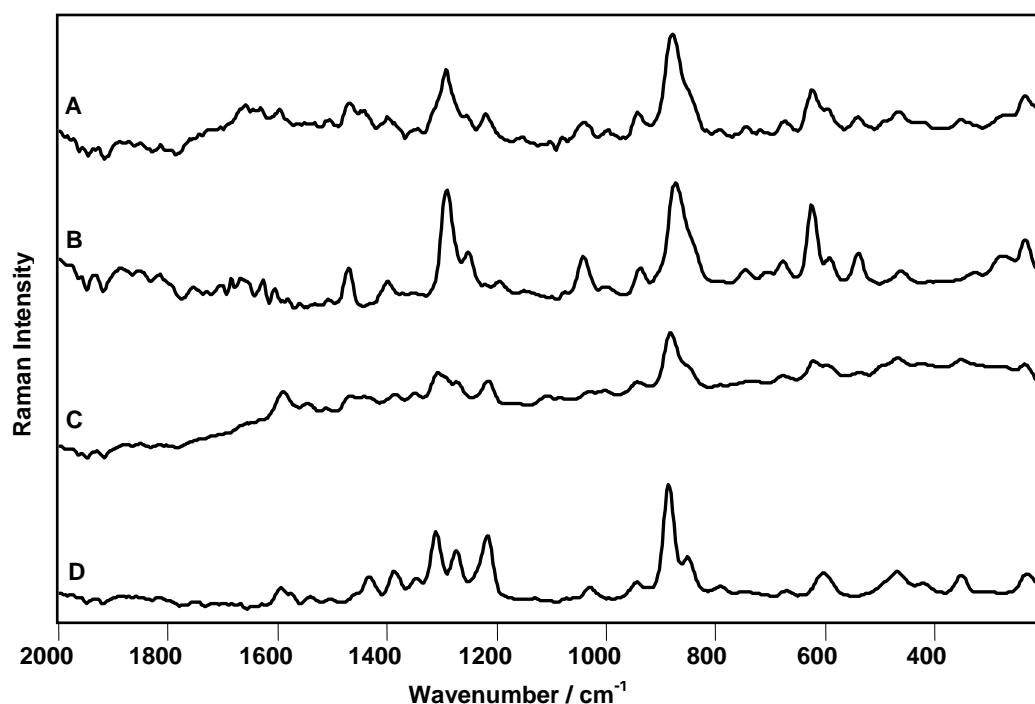


Figure 10.25 Raman spectra of the plastic explosives

- A: Semtex (sample 1), Advantage 1064 nm , 10 second exposure, 1 accumulation
- B: PETN, Advantage 1064 nm , 10 second exposure, 1 accumulation
- C: Semtex (sample 2), Advantage 1064 nm , 10 second exposure, 1 accumulation
- D: RDX, Advantage 1064 nm , 10 second exposure, 1 accumulation

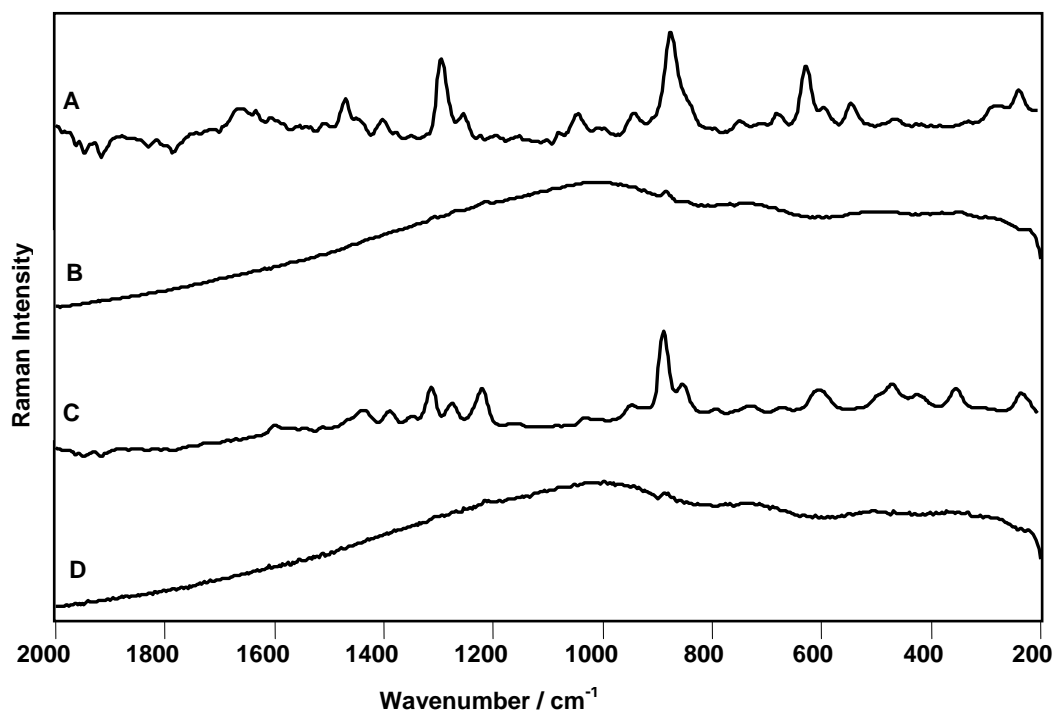


Figure 10.26 Raman spectra of the plastic explosives

A: Semtex (sample 3), Advantage 1064 nm , 10 second exposure, 1 accumulation

B: Semtex(sample 3), DeltaNu, 785 nm, 10 second exposure, 1 accumulation

C: Semtex (sample 4), Advantage 1064 nm , 10 second exposure, 1 accumulation

D: Semtex(sample 4), DeltaNu, 785 nm, 10 second exposure, 1 accumulation

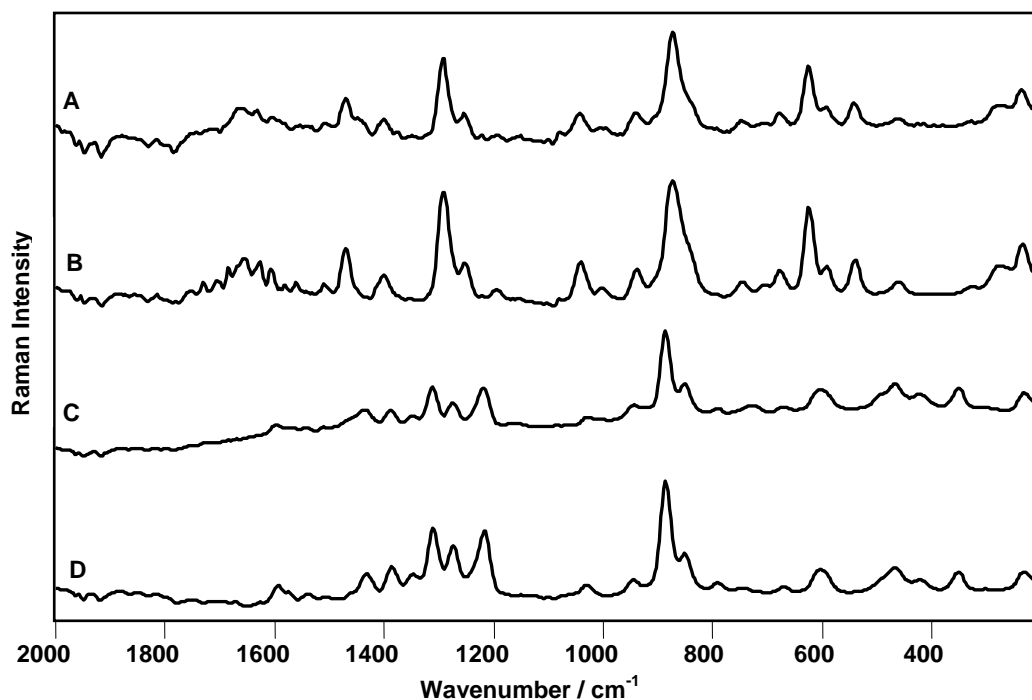


Figure 10.27 Raman spectra of the plastic explosives

A: Semtex (sample 3), Advantage 1064 nm , 10 second exposure, 1 accumulation

B: PETN, Advantage 1064 nm , 10 second exposure, 1 accumulation

C: Semtex (sample 4), Advantage 1064 nm , 10 second exposure, 1 accumulation

D: RDX, Advantage 1064 nm , 10 second exposure, 1 accumulation

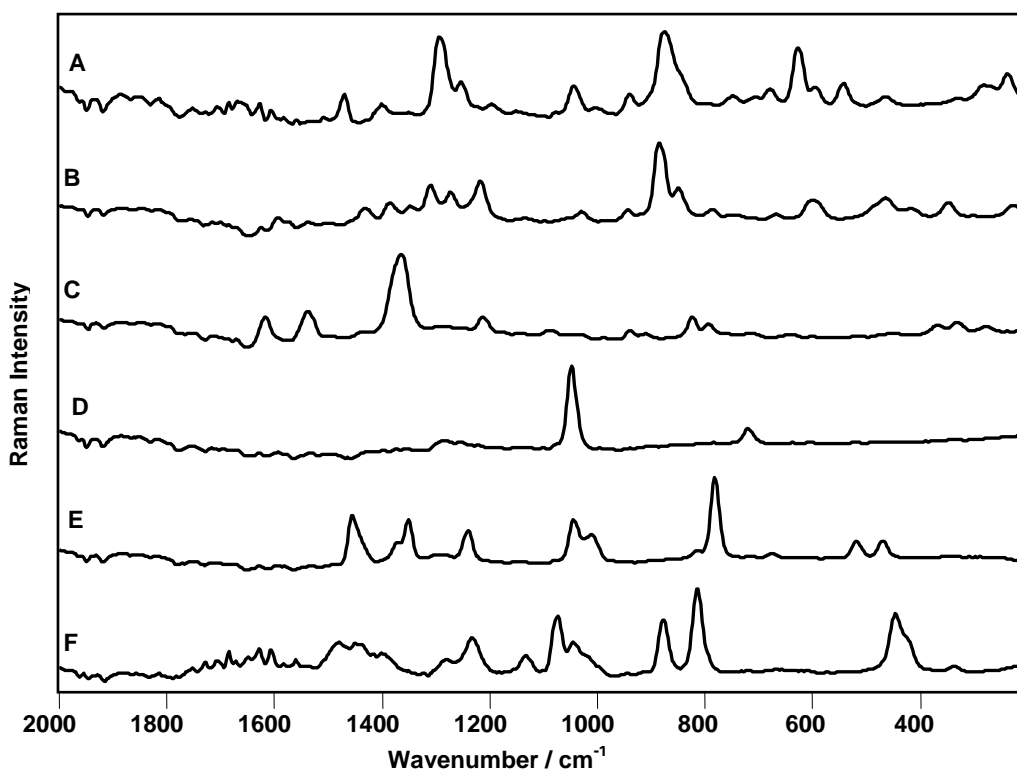


Figure 10.28 Raman spectra of the explosives and precursors inside plastic bags
 A: RDX
 B: PETN
 C: TNT
 D: Ammonium nitrate
 E: Hexamethylenetetramine (HMTA)
 F: Pentaerythritol

identify the explosives while inside their containers eliminates the chance of exposure to possible harmful substances in such containers and prevent evidence contamination.

10.3.7 Analysis of explosives and explosive precursors inside glass containers

10.3.7.1 Analysis of explosives and explosive precursors inside clear glass vials

The spectra acquired from the explosives and explosive precursors whilst held in clear glass containers are shown in figure (10.29). The characteristic Raman features of the explosives can be clearly identified and the glass containers did not interfere with the identification of the explosives. This can be attributed to the explosives being excellent Raman scatterers and the glass container being a relatively poorer Raman scatterer. Also, it was possible to acquire Raman spectra from two samples of Semtex inside clear glass containers (Figure 10.30) which were identified as predominantly composed of RDX.

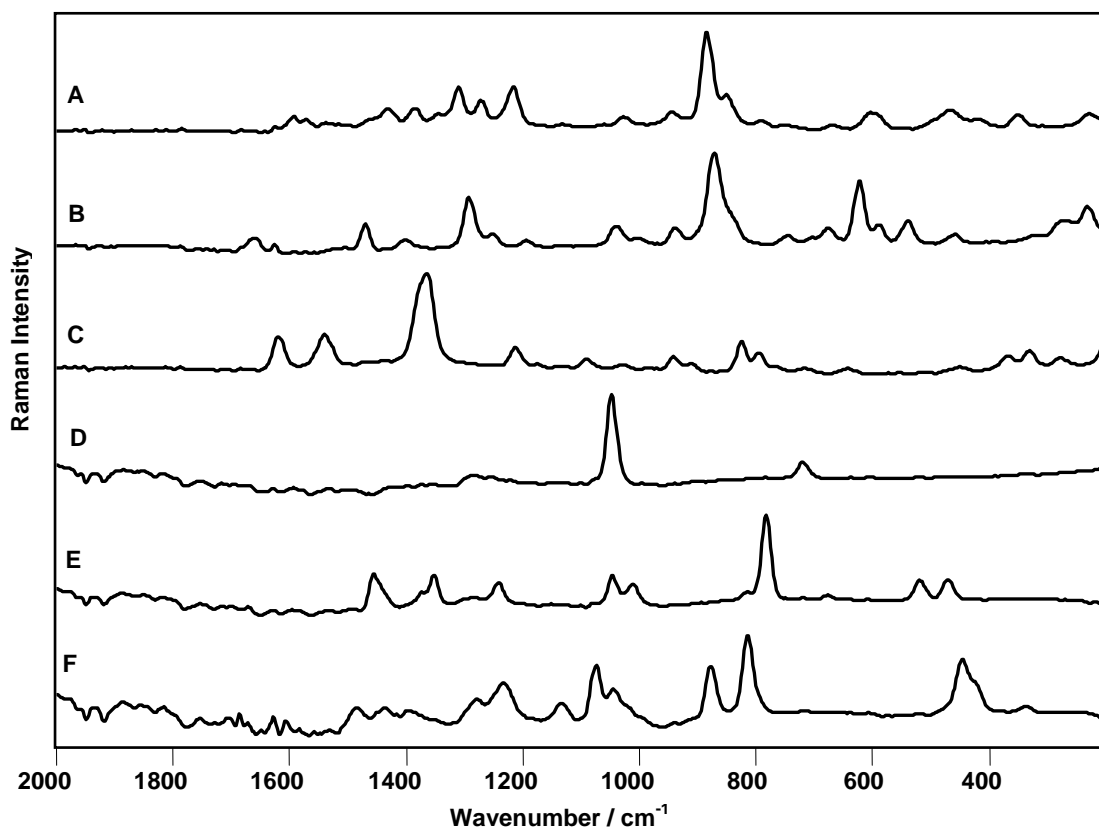


Figure 10.29 Raman spectra of the explosives and precursors inside clear glass vials

- | | |
|----------------------------------|---------------------|
| A: RDX | B: PETN |
| C: TNT | D: Ammonium nitrate |
| E: Hexamethylenetetramine (HMTA) | F: Pentaerythritol |

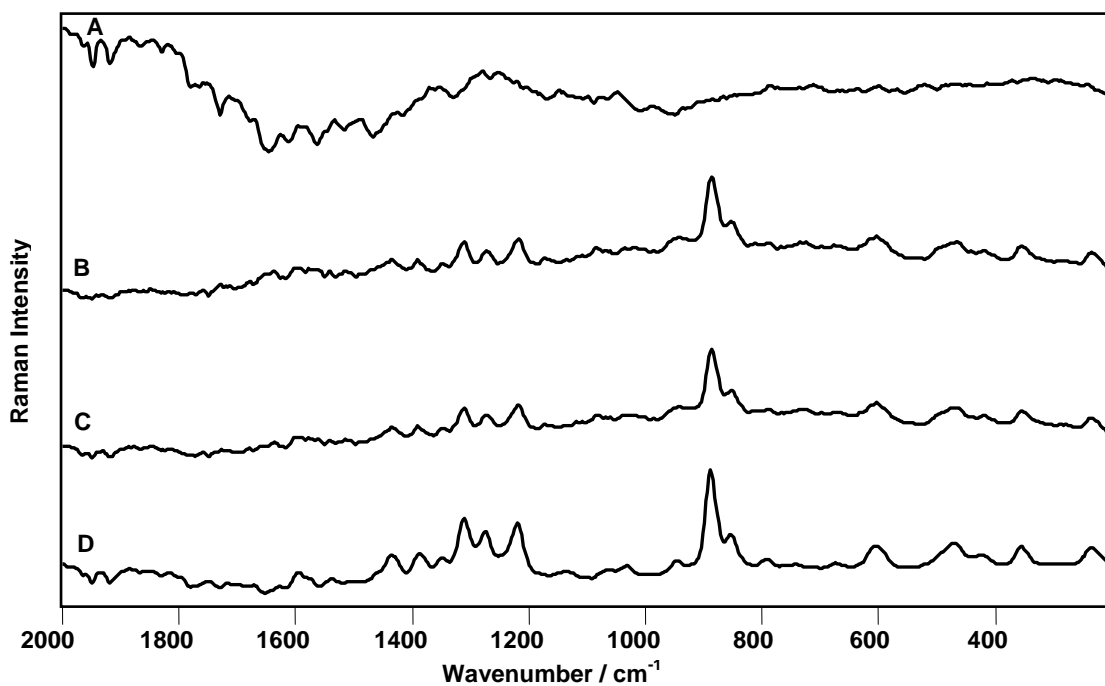


Figure 10.30 Raman spectra of Semtex inside clear glass vials

- | | |
|--------------------------|----------------------|
| A: Clear glass container | B: Semtex (sample 1) |
| C: Semtex (sample 2) | D: RDX |

10.3.7.2 Analysis of explosives and explosive precursors inside green vials

The spectra acquired from the explosives and explosive precursors are shown in figure (10.31) from which all the compounds studied can be identified. There is no fluorescence background can be seen in the spectra. The green colour of the glass containers did not interfere with the sampling of the explosives *in-situ*.

10.3.7.3 Analysis of explosives and explosive precursors inside brown containers

A broad emission background can be seen in the spectra obtained from some of the explosives and explosive precursors but in all cases the principal bands of the explosives can be identified. This can be seen in the Raman spectra obtained from RDX (Figure 10.32) and PETN (Figure 10.33) inside brown glass containers, respectively. However, spectral subtraction has been applied and the resulting

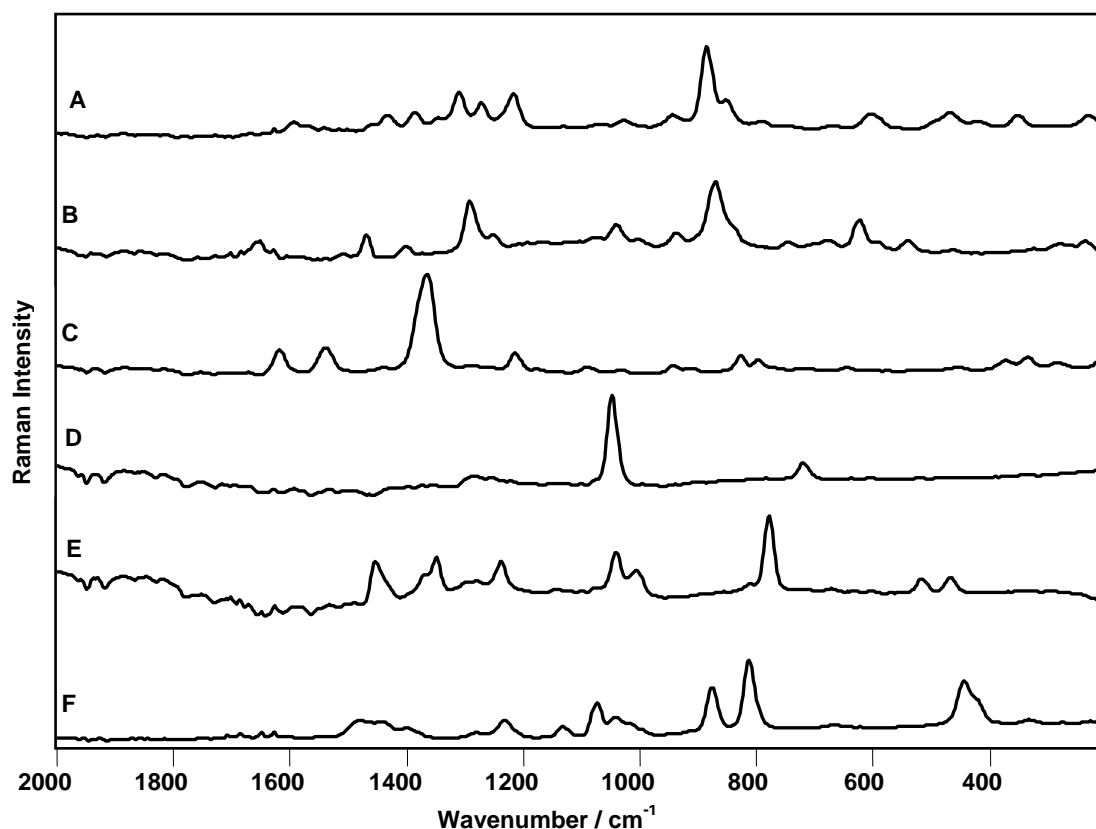


Figure 10.31 Raman spectra of explosives and precursors inside green-coloured vials
A: RDX
B: PETN
C: TNT
D: Ammonium nitrate
E: Hexamethylenetetramine (HMTA)
F: Pentaerythritol

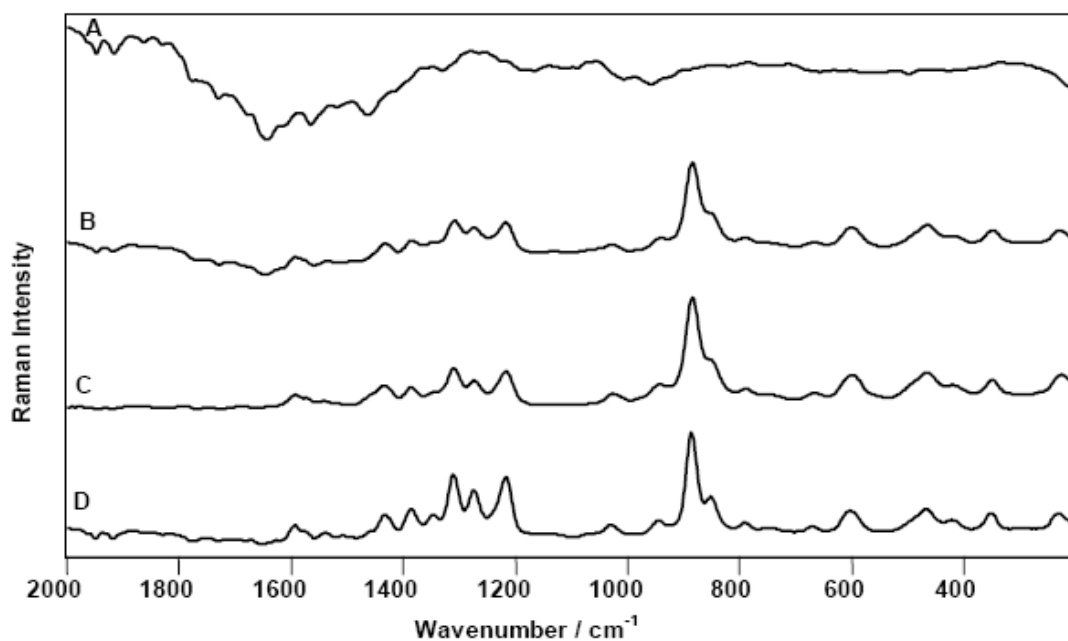


Figure 10.32 Raman spectra of RDX inside brown glass container

- A: Brown glass
- B: RDX
- C: Subtract spectrum (B-A)
- D: Reference RDX

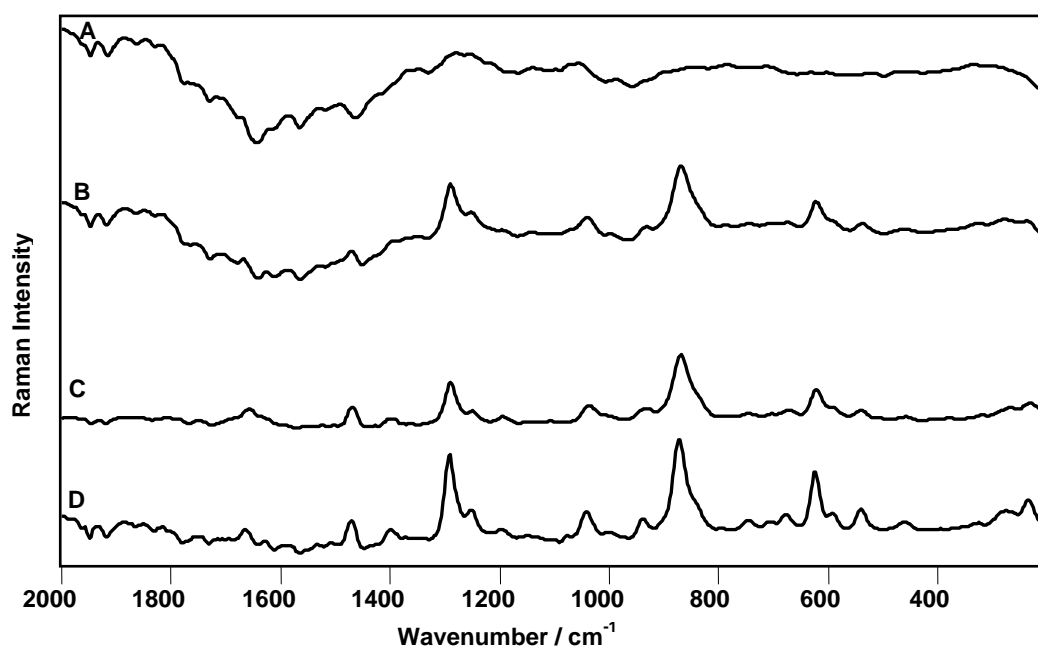


Figure 10.33 Raman spectra of PETN inside brown glass container

- A: Brown glass
- B: PETN
- C: Subtract spectrum (B-A)
- D: Reference PETN

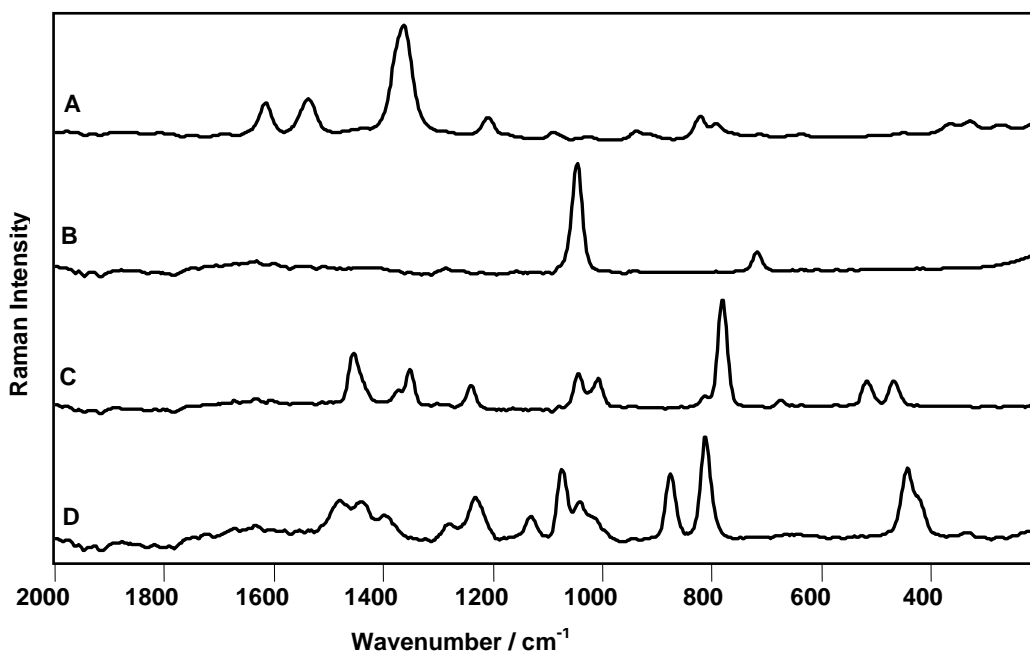


Figure 10.34 Raman spectra of explosives and precursors inside brown glass container

A: TNT

B: Ammonium nitrate

C: Hexamethylenetetramine (HMTA)

D: Pentaerythritol

subtracted spectra agree well with the reference spectra of the explosives and even the weaker bands can be identified. This background cannot be observed in the Raman spectra obtained from the rest of the explosives and explosive precursors (Figure 10.34) and the vibrational bands of the explosives are clearly identified.

10.3.8 Analysis of drugs of abuse and explosives inside opaque polymer containers

Polymers are common containers of drugs of abuse and explosives. The ability to acquire Raman spectra from materials held within these containers will depend on the Raman cross-section of the material itself and the absorption and scattering properties of the containers. The Raman spectrum acquired from HMTA inside a white plastic bottle (Figure 10.35) shows only the bands of the bottle container and no band can be assigned to the explosive precursor. However, after spectral subtraction of the bottle spectrum (Figure 10.35 C) the Raman bands of HMTA can be identified, such as those

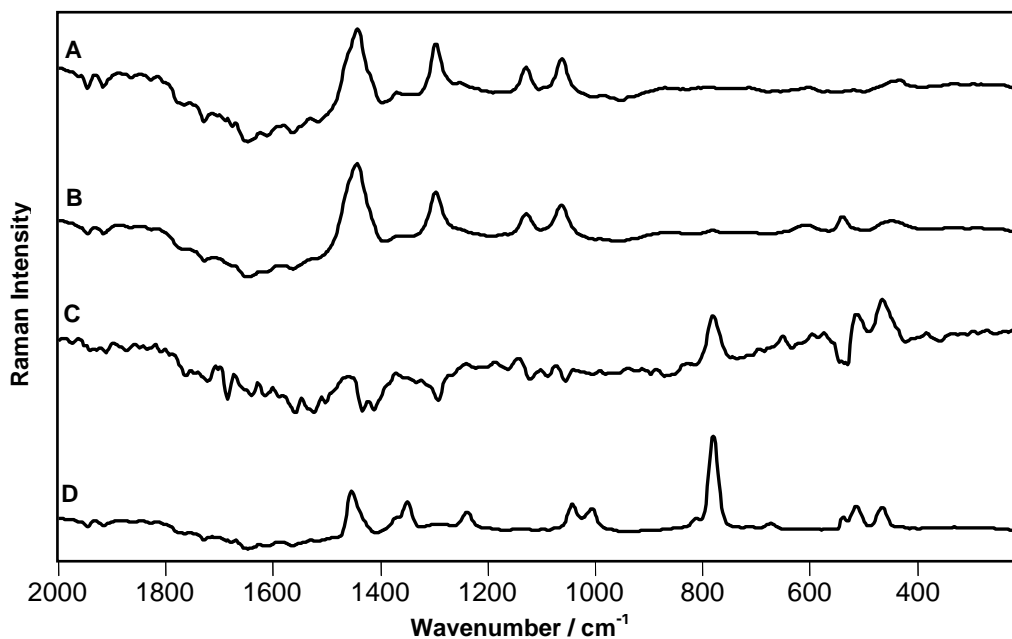


Figure 10.35 Raman spectra of HMTA inside white plastic bottle
 A: White plastic bottle
 B: HMTA inside white plastic bottle
 C: Subtract spectrum (B-A)
 D: Reference HMTA

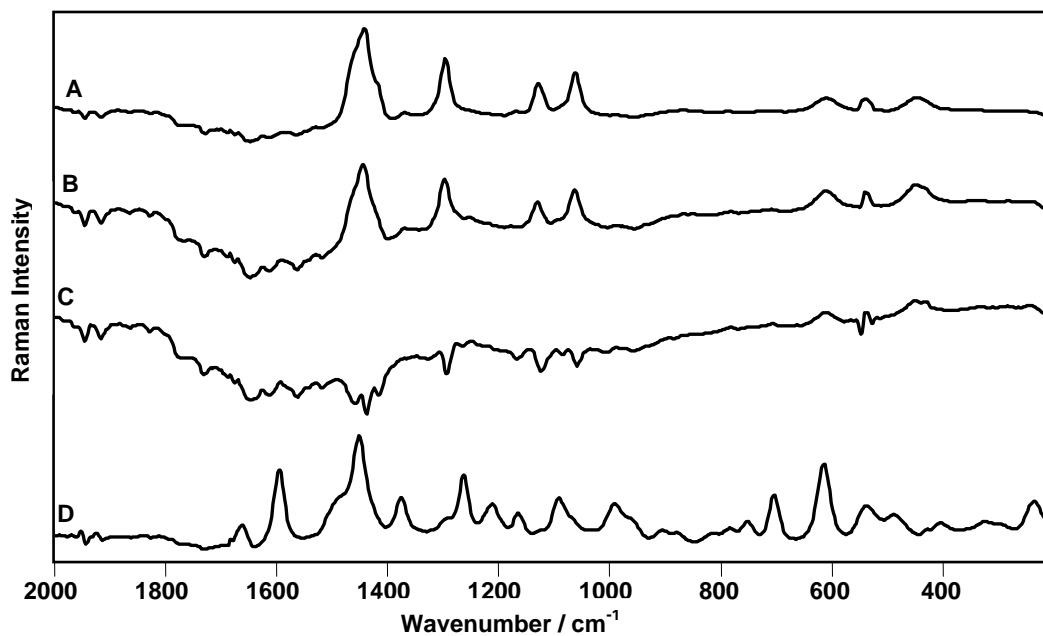


Figure 10.36 Raman spectra of lidocaine inside white plastic bottle
 A: White plastic bottle
 B: Lidocaine inside white plastic bottle
 C: Subtract spectrum (B-A)
 D: Reference lidocaine

at 780, 508 and 462 cm^{-1} . In another case studied here, The Raman spectrum obtained from lidocaine inside a white plastic bottle is shown in figure (10.36). The intense signal emanating from the plastic bottle overwhelms that of the drug and even after spectral subtraction of the bottle spectrum, no significant band can be assigned to the drug contained inside. Also, samples of cocaine hydrochloride and PETN were examined whilst held inside a red / brown polypropylene pharmaceutical dispensing bottle. Setting the laser power to a higher level has resulted in burning of the wall of the containers and no signal can be detected at medium laser power level.

These results demonstrate that this prototype operating with 1064 nm excitation has an excellent potential for the analysis of drugs of abuse and explosives. Street samples of drugs of abuse and plastic explosives which usually fluoresce with visible or 785 nm excitations were successfully analysed without interfering fluorescence backgrounds. Spectra have been obtained for drugs of abuse and explosives, both neat and in plastic and glass containers. Sampling drugs of abuse and explosives through coloured glass, which is highly fluorescent in the visible, was also feasible. This dispersive system operating at 1064 nm excitation and coupled with transfer electron (TE) InGaAs photocathode and electron bombardment (EB) CCD technology can rapidly analyze samples with good S/N ratios. The right-angled optical head allows for a flexible positioning of the sample to be analyzed. The portability and rapidity of the analysis are significant advantages of the 1064 Advantage system. These criteria are significantly important for law enforcement agencies working in the field and dealing with relatively large numbers of samples on a daily basis. Hence, the prototype tested here brings a new potential to detect compounds which are fluorescing at lower excitation wavelengths and broadens the number of samples that can be analyzed by Raman spectroscopy.

The main disadvantage of this prototype is the need for a power connection which can limit the use of the instrument in the field. Despite this, the instrument can be used in airports or through the adoption a battery-operated configuration. A weak spectral artefact can be seen in the spectra at approximately 1950 cm^{-1} , but this is well removed in wavenumber from the characteristic vibrational bands of explosives and drugs of abuse and their precursor materials.

Chapter 11

Conclusions and Future Work

This the first study that illustrates the use of Raman microscopy for the detection and identification of drugs of abuse, explosives and their precursors on some biomaterials of forensic relevance such as textiles, nail and skin. The technique has proven to be effective in discriminating between the analyte and the substrate. The presence of some spectral bands arising from the biomaterial substrate did not interfere with the identification of the drugs of abuse and explosives, which could be unambiguously identified by their characteristic Raman bands. If necessary, interfering bands could be successfully removed by spectral subtraction. Raman spectra could be acquired from drug particles embedded within highly fluorescent specimens such as a coloured T-shirt. Also, confocal Raman microspectroscopy can be an invaluable tool for the detection and identification of drugs of abuse and explosives in obscured situations; interference-free Raman spectra as well as two-dimensional Raman maps could be acquired from contaminant particles under a coating of nail varnish. The use of near-infrared lasers to excite samples is an added advantage of the technique because the likelihood of generation of fluorescence is much less than with the use of visible lasers. Raman spectra of selected drugs of abuse and explosive substances could be readily obtained *in-situ* non-destructively without sample preparation or chemical pretreatment. The results can be of evidential value to establish a link between these substances and individuals involved in activities related to the drug trade, drug abuse or terrorism. As this work has been carried out in a laboratory-based environment, the viability of the results for field applications has to be thoroughly investigated further. The results can be of evidential value in several forensic scenarios, such as the detection of drugs of abuse on the nails or skin of drug-intoxicated victims *in-situ*,

which gives an insight and possibility of identification of intoxication and allows the emergency team to resuscitate the victim properly. Another scenario is the detection of explosives or explosives residues on the nails, skin or clothing of a person will help to identify persons involved in suicidal bomber attacks.

Also, this study reports for the first time the application of fibre-optic Raman spectroscopy for the detection and identification of drugs of abuse in clothing impregnated with these drugs. The presence of spectral bands arising from the fibre polymers and/or dyes in textiles presented no difficulty in establishing the identity of the drugs of abuse. Raman spectra of the drugs could be readily obtained *in-situ* non-destructively within 20–60 seconds and without necessitating sample extraction or pre-treatment. The spectra obtained were identified by searching against an identification library, which is highly desirable for automated database recognition algorithms. These results show a clear application of portable Raman spectroscopy as a primary screening technique for drugs-of-abuse in live situations. The rapid acquisition of Raman spectra *in-situ* and in the field offers a reliable method for forensic scientists and police agencies that has the potential for rapidly identifying unknown samples.

Lastly, the tested prototype operating with 1064 nm excitation has excellent potential for the analysis of drugs of abuse and explosives. Street samples of drugs of abuse and plastic explosives, usually fluorescing with visible and 785 nm laser excitation, were analyzed successfully. The samples were analyzed both as neat materials and whilst contained in plastic and glass containers. Sampling drugs of abuse and explosives through coloured glass, which is highly fluorescent in the visible region, was also feasible. The portability and rapidity of analysis are significant advantages of the 1064 DeltaNu Advantage system. These criteria are significantly important for law

enforcement agencies working in the field and dealing with relatively large numbers of samples on a daily basis. The prototype tested here brings a new potential for the detection of compounds which are fluorescing at lower excitation wavelengths and broadens the number of samples that can be analyzed by Raman spectroscopy.

References

- [1] King, L. A. and McDemontt , S. D. in: Clarke's analysis of drugs and poisons by Moffat , A. C., Osselton, M. D. and Widdop , B. (Eds.), 3rd edition, London, Pharmaceutical press, 2004,Vol. 1, chapter 2, p.p.37-52.
- [2] Wills, S., Drugs of abuse, 2nd edition, London, Pharmaceutical press, 2005, p.p.1-225.
- [3] World Health Organization, The global burden.
www.who.int/substance_abuse/facts/global_burden/en/index (Accessed 6 September 2010).
- [4] King, L. A., The misuse of drugs act: A guide for forensic scientists, Cambridge, UK,Royal Society of Chemistry,2003,chapter1,p.p.1-6;
- [5] The Misuse of Drugs Regulations 2001, Statutory Instrument 2001 No. 3998.
www.opsi.gov.uk/si/si2001/20013998; www.homeoffice.gov.uk/drugs/drug-law/ ;
www.homeoffice.gov.uk/about-us/home-office-circulars/circulars-2009/021-2009/21-2009?view=Binary (Accessed 6 September 2010).
- [6] Goldstein, A., Addiction: from biology to drug policy, New York, USA, W.H. Freeman and Company, 1994, Chapter6, p.p.73-98.
- [7] Wijesekera, A.R., Henry ,K.D., Ranasinghe, P., The detection and estimation of (A) arsenic in opium, and (B) strychnine in opium and heroin, as a means of identification of their respective sources, Forensic Sci Int., 36 (3-4),1988,193-209.
- [8] Warkentin,T.E., Thrombocytopenia and Illicit Drug Use, Annals of Internal Medicine, 120(8),1994,p.p. 693.
- [9] Nogué S., Sanz P., Munné P., de la Torre R. , Acute scopolamine poisoning after sniffing adulterated cocaine, Drug and alcohol dependence, 27(2), 1991, 115-6.
- [10] Fucci, N., De Giovanni N., Adulterants encountered in the illicit cocaine market,

Forensic Sci Int, 95(3),1998 , 247-52.

[11] Perrine,D.M., The Chemistry of Mind-Altering Drugs: History, Pharmacology and cultural context, Washington, DC, American Chemical Society, 1996, chapter 4, p.p.171-205.

[12] Yudko, E., Hall, H. V. and McPherson, S. B., Methamphetamine Use: Clinical and Forensic Aspects, Florida, USA, CRC Press, 2003, chapters 3&4, p.p.15-30.

[13] Cole, M. D., The analysis of Controlled Substances, Chichester, England, John Wiley & Sons Ltd , 2003, chapter 2, p.p.13-36.

[14] Bell, S. Forensic Chemistry, New Jersey, USA, Pearson Education, Inc., 2006, Part III. , Chapter 6, 212-264.

[15] A C Moffat. Drugs of abuse.Science & Justice, 40(2) , 2000, 89-92.

[16] United Nations Office on Drugs and Crimes, 2009 World Drug Report.

http://www.unodc.org/documents/about-unodc/AR09_LORES.pdf (Accessed 6 September 2010).

[17] Scott-Ham, M. and Burton, F. C., Toxicological findings in cases of alleged drug-facilitated sexual assault in the United Kingdom over a 3-year period, Journal of clinical forensic medicine, 12, 2005, 175-186.

[18] LeBeau, M. A. and Mozayani, A., Drug – Facilitated Sexual Assault: A Forensic Handbook, San Diego, Academic Press, 2001, chapter5, p.p.107.

[19] Marshall, M. and Oxley, J.C., Aspects of Explosives Detection, First edition, Oxford, UK, Elsevier, 2009,p.p.12-20.

[20] Beveridge, A., Forensic Investigation of Explosions, London,UK, Taylor & Francis , 1998,p.p.1-71.

[21] Anderson , J.L., Cantu, A. A., Chow, A.W., Fussell ,P. S., Nuzzo ,R. G., Parmeter ,J. E., Sayler ,G. S., Shreeve ,J. M. , Slusher ,R. E., Story ,M., Trogler, W.,

Venkatasubramanian, V., Waller , L. A., Young , J., Zukoski,C.F., Existing and Potential Standoff Explosives Detection Techniques, Washington DC,USA, The National Academies Press, , 2004,p.p 8-11.

[22] Akhavan, J., The Chemistry of Explosives, Second Edition, Cambridge, UK, Royal Society of Chemistry, 2004,p.p.1-47.

[23] Bell, S., Drugs, Poisons, and Chemistry, New York, USA, Facts On File, Inc., 2009, Chapter 4, p.p.88.

[24] O'Neal, C. L., Crouch, D. J., Fatah, A. A., Validation of twelve chemical spot tests for the detection of drugs of abuse, Forensic Science International, 109, 2000, 189–201.

[25] Kitson, F.G., Larsen, B.S, McEwen, C.N., Gas Chromatography and Mass Spectrometry-A practical guide, California, USA, Academic Press, 1996, p1-5.

[26] Yinon, J., Advances in Forensic Applications of Mass Spectrometry,Washington D.C., USA, CRC Press, 2004,14-18.

[27] de Korompay, A., Hill, J. C., Carter, J. F., NicDaeid, N., Sleeman, R., Supported liquid-liquid extraction of the active ingredient (3,4-methylenedioxymethylamphetamine) from ecstasy tablets for isotopic analysis, Journal of Chromatography A ,1178 (1-2), 2008,1-8 .

[28] Cheng , W.C., Poon ,N.L., Chan, M.F., Chemical profiling of 3,4-methylenedioxymethamphetamine (MDMA) tablets seized in Hong Kong, Journal of Forensic Sciences , 48(6) ,2003 , 1249-1259 .

[29] O'Connell, D., Heffron, J.J.A., Rapid analysis of illicit drugs by mass spectrometry: Results from seizures in Ireland, Analyst, 125(1), 2000, 119-121.

[30] Jenkins, A.J., Drug contamination of US paper currency, Forensic Science International , 121(3), 2001, 189-193.

- [31] Esteve-Turrillas, F.A., Armenta ,S. , Moros , J., Garrigues, S., Pastor , A. , de la Guardia , M., Validated, non-destructive and environmentally friendly determination of cocaine in euro bank notes, *Journal of Chromatography A* ,1065 (2),2005,321-325.
- [32] Kalasinsky, K.S., Levine, B., Smith, M.L., Feasibility of using GC/FT-IR for drug analysis in the forensic toxicology laboratory, *J Anal Toxicol.*,16(5), 1992 , 332-336.
- [33] Kalasinsky, K.S., Levine, B., Smith, M.L., Magluilo, J., Schaefer, T., Detection of amphetamine and methamphetamine in urine by gas chromatography/Fourier transform infrared(GC/FTIR) spectroscopy, *J Anal Toxicol.*, 17(6),1993,359-64.
- [34] Duncan, W. and Soine, W.H., Identification of Amphetamine Isomers by GC/IR/MS, *J. Chromatogr. Sci.*, 26, 1988, 521-526.
- [35] Lee, M.S., *LC/MS Applications in Drug Development*, New York, USA, John Wiley & Sons, 2002, p.34.
- [36] da Costa, J.L., Pintao, E.R., Corrighiano, C.M.C., Neto ,O.N. , determination of 3,4-methylenedioxymethamphetamine (MDMA) in ecstasy tablets by high performance liquid chromatography with fluorescence detection (HPLC-FD), *Quimica Nova* , 32(4),2009, 965-969.
- [37] Sadeghipour, F., Veuthey, J.L., sensitive and selective determination of methylenedioxyated amphetamines by high-performance liquid chromatography with fluorimetric detection, *Journal of Chromatography A* , 787(1-2),1997,137-143.
- [38] Atay ,O., Oztop, F. , Quantitative determination by using HPLC and GLC methods for cocaine HCl in synthetic binary mixtures with procaine HCl, lidocaine HCl and caffeine, *Analytical Letters* , 30(3),1997, 565-584.
- [39] Stein, K. , Kraatz, A., Comparative study of illegal cocaine samples with high pressure liquid chromatography and photodiode array detection, *Arch Kriminol* ,

197(1-2),1996, 16-26.

[40] Besacier, F., Chaudron, T. H., Rousseau, T. M., Girard, J., Lamotte, A. Comparative chemical analyses of drug samples: General approach and application to heroin, *Forensic Science International*, 85(2),1997, 113-125.

[41] Veress, T., Szanto, J.I., Leisztner, L., determination of the characteristic components from Hashish and Marijuana type drugs of abuse .2. determination of Cannabinoid acids applying decarboxylation and HPLC, *Magyar Kemiai Folyoirat*, 95(2),1989,59-65.

[42] Shimamine, M., Masunari, T., Nakahara, Y., Studies on identification of drugs of abuse by diode array detection. I. Screening-test and identification of benzodiazepines by HPLC-DAD with ICOS software system, *Eisei Shikenjo Hokoku*, 11, 1993, 47-56.

[43] Ardrey, R.E., *Liquid Chromatography– Mass Spectrometry: an introduction*, John Wiley & Sons, Chichester, England. , 2003, P.2

[44] Laks, S., Pelander, A., Vuori, E., Tolppa, E. A., Sippola, E., Ojanperä, J., Analysis of Street Drugs in Seized Material without Primary Reference Standards, *Analytical Chemistry*, 76 (24), 2004, pp 7375–7379.

[45] Postigo, C., de Alda, M.J.L., Viana, M., Querol, X., Alastuey, A., Artinano, B., Barcelo, D., Determination of Drugs of Abuse in Airborne Particles by Pressurized Liquid Extraction and Liquid Chromatography-Electrospray-Tandem Mass Spectrometry, *Analytical Chemistry*, 81(11),2009,4382-4388.

[46] Uchiyama, N., Kikura-Hanajiri, R., Kawahara, N., Goda, Y., Analysis of designer drugs detected in the products purchased in fiscal year 2006, *Yakugaku Zasshi-journal of the Pharmaceutical Society of Japan*, 128(10),2008, 1499-1505.

[47] Bones, J., Macka, M., Paull, B., Evaluation of monolithic and sub 2 mm particle packed columns for the rapid screening for illicit drugs - application to the

determination of drug contamination on Irish euro banknotes, *Analyst* ,132(3), 2007, 208-217.

[48] Somsen, G.W. , Gooijer, C. , Brinkman, U.A.Th., Liquid chromatography–Fourier-transform infrared spectrometry, *Journal of Chromatography A*, 856 ,1999, 213–242.

[49] Montaudo ,G., Lattimer , R. P., *Mass Spectrometry of Polymers*, CRC Press , Florida , USA, 2002, chapter1, p.1-10.

[50] Steiner, R.R., Larson, R.L. , Validation of the Direct Analysis in Real Time Source for Use in Forensic Drug Screening, *Journal of Forensic Sciences*,54(3), 2009, 617-622.

[51] Rowell, F., Hudson, K., Seviour, J., Detection of drugs and their metabolites in dusted latent finger marks by mass spectrometry, *Analyst* , 134(4), 2009, 701-707.

[52] Kothari, S., Song, Q.Y., Xia, Y., Fico, M., Taylor, D, Amy, J.W., Stafford, G., Cooks, R.G., Multiplexed Four-Channel Rectilinear Ion Trap Mass Spectrometer, *Analytical Chemistry*,81(4), 2009,1570-1579.

[53] Luosujärvi, L., Laakkonen, U.M., Kostianen, R., Kotiaho, T., Kauppila, T.J., Analysis of street market confiscated drugs by desorption atmospheric pressure photoionization and desorption electrospray ionization coupled with mass spectrometry , *Rapid Communications in Mass Spectrometry* , 23(9), 2009,1401-1404.

[54] Talaty, N., Mulligan, C.C., Justes, D.R., Jackson, A.U., Noll, R.J., Cooks, R.G., Fabric analysis by ambient mass spectrometry for explosives and drugs, *Analyst* , 133(11),2008,1532-1540.

[55] Rouessac,F., Rouessac, A., *Chemical Analysis: Modern Instrumentation Methods and Techniques* , John Wiley & Sons, Chichester , England, 6th edition, 2007, p.263.

- [56] Hu ,X.Z., Kan, J.D., Yuan, B., X-ray diffraction spectrum of heroin, *Spectroscopy and Spectral Analysis* ,19(3),1999, 434-436.
- [57] Cook, E. , Fong, R., Horrocks, J., Wilkinson, D., Speller, R., Energy dispersive X-ray diffraction as a means to identify illicit materials: A preliminary optimisation study, *Applied Radiation and Isotopes*, 65(8), 2007, 959-967.
- [58] Muratsu, S., An application of synchrotron radiation to the analysis of forensic samples, mainly drugs of abuse, *Bunseki Kagaku*, 52(11), 2003, 1061-1062.
- [59] Muratsu ,S., Ninomiya, T., Kagoshima, Y., Matsui, J., Trace elemental analysis of drugs of abuse using synchrotron radiation total reflection X-ray fluorescence analysis (SR-TXRF), *Journal of Forensic Sciences* ,47(5), 2002 , 944-949.
- [60] Macomber, R.S., A complete introduction to modern NMR spectroscopy, John Wiley & Sons, New York , USA, 1998, p.1-5.
- [61] Doi, K., Miyazawa, M., Fujii, H., Kojima, T., The analysis of the chemical drugs among structural isomer, *Yakugaku Zasshi-Journal of the Pharmaceutical Society of Japan*, 126(9), 2006, 815-823.
- [62] Blachut, D., Wojtasiewicz, K., Czarnocki, Z., Identification and synthesis of some contaminants present in 4-methoxyamphetamine (PMA) prepared by the Leuckart method, *Forensic Science International* , 127(12), 2002, 45-62.
- [63] Baudot, P., Vicherat, A., Viriot, M.L., Carre, M.C., Identification of N-methyl-1-(1,3-benzodioxol-5-yl)-2-butanamine (MBDB), an homologue derivative of "ecstasy", *Analisis* , 27(6), 1999, 523-532.
- [64] Brewster, M.E., Davis, F.T., Appearance of Aminorex as a designer analog of methylaminorex, *Journal of Forensic Sciences* ,36(2),1991,587-592.
- [65] Fifield , F.W. ,Kealey, D., Principles and Practice of Analytical Chemistry, Blackwell Science, Cambridge, UK, 2000, Fifth Edition , p.2363-369.

- [66] Lawrence, A.H., Macneil, J.D., identification of amphetamine and related illicit drugs by 2nd derivative ultraviolet spectrometry, *Analytical Chemistry*, 54(13), 1982, 2385-2387.
- [67] Maeder, G., Pelletier, M., Haerdi, W., determination of amphetamines by high-performance liquid-chromatography with ultraviolet detection-online precolumn derivatization with 9 fluorenylmethyl chloroformate and preconcentration, *Journal of Chromatography*, 593(1-2), 1992, 9-14.
- [68] Cheng, W.C., Lee, W.M., Chan, M.F., Tsui, P., Dao, K.L., Enantiomeric separation of methamphetamine and related analogs by capillary zone electrophoresis: Intelligence study in routine methamphetamine seizures, *Journal of Forensic Sciences*, 47(6), 2002, 1248-1252.
- [69] Stuart, B., *Infrared Spectroscopy: Fundamentals and Applications*, John Wiley & Sons, Chichester, England, 2004, 1-6.
- [70] Smith, E., Dent, G., *Modern Raman Spectroscopy— A Practical Approach*, John Wiley & Sons, Chichester, England, 2005, chapter 3, 71-86.
- [71] Ricci, C., Chan, K.L.A., Kazarian, S.G., Combining the tape-lift method and Fourier transform infrared spectroscopic imaging for forensic applications, *Applied Spectroscopy*, 60 (9), 2006, 1013-1021.
- [72] Duncan, W.P., The use of GC/IR/MS for determination of drugs of abuse, *Clinical Chemistry*, 34(6), 1988, 1185-1185.
- [73] Kawase, K., Dobroiu, A., Yamashita, M., Sasaki, Y., Otani, C., Terahertz rays to detect drugs of abuse, in Miles, R.E., Zhang, X.C. Eisele, H., Krotkus, A., Terahertz frequency detection and identification of materials and objects, 2007, 241-250.
- [74] Burnett, A.D., Fan, W.H., Upadhyaya, P.C., Cunningham, J.E., Hargreaves, M.D., Munshi, T., Edwards, H.G.M., Linfield, E.H., Davies, A.G., Broadband terahertz time-

- domain spectroscopy of drugs-of-abuse and the use of principal component analysis, *Analyst*, 134(8), 2009,1658-1668.
- [75] Yinon, J., Field detection and monitoring of explosives, trends in analytical chemistry, 21(4), 2002, 292-301.
- [76] Arunachalam, K., , Udpa, S.S., Udpa, L., An X-ray security screening technique with limited field-of-view, *International Journal of Applied Electromagnetics and Mechanics* ,24(1-2), 2006,79-89.
- [77] Zentai, G., X-ray Imaging for Homeland Security, *IEEE International Workshop on Imaging Systems and Techniques*, 2008, 1-6.
- [78] Madden,R.W., Mahdavih,J.,Smith,R.C.,Subramanian,R., an explosives detection system for airline security using coherent x-ray scattering technology-art. no. 707915, in: *Proceedings of the society of photo-optical instrumentation engineers (spie)* , by Burger, A., Franks, L.A., James, R.B. (Eds.),7079,2008,7915-7915.
- [79] Ying, Z.R., Naidu, R., Crawford, C.R., Dual energy computed tomography for explosive detection, *Journal of x-ray science and technology*,14(4),2006,235-256 .
- [80] Liu, Y., Sowerby, B.D., Tickner, J.R., Comparison of neutron and high-energy X-ray dual-beam radiography for air cargo inspection, *Applied Radiation and Isotopes* , 66(4),2008, 463-473.
- [81] Bendahan, J., Garms, W., Megavolt computed tomography for air cargo container inspection, *IEEE conference on technologies for homeland security*, vol.(1,2), 2008, 7-11.
- [82] Bruning, H., Wolff, S., Automated explosive detection systems based upon CT technology, in: *32nd annual international carnahan conference on security technology*, by Sanson, L.D. (Eds), 1998, 55-58.

- [83] Farsoni ,A.T., Miresghi, S.A., Design and evaluation of a TNA explosive-detection system to screen carry-on luggage, *Journal of radioanalytical and nuclear chemistry*, 248(3), 2001, 695-697.
- [84] Ipe ,N.E.,Olsher, R.,Ryge, P., Mrozack, J., Thieu, J., A cargo inspection system based on pulsed fast neutron analysis (PFNA (TM)), *Radiation protection dosimetry* , 116 (1-4), 2005, 343-346.
- [85] Feldman, G. ,Vartsky , D., Goldberg, M.B., Bar, D., Krauss, R.A., Analysis of gamma-ray nuclear resonant absorption (NRA) images for automatic explosives detection ,seventh international conference on image processing and its applications , IEE conference publications,465,1999,789-793.
- [86] Somasundaram, S.D., Jakobsson, A., Smith, J. A. S., Analysis of nuclear quadrupole resonance signals from mixtures, *Signal processing*, 88(1),2008,146-157.
- [87] Jakobsson, A., Mossberg, M. , Using spatial diversity to detect narcotics and explosives using NQR signals, *IEEE transactions on signal processing* ,55(9), 2007, 4721-4726 .
- [88] Hoshina, H., Sasaki, Y.,Hayashi, A., Otani, C.,Kawase, K., Noninvasive Mail Inspection System with Terahertz Radiation, *Applied Spectroscopy*,63(1),2009, 81-86.
- [89] Liu, G.F., Zhao, F.W., Ge, M., Wang, W.F., Application of terahertz time domain spectroscopy to explosive and illegal drug ,*Spectroscopy and spectral analysis*, 28(5) , 2008, 966-969.
- [90] Davies, A.G., Burnett, A. D., Fan ,W., Linfield, E.H., Cunningham, J.E., Terahertz spectroscopy of explosives and drugs, *Materials Today*, 11(3), 2008, 18-26.
- [91] Woodfin , R.L., Trace chemical sensing of explosives, John Wiley & Sons, New Jersey, USA , 2007, p.5.

- [92] Yinon, J., detection of hidden explosives: an overview, *American Laboratory*, 38(12), 2006, 18-23.
- [93] Ewing, R.G., Atkinson, D.A., Eiceman, G.A., Ewing, G.J., A critical review of ion mobility spectrometry for the detection of explosives and explosive related compounds, *Talanta*, 54, 2001, 515–529.
- [94] Keller, T., Keller, A., Tutsch-Bauer, E., Monticelli, F., Application of ion mobility spectrometry in cases of forensic interest, *Forensic Science International*, 161, 2006, 130–140.
- [95] Fetterolf, D. D., Clark, T. D., Detection of Trace Explosive Evidence by Ion Mobility Spectrometry, *Journal of Forensic Sciences*, 38(1), 1993, 28-39.
- [96] Wu, Z., Hendrickson, C. L., Rodgers, R. P., Marshall, A. G., Composition of Explosives by Electrospray Ionization Fourier Transform Ion Cyclotron Resonance Mass Spectrometry, *Analytical Chemistry*, 74 (8), 2002, pp 1879–1883.
- [97] Cotte-Rodríguez, I., Chen, H., Cooks, R. G., Rapid trace detection of triacetone triperoxide (TATP) by complexation reactions during desorption electrospray ionization, *Chemical Communication*, 2006, 953-955.
- [98] Tachona, R., Pichon, V., Le Borgne, M. B., Mineta, J., Use of porous graphitic carbon for the analysis of nitrate ester, nitramine and nitroaromatic explosives and by-products by liquid chromatography–atmospheric pressure chemical ionisation-mass spectrometry, *Journal of Chromatography A*, 1154(1-2), 2007, 174-181.
- [99] Mathis, J.A., McCord, B.R., The analysis of high explosives by liquid chromatography/ electrospray ionization mass spectrometry: multiplexed detection of negative ion adducts, *Rapid Communications in Mass Spectrometry*, 19(2), 2004, 99-104.

- [100] Sigman, M.E., Ma, C.Y., Detection limits for GC/MS analysis of organic explosives, *Journal of Forensic Sciences*, 46(1) , 2001, 6-11.
- [101] Popov, I. A., Chen, H., Kharybin , O. N., Nikolae , E. N. , Cooks , R. G. , Detection of explosives on solid surfaces by thermal desorption and ambient ion/molecule reactions, *Chemical Communication* , 2005, 1953–1955.
- [102] McLuckey, S. A., Goeringer, D.E., Asano, K.G., Vaidyanathan ,G., Stephenson, J. L., High Explosives Vapor Detection by Glow Discharge-Ion Trap Mass Spectrometry, *Rapid Communications in Mass Spectrometry*, 10, 1996, 287-298.
- [103] Furton , K. G., Myers , L. J., The scientific foundation and efficacy of the use of canines as chemical detectors for explosives, *Talanta* , 54 , 2001, 487–500.
- [104] Yinon, J., Detection of Explosives by Electronic Noses, *Analytical Chemistry*, 75, 2003, 99A-105A.
- [105] Chalmers, J.M., Dent, J., *Industrial analysis with vibrational spectroscopy*, The Royal Society of Chemistry, Athenaeum Press Ltd., 1997, chapter 1, p.1.
- [106] Hendra, P., Jones, C., Warnes, G., *Fourier Transform Raman spectroscopy: Instrumentation and chemical applications*, Ellis Horwood Limited, Chichester, England, 1991, chapter 2, p.p.17-20.
- [107] Raman, C.V., Krishnan, K.S., *Nature*, 121, 1928, 50.
- [108] Pelletier, E.M., *Analytical applications of Raman spectroscopy*, Blackwell Science, London, UK, 1999, chapter 1, pp.1-3.
- [109] McCreery, R.L., *Raman spectroscopy for chemical analysis*, John Wiley & Sons , New York, USA, 1999, pp.1-247.
- [110] Šašić, S., *Pharmaceutical Applications of Raman Spectroscopy*, John Wiley & Sons, New York, USA, 2008, chapter 1, pp.1-5.

- [111] Griffiths, P. R., De Haseth, J. A., *Fourier Transform Infrared Spectrometry*, John Wiley and Sons., New Jersey, USA, 2007, Second Edition, Chapter 1, pp.16-18.
- [112] Couling, V.W., Fischer, P., Klenerman, D., Huber, W., Ultraviolet resonance Raman study of drug binding in dihydrofolate reductase, gyrase, and catechol O-methyltransferase, *Biophysical Journal*, 75, 1998, 1097–1106.
- [113] Graham, D., Goodacre, R., Chemical and bioanalytical applications of surface enhanced Raman scattering spectroscopy, *Chemical Society Reviews*, 37, 2008, 883-884.
- [114] Macdonald, A. M., Wyeth, P., On the use of photobleaching to reduce fluorescence background in Raman spectroscopy to improve the reliability of pigment identification on painted textiles, *Journal of Raman Spectroscopy*, 37(8), 2006, 830-835.
- [115] Chalmers, J.M., Griffiths, P.R., *Handbook of Vibrational Spectroscopy*, John Wiley and Sons, Chichester, U.K., 2002.
- [116] Pellow-Jarman, M. V., Hendra, P. J., Lehnert, R. J., The dependence of Raman signal intensity on particle size for crystal powders, *Vibrational Spectroscopy*, 12, 1996, 257-261.
- [117] Wang, H., Mann, C. K., Vickers, T. J., Effect of powder properties on the intensity of Raman scattering by crystalline solids, *Applied Spectroscopy*, 56(12), 2002, 1538-1544.
- [118] Hollas, J. M., *Modern Spectroscopy*, John Wiley & Sons, Chichester, England, Fourth Edition, 2004, pp.166.
- [119] Ferraro, J. R., Nakamoto, K., Brown, C. W., *Introductory Raman Spectroscopy*, Elsevier, California, USA, 2003, Second edition, pp.18.

- [120] Bondesson , L., Mikkelsen ,K. V., Luo, Y., Garberg, P., Ågren , H., Hydrogen bonding effects on infrared and Raman spectra of drug molecules, *Spectrochimica Acta Part A*, 66, 2007, 213–224.
- [121] Turrell, G., Corset, J., *Raman microscopy: Developments and applications*, Academic Press Limited, London, UK, 1996, chapter 3, pp.51-
- [122] Lewis, I.R., Edwards, H.G.M., *Handbook of Raman Spectroscopy from the Research Laboratory to the Process Line*, Marcel Dekker, Inc., New York,USA, 2001.
- [123] Chase, B., Fourier transform Raman spectroscopy, *Microchimica Acta* 93(1), 1987, 81-91.
- [124] Edwards, H.G.M., Chalmers, J. M., *Raman spectroscopy in archaeology and art history*, The Royal Society of Chemistry, Cambridge,UK,2005,pp.48-51.
- [125] Kuptsov , A.H., Applications of Fourier transform Raman spectroscopy in forensic science, *Journal of Forensic Science*, 39 ,1994, 305–318.
- [126] Hodges, C.M., Hendra, P.J., Willis, Farley, T., Fourier transform Raman spectroscopy of illicit drugs, *Journal of Raman Spectroscopy*, 20, 1989, 745-749.
- [127] Hodges, C.M, Akhavan, J., The use of Fourier transform Raman spectroscopy in the forensic identification of illicit drugs and explosives, *Spectrochimica Acta* ,46A(2) ,1990,303-307.
- [128] Neville,G.A., Shurvell,H.F., Fourier transform Raman and infrared vibrational study of diazepam and four closely related 1,4-benzodiazepines, *Journal of Raman Spectroscopy*,21, 1990,9-19.
- [129] Neville, G.A., Beckstead, H.D., Shurvell, H.F., Fourier transform Raman and infrared study of nitrazepam, nimetazepam, clonazepam and flunitrazepam, *Vibrational Spectroscopy*, 1, 1991, 287-297.

- [130] Tsuchihashi, H., Katagi, M., Nishikawa, M., Tatsuno, M., Nishioka, H., Nara, A., Nishio, E., Petty, C., Determination of methamphetamine and its related compounds using Fourier transform Raman spectroscopy, *Applied spectroscopy*, 51(12), 1997, 1796-1799.
- [131] Petty, C., Garland, B., Screening Controlled Substances Using the Near-infrared Fourier Transform Raman Technique, Thermo Fisher Scientific Application Note: 51242 (Thermo Fisher Scientific, Madison, WI, USA).
- [132] Burnett, A., Fan, W., Upadhyaya, P., Cunningham, J., Edwards, H.G.M., Munshi, T., Hargreaves, M., Linfield, E., Davies, G., Complementary spectroscopic studies of materials of security interest, *Optics and Photonics for Counterterrorism and Crime Fighting*. Edited by Lewis, C., Owen, G. P., Proceedings of the SPIE, Volume 6402, 2006, pp. 64020B.
- [133] Passingham, C., Hendra, P. J., Hodges, C., Willis, H. A., The Raman spectra of some aromatic nitro compounds, *Spectrochimica Acta A*, 47(9-10), 1991, 1235-1245.
- [134] Akhavan, J., Analysis of high-explosive samples by Fourier transform Raman spectroscopy, *Spectrochimica Acta A*, 47(9-10), 1991, 1247-1250.
- [135] McNesby, K.L., Wolfe, J.E., Morris, J.B., Pesce-Rodriguez, R. A., Fourier Transform Raman Spectroscopy of Some Energetic Materials and Propellant Formulations, *Journal of Raman Spectroscopy*, 25, 1994, 75-87.
- [136] Fell, N. F., Widder, J. M., Medlin, S. V., Morris, J. B., Pesce-Rodriguez, R. A., McNesby, K.L., Fourier Transform Raman Spectroscopy of Some Energetic Materials and Propellant Formulations (II), *Journal of Raman Spectroscopy*, 27, 1996, 97-104.
- [137] Lewis, I. R., Daniel, N. W., JR., Griffiths, P. R., Interpretation of Raman Spectra of Nitro-Containing Explosive Materials. Part I: Group Frequency and Structural Class Membership, *Applied Spectroscopy*, 51(12), 1997, 1854-1867.

- [138] Willis, J.N., Cook, R.B., Jankow, R., Raman spectrometry of some common barbiturates, *Analytical Chemistry*, 44(7),1972,1228-1234.
- [139] Vergoten , G., Fleury,G., Gamot ,A.P., Lattice vibrations of crystalline l-cocaine hydrochloride, *Journal of Raman Spectroscopy*, 14(6),1983,371 – 374.
- [140] Gamot, A.P., Vergoten ,G., Fleury , G., Raman spectroscopic study of cocaine chlorhydrate , *Talanta* ,32(5),1985,363-372.
- [141] Morssli , M., Cassanas, G., Bardet, L., Vibrational analysis of sodium α -, β -, and γ - hydroxybutyrates. Inter- and intramolecular hydrogen bonds, *Spectrochimica Acta A*, 47(5),1991, 529-541.
- [142] Sands,H.S.,Hayward,I.P.,Kirkbride,T.E.,Bennet,R.,Lacey,R.J.,Batchelder, D.N., UV-excited resonance Raman spectroscopy of narcotics and explosives, *Journal of Forensic Sciences*,43(3),1998,509-513.
- [143] Bell, S.E.J., Burns, D.T., Dennis, A. C., Matchett, L. J., Speers,J. S., Composition profiling of seized ecstasy tablets by Raman spectroscopy, *Analyst*, 125, 2000,1811–1815.
- [144] Bell, S. E. J., Burns, D. T., Dennis, A. C., Dennis, A.C., Speers, J. S., Rapid analysis of ecstasy and related phenethylamines in seized tablets by Raman spectroscopy, *Analyst*,125,2000,541-544.
- [145] Bell, S. E. J., Barrett, L.J., Burns, D. T., Dennis, A. C., Dennis, A.C., Speers, J. S, Tracking the distribution of “ecstasy” tablets by Raman composition profiling: A large scale feasibility study, *Analyst*, 128, 2003, 1331-1335.
- [146] Day, J.S., Edwards, H.G.M., Dobrowski, S.A. , Voice, A.M., the detection of drugs of abuse in fingerprints using Raman spectroscopy I:latent fingerprints, *Spectrochimica Acta A*,60,2004,563-568.

- [147] Day, J.S., Edwards, H.G.M., Dobrowski, S.A., Voice, A.M., the detection of drugs of abuse in fingerprints using Raman spectroscopy II: cyanoacrylate-fumed fingerprints, *Spectrochimica Acta A*, 60, 2004, 1725-1730.
- [148] West, M.J., Went, M.J., The spectroscopic detection of exogenous material in fingerprints after development with powders and recovery with adhesive lifters, *Forensic Science International*, 174, 2008, 1-5.
- [149] West, M.J., Went, M.J., The spectroscopic detection of drugs of abuse in fingerprints after development with powders and recovery with adhesive lifters, *Spectrochimica Acta A*, 71(5), 2009, 1984-1988.
- [150] West, M.J., Went, M.J., The spectroscopic detection of drugs of abuse on textile fibres after recovery with adhesive lifters, *Forensic Science International*, 189(1-3), 2009, 100-103.
- [151] Frederick, K.A., Pertaub, R., Kam, N.W.S., Identification of individual drug crystals on paper currency using Raman microspectroscopy, *Spectroscopy Letters*, 37(3), 2004, 301-310.
- [152] Noonan, K.Y., Beshire, M., Darnell, J., Frederick, K.A., Qualitative and quantitative analysis of illicit drug mixtures on paper currency using Raman microspectroscopy, *Applied Spectroscopy*, 59(12), 2005, 1493-1497.
- [153] Vergoten, G., Fleury, G., Blain, M., Odier, S., Structure Moléculaire des Dérivés Nitres Aromatiques 5-Spectres de Vibration et Analyse par Coordonnées Normales du 1,3,5-Triamino-2,4,6-trinitrobenzène, *Journal of Raman Spectroscopy*, 16(3), 1985, 143-148.
- [154] Gruzdkov, Y.A., Gupta, Y.M., Vibrational properties and structure of pentaerythritol tetranitrate, *J. Phys. Chem. A*, 105, 2001, 6197-6202.

- [155] Cheng, C., Kirkbride, T. E., Batchelder, D. N., Lacey, R. J., Sheldon, T. G., In Situ Detection and Identification of Trace Explosives by Raman Microscopy, *Journal of Forensic Sciences*, 40(1), 1995, 31-37.
- [156] Angel, S.M., Carter, J.C., Stratis, D.N., Marquardt, B.J., Brewer, W.E., Some new uses for filtered fiber-optic Raman probes: In situ drug identification and in situ and remote Raman imaging, *Journal of Raman Spectroscopy*, 30, 1999, 795-805.
- [157] Carter, J. C., Brewer, W. E., Angel, S. M., Raman spectroscopy for the in situ identification of cocaine and selected adulterants, *Applied Spectroscopy*, 54(12), 2000, 1876-1881.
- [158] Hargreaves, M. D., Page, K., Munshi, T., Tomsett, R., Lynch, G., Edwards, H.G.M., Analysis of seized drugs using portable Raman spectroscopy in an airport environment – a proof of principle study, *Journal of Raman Spectroscopy*, 39, 2008, 873–880.
- [159] Brewster, V.L., Edwards, H.G.M., Hargreaves, M. D., Munshi, T., Identification of the date-rape drug GHB and its precursor GBL by Raman spectroscopy, *Drug Testing and Analysis*, 1, 2009, 25–31.
- [160] Hayward, I. E., Kirkbride, T.E., Batchelder, D.N., Lacey, R. J., Use of a fiber optic probe for the detection and identification of explosive materials by Raman spectroscopy, *Journal of Forensic Sciences*, 40(5), 1995, 883-884.
- [161] Lewis, I.R., Daniel, N.W., Chaffin, N.C., Griffiths, P.R., Tungol, M.W., Raman spectroscopic studies of explosive materials: towards a fieldable explosives detector, *Spectrochimica Acta Part A*, 51, 1995, 1985-2000.
- [162] Gupta, N., Dahmani, R., AOTF Raman spectrometer for remote detection of explosives, *Spectrochimica Acta Part A*, 56, 2000, 1453-1456.

- [163] Harvey, S.D., Vucelick, M.E., Lee, R.N., Wright, B.W., Blind field test evaluation of Raman spectroscopy as a forensic tool, *Forensic Science International*, 125, 2002, 12-21.
- [164] Lewis, M.L., Lewis, I.R., Griffiths, P.R., Anti-Stokes Raman Spectrometry with 1064-nm Excitation: An Effective Instrumental Approach for Field Detection of Explosives, *Applied Spectroscopy*, 58(4), 2004, 420- 427.
- [165] Lewis, M.L., Lewis, I.R., Griffiths, P.R., Raman spectrometry of explosives with a no-moving-parts fiber coupled spectrometer: A comparison of excitation wavelength, *Vibrational Spectroscopy*, 38, 2005, 17-28.
- [166] Sharma, S.K., Misra, A.K., Sharma, B., Portable remote Raman system for monitoring hydrocarbon, gas hydrates and explosives in the environment, *Spectrochimica Acta Part A*, 61, 2005, 2404–2412.
- [167] Carter, J. C., Angel, S. M., Lawrence-Snyder, M., Scaffidi, J., Whipple, R. E., Reynolds, J. G., Standoff detection of high explosive materials at 50 meters in ambient light conditions using a small Raman instrument, *Applied Spectroscopy*, 59(6), 2005, 769- 775.
- [168] Pinzaru, S. C., Pavel, I., Leopold, N., Kiefer, W., Identification and characterization of pharmaceuticals using Raman and surface-enhanced Raman scattering, *Journal of Raman Spectroscopy*, 35, 2004, 338–346.
- [169] Vo-Dinh, T., Stokes, D. L., Griffin, G. D., Volkan, M., Kim, U. J., Simon, M. I., Surface-enhanced Raman Scattering (SERS) Method and Instrumentation for Genomics and Biomedical Analysis, *Journal of Raman Spectroscopy*, 30, 1999, 785–793.
- [170] Ruperez, A., Montes, R., Laserna, J.J., Identification of stimulant drugs by surface-enhanced Raman spectrometry on colloidal silver, *Vibrational Spectroscopy*,

2, 1991,145-154.

[171] Sägmüller, B., Schwarze, B., Brehma, G., Schneider, S., Application of SERS spectroscopy to the identification of (3, 4-methylenedioxy) amphetamine in forensic samples utilizing matrix stabilized silver halides, *Analyst*, 126, 2001, 2066–2071.

[172] Faulds, K., Smith, W. E., Grahama, D., Lacey, R. J., Assessment of silver and gold substrates for the detection of amphetamine sulfate by surface enhanced Raman scattering (SERS), *Analyst*, 127, 2002,282–286 .

[173] Trachta, G.,Schwarze,B., Brehm, G., Schneider, S., Hennemann, M., Clark, T., Near-infrared Fourier transform surface-enhanced Raman scattering spectroscopy of 1,4-benzodiazepine drugs employing gold films over nanospheres, *Journal of Raman Spectroscopy*, 35, 2004,368–383.

[174] Kneipp, K., Wang, Y., Dasari, R.R., Feld, M.S., Gilbert, B.D., Janni, J., Steinfeld, J. I., Near-infrared surface-enhanced Raman scattering of trinitrotoluene on colloidal gold and silver, *Spectrochimica Acta Part A*, 51,1995,2171-2175 .

[175] Kawai, N.T.,Spencer, K. M., InPhotonics and EIC Laboratories, Raman spectroscopy for homeland defense applications, *InPhotonics*, Application Note #18, 2004. www.inphotonics.com

[176] Fang, X., Ahmad, S.R., Detection of explosive vapour using surface-enhanced Raman spectroscopy, *Applied Physics B: Lasers and Optics*, 97(3),2009,723-726.

[177] Eliasson, C., Claybourn,M., Matousek,P., Deep subsurface Raman spectroscopy of turbid media by a defocused collection system, *Applied Spectroscopy*, 61(10), 2007,1123- 1127.

[178] Eliasson, C., Macleod, N.A., Matousek,P., Non-invasive detection of cocaine dissolved in beverages using displaced Raman spectroscopy, *Analytica Chimica Acta*, 607, 2008, 50–53.

- [179] Eliasson, C., Macleod, N.A., Matousek, P., Non-invasive detection of cocaine in rum using displaced Raman spectroscopy, Central Laser Facility Annual Report, (7), 2007/2008, 254- 255.
- [180] Eliasson, C., Macleod, N.A. , Matousek, P., Noninvasive detection of concealed liquid explosives using Raman spectroscopy, Analytical Chemistry,79(21),2007, 8185–8189.
- [181] Macleod, N.A., Eliasson, C., Matousek, P., Hidden depths ? New techniques for subsurface spectroscopy, Spectroscopy Europe, 19 (5), 2007, 7-10.
- [182] Eliasson ,C., Macleod, N. A. , Matousek,P., Non-invasive detection of concealed liquid and powder explosives using spatially offset Raman spectroscopy, Central Laser Facility Annual Report, (6), 2007/2008, 203-206.
- [183] Eliasson ,C., Macleod, N. A. , Matousek,P., Non-invasive detection of powders concealed within diffusely scattering plastic containers, Vibrational Spectroscopy, 48 ,2008, 8–11.
- [184] Pelletier, M. J., Quantitative analysis using Raman spectrometry, Applied Spectroscopy, 57(1) , 2003, 20A-42A.
- [185] Ryder, AG, O'Connor, GM, Glynn, TJ, Identifications and quantitative measurements of narcotics in solid mixtures using near-IR Raman spectroscopy and multivariate analysis, Journal of Forensic Sciences ,44(5), 1999,1013-1019.
- [186] Ryder, AG, O'Connor, GM, Glynn, TJ, Quantitative analysis of cocaine in solid mixtures using Raman spectroscopy and chemometric methods, Journal of Raman spectroscopy,31(3),2000, 221-227.
- [187] Ryder, AG, Classification of narcotics in solid mixtures using Principal Component Analysis and Raman spectroscopy, Journal of Forensic Sciences,(47) 2, 2002, 275-284.

- [188] Leger, M.N., Ryder, A.G., Comparison of derivative preprocessing and automated polynomial baseline correction method for classification and quantification of narcotics in solid mixtures, *Applied Spectroscopy*,60(2),2006,182-193.
- [189] Dujourdy, L., Pocognoli, S., Hess, S., Buzzini, P., Massonnet, G., Margot, P., Chemometric analysis of Raman spectroscopy data on MDMA in "Ecstasy" tablets, *Forensic Science International*,136,2003,Suppl.1, 91-92.
- [190] Katainen, E., Elomaa, M., Laakkonen, U., Sippola, E., Niemelä, P., Suhonen, J., Järvinen, K., Quantification of the amphetamine content in seized street samples by Raman spectroscopy, *Journal of Forensic Sciences*,52(1),2007,88-92.
- [191] Renishaw plc, Combined Raman and FT-IR spectroscopy, Application Note 101, Issue 1.0, April 2004.
- [192] Adar, F., leBourdon, G., Reffner, J., Whitley, A., FT-IR and Raman Microscopy on a United Platform: A Technology Whose Time Has Come, *Spectroscopy*, 18(2), 2003,34-40.
- [193] Sägmüller, B., Schwarze, B., Brehm, G., Trachta, G., Schneider, S., Identification of illicit drugs by a combination of liquid chromatography and surface-enhanced Raman scattering spectroscopy, *Journal of Molecular Structure*, 661-662, 2003, 279-290.
- [194] Otieno-Alego, V., Some forensic applications of a combined micro-Raman and scanning electron microscopy system, *Journal of Raman Spectroscopy*, 40(8), 2009, 948-953.
- [195] Irving, R. C., Dickson, S. J., The detection of sedatives in hair and nail samples using tandem LC-MS-MS, *Forensic Science International*,166 2007,58-67.

- [196] Musshoff, F., Driever, F., Lachenmeier, K., Lachenmeier, D.W., Banger, M., Madea, B., Results of hair analyses for drugs of abuse and comparison with self-reports and urine tests. *Forensic Science International*, 156, 2006, 118–123.
- [197] Gambelunghe, C., Rossi, R. , Ferranti, C., Rossi, R. , Bacci, M., Hair analysis by GC/MS/MS to verify abuse of drugs, *Journal of Analytical Toxicology*, 25, 2005, 205–221.
- [198] Cognard, E., Rudaz, S. , Bouchonnet ,S. , Staub,C, Analysis of cocaine and three of its metabolites in hair by gas chromatography-mass spectrometry using ion-trap detection for CI/MS/MS, *Journal of Chromatography B*, 826 ,2005, 17–25.
- [199] Lachenmeier, K., Musshoff, F., Madea, B., Determination of opiates and cocaine in hair using automated enzyme immunoassay screening methodologies followed by gas chromatographic–mass spectrometric (GC–MS) confirmation, *Forensic Science International*, 159, 2006, 189–199.
- [200] Suzuki,O., Hattori, H., Asano, M., Nails as useful materials for detection of methamphetamine or amphetamine abuse, *Forensic Science International* , 24,1984, 9-16.
- [201] Lemos, N.P., Anderson, R.A., Robertson, J.R., Nail analysis for drugs of abuse: extraction and determination of cannabis in fingernails by RIA and GC-MS, *Journal of Analytical Toxicology*, 23(3), 1999, 147-152.
- [202] Engelhart, D.A., Jenkins, A.J., Detection of cocaine analytes and opiates in nails from postmortem cases, *Journal of Analytical Toxicology*, 26(7), 2002, 489-492.
- [203] Garside, D., Roper-Miller, J.D., Goldberger, B.A., Hamilton, W.F., Maples, W.R., Identification of cocaine analytes in fingernail and toenail specimens, *Journal of Forensic Science*, 43(5), 1998, 974-979.

- [204] Lemos, N.P., Anderson, R.A., Valentini, R., Tagliaro, F., Scott, R.T., Analysis of morphine by RIA and HPLC in fingernail clippings obtained from heroin users, *Journal of Forensic Science*, 45(2), 2000, 407-412.
- [205] Engelhart, D.A., Lavins, E.S., Sutheimer, C.A., Detection of drugs of abuse in nails, *Journal of Analytical Toxicology*, 22(4) 1998, 314-318.
- [206] Valente-Campos, S., Yonamine, M., de Moraes, M. R.L., Silva, O.A., Validation of a method to detect cocaine and its metabolites in nails by gas chromatography-mass spectrometry, *Forensic Science International*, 159(2-3), 2006, 218-222.
- [207] Gangitano, D.A., Garofalo, M.G., Juvenal, G.J., Budowle, B., Padula R.A., Typing of the locus DYS19 from DNA derived from fingernail clippings using PCR Concert rapid purification system, *Journal of Forensic Science*, 47(1), 2002, 175-177.
- [208] Anderson, T.D., Ross, J.P., Roby, R.K., Lee, D.A., Holland, M.M., Validation study for the extraction and analysis of DNA from human nail material and its application to forensic casework, *Journal of Forensic Science*, 44(5), 1999, 1053-1056.
- [209] Wiegand, P., Bajanowski, T., Brinkmann, B., DNA typing of debris from fingernails, *Int. J. Legal Med.*, 106, 1993, 81-83.
- [210] de Faria, D. L. A., de Souza, M. A., Raman spectra of human skin and nail excited in the visible region, *Journal of Raman Spectroscopy*, 30, 1999, 169-171.
- [211] Williams, A. C., Edwards, H. G. M., Barry, B.W., Raman spectra of human keratotic biopolymers: Skin, callus, hair and nail, *Journal of Raman Spectroscopy*, 25(1), 1994, 95-98.
- [212] Akhtar, W., Edwards, H. G. M., Fourier-transform Raman spectroscopy of mammalian and avian keratotic biopolymers, *Spectrochimica Acta Part A*, 53, 1997, 81-90.

- [213] Widjaja, E. ,Seah, R.K., Use of Raman spectroscopy and multivariate classification techniques for the differentiation of fingernails and toenails, *Applied spectroscopy*, 60(3), 2006, 343-345.
- [214] Widjaja, E., Lim, G. H., An, A., A novel method for human gender classification using Raman spectroscopy of fingernail clippings, *Analyst*, 133, 2008 , 493-498 .
- [215] Fang , Z., Wang, S., Li, F., Study on the nitrolysis of hexamethylenetetramine by NMR-spectrometry, Part IV: A novel mechanism of the formation of RDX from HA, *Propellants, Explosives, Pyrotechnics*, 23, 1998, 317-319.
- [216] Carter, E.A., Edwards, H.G.M., in: Gremlich, H., Yan, B., (Eds.), *Infrared and Raman spectroscopy of biological materials*, Marcel Dekker, Inc., New York, USA, 2001, 429.
- [217] Herzberg, G., *Molecular spectra and molecular structure*, D.Van Nostrand Company, New York, USA, 1945, p. 179.
- [218] Degen, I.A., Newman, G.A., Raman spectra of inorganic ions, *Spectrochimica Acta A*, 49, 1993, 859- 887.
- [219] Jensen,J.O., Vibrational frequencies and structural determinations of hexamethylenetetramine, *Spectrochimica Acta Part A*, 58 , 2002, 1347-1364.
- [220] Ramamoorthy, P., Krishnamurthy, N., Vibration spectrum of pentaerythritol , *Spectrochimica Acta Part A*, 53, 1997, 655-663.
- [221] Marzocchi, M. P., Castellucci, E., Vibrational crystal spectra of pentaerythritol- d_0 and $-d_4$, *Journal of Molecular Structure*, 9, 1971, 129-137.
- [222] Schlucker, S., Schaeberle, M.D., Huffman, S.W. , Levin, I.W., Raman micro-spectroscopy: A comparison of point, line and wide-field imaging methodologies, *Analytical Chemistry*,75,2003, 4312-4318.

- [223] Overall, N., Depth profiling with confocal Raman microscopy, part I, *Spectroscopy*, 14(10), 2004, 22-27.
- [224] Glatstein, B., Vinokurov, A., Levin, N., Zeichner, A., Improved method for shooting distance estimation. Part1. Bullet holes in clothing items, *Journal of Forensic Sciences*, 45(4), 2000, 801-806.
- [225] Brazeau, J., Wong, R.K., Analysis of gunshot residues on human tissues and clothing by X-ray microfluorescence, *Journal of Forensic Sciences*, 42(3), 1997, 424-428.
- [226] Andrasko, J., Characterization of Smokeless Powder Flakes from Fired Cartridge Cases and from Discharge Patterns on Clothing, *Journal of Forensic Sciences*, 37(4), 1992, 1030-1047.
- [227] Boland, C.A. , McDermott, S.D. , Ryan, J. , Clothing damage analysis in alleged sexual assaults—The need for a systematic approach, *Forensic Science International*, 167 , 2007, 110-115.
- [228] Petricevic, S.F. , Bright, J. , Cockerton, S.L. , DNA profiling of trace DNA recovered from bedding , *Forensic Science International* 159 (1) ,2006, 21-26.
- [229] Wayne, J.S., Michaud, D., Bowen, J.H., Fournery, R.M., Sensitive and Specific Quantification of Human Genomic Deoxyribonucleic Acid (DNA) in Forensic Science Specimens: Casework Examples, *Journal of Forensic Sciences*, 36(4), 1991, 1198-1203.
- [230] Al-Dirbashi, O.Y., Ikeda, k., Takahashi, M., Kuroda, N., Ikeda, S., Nakashima, K. , Drugs of abuse in a non-conventional sample ;detection of methamphetamine and its main metabolite, amphetamine in abusers' clothes by HPLC with UV and fluorescence detection, *Biomedical chromatography*, 15,2001, 457-463.

- [231] Tracqui, A., Kintz, P., Lades, B., Jamey, C., Mangin, P., The detection of opiate drugs in non-traditional specimens (clothing): A report of ten cases, *Journal of Forensic Sciences*, 40(2), 1995, 263-265.
- [232] Crowson, C. A. , Cullum, H. E. , Hiley, R. W. , Lowe, A. M. , A survey of high explosives traces in public places , *Journal of Forensic Sciences*,41(6), 1996, 980-989.
- [233] Cullum, H. E. , McGavigan, C. , Uttley, C. Z. , Stroud, M. A. M. , Warren, D. C., A second survey of explosive traces in public places , *Journal of Forensic Sciences*, 49(4), 2004,1-7.
- [234] Locard, E., *The Analysis of Dust Traces*, *American Journal of Police Science* , 1, 1930, 276-298.
- [235] Edwards, H.G.M., Farwell, D.W.,Webster, D., FT Raman microscopy of untreated natural plant fibres, *Spectrochimica Acta Part A*, 53, 1997, 2383-2392.
- [236] Edwards, H.G.M., Farwell, D.W., Raman spectroscopic studies of silk , *Journal of Raman Spectroscopy*, 26 (8-9), 1995, 901-909.
- [237] Skrifvars, M., Niemelä, P., Koskinen, R. , Hormi , O., Process cure monitoring of unsaturated polyester resins, vinyl ester resins and gel coats by Raman spectroscopy , *Journal of Applied Polymer Science* , 93(3) , 2004, 1285-1292.
- [238] Claudio,A.,Te llez, S.,Hollauer, E., Mondragon, M.A., Castano, V.M., Fourier transform infrared and Raman spectra, vibrational assignment and ab initio calculations of terephthalic acid and related compounds, *Spectrochimica Acta Part A*, 57(5), 2001, 993-1007.
- [239] Hogg, L.J., Edwards, H.G.M., Farwell, D.W. , Peter, A.T. , FT Raman spectroscopic studies of wool, *Journal of the Society of Dyers and Colourists*, 110 (56),1994,196-199.

- [240] Na, N. , Zhang, C. , Zhao, M. , Zhang, S. , Yang, C. , Fang, X. , Zhang, X., Direct detection of explosives on solid surfaces by mass spectrometry with an ambient ion source based on dielectric barrier discharge, *Journal of Mass Spectrometry*,42, 2007,1079-1085.
- [241] Cotte-Rodríguez, I., Cooks, R. G., Non-proximate detection of explosives and chemical warfare agent simulants by desorption electrospray ionization mass spectrometry, *Chemical Communications*, 28, 2006, 2968-2970.
- [242] Takáts, Z., Cotte-Rodríguez, I., Talaty, N., Chen, H., Cooks, R. G., Direct, trace level detection of explosives on ambient surfaces by desorption electro electrospray ionization mass spectrometry, *Chemical Communications*, 15 , 2005 , 1950-1952.
- [243] Cotte-Rodríguez, I., Takáts, Z., Talaty, N.,Chen, H., Cooks, R. G., Desorption electrospray ionization of explosives on surfaces: sensitivity and selectivity enhancement by reactive desorption electrospray ionization, *Analytical Chemistry*,77,2005,6755-6764.
- [244] Grabherr, S. , Ross, S. , Regenscheit, P. , Werner, B. , Oesterhelweg, L. , Bolliger, S. , Thali, M. J. , *American Journal of Roentgenology*,190, 2008,1390-1395.
- [245] U S Drug Enforcement Administration, *Microgram Bulletins*, 38, 2005, 48.
- [246] U S Drug Enforcement Administration, *Microgram Bulletins*, 36, 2003,199.
- [247] U S Drug Enforcement Administrations, *Microgram Bulletins*, 39, 2006, 72.
- [248] Australian Illicit Drug Report 2001-02, p91. http://www.crimecommission.gov.au/publications/ iddr/2001_02.htm, [accessed 6 September 2010].
- [249] U S Drug Enforcement Administration, *Microgram Bulletins*, 38, 2005,137.
- [250] U S Drug Enforcement Administration, *Microgram Bulletins*, 2003, 36, 271.

- [251] McDermott, S. D. , Power, J.D. , Drug smuggling using clothing impregnated with cocaine, *Journal of Forensic Sciences*,50, 2005, 50 (6) ,1423-1425.
- [252] Chase , B., A new generation of Raman instrumentation, *Applied Spectroscopy*, 48, 1994, 14A-19A.
- [253] Barry, B. W., Edwards, H. G. M., Williams, A. C., Fourier transform Raman and infrared vibrational study of human skin: Assignment of spectral bands, *Journal of Raman Spectroscopy* , 23 (11),1992, 641-645.
- [254] Barry, B. W., Edwards, H. G. M., Williams, A. C., Fourier transform Raman and IR spectra of snake skin, *Spectrochimica Acta Part A*, 49 (5-6) ,1993, 801-807.
- [255] Williams, A. C., Barry, B. W., Edwards, H. G. M., Comparison of Fourier-transform Raman spectra of mammalian and reptilian skin, *Analyst*, 119, 1994, 563-566.
- [256] Caspers, P., Lucassen, G.W., Wolthuis, R., Bruining,H.A., Puppels, G., in vitro and in vivo Raman spectroscopy of human skin, *Biospectroscopy*,4, 1998, S31-S39.
- [257] Caspers, P. J. , Lucassen, G. W. , Puppels, G. J., Combined in vivo confocal Raman spectroscopy and confocal microscopy of human skin, *Biophysical Journal* , 85, 2003, 572–580.
- [258] Williams, A. C., Barry, B. W., Edwards, H. G. M., The ‘Iceman’: molecular structure of 5200-year-old skin characterized by Raman spectroscopy and electron microscopy, *Biochimica et Biophysica Acta*, 1246, 1995, 98-105.
- [259] Petersen, S., Nielsen, O.F., Christensen, D.H., Edwards, H.G.M., Farwell, D.W., David, Rosalie, Lambert, P., Gniadecka, M., Wulf, H.C., Near-infrared Fourier-transform Raman spectroscopy of skin samples from the ‘Tomb of the Two Brothers’, Khnum-Nakht and Nekht-Ankh, XIIth Dynasty Egyptian mummies (ca 2000 BC), *Journal of Raman spectroscopy*,34,2003, 375-379.

- [260] Edwards, H.G.M., Farwell, D.W., Williams, A. C., Barry, B. W., Rull , F., Novel spectroscopic deconvolution procedure for complex biological systems: vibrational components in the FT-Raman spectra of ice-man and contemporary skin, Journal of the Chemical Society, Faraday Transactions, 91(21) , 1995 ,3883-3887.
- [261] Edwards, H.G.M., Gniadecka , M., Petersen, S., Hansen, J.P.H., Nielsen, O.F., Christensen, D.H., Wulf, H.C., NIR-FT Raman spectroscopy as a diagnostic probe for mummified skin and nails, Vibrational spectroscopy, 28,2002,3-15.
- [262] Gniadecka , M., Wulf , H.C., Mortensen, N.N., Nielsen, O.F., Christensen, D.H., Diagnosis of basal cell carcinoma by Raman spectroscopy, Journal of Raman spectroscopy,28, 1997, 125-129.
- [263] Justes ,D.R., Talaty,N., Cotte-Rodriguez, I., Cooks, G., Detection of explosives on skin using ambient ionization mass spectrometry, Chemical communications, 2007, 2142-2144.
- [264] Lewis, M. L., Lewis, I. R., Griffiths, P. R., Evaluation of a dispersive Raman spectrometer with a Ge array detector and a 1064 nm laser for the study of explosives, Vibrational Spectroscopy, 38 , 2005,11–16.
- [265] http://www.andor.com/scientific_cameras/idus-ingaas/ accessed 23 February 2010.
- [266] <http://www.rta.biz/Content/IRA.asp/> accessed 23 February 2010.
- [267] <http://deltanu.com/1064-raman-spectrometer/> accessed 1 March 2010.
- [268] <http://www.intevac.com/intevacphotonics/products/mosir950/>
Accessed 26 February 2010.
- [269] http://www.laser2000.co.uk/pdfs/download/test_&_measurement.pdf
Accessed 26 February 2010.